Generation and analysis of mammalian cells containing various Raf mutations

Thesis submitted for the degree of

Doctor of Philosophy

at the University of Leicester

by

Kathryn Elizabeth Mercer (B.Sc. Hons. UMIST)

Department of Biochemistry

University of Leicester

June 2002

ProQuest LLC
789 East Eisenhower Parkway
P.O. Box 1346
Ann Arbor, MI 48106-1346

CONTENTS

ABBREVIATIONS

amp^R	ampicillin resistance
AP-1	activating protein-1
Apaf-1	apoptotic protease activating factor-1
APS	ammonium persulphate
ASK1	apoptosis signal regulating kinase 1
ATF2	activating transcription factor 2
bp	base pairs
BrdU	bromodeoxyuridine
BSA	bovine serum albumin
cAMP	adenosine 3', 5'- cyclic manophosphate
CDK	cyclin dependent kinase
cDNA	complementary DNA
C. elegans	*Caenorhabditis elegans*
CIP	CDK-interacting protein
CK2	casein kinase 2
CR	conserved region
CRD	cysteine rich domain
DAG	diacylglycerol
dCTP	deoxy-cytidine triphosphate
DISC	death-inducing signalling complex
D. melanogaster	*Drosophila melanogaster*
DMEM	Dulbecco's modified Eagle's medium
DMSO	dimethyl sulphoxide
DNA	deoxyribonucleic acid
dNTP	deoxy-nucleoside triphosphate
E	embryonic day
E2F	E2 promoter binding factor

E. coli	*Escherichia coli*
EDTA	diaminoethane-tetra acetic acid
EGF	epidermal growth factor
ER	estrogen receptor
ERK	extracellular-signal-regulated kinase
ES cell	embryonic stem cell
FADD	Fas-associated death domain
FCS	foetal calf serum
FITC	fluorescein isothiocyanate
GADD	growth arrest and DNA damage
h	hour(s)
HEPES	N-[2-hydroxyethyl] piperazine-N'-[2-ethanesulphonic acid]
HPRT	hypoxanthine guanine phosphoribosyl transferase
Hsp90	heat-shock protein of 90 kDa
hyg^R	hygromycin resistance
IAP	inhibitor of apoptosis protein
IKK	IκB kinase
IL3	interleukin 3
INK4	inhibitor of cyclin-dependent kinase 4
kb	kilobase(s)
kDa	kiloDalton
KIP	kinase-interacting protein
KSR	kinase suppressor of Ras
LIF	leukaemia inhibitory factor
LPA	lysophosphatidic acid
MAPK	mitogen activated protein kinase
MEF2C	myocyte enhancer factor-2C
MEFs	mouse embryonic fibroblasts
MEK	MAPK/ERK kinase
min	minute(s)
MKK	MAPK kinase

MLC-2	myosin light chain-2
MLK	mixed lineage protein kinase
mRNA	messenger RNA
neo^R	neomycin resistance
NFκB	nuclear factor κB
NGF	nerve growth factor
OLB	oligonucleotide labelling buffer
PBS	phosphate buffered saline
PCR	polymerase chain reaction
PDGF	platelet derived growth factor
PFA	paraformaldehyde
PI3-K	Phosphoinositide 3-kinase
PKA	protein kinase A
PKC	protein kinase C
PMA	phorbol 12-myristate 13-acetate
PMSF	phenylmethylsulphonyl fluoride
PP2A	protein phosphatase 2A
pRb	retinoblastoma protein
PTB	phosphotyrosine binding
puro^R	puromycin resistance
RBD	Ras binding domain
RKIP	Raf kinase inhibitor protein
RNA	ribonucleic acid
RNase	ribonuclease
rpm	evolutions per minute
S. cerevisiae	*Saccharomyces cerevisiae*
SDS-PAGE	sodium dodecyl sulphate- polyacrylamide gel electrophoresis
sec	second(s)
Ser	serine
SGK	serum- and glucocorticoid-inducible kinase
SH2	Src homology 2
SoS	son of sevenless

SRE	serum response element
SRF	serum response factor
Sur-8	suppressor of Ras-8
TAE	Tris-acetate-EDTA
TAK1	transforming growth factor beta-activated kinase 1
TBS	Tris-buffered saline
TE	Tris-EDTA
TEMED	tetramethyl-ethylenediamine
Thr	threonine
TK	thymidine kinase
TNFα	tumour necrosis factor α
TNFR1	tumour necrosis factor receptor 1
TPA	12-O-tetradecanoyl-phorbol-13-acetate
TPL-2	tumor progression locus 2
TRADD	TNFR-associated death domain
Tris	tris (hydroxymethyl) aminomethane
Tyr	tyrosine
UTR	untranslated region
UV	ultraviolet
V	volts
v/v	volume to volume
WT	wild-type
w/v	weight to volume
X. laevis	*Xenopus laevis*

ACKNOWLEDGEMENTS

I would like to thank my supervisor Dr. Catrin Pritchard both for giving me the opportunity to work with her and for her excellent guidance throughout my PhD. I would like to thank Martin who always had an answer to all of my questions. I would also like to thank both past and present members of lab 208 for their helpful input and of Gerry Cohen's lab members for their expert apoptosis help and advice. In addition I give thanks to Jane Brown for her micromanipulation expertise. I finally want to thank my darling Lee for his immense statistical knowledge and more importantly for being my rock.

ABSTRACT

Generation and analysis of mammalian cells containing various Raf mutations

Kathryn E. Mercer

The generation of a *raf-1* allele where the gene is flanked by two *lox*P sites ('floxed') in ES cells was described with the aim to enable the conditional deletion of *raf-1* in mice generated from the mutated ES cells. Two separate targeting vectors were designed that each harboured a *lox*P site flanked by homologous *raf-1* sequences, with one targeted to the 5' end of *raf-1* and the other targeted to the 3' end of *raf-1*. These vectors were used for gene targeting and eight ES cell clones were identified that had undergone homologous recombination with both targeting vectors. These ES clones were used to generate chimaeric mice and germline transmission was achieved from one of the targeted ES cell clones. A Cre expression plasmid was used to successfully mediate the deletion of the *raf-1* floxed gene in ES cells.

The role of A-Raf and Raf-1 in cell growth and survival was investigated by using primary mouse embryonic fibroblasts that either lacked A-Raf, Raf-1, or that contained a mutation of the two endogenous tyrosine residues at 340/341 of Raf-1 to phenylalanine residues (RafFF) which result in undetectable kinase activity towards MEK. No differences were observed with growth and proliferation of the A-Raf deficient, Raf-1 deficient or RafFF MEFs as compared with wild-type MEFs. An increased susceptibility of the Raf-1 deficient MEFs to undergo apoptosis was observed upon treatment with etoposide and upon treatment with an anti-CD95 antibody plus cycloheximide. However, the RafFF MEFs did not exhibit the same susceptibility to undergo apoptosis. These results suggest that Raf-1 has a role in cell survival that is independent from its role in the Ras/Raf/MEK/ERK cascade.

1 INTRODUCTION

1.1 Cell signalling

The ability of a cell to sense its own environment and respond to extracellular signalling molecules is essential for the correct functioning of multicellular organisms. Generally, extracellular signalling molecules interact with transmembrane receptors which transduce the signal across the plasma membrane. This causes the initiation of distinct intracellular signal transduction pathways that directly affect different kinds of cytoplasmic machinery or lead to the cell nucleus where they have an impact on gene transcription. Cell signalling is not only important for understanding the function of a normal cell, but is also of vital importance in understanding the growth and activity of an aberrant cell. It is the altered regulation of intracellular signalling events which is the precursor of cellular transformation.

1.1.1 Conserved signalling pathways

Mitogen-activated protein kinases (MAPKs) are important intermediates in signal transduction pathways that are initiated by many types of cell surface receptors. A common pathway that is activated by these diverse agents and exists in all eukaryotes, is a three-tiered protein kinase cascade known as the mitogen-activated protein kinase (MAPK) signalling cascade. This cascade involves MAPK kinase kinases (MAPKKK) that phosphorylate and activate a MAPK kinase (MAPKK) which in turn phosphorylate and activate a MAPK (Figure 1.1). The MAPK signalling cascade not only allows for signal amplification, but also allows for fine regulation of the activation of each of the cascade components.

An understanding of MAPK signalling has arisen by its analysis in lower organisms, especially yeast. For example, in *Saccharomyces cerevisiae*, there are five MAPK pathways involved in mating, cell wall remodelling, nutrient deprivation, and responses to stress stimuli such as osmolarity changes. Each of the three MAPK cascade components of the yeast pathways have conserved counterparts in mammalian cells. In the case of the mating pathway in *S. cerevisiae*, the MAPKKK is Ste11 (Stevenson *et al.*, 1992), the

MAPKK is Ste7 (Cairns *et al.*, 1992), and the MAPKs are Fus3 and Kss1 (Gartner *et al.*, 1992).

1.1.2 Multiple MAPK pathways exist in mammalian cells

Similar to yeast, multiple MAPK pathways exist in mammalian cells that are each activated by distinct stimuli, although some cross talk between the pathways does appear to exist. Mammals express at least four distinctly regulated groups of MAPKs: extracellular signal-regulated kinase 1/2 (ERK1/2), c-Jun N-terminal kinase 1/2/3 (JNK1/2/3), p38 α/β/γ/δ MAPK and ERK5. Each are activated by specific MAPKKs: MAPK/ERK kinase 1/2 (MEK1/2) for ERK1/2 (Seger *et al.*, 1992b; Zheng and Guan, 1993), MAPK kinase 3/6/4 (MKK3/6/4) for p38MAPKs (Derijard *et al.*, 1995; Han *et al.*, 1996; Moriguchi *et al.*, 1996), MKK4/7 for JNKs (Sanchez *et al.*, 1994; Derijard *et al.*, 1995; Lin *et al.*, 1995; Gerwins *et al.*, 1997) and MEK5 for ERK5 (Kato *et al.*, 1997). Each MAPKK can be activated by more than one MAPKKK. Raf (Kyriakis *et al.*, 1992), MEK kinase (MEKK) (Lange-Carter *et al.*, 1993), Mos (Pham *et al.*, 1995) and Tumor progression locus 2 (Tpl-2) (Salmeron *et al.*, 1996) can activate MEK1/2. MEKK (Yan *et al.*, 1994), apoptosis signal regulating kinase 1 (ASK1) (Ichijo *et al.*, 1997), mixed lineage protein kinase (MLK) (Rana *et al.*, 1996), transforming growth factor beta-activated kinase 1 (TAK1) (Wang *et al.*, 2001) and tumour progression locus-2 (TPL-2) (Salmeron *et al.*, 1996) can activate MKK3/6/4/7. Finally, MEKK3 can activate MEK5 (Chao *et al.*, 1999) (Figure 1.1). This therefore allows a diversity of inputs to activate the various MAPK pathways. Along with the regulation of enzyme activation, other key components of signal transduction pathways include adaptor, scaffold and anchor proteins which enable the formation of large multiprotein signalling complexes.

The ERKs are predominantly activated by mitogenic stimuli. Their substrates include transcription factors such as Elk-1 (Marais *et al.*, 1993), Nuclear factor for IL-6 expression (NF-IL6) (Nakajima *et al.*, 1993) also known as CCAAT/enhancer-binding protein β (C/EBPβ), activating transcription factor 2 (ATF2) (Abdel-Hafiz *et al.*, 1992) and c-Myc (Seth *et al.*, 1992) and other protein kinases such as the p90 ribosomal S6 kinase family ($p90^{RSK}$) (Sturgill *et al.*, 1988) also known as MAPK activated protein kinase-2 (MAPKAP

Fig. 1.1. The MAPK modules that exist in mammalian cells.

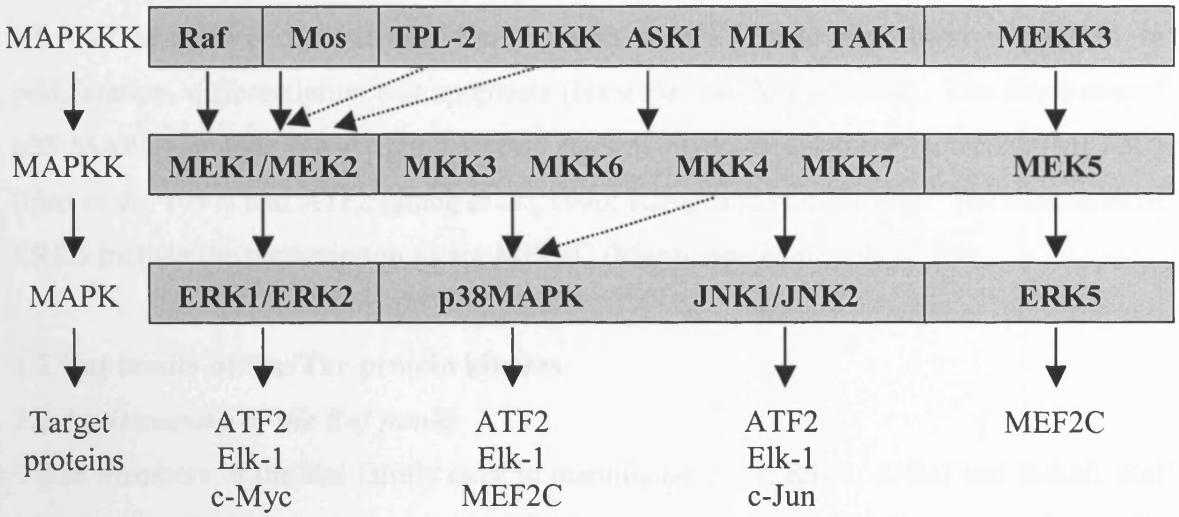

kinase-2). The JNK family is activated in response to stress conditions such as ultraviolet (UV) irradiation (Derijard *et al.*, 1994), changes in osmolarity and temperature (Galcheva-Gargova *et al.*, 1994) and in response to pro-inflammatory cytokines such as tumour necrosis factor-α (Sluss *et al.*, 1994). JNKs have also been implicated in apoptosis (Xia *et al.*, 1995; Tournier *et al.*, 2000). The substrates of activated JNKs include transcription factors such as c-Jun and ATF2 (Derijard *et al.*, 1994; Gupta *et al.*, 1995). The p38 MAPK family is also activated in response to stress conditions and pro-inflammatory cytokines (Han *et al.*, 1994; Lee *et al.*, 1994). p38 MAPKs have also been implicated in proliferation, differentiation and apoptosis (Nebreda and Porras, 2000). The substrates of p38 MAPKs include transcription factors such as myocyte enhancer factor-2C (MEF2C) (Han *et al.*, 1997) and ATF2 (Jiang *et al.*, 1996; Raingeaud *et al.*, 1996). The substrates of ERK5 include the transcription factor MEF2C (Marinissen *et al.*, 1999).

1.2 Raf family of Ser/Thr protein kinases

1.2.1 Discovery of the Raf family

Three members of the Raf family exist in mammalian cells; Raf-1, A-Raf and B-Raf. Raf kinases were first discovered as gain of function mutants with the ability to transform cells oncogenically. The mammalian *raf-1* gene was first identified as the cellular homologue of *v-raf*, the transforming gene of the 3611-murine sarcoma virus (Rapp *et al.*, 1983). *v-raf* was shown to transform fibroblasts and epithelial cells *in vitro* and cause the induction of fibrosarcomas in new-born mice (Rapp *et al.*, 1983). Subsequently, the *v-mil* oncogene of the avian retrovirus MH2 was identified as being the avian homologue of *v-raf* (Sutrave *et al.*, 1984). Both viruses express the *mil/raf* oncogene product as a gag-fusion protein. *A-raf* was originally discovered through the screening of a mouse spleen DNA library using the *v-raf* sequence as the probe (Huleihel *et al.*, 1986). *B-raf* was identified by homology to the avian homologue v-R*mil* (Marx *et al.*, 1988) and as the transforming gene isolated from NIH 3T3 cells transformed with human Ewing sarcoma DNA (Ikawa *et al.*, 1988). It became apparent that the amino-terminal portions of the gene products of the Raf family of proto-oncogenes have a regulatory role which acts to suppress Raf-1 kinase activity, as loss of this sequence results in deregulation of the carboxyl-terminal kinase domain and hence cellular transformation.

1.2.2 Discovery of Raf homologues in other organisms

The Raf kinases are evolutionarily highly conserved, a fact that facilitated the isolation of homologues in other organisms except yeast. A role for the Raf protein in a variety of developmental processes in other organisms is well established. The single *Drosophila melanogaster raf* gene, *Draf*, is involved in the determination of the dorsoventral polarity of the egg (Brand and Perrimon, 1994), the formation of the terminal structures of the larva (Ambrosio *et al.*, 1989), and the specification of the R7 photoreceptor (Dickson *et al.*, 1992). *lin-45* is the *raf* homologue in *Caenorhabditis elegans*; this gene is essential for differentiation of the vulva and it appears to act downstream of Ras (*let-60*) in this pathway (Han *et al.*, 1993). The Raf homologue in *Xenopus laevis* is essential for fibroblast growth factor induced differentiation of mesoderm (MacNicol *et al.*, 1993). Therefore it was apparent that Raf played a key role in cell differentiation in various organisms.

1.2.3 Expression of the three Raf isoforms

All three Raf isoforms are ubiquitously expressed in the mouse as determined by the detection of mRNA transcripts, however the levels of expression vary enormously (Storm *et al.*, 1990). A-Raf protein is highly expressed in components of the male reproductive tract such as the epididymis and seminal vesicles. High levels of A-Raf are also detected in testis, ovary, uterus, bladder, and kidney. A number of nonurogenital tissues also express significant levels of A-Raf, including liver, heart, intestine, spleen, thymus and cerebellum. Both the cerebral cortex and skeletal muscle express barely detectable amounts of A-Raf (Luckett *et al.*, 2000). *B-raf* RNA is highly expressed in neural tissues such as the brain and spinal cord. *B-raf* RNA is also highly expressed in the testis and spleen. Other tissues such as skeletal muscle and lung are found to express relatively low amounts of *B-raf* transcripts, furthermore B-Raf proteins can only be detected in cell lines of a neuronal origin such as in the rat pheochromocytoma PC12 cell line (Storm *et al.*, 1990; Barnier *et al.*, 1995). Raf-1 is ubiquitously expressed in all tissues and cell lines tested (Storm *et al.*, 1990) and because of this, most studies of the Raf proteins have focused on Raf-1.

1.2.4 Comparison of the structure of the three Raf isoforms

Amino-terminal truncations of the Raf proteins result in their constitutive activation and ability to transform NIH3T3 cells. The minimal transforming sequence was identified as the kinase domain (Beck *et al.*, 1987; Stanton and Cooper, 1987; Ikawa *et al.*, 1988; Stanton *et al.*, 1989; Heidecker *et al.*, 1990). This means that the amino-terminus normally serves a regulatory function to suppress the activity of the carboxy-terminal kinase domain. Moreover, when the kinase domain and the regulatory domain are expressed as separate proteins, the regulatory domain suppresses the biological and enzymatic activity of the catalytic domain (Cutler *et al.*, 1998). All three Raf proteins share three highly conserved regions (CR1, CR2 and CR3) embedded in variable sequences with the variable sequences differing greatly between the three Raf proteins (Bonner *et al.*, 1986; Beck *et al.*, 1987; Sithanandam *et al.*, 1990; Figure 1. 2). In Raf-1, CR1 encompasses residues 62-194 and contains two domains that have been reported to bind to Ras-GTP; the Ras binding domain (RBD) which spans residues 51-131 of Raf-1 (Vojtek *et al.*, 1993; Scheffler *et al.*, 1994) and the cysteine rich domain (CRD) which spans residues 139-184 of Raf-1 (Mott *et al.*, 1996). CR1 also contains a putative zinc binding domain (Beck *et al.*, 1987; Ghosh *et al.*, 1994). CR2 encompasses residues 229-254 of Raf-1 and is rich in serine and threonine residues, some of which are regulatory phosphorylation sites. Two domains, CR1 and CR2 constitute the regulatory domain of Raf, which serves to suppress Raf kinase activity in unstimulated cells and reverse this inhibition when cells are stimulated. CR3 encompasses residues 330-627 of Raf-1 and contains the kinase domain which is the most homologous domain between the Raf proteins (Daum *et al.*, 1994; Morrison and Cutler, 1997).

In the mouse, different sizes of B-Raf proteins have been identified. For example, in the PC12 cell line, B-Raf is observed as a 95 kDa protein (Stephens *et al.*, 1992) whereas in mouse testis two B-Raf proteins of 75 kDa and 77 kDa can be identified (Sithanandam *et al.*, 1990). B-Raf differs from the other Raf proteins because the region in between CR2 and CR3 is subjected to alternative splicing of two exons (exon 8b and exon 10) and results in the synthesis of four distinct isoforms (Barnier *et al.*, 1995). In addition exons 1 and 2 are present in some B-Raf proteins but not in others (Barnier *et al.*, 1995). At least 10 isoforms of B-Raf have been identified in adult mouse tissues which means additional alternative splicing events occur within *B-raf* (Barnier *et al.*, 1995). It has been proposed

Fig. 1.2 Comparison of the domain structure of the three Raf family members highlighting the three conserved regions (CR1, CR2 and CR3). Within the CR1 domain is the Ras binding domain (RBD) and the cysteine rich domain (CRD). These are the two interaction sites for Ras.

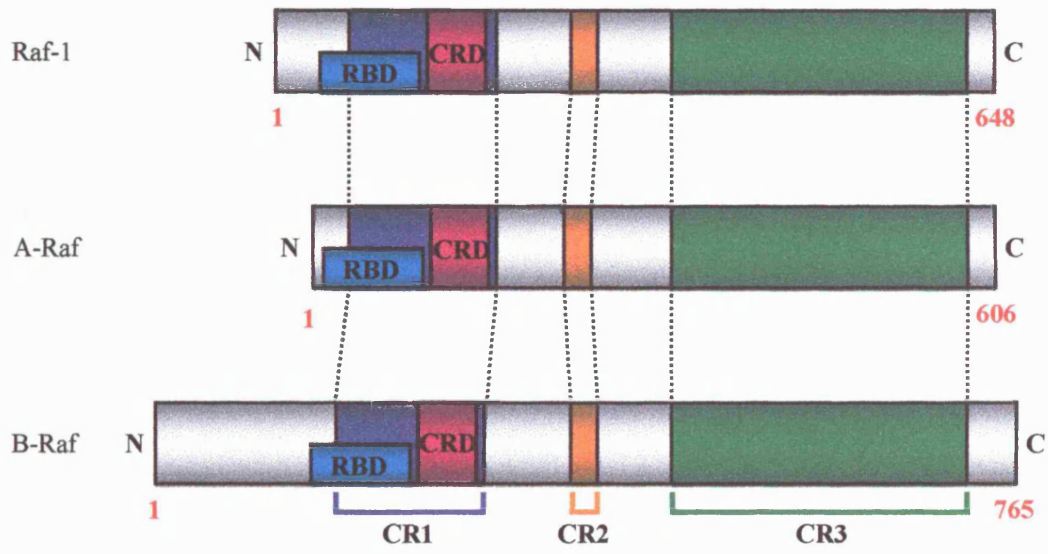

that the alternative splicing of exon 8b and exon 10 present in *B-raf* influences its kinase activity and therefore suggests that B-Raf is probably regulated in a different way to A-Raf and Raf-1 (Papin *et al.*, 1998).

1.3 Activation of Raf proteins

1.3.1 Signalling through receptor tyrosine kinases

Receptors that regulate Raf kinases include members of the serpentine family that contain seven transmembrane helices, transmembrane receptor tyrosine kinase (RTKs), and cytokine receptors that regulate intracellular protein tyrosine kinases. Activation of these receptors leads to a large variety of biochemical events in which small GTPases play a crucial role. The events leading from RTKs to the activation of the Ras/Raf/MEK/ERK signal transduction cascade is the best understood at present and is shown in Figure 1.3. All RTKs such as the epidermal growth factor receptor (EGFR) and platelet derived growth factor receptor (PDGFR) are monomers that traverse the cell membrane once (except the insulin receptor family). RTKs are activated by ligand binding to the extracellular domain which induces dimerisation. Different ligands employ different strategies to induce the active dimeric state. Receptor dimerisation is further stabilised by receptor:receptor interactions (Heldin, 1995). Dimerisation of RTKs promotes tyrosine autophosphorylation of their cytoplasmic domains (Schlessinger, 1988; Lemmon and Schlessinger, 1994; Jiang and Hunter, 1999). Tyrosine autophosphorylation sites serve as binding sites for Src homology 2 (SH2) or phosphotyrosine binding (PTB) domains of a variety of signalling proteins, such as Grb2, resulting in the recruitment of signalling complexes at the plasma membrane. (Songyang *et al.*, 1993; Kavanaugh *et al.*, 1995). Grb2 can both interact with activated RTKs and associated adapter proteins such as Shc, Crk and Syp via its SH2 domain. Grb2 also interacts with the guanine nucleotide exchange factor (GNEF) Son of Sevenless (SoS). Therefore upon receptor activation, Grb2 recruits SoS to its target protein Ras which is located at the plasma membrane (Rozakis-Adcock *et al.*, 1993; Li *et al.*, 1994; Matsuda *et al.*, 1994). SoS activates Ras by promoting the exchange of bound GDP for GTP (Pawson, 1995; Bar-Sagi and Hall, 2000). Therefore, this cascade of protein-protein interactions transmits signals from autophosphorylated receptors to Ras in part by redistributing SoS to the plasma membrane where Ras is located (Aronheim *et al.*, 1994).

Fig. 1.3 Role of the Raf family in the transduction of signals received at the plasma membrane resulting in activation of the MAPK cascade and leading to altered patterns of gene expression and determination of cell fate.

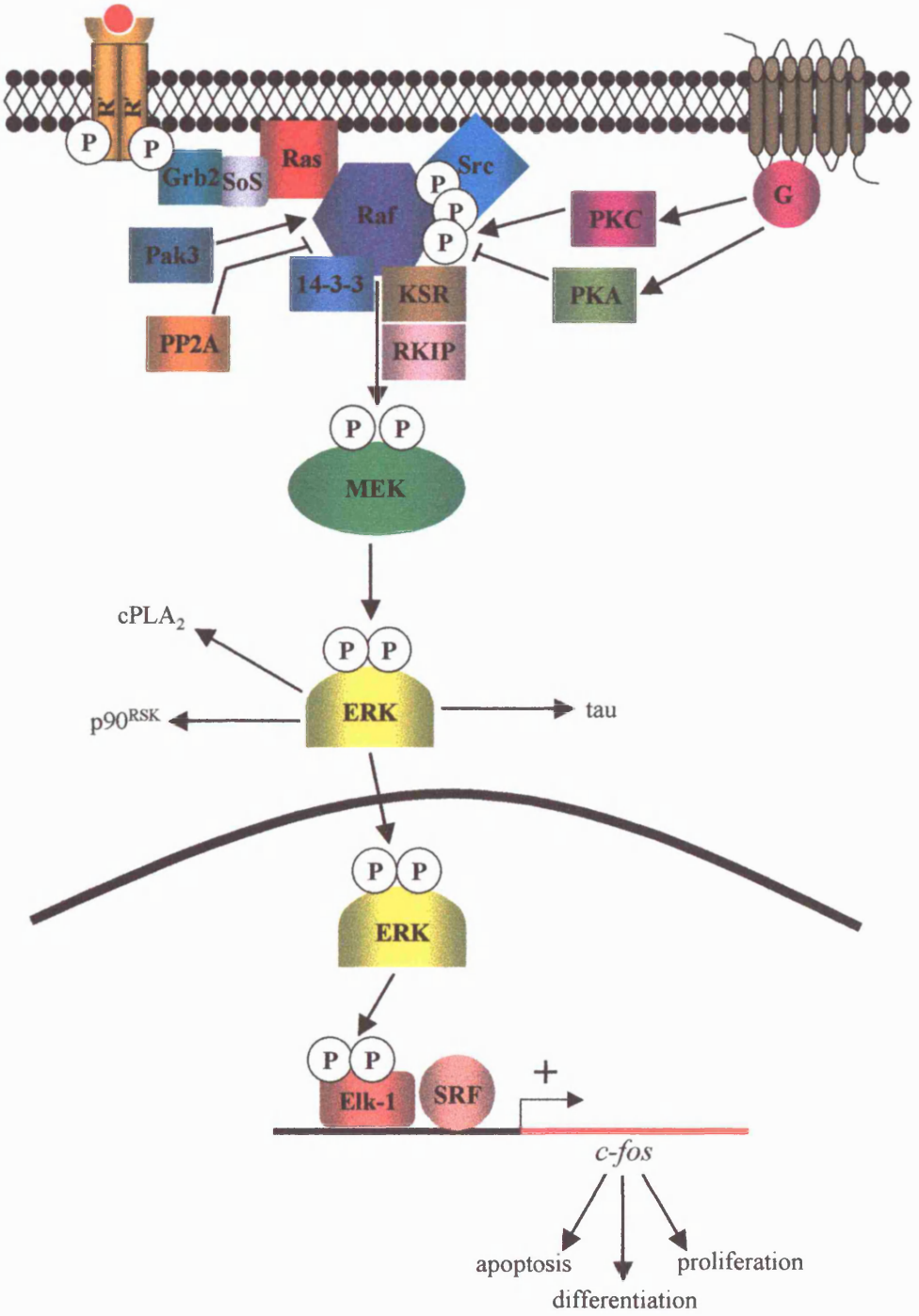

1.3.2 Activation of Ras

Five Ras proteins have been identified in human cells: Ha-ras, N-ras, Ki-ras 4A, Ki-ras 4B and R-ras. The two Ki-Ras proteins result from alternative splicing events. Mutations of *ras* genes have been found in 30% of human cancers including pancreatic, colon and lung cancers, although the incidence and the specific *ras* gene that is mutated varies considerably with the type of malignancy (Bos, 1989). It was these findings that linked Ras with the control of cell growth, along with the finding that activated Ras induced DNA synthesis and morphological transformation in NIH3T3 cells (Feramisco *et al.*, 1984; Stacey and Kung, 1984). Ras proteins are 21 kDa membrane associated guanine nucleotide binding proteins that function as molecular switches, cycling between a GDP-bound and a GTP-bound state. This process is tightly regulated by the activities of GNEFs such as SoS, which accelerate GTP loading and therefore activate Ras (Bar-Sagi, 1994), and GTPase-activating proteins (GAPs) such as p120GAP and Neurofibromin which stimulate the intrinsic weak GTP-ase activity of Ras therefore inactivating Ras (Lowy *et al.*, 1991). The GTP-bound form of Ras is active as it results in a conformational change resulting in the exposure of its effector domain (residues 32-40) which is the region to which the effectors of Ras bind (Boguski and McCormick, 1993; Schlessinger, 1993).

1.3.3 Downstream of Ras

The best characterised protein that is activated by Ras is Raf-1. Others include A-Raf and B-Raf, members of the Ral-GNEF family (Wolthuis *et al.*, 1998) and phosphoinositide 3-kinase (PI3-K) (Rodriguez-Viciana *et al.*, 1994). Ral-GNEFs (Ral-GDS, Rgl and Rlf) exhibit exhange activity towards the small GTPases RalA and RalB (Murai *et al.*, 1997; Urano *et al.*, 1996; Wolthuis *et al.*, 1997). PI3-K catalyses the phosphorylation of phosphoinositides at the D3 position. These PI3-K generated phospholipids then elicit a diverse set of cellular responses, including the regulation of the Ser/Thr kinase Akt which has been implicated in cell survival signalling (Burgering and Coffer, 1995; Datta *et al.*, 1996) and possibly the regulation of Rac GNEFs that are implicated in cytoskeletal organisation (Hawkins *et al.*, 1995).

1.3.4 *Interaction of Raf with Ras*

Most studies of the Raf family have focussed on Raf-1 in particular. Raf-1 was first implicated as an essential cofactor in Ras-induced cellular transformation (Kolch *et al.*, 1991) and it was thought to function downstream of Ras because dominant negative mutations of Raf-1 blocked proliferation and transformation induced by an activated form of Ras (Rapp, 1991). Moreover, hyperphosphorylated Raf-1 was observed in cells treated with agonists that were known to activate Ras, and in cells containing the activated Ras oncogene itself (Morrison *et al.*, 1988; Wood *et al.*, 1992).

Using *in vitro* protein binding assays and the *in vivo* yeast two-hybrid system, a direct physical interaction between Ras-GTP and the N-terminal region of Raf was observed by several groups (Koide *et al.*, 1993; Van Aelst *et al.*, 1993; Vojtek *et al.*, 1993; Warne *et al.*, 1993; Zhang *et al.*, 1993). Ras is reported to coimmunoprecipitate with Raf-1 from stimulated, but not unstimulated mammalian cells (Hallberg *et al.*, 1994). Ras specifically interacts with two domains in the amino terminal of Raf-1; the Ras binding domain (RBD; amino acids 51-131) and the cysteine-rich domain (CRD; amino acids 139-184) (Brtva *et al.*, 1995; Hu *et al.*, 1995). The strongest interaction is between Ras-GTP and the RBD of Raf-1 and was found to be essential for Raf-1 activation (Chuang *et al.*, 1994). The lower affinity interaction of Ras with the CRD of Raf-1 also appears to be essential in Raf-1 activation, as mutations that disrupt the structure of the CRD also reduce binding of Raf-1 to Ras *in vitro*, suggesting that both the RBD and CRD contribute to Raf-1 binding (Hu *et al.*, 1995; Drugan *et al.*, 1996; Luo *et al.*, 1997; Mineo *et al.*, 1997; Roy *et al.*, 1997). The CRD also binds to 14-3-3 (Michaud *et al.*, 1995; Clark *et al.*, 1997), zinc and phosphatidylserine (Ghosh *et al.*, 1994; Mott *et al.*, 1996).

1.3.5 *Ras is required to localise Raf-1 to the plasma membrane*

The interaction between Raf-1 and Ras is not sufficient for full Raf-1 activation, because Ras-GTP cannot activate Raf-1 *in vitro* unless Ras-GTP is membrane bound and an unidentified cytosolic factor is present (Traverse *et al.*, 1993; Zhang *et al.*, 1993; Dent and Sturgill, 1994; Stokoe and McCormick, 1997). Inactive Raf-1 is located in the cytosol in an inactive complex (Wartmann and Davis, 1994). In cells expressing oncogenic Ras it was found that Raf-1 translocates to the plasma membrane, suggesting that Ras-GTP

activates Raf-1 by altering its cellular distribution (Traverse *et al.*, 1993; Wartmann and Davis, 1994). This hypothesis was tested by examining the activity of a membrane-bound version of Raf-1 (RafCAAX) which was generated by fusing the Ki-Ras membrane localisation signals onto the carboxyl-terminal of Raf-1 (Leevers *et al.*, 1994; Stokoe *et al.*, 1994). RafCAAX is constitutively active, and can be further stimulated by epidermal growth factor (EGF). Moreover, both the constitutive and the ligand-stimulated activation of RafCAAX is independent of Ras activation, as it is not potentiated by oncogenic Ras or abrogated by dominant negative Ras (Leevers *et al.*, 1994; Stokoe *et al.*, 1994). These results suggest that the primary role of Ras in Raf-1 activation is to mediate translocation of Raf-1 from the cytosol to the plasma membrane, where it is fully activated by other membrane-localised events.

The dimerisation of Raf-1 is thought to be important for its activation. A Raf-1 mutant that undergoes oligomerisation upon the addition of a synthetic dimeriser FK1012A resulted in Raf-1 activation (Luo *et al.*, 1996). In addition, coumermycin-induced dimerisation of Raf-1 resulted in activation of the MAP kinase cascade (Farrar *et al.*, 1996).

1.3.6 Other Ras family members

Other members of the Ras family of small GTP binding proteins can interact with Raf proteins. These include TC21 which interacts with Raf-1 and B-Raf but not with A-Raf (Rosario *et al.*, 1999). It was shown that, like Ras, oncogenic TC21 can translocate these Raf proteins to the plasma membrane which results in their activation (Rosario *et al.*, 1999). Also Rap1A interacts with Raf proteins, but with differing effects on their activation. Rap1A not only is incapable of activating Raf-1, but also antagonizes Ras-dependent activation of Raf-1 (Cook *et al.*, 1993). However, Rap1A is capable of activating B-Raf (Ohtsuka *et al.*, 1996). Moreover, in PC12 cells, B-Raf activation induced by nerve growth factor (NGF) appears to be mediated by Rap1A rather than Ras (Vossler *et al.*, 1997; York *et al.*, 1998). This difference in activation of Raf-1 and B-Raf by Rap1A appears to be due to a difference in the strength of interaction between Rap1A and the CRD of each Raf protein, with the strongest interaction being with the CRD of Raf-1. A domain-shuffling experiment was performed whereby the CRD of Raf-1 was replaced by the CRD of B-Raf. This version of Raf-1 subsequently became activatable by

Rap1A. Also, the CRD of B-Raf was replaced by the CRD of Raf-1 and subsequently, this protein could not be activated by Rap1A. Therefore the difference in the CRD of Raf-1 and B-Raf appears to dictate the specific response to Rap1A (Okada *et al.*, 1999). The possibility that A-Raf binds to Rap1A has not been established.

1.4 Phosphorylations of Raf-1

Both phosphorylation and dephosphorylation events appear to be required for activation of Raf-1. For example, in unstimulated cells, Raf-1 is phoshorylated on serine 259 (Ser259) which acts as one of the two binding sites for 14-3-3 and inhibits the activity of Raf-1 (Morrison *et al.*, 1993; Clark *et al.*, 1997). Whereas in stimulated cells, after Raf-1 has been recruited to the plasma membrane by Ras, distinct serine/threonine and tyrosine phosphorylation events appear to be involved in the activation of Raf-1 (Figure 1.4.). Candidate kinases thought to be involved in phosphorylating Raf-1 include; Src family members, PKC, Pak and PKA.

1.4.1 Tyr341 phosphorylation

The *src* gene product of the Rous sarcoma virus (v-Src) is a membrane associated protein tyrosine kinase with a constitutively active kinase activity that transforms cells in culture and induces tumours in animals (Jove and Hanafusa, 1987). When a v-Src transformed cell line was transfected with a Raf-1 dominant negative mutant, the cells reverted to a non-transformed phenotype preventing their growth in soft agar (Qureshi *et al.*, 1993). Moreover, expression of dominant negative mutants of MEK-1 also block transformation induced by v-Src (Cowley *et al.*, 1994). Therefore signalling through Raf-1 and the MAP kinase pathway is necessary for transformation by v-Src.

Overexpression studies have shown that the expression of Raf-1 alone has relatively low activity as assayed by the phosphorylation of MEK. However when Raf-1 is co-expressed with either oncogenic Ras or v-Src a significant increase in Raf-1 phosphorylation occurs. Furthermore, when all three proteins are expressed, a synergistic activation of Raf-1 activity is observed (Williams *et al.*, 1992; Fabian *et al.*, 1993; Dent and Sturgill, 1994; Marais *et al.*, 1995). Raf-1 activation induced by v-Src is accompanied by the phosphorylation of two tyrosine residues 340 and 341 both *in vivo* and *in vitro*

Fig. 1.4 Domain structures of the three Raf family members indicating the positions of potentially important phosphorylation sites involved in the regulation of activation. Also indicated are the kinases/phosphatases thought to be responsible for the phosphorylation/dephosphorylation events.

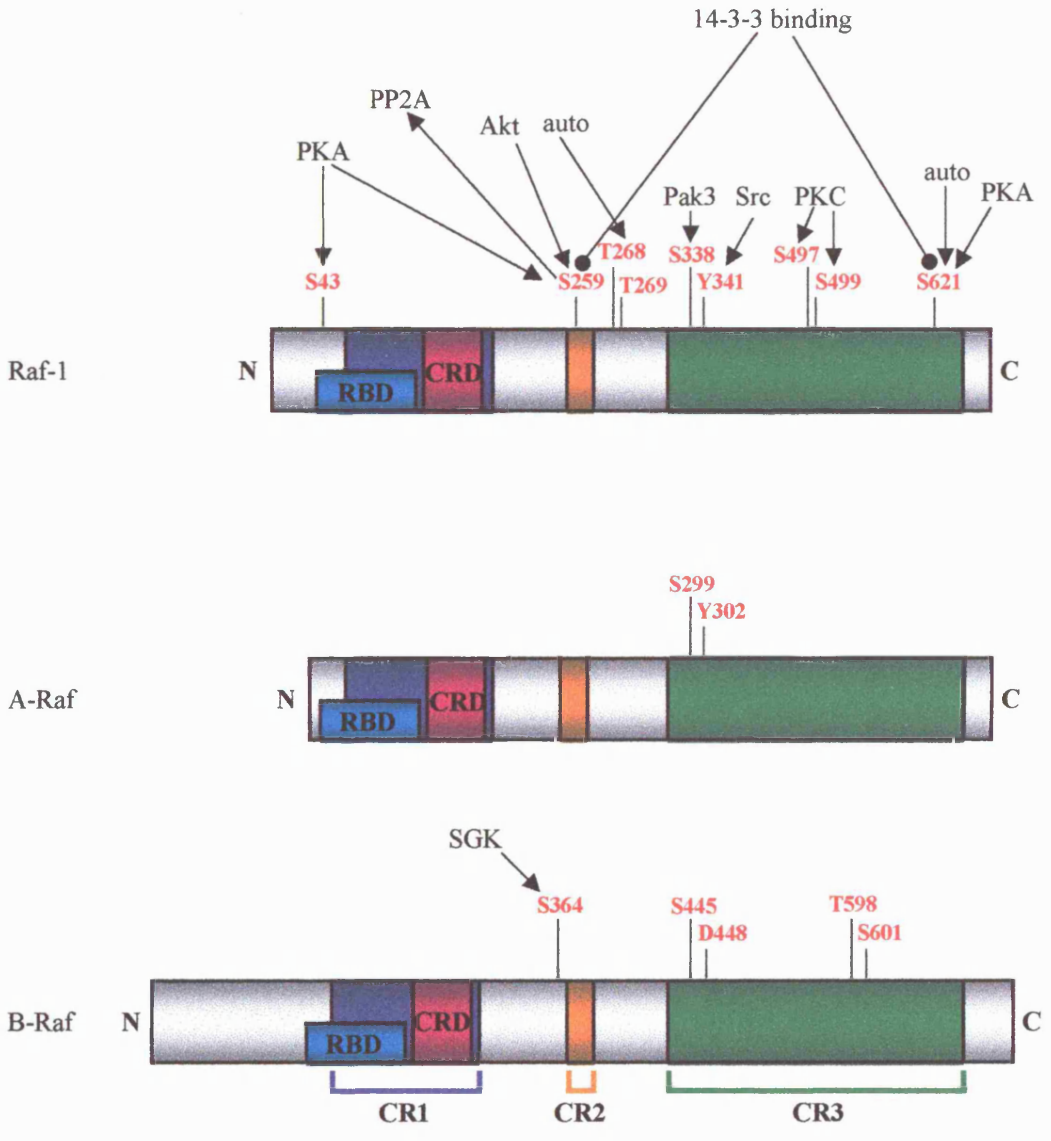

(Fabian *et al.*, 1993; Marais *et al.*, 1995). Mutation of these two tyrosine residues to phenyalanine residues, creating RafFF, prevents activation of Raf-1 by oncogenic Ras and v-Src, or by ligand stimulation (Fabian *et al.*, 1993; Marais *et al.*, 1995). Therefore it is proposed that Src is involved in the phosphorylation of Tyr340 and Tyr341 of Raf-1. Further experiments identified that the phosphorylation of Tyr341 by Src is a critical event in the activation of Raf-1 whereas the phosphorylation of Tyr340 is not essential (Mason *et al.*, 1999). Tyr341 is located at the very N-terminus of the catalytic domain, approximately 20 amino acids upstream of the putative ATP binding site. The equivalent tyrosines at this position are conserved in A-Raf (amino acids 301/302), and similar to Raf-1, the mutation of these two residues to phenylalanine residues prevents activation of A-Raf by oncogenic Src indicating that it may also be a substrate for Src-like kinases (Marais *et al.*, 1997). In contrast to Raf-1 and A-Raf, at the equivalent position in B-Raf are aspartic acid residues (amino acids 447/448). Aspartic acid residues mimic that of a phosphorylated residue due to the negative charge, and as a result B-Raf only requires Ras for maximal activation whereas Raf-1 and A-Raf require both Ras and Src for maximal activation (Marais *et al.*, 1997).

1.4.2 Ser338 phosphorylation

The phosphorylation of Ser338 of Raf-1 is stimulated by Ras and is essential for the activation of Raf-1 as it was shown that mutation of Ser338 to alanine diminishes Raf activation by Ras, Src and ligand stimulation. (Diaz *et al.*, 1997; Barnard *et al.*, 1998; Mason *et al.*, 1999). King *et al.* (1998) suggested that the p21-activated kinase 3 (Pak3) may be responsible for the phosphorylation of Ser338 *in vitro* and *in vivo* (King *et al.*, 1998). Pak-3 is a serine/threonine protein kinase that is activated by direct binding to the small G proteins Cdc42 and Rac which are in turn phosphorylated and activated by PI3-K, another well known effector of Ras (Bagrodia and Cerione, 1999; Daniels and Bokoch, 1999). Raf-1 mutants that are defective in Ras binding are readily activated by a constitutively active Ras mutant. This indirect activation of Raf-1 by Ras can be blocked by a dominant-negative mutant of Pak, implicating an alternative Ras effector pathway involved in Pak-mediated Raf-1 activation. Pak-mediated Raf-1 activation can be upregulated by both a selective activator of PI 3-kinase, and a constitutively active PI 3-kinase. In addition, a dominant negative mutant of the PI 3-kinase regulatory subunit can

inhibit the stimulated activity of Raf-1. Therefore, implying that Ras indirectly activates Raf-1 by activating Pak3 (Sun *et al.*, 2000). However, Chiloeches *et al.* (2001) argue against the involvement of Pak3 in Raf-1 activation as they show that PI3-K inhibitors can not prevent Ser338 phosphorylation indicating that PI3-K is not required for this event. Furthermore, Pak3 activation does not correlate with Ser338 phosphorylation as activated mutants of Pak3 are able to induce Ser338 phosphorylation but not Raf-1 activation (Chiloeches *et al.*, 2001).

The equivalent serine at this position is conserved in A-Raf (amino acid 299), but its effect on the activity of A-Raf has not been investigated. B-Raf also has a conserved serine at the position equivalent to Ser338 of Raf-1 (Ser445 in B-Raf). S445 is constitutively phosphorylated in B-Raf and this phosphorylation together with the Asp448 (equivalent to Tyr341 of Raf-1) is thought to contribute to the high basal kinase activity of B-Raf, with B-Raf basal kinase activity being 15-20 times that of either Raf-1 or A-Raf (Mason *et al.*, 1999).

In the proposed model, Ras activation results in the recruitment of Raf-1 to the plasma membrane where it is fully activated by phosphorylation of Tyr341 by Src-like kinases and by phosphorylation of Ser338 by Pak3 or an unidentified kinase. These phosphorylation events in CR3 are essential for Raf-1 regulation. However their precise role in Raf-1 regulation is unclear. They could either directly influence the catalytic activity of Raf-1 or they could act in concert with Ras to relieve the amino-terminal inhibition. The model for A-Raf activation is proposed to be similar to that of Raf-1. However, the model for the activation of B-Raf is different, as the basal kinase activity of B-Raf is 15-20 times that of either Raf-1 or A-Raf. However, Ras activation results in the recruitment of B-Raf to the plasma membrane which appears to fully activate B-Raf (Marais *et al.*, 1997; Mason *et al.*, 1999).

1.4.3 PKA, Rap1 and cAMP

Cyclic AMP (cAMP) is a major second messenger. Some of the hormones that have their cellular effects mediated by cAMP include glucagon, epinephrine and vasopressin. cAMP is produced from ATP at the plasma membrane by a family of membrane-bound adenylyl

cyclases (Taussig and Gilman, 1995). Hormone binding to the G-protein-coupled receptor stimulates exchange of bound GDP for GTP on the α-subunit of inactive heterotrimeric G proteins (Collins *et al.*, 1992). The α-GTP dissociates from the βγ components and activates the cyclase leading to the production of cAMP (Collins *et al.*, 1992). The elevation of cAMP levels in the cell correlates with the inhibition of Raf-1. It has been suggested that this effect is due to the activation of cAMP-dependent protein kinase A (PKA). However, the mechanism of this inhibition is not fully understood. Three different sites in Raf-1 have been implicated as PKA inhibitory phosphorylation sites; that of Ser43 (Morrison *et al.*, 1993; Wu *et al.*, 1993a), Ser621 (Hafner *et al.*, 1994; Mischak *et al.*, 1996) and recently Ser259 (Dhillon *et al.*, 2002b). Studies have shown that deletion of Ser43 does not prevent the cAMP-dependent inhibition of Raf-1 *in vivo* (Sidovar *et al.*, 2000; Dhillon *et al.*, 2002b). In addition, Ser621 is an autophosphorylation site required for 14-3-3 binding and Raf-1 activation (Thorson *et al.*, 1998). Therefore it seems unlikely that a phosphorylation site that is essential for Raf-1 activity would also be required for inhibition. Recent data gives evidence to suggest that Ser259 is the major target for inhibitory phosphorylation by PKA (Dhillon *et al.*, 2002b). Moreover, the mutation of Ser259 appears to enhance the affinity of Raf-1 towards Ras (Dhillon *et al.*, 2002a). The authors suggest that the phosphorylation of Ser259 affects the conformation of Raf-1, and its dephosphorylation is a major step towards its activation.

Rap1 is a small G-protein and two isoforms exist in humans; Rap1a and Rap1b (Pizon *et al.*, 1988). Rap1 can be activated by cAMP and is phosphorylated by PKA (Altschuler and Lapetina, 1993; Altschuler *et al.*, 1995). A constitutively active mutant of Rap1 when expressed in rat-1 fibroblasts interferes with ERK activation in response to EGF and LPA (Cook *et al.*, 1993). In contrast, Rap1 activates the ERKs in PC12 cells despite Raf-1 being inhibited (Vossler *et al.*, 1997; York *et al.*, 1998). The difference between these two cell types is suggested to be due to B-Raf as its expression is much greater in PC12 cells, in addition B-Raf has been found to be activated by Rap1 *in vitro* (Ohtsuka *et al.*, 1996; Vossler *et al.*, 1997). The formation of a Rap1/B-Raf complex was observed in PC12 cells stimulated with NGF and cAMP (Vossler *et al.*, 1997; York *et al.*, 1998). This allows Ras-independent activation of the ERKs via B-Raf which leads to differentiation of PC12 cells

(Vossler *et al.*, 1997; York *et al.*, 1998). The effect of PKA or Rap1 on A-Raf has not been investigated.

1.4.4 PKC

Members of the protein kinase C (PKC) family, of which there are at least 11 members, are activated by the second messenger diacylglycerol (DAG). This lipid is derived from phosphatidyl inositol phosphate metabolism in response to a variety of cellular agonists operating through tyrosine-kinase-linked receptors and seven-transmembrane receptors (Liscovitch, 1992). PKCs are also activated by tumour-promoting phorbol esters such as 12-O-tetradecanoyl-phorbol-13-acetate (TPA) (Rapp, 1991). PKCα has been shown to directly phosphorylate Raf-1 both *in vitro* and *in vivo* on several sites, including Ser497 and Ser499 and this was found to be sufficient to activate the enzymatic function of Raf-1 *in vitro* and *in vivo* (Kolch *et al.*, 1993; Carroll and May, 1994). The mutation of Ser499 blocks Raf-1 activation by PKCα, but has no effect on Raf-1 activation by Ras and Src. Also, Raf-1 and PKCα co-operate in the transformation of NIH3T3 cells, and this is dependent on Ser499 (Kolch *et al.*, 1993). In three separate studies however, the loss of these sites is shown to have no effect on Raf-1 activation by PKC and Ras (Barnard *et al.*, 1998; Schonwasser *et al.*, 1998; Chong *et al.*, 2001). Instead, it is observed that the primary effect of phorbol ester treatment is to promote an increase in Ras-GTP which then activates Raf-1 by the same mechanisms as those utilized by EGF (Barnard *et al.*, 1998). Also, Raf-1 mutations that prevent its association with Ras block the activation of Raf-1 by PKC (Marais *et al.*, 1998). However, dominant negative Ras does not prevent Raf-1 activation by PKC. This indicates that Raf-1 activation by PKC involves Ras, but via a different mechanism than that which occurs downstream of activated receptor tyrosine kinases (Marais *et al.*, 1998).

1.4.5 B-Raf specific Phosphorylations

Thr598 and Ser601 have been identified as the additional major phosphorylation sites of B-Raf in response to oncogenic Ras and phosphorylation of these two residues is thought to be required for full activation (Zhang and Guan, 2000). The kinase responsible for these phosphorylation events has not been identified. The equivalent residues in Raf-1 and A-Raf are conserved but have not been identified as major phosphorylation sites.

In addition, the phosphorylation of Ser364 appears to negatively regulate B-Raf activity. The expression of Serum- and glucocorticoid-inducible kinase (SGK) prevents the activation of B-Raf in response to serum via the phosphorylation of Ser364. The mutation of Ser364 to alanine prevents this inhibition of B-Raf by SGK (Zhang *et al.*, 2001). Ser259 is the equivalent residue in Raf-1 which also serves as a negative regulatory site when phosphorylated.

1.5 Chaperones

Several chaperones have been reported to interact with Raf-1 including: 14-3-3 proteins, heat-shock protein of 90 kDa (Hsp90), p50 (Cdc37), Raf kinase inhibitor protein (RKIP), kinase suppressor of Ras (KSR), Suppressor of Ras-8 (Sur-8), FKBP65 and Bag-1. The interaction of Raf-1 with Hsp90 and p50 (Cdc37) is widely accepted. However its interaction with FKBP65 and Bag-1 has not been thoroughly investigated. These observations suggest that Raf-1 is part of a large signalling complex.

1.5.1 14-3-3

Members of the 14-3-3 family of proteins are highly conserved phosphoserine-specific adapter proteins which are ubiquitously expressed and assemble as dimers (Tzivion *et al.*, 2001). 14-3-3 proteins have been reported to interact with many signalling proteins and in many cases this causes the inactivation of the target protein by changing its subcellular localisation or protein associations (Tzivion *et al.*, 2001). Using both biochemical and genetic approaches 14-3-3 is able to bind to Raf-1 as identified by several groups (Fantl *et al.*, 1994; Freed *et al.*, 1994; Fu *et al.*, 1994; Irie *et al.*, 1994; Yamamori *et al.*, 1995). 14-3-3 has been reported to bind to at least two distinct phosphorylated sites of Raf-1; Ser259 in CR2 and Ser621 in CR3 (Morrison *et al.*, 1993; Morrison, 1995), although the role of 14-3-3 in Raf-1 activation is not fully understood. Mutation of Ser259 to alanine results in the constitutive activation of Raf-1, suggesting that the phosphorylation of this particular serine residue is inhibitory (Morrison *et al.*, 1993; Clark *et al.*, 1997). Moreover, Akt and PKA are reported to phosphorylate Ser259 which results in the inhibition of Raf-1 activity (Zimmermann and Moelling, 1999; Dhillon *et al.*, 2002b). The serine/threonine protein phosphatase 2A (PP2A) is reported to affect the phosphorylation state of Ser259 in macrophages. Use of the specific PP2A inhibitor prevents the full activation of Raf-1 by

CSF-1 which correlates with an increase in the phosphorylation status of Ser259 (Abraham *et al.*, 2000). This indicated that PP2A is required for full Raf-1 activation by dephosphorylating Ser259. The mutation of Ser621 to alanine results in a kinase inactive version of Raf-1, suggesting that the phosphorylation of this particular serine residue is required for Raf-1 activation. This residue has also been identified as an autophosphorylation site (Morrison *et al.*, 1993; Thorson *et al.*, 1998). There is conflicting data as to whether 14-3-3 contributes to the activation of Raf-1. Several groups report that 14-3-3 has a positive role in Raf-1 activation (Fantl *et al.*, 1994; Freed *et al.*, 1994; Irie *et al.*, 1994; Tzivion *et al.*, 1998), others have reported that it has no effect (Michaud *et al.*, 1995; Suen *et al.*, 1995), or that it has an inhibitory effect (Clark *et al.*, 1997; Rommel *et al.*, 1997). In reality 14-3-3 seems to play opposite roles in the activation of Raf-1.

A model for the activation of Raf-1 has been proposed by Kolch, 2000. It appears that in resting cells, dimeric 14-3-3 is required to maintain Raf-1 in an inactive conformation by binding to both phosphorylated Ser259 and Ser621. Upon stimulation, the active conformation of Raf-1 is stabilized as Ras-GTP destabilises the interaction of 14-3-3 with phosphorylated Ser259 (Rommel *et al.*, 1996) allowing protein phosphatase 2A to access this site and remove the phosphate (Abraham *et al.*, 2000). Thus as half of the 14-3-3 dimer is now free, it has been suggested that it binds to a new phosphoserine resulting in stabilisation of an active Raf-1 conformation (Tzivion *et al.*, 1998).

A-Raf has not been reported to bind to 14-3-3 proteins. However since the 14-3-3 binding sites are conserved in all three Raf proteins, the interaction is proposed to be similar. B-Raf was shown to interact with 14-3-3 proteins *in vitro* (Papin *et al.*, 1996). Through the analysis of four different cell types that all expressed similar amounts of 14-3-3 proteins, it was discovered that cAMP was inhibitory in cells where less 14-3-3 was associated with B-Raf than in cells where more 14-3-3 was associated with B-Raf. This observed cell type-specific inhibition of B-Raf can be prevented by overexpression of 14-3-3 proteins, whereas the expression of a dominant negative 14-3-3 mutant results in partial inhibition of B-Raf activity. The authors suggest that the amount of 14-3-3 associated with B-Raf may explain the tissue-specific effects of cAMP on B-Raf kinase activity, implying that 14-3-3 protects B-Raf from inhibition by cAMP (Qiu *et al.*, 2000).

1.5.2 Hsp90 and p50

The drug geldanamycin binds to Hsp90 and prevents its interaction with its binding partners (Schulte *et al.*, 1995). It is observed that treatment of cells with geldanamycin almost completely depletes cells of Raf-1 within a few hours by targeting the protein for degradation (Schulte *et al.*, 1995; Schulte *et al.*, 1997). The association of Raf-1 with Hsp90 is thought to be mediated by p50 (Cdc37) (Silverstein *et al.*, 1998; Grammatikakis *et al.*, 1999). Overexpression of a p50 mutant deficient in binding Hsp90 impairs growth factor stimulation of the ERK pathway in mammalian cells, whereas the co-expression of p50 in insect cells enhances both the basal and the Ras- and Src-induced activity of Raf-1 (Grammatikakis *et al.*, 1999). Thus, formation of a ternary Raf-1-p50-Hsp90 complex is crucial for Raf-1 activity and MAPK pathway signaling (Grammatikakis *et al.*, 1999). The p50-Hsp90 complex has been shown to associate with v-Src and other tyrosine kinases. Therefore p50 could potentially link Raf-1 to tyrosine phosphorylation (Kimura *et al.*, 1997). Moreover, MEK is also found in a high-molecular weight complex with p50 and Hsp90 leading to the possibility that p50 couples Raf-1 to MEK (Stewart *et al.*, 1999). It is postulated that the function of these chaperones is not simply to prevent degradation, but also to allow the recruitment of specific activators to allow signalling pathway specificity.

B-Raf is also found in a complex containing Hsp90 upon treatment of PC12 cells with NGF (Jaiswal *et al.*, 1996). However whether A-Raf exists in a complex with Hsp90 has not been investigated.

1.5.3 Sur-8

The *Caenorhabditis elegans* suppressor of Ras-8 (Sur-8) was isolated in a genetic screen for mutations that could suppress the multivulva phenotype that resulted from an activated *let-60* (Ras) mutation (Sieburth *et al.*, 1998). Sur-8 expression in mammalian cells enhances Ras- or EGF-induced Raf and ERK activation but has no effect on ERK activation induced by active Raf or MEK and therefore functions as a positive regulator of Ras signalling (Sieburth *et al.*, 1998). Sur-8 forms a ternary complex with Ras and Raf and its role may be as a scaffold that enhances Ras-MAP kinase signal transduction by facilitating the interaction between Ras and Raf (Li *et al.*, 2000).

1.5.4 KSR

Kinase Suppressor of Ras (KSR) was first identified by genetic studies performed in *D. melanogaster* and *C. elegans*. In both organisms, inactivating mutations in KSR suppress the phenotypic effects induced by activated Ras thereby functioning as a positive mediator of Ras signalling either upstream of or parallel to Raf-1 (Downward, 1995; Kornfeld *et al.*, 1995; Sundaram and Han, 1995; Therrien *et al.*, 1995). KSR has been shown to interact with several components of the MAP kinase cascade in mammalian cells, including Raf-1 (Michaud *et al.*, 1997), MEK1/2 and ERK1/2 (Yu *et al.*, 1998), plus 14-3-3, p50 (Cdc37) and Hsp90 (Stewart *et al.*, 1999). In light of the fact that KSR can interact with many proteins, that KSR kinase activity *in vitro* cannot be detected and that a version of KSR in which the kinase domain was removed was shown to stimulate Raf-1 activity (Michaud *et al.*, 1997; Stewart *et al.*, 1999), it was proposed that KSR functions as a scaffold protein to assemble a signalling complex in mammalian cells.

It has also been suggested that KSR is a ceramide-activated protein kinase that is able to phosphorylate Thr269 of Raf-1 in response to ceramide or tumour necrosis factor-α (Yao *et al.*, 1995; Zhang *et al.*, 1997). Furthermore, it was shown that the phosphorylation of this site by KSR was essential for Raf-1 activation *in vitro* and for optimal activation of Raf-1 by KSR in response to EGF stimulation *in vivo* (Xing and Kolesnick, 2001).

1.5.5 RKIP

An interaction between Raf-1 and Raf kinase inhibitor protein (RKIP) was identified in a yeast two hybrid screen (Yeung *et al.*, 1999). RKIP was also shown to bind to MEK1 and ERK2 *in vitro* and *in vivo* but did not bind to Ras. RKIP was shown by overexpression experiments to suppress the Raf/MEK/ERK pathway. Moreover it was shown to interfere with Raf-mediated proliferation and transformation by inhibiting Raf-1 (Yeung *et al.*, 1999). RKIP decreases the phosphorylation of MEK by Raf-1 *in vitro*, but does not inhibit ERK phosphorylation by MEK or Elk phosphorylation by ERK. In addition RKIP does not prevent MEK phosphorylation by MEKK-1 and it does not interfere with Raf-1 autophosphorylation. Taken together these data indicate that RKIP is a selective inhibitor of the activation of MEK by Raf-1. In effect it acts as a competitive inhibitor by dissociating the Raf-1-MEK complex (Yeung *et al.*, 2000). RKIP therefore appears to

function as a physiological regulator of ERK signalling whereby its overexpression blocks ERK-dependent processes such as gene transcription and cellular transformation, whereas lowering the levels of RKIP by using antisense RNA causes activation of the pathway (Yeung *et al.*, 1999).

1.6 Downstream of Raf

1.6.1 MEKs and ERKs

A link between Ras and activation of the ERKs was discovered by the expression of oncogenic Ras which resulted in activation of ERK1 and ERK2 (Leevers and Marshall, 1992; Wood *et al.*, 1992). Moreover, the use of a dominant negative Ras mutant prevented ERK activation in response to growth factor stimulation (de Vries-Smits *et al.*, 1992; Thomas *et al.*, 1992; Wood *et al.*, 1992). Therefore as Raf proteins functioned downstream of Ras, Raf appeared to be the kinase responsible for activating the ERKs. It was shown that ERK2 was activated in *v-raf* transformed cells, and in cells transfected with activated Raf-1. This was found to be independent of Ras as shown by using a dominant negative mutant of Ras (Dent *et al.*, 1992; Howe *et al.*, 1992).

MEK1 and MEK2 were identified as dual specificity serine/threonine and tyrosine kinases as they are capable of specifically phosphorylating ERK1/2 on regulatory tyrosine and threonine residues (Payne *et al.*, 1991). Moreover, MEK1 and MEK2 were found to become activated in response to serum (Crews and Erikson, 1992; Nakielny *et al.*, 1992; Seger *et al.*, 1992b; Wu *et al.*, 1993b; Zheng and Guan, 1993).

MAPK/ERK kinase (MEK) is the only commonly accepted downstream substrate for the three Raf proteins. Two different MEK cDNAs (MEK1 and MEK2) were cloned from mouse, rat, human and *Xenopus* (Seger *et al.*, 1992c; Wu *et al.*, 1993b; Zheng and Guan, 1993). All three Raf isoforms are able to phosphorylate and activate MEK1 (44kDa) and MEK2 (45kDa) *in vitro* (Dent *et al.*, 1992; Howe *et al.*, 1992; Kyriakis *et al.*, 1992; Catling *et al.*, 1994; Pritchard *et al.*, 1995; Reuter *et al.*, 1995). However, data from one group suggest that A-Raf can only phosphorylate and activate MEK1, but not MEK2 (Wu *et al.*, 1996). Although Raf isoforms are the predominant MEK activators, MEKK-1 [Lange-Carter *et al.*, 1993), Mos (Pham *et al.*, 1995) and Tpl-2 (Salmeron *et al.*, 1996) can also

phosphorylate and activate MEK1 and MEK2. MEK1 is activated by phosphorylation of two serine residues at positions 218 and 222 present in the activation loop (Alessi *et al.*, 1994; Yan and Templeton, 1994; Zheng and Guan, 1994). MEK1 and MEK2 contain a proline rich sequence that is thought to be required for recognition and activation by Raf proteins (Catling *et al.*, 1995). This sequence is not present in other MAPKKs and therefore is a basis for specific signalling from Raf proteins to MEK1/2 rather than to MKK4 (activator of JNK and p38MAPK) for example (Catling *et al.*, 1995).

A striking biochemical difference between the three Raf isoforms is in their abilities to phosphorylate and activate MEK, their most widely accepted substrate. It is evident that B-Raf activates MEK to a much greater extent than Raf-1, and subsequently Raf-1 activates MEK to a greater extent than A-Raf. In fact A-Raf activity towards MEK is barely detectable (Pritchard *et al.*, 1995; Marais *et al.*, 1997; Papin *et al.*, 1998; Huser *et al.*, 2001). These differing abilities of the Raf isoforms to activate MEK could have profound implications on cell proliferation and cell cycle arrest (discussed in Section 1.5).

Two different ERK isoforms exist in mammalian cells; p44 and p42 MAPK or ERK1 and ERK2 respectively. ERK1 and ERK2 are activated by phosphorylation of a threonine and tyrosine residue in the sequence -Thr-Glu-Tyr- by MEK which displays a high substrate selectivity towards ERK and are the only identified ERK activators (Crews *et al.*, 1991; Matsuda *et al.*, 1992; Nakielny *et al.*, 1992; Seger *et al.*, 1992a). The phosphorylation sites have been mapped to Thr183 and Tyr185 in ERK2 (Payne *et al.*, 1991). The ERKs are serine/threonine protein kinases that recognise a minimal consensus sequence of Ser/Thr-Pro and have at least 50 substrates. The ERKs are located both in the cytosol and in the nucleus and translocation of the ERKs from the cytosol to the nucleus occurs after mitogen stimulation (Chen *et al.*, 1992; Sanghera *et al.*, 1992). Therefore the ERKs provide a physical link in the signal transduction pathway from the cytoplasm to the nucleus.

1.6.2 Downstream of ERKs

The ERKs phosphorylate and activate a wide variety of substrates including upstream protein kinases such as Raf-1 (Anderson *et al.*, 1991; Lee *et al.*, 1992) and MEK (Matsuda *et al.*, 1993). The function of this may be to serve as a feedback mechanism for the

upstream components that lead to the activation of the ERKs. p90 ribosomal S6 kinase ($p90^{RSK}$) also known as MAPKAP kinase-2 is phosphorylated and activated by the ERKs (Sturgill *et al.*, 1988). $p90^{RSK}$ is able to translocate to the nucleus (Chen *et al.*, 1992) where it has been reported to phosphorylate and activate several transcription factors such as c-Fos (Chen *et al.*, 1993) and serum response factor (Rivera *et al.*, 1993). The ERKs phosphorylate cytoskeletal proteins such as tau which is a microtubule associated protein (Drewes *et al.*, 1992) leading to the regulation of cytoskeletal rearrangements and cellular morphology. The ERKs phosphorylate cell membrane enzymes such as the EGF receptor (Northwood *et al.*, 1991; Takishima *et al.*, 1991) and cytoplasmic phospholipase A_2 ($cPLA_2$) (Lin *et al.*, 1993; Nemenoff *et al.*, 1993). The phosphorylation of $cPLA_2$ causes an increase in its enzymatic activity resulting in an increased arachidonic acid release and formation of lysophospholipids from membrane phospholipids (Lin *et al.*, 1993). ERKs can therefore trigger the formation of multiple secondary signalling pathways. The ERKs also phosphorylate transcription factors such as c-Myc (Alvarez *et al.*, 1991; Gupta *et al.*, 1993), NF-IL6 (Nakajima *et al.*, 1993), Elk-1 (Gille *et al.*, 1992; Marais *et al.*, 1993), Ets-2 (McCarthy *et al.*, 1995; McCarthy *et al.*, 1997), ATF-2 (Abdel-Hafiz *et al.*, 1992) and c-Jun (Pulverer *et al.*, 1991; Smeal *et al.*, 1991). The ERKs also influence cell shape and motility via interaction with integrins (Hughes *et al.*, 1997), activation of myosin light chain kinase (MLCK) (Klemke *et al.*, 1997) and activation of Calpain II (Glading *et al.*, 2000).

1.7 Other binding partners for the Raf proteins

Each of the Raf family members have been reported to interact with substrates other than MEK. A-Raf has been reported to interact with the β regulatory subunit of casein kinase 2 (CK2) using yeast two-hybrid assays and this binding was specific for A-Raf (Boldyreff and Issinger, 1997; Hagemann *et al.*, 1997). A-Raf was also shown to interact with hTOM and hTIM. These are novel proteins that are thought to be involved in mitochondrial transport implicating their involvement in the transport of A-Raf to the mitochondria where it was shown to be localised (Yuryev *et al.*, 2000). Raf-1 has been reported to interact with the antiapoptotic protein Bcl-2 (Wang *et al.*, 1994), Bag1 (Wang *et al.*, 1996b), KSR (Michaud *et al.*, 1997) and Cdc25 phosphatase (Galaktionov *et al.*, 1995). These interactions have been discussed in detail elsewhere in the chapter. Many more proteins

that interact with the Raf proteins have been identified (presented in the review by Kolch, 2000).

1.8 Proliferation

Growth factors stimulate the entry of quiescent cells into the cell cycle. The presence of growth factors is essential for the progression of cells through the G1 phase and past the restriction point at which cell cycle progression is independent of growth factor stimulation. This then allows entry into S phase which is when chromosome duplication occurs. This is followed by the G2 phase which is then followed by M phase which is when chromosome segregation plus cytokinesis occurs. There are many checkpoints during the cell cycle which each monitor the execution of a particular cell cycle event for example; DNA synthesis and spindle assembly. These safeguard against mistakes in cell duplication.

Progression through the initial phases of G1 appears to be regulated by Cyclins D1, D2 and D3 in conjunction with their catalytic partners, the cyclin-dependent protein kinases (Cdks), cdk4 and cdk6. The major target of these complexes is the retinoblastoma protein (pRb) (Kato *et al.*, 1993). At least in part, pRb is thought to control G1 progression by regulating the activity of the transcription factor E2 promoter binding factor (E2F). E2F activates the transcription of many genes necessary for DNA replication and is sequestered into an inactive complex by association with pRb (Nevins, 1992). CyclinD1-Cdk4 kinase complexes phosphorylate pRb during mid to late G1. Also, very close to the G1/S phase transition, cyclin E accumulates and specifically activates cdk2 which has a secondary role in the phosphorylation of pRb (Harbour *et al.*, 1999). Hyperphosphorylated pRb is unable to bind E2F, which enables free E2F to promote expression of genes necessary for entry into S phase. G1 progression depends on the sustained expression of D-type cyclins, which, in turn depends on continuous mitogenic stimulation up until the restriction point when E2F is released from Rb. Moreover, overexpression of D-type cyclins or cyclin E during early G1 leads to premature S phase entry (Ohtsubo and Roberts, 1993; Quelle *et al.*, 1993; Resnitzky *et al.*, 1994). Therefore, D-type cyclins provide a link between mitogen signalling and the cell-cycle machinery.

The cyclin-cdk complexes are targets for negative regulators referred to as cyclin-dependent kinase inhibitors (CKIs). Two classes of CKIs exist: the CDK-interacting protein/kinase-interacting protein (Cip/Kip) family ($p21^{WAF1/Cip1}$, $p27^{Kip1}$ and $p57^{Kip2}$) and the inhibitor of cyclin-dependent kinase 4 (INK4) family (p15, p16, p18 and p19) (Sherr and Roberts, 1999). Cip/Kip family members can inhibit both cyclin-D-Cdk4/6 kinases and cyclin-E/A-Cdk2 (Blain *et al.*, 1997). INK family members specifically inhibit cyclin-D-Cdk4/6 kinases (Sherr and Roberts, 1999).

1.8.1 Raf-1 and proliferation

A role for Raf-1 in cell proliferation was first indicated by experiments showing that the microinjection of Raf-1 protein was sufficient to induce DNA synthesis in quiescent cells (Smith *et al.*, 1990). Furthermore it was shown that antisense Raf-1 or kinase-defective Raf-1 interfered with the proliferation of NIH3T3 cells, whereas a constitutively active form of Raf-1 had an accelerated effect on proliferation (Kolch *et al.*, 1991; Miltenberger *et al.*, 1993). It was also shown that Raf-1 was both necessary and sufficient to activate a subset of early and late growth response genes (Miltenberger *et al.*, 1993).

1.8.2 The Ras/Raf/MEK/ERK cascade and proliferation

A direct connection between activation of the Ras/Raf/MEK/ERK cascade and transcriptional changes that are believed to induce cell proliferation has been demonstrated. The transcription of the prominent early response gene *c-fos* appears to be regulated by two proteins, the serum response factor (SRF) and Elk-1, which both bind to the promoter of the *c-fos* gene. This promoter is activated upon phosphorylation of Elk-1 by the ERKs (Treisman, 1996). c-Fos is one of the components of activating protein-1 (AP-1). AP-1 is a collective term referring to dimeric transcription factors composed of Jun, Fos or ATF family members that bind to a common DNA site, the AP-1 binding site which is found in the promoters of many genes, including the promoter of cyclin D1 (Angel and Karin, 1991; Albanese *et al.*, 1995). The abundance of AP-1 proteins is most commonly regulated by controlling the transcription of their genes as described for c-Fos, but can also be regulated by modulation of their stability, for example by preventing their degradation (Karin, 1995).

1.8.3 Use of inducible Raf proteins to investigate the role of Raf in proliferation

Detailed studies on the role of the Raf proteins in cell proliferation have been performed by using a system in which Raf-1 kinase activity could be rapidly and conditionally activated in mammalian cells. This was achieved by fusing the CR3 domain of each of the 3 Raf isoforms to the human hormone-binding domain of the estrogen receptor (hbER) (Figure 1.5) resulting in the creation of ΔRaf-1:ER, ΔB-Raf:ER and ΔA-Raf:ER (Samuels *et al.*, 1993; Pritchard *et al.*, 1995). In the absence of estradiol the hybrid proteins are maintained in an inactive state due to formation of a complex including Hsp90, which results in steric hindrance of other activities. Estradiol binding results in release of the Hsp90 complex and hence derepression leading to oncogenic activation of each of the Raf proteins (Picard, 1993). The addition of estradiol to quiescent 3T3 cells expressing either ΔRaf-1:ER or ΔB-Raf:ER does not allow cell cycle progression and inhibits the response of the cells to EGF and platelet derived growth factor (PDGF). Moreover ΔB-Raf:ER inhibits the mitogenic response of these cells to serum. In contrast, the addition of estradiol to quiescent 3T3 cells expressing ΔA-Raf:ER leads to cell cycle progression. Unlike the other Raf kinases, ΔA-Raf:ER has no effect on the mitogenic responses of cells to growth factor stimulation (Pritchard *et al.*, 1995). The reason for the different responses of the cells to the activation of the three Raf proteins is thought to be due to their differing abilities to activate MEK/ERK. All three Raf proteins, when activated, could activate MEK. However their individual efficiencies at doing so varied significantly, with ΔB-Raf:ER activating MEK to the greatest extent, ΔRaf-1:ER to a lesser extent, and ΔA-Raf:ER activating MEK to an even lesser extent (Pritchard *et al.*, 1995).

With the use of the estradiol regulated Raf proteins, further experiments were performed to analyse the regulation of various cell cycle proteins. It was found that all of the active forms of the Raf proteins induce cyclin D1 and cyclin E expression and cause a decrease in the expression of $p27^{Kip1}$ which is consistent with a positive effect on proliferation (Woods *et al.*, 1997). However, ΔRaf-1:ER and ΔB-Raf:ER strongly induced the expression of $p21^{Cip1}$ which is the probable cause of the observed cell cycle arrest, whereas ΔA-Raf:ER did not induce $p21^{Cip1}$ expression (Woods *et al.*, 1997). Moreover, the activation of the hybrid proteins was manipulated by adjusting the concentration of estradiol. It was concluded from these experiments that each of the Raf proteins could elicit either cell cycle

Fig. 1.5 Generation of a conditionally activated form of Raf. **(A)** Domain structure of Raf highlighting the three conserved regions (CR1, CR2 and CR3). **(B)** Fusion of the human binding domain of the estrogen receptor to the CR3 domain of Raf in which Raf only becomes activated upon the addition of estradiol.

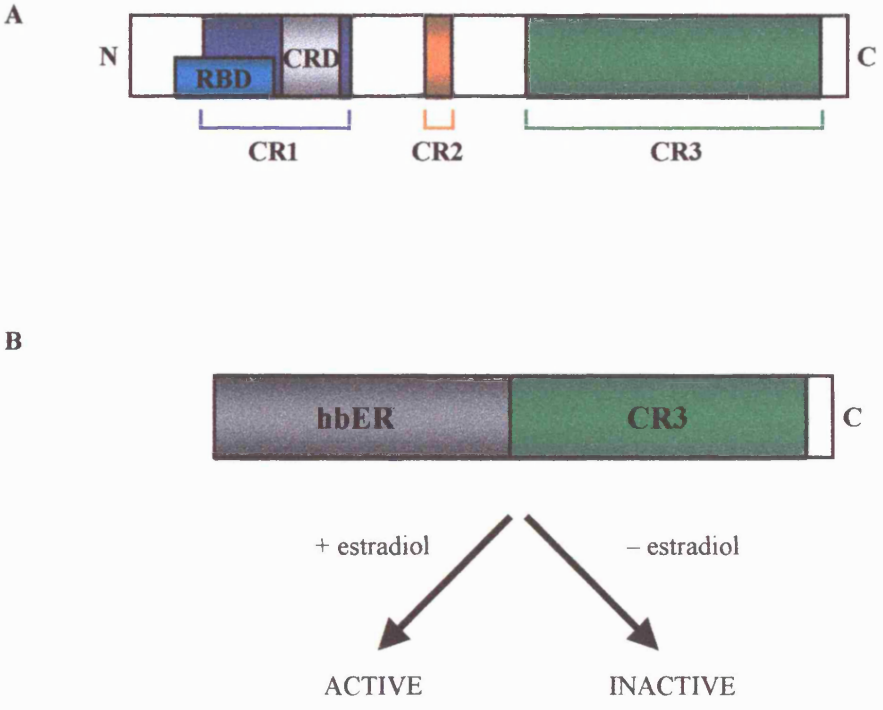

progression or cell cycle arrest depending upon the level of Raf kinase activity, with low levels of Raf activity eliciting cell cycle progression and high levels of Raf activity eliciting cell cycle arrest (Woods *et al.*, 1997). The activation of ΔRaf-1:ER in $p21^{Cip1-/-}$ MEFs led to a robust mitogenic response, supporting the theory that $p21^{Cip1}$ is involved in Raf-induced cell cycle arrest and by the use of $p53^{-/-}$ MEFs it was shown that the induction of $p21^{Cip1}$ was independent of p53 (Sewing *et al.*, 1997; Woods *et al.*, 1997). Therefore the induction of $p21^{Cip1}$ and consequently cell cycle arrest requires high levels of signalling through the Raf/MEK/ERK signalling pathway whereas cell cycle progression requires low levels of signalling through the Raf/MEK/ERK signalling pathway to prevent $p21^{Cip1}$ induction in NIH3T3 cells.

1.9 Differentiation

One of the most studied differentiation systems in culture is that of the rat pheochromocytoma cell line (PC12 cells) in which both EGF and NGF activate the MAPK cascade. However, EGF treatment induces proliferation (Huff *et al.*, 1981) whilst NGF treatment induces differentiation into sympathetic neuron-like cells (Greene and Tischler, 1976; Qui and Green, 1992). It is thought that the difference between the EGF and NGF responses may be derived from differences in the duration of MAPK signalling (Qui and Green, 1992; Traverse *et al.*, 1992; Nguyen *et al.*, 1993). EGF and other mitogens promote the brief activation of the MAPK pathway, whereas NGF promotes the sustained activation of this signal transduction pathway (Qui and Green, 1992; Traverse *et al.*, 1992; Nguyen *et al.*, 1993). When the number of EGF receptors is increased in PC12 cells it changes their response to EGF, MAPK is sustained and the cells undergo differentiation rather than proliferation (Dikic *et al.*, 1994; Traverse *et al.*, 1994). The difference in strengths of signalling may be as a result of different rates of receptor downregulation, as the EGF receptor is downregulated much faster than the TrkA receptor (Countaway *et al.*, 1992).

These results are consistent with the findings that both oncogenic Ras and oncogenic Raf mimic the effect of NGF in stimulating neurite outgrowth (Bar-Sagi and Feramisco, 1985; Noda *et al.*, 1985; Wood *et al.*, 1993), as both of these oncoproteins produce prolonged activation of the ERKs (Leevers and Marshall, 1992). NGF treatment and thus sustained

ERK activation leads to nuclear translocation of ERK whereas EGF and thus transient ERK activation does not lead to nuclear translocation of ERK (Nguyen *et al.*, 1993; Dikic *et al.*, 1994). Therefore this difference in the nuclear translocation of ERK is probably the mechanism behind the different biological responses of PC12 cells to EGF and NGF as for example, it was observed that NGF stimulates the activation of Elk-1 more markedly than EGF (York *et al.*, 1998). It appears that in the case of PC12 cells the strength and duration of signals transmitted through the MAPK cascade are themselves sufficient to determine the responses of PC12 cells to stimuli, with prolonged MAPK signalling leading to differentiation and transient MAPK signalling leading to proliferation. These differences in strengths of signalling to the ERKs may be provided for by the different Raf isoforms. For example, NGF specifically activates B-Raf in PC12 cells. In addition this appears to be mediated by Rap1 which leads to sustained activation of the ERKs and differentiation (Vossler *et al.*, 1997; York *et al.*, 1998).

1.10 Cellular transformation

Oncogenes were first described as retrovirus-encoded genes that produced tumours in rodents and birds as was the case for the discovery of the Raf proteins. Most oncogenes discovered encode proteins that participate in the various signalling cascades through which growth factors stimulate normal cell division. However, no direct links have been observed between Raf and human cancers even though amino-terminal truncations of all three Raf proteins leads to cellular transformation. The main reason for studying the involvement of Raf proteins in cellular transformation is due to the fact that mutations of *ras* genes have been found in 30% of human cancers (Bos, 1989). Therefore the main role for Raf proteins in tumour cells is thought to be mediated by their participation in the Ras/Raf/MEK/ERK cascade.

1.10.1 Transforming abilities of the Raf proteins

A critical role for Raf-1 in oncogenic transformation of 3T3 cells by v-Ha-ras, v-Ki-ras (Kolch *et al.*, 1991) and v-src (Qureshi *et al.*, 1993) was demonstrated by inhibition studies using dominant negative and antisense RNA constructs, which serve to block transformation normally induced by these oncogenes. Also, constitutively activated mutants of all Raf proteins exhibit transforming activities in fibroblast transformation

assays, although A-Raf displays the weakest transforming ability compared to the other two Raf proteins (Pritchard *et al.*, 1995). This difference correlates with the individual abilities of the Raf proteins to activate MEK, with A-Raf activating MEK to a much lesser extent than B-Raf and Raf-1 (Pritchard *et al.*, 1995).

We recently assessed the ability of *A-Raf*$^{-/Y}$ and *A-Raf*$^{+/Y}$ mouse embryonic fibroblasts (MEFs) immortalised with the SV40T antigen and transfected with either Ras or Src oncogenes to undergo anchorage independent growth. No difference was observed in the ability of the *A-Raf*$^{-/Y}$ MEFs to form colonies in soft agar in comparison to *A-Raf*$^{+/Y}$ MEFs (Mercer *et al.*, 2002). This shows that A-Raf is not required for transformation with either of these two particular oncogenes, which possibly reflects its lack of a major involvement in the Ras/Raf/MEK/ERK pathway in MEFs.

As discussed, the ERKs provide a link between the cytoplasmic signalling cascade and transcription of genes controlling cellular proliferation, therefore the Ras/Raf/MEK/ERK cascade is an important mediator of activated oncogenes. Furthermore, the involvement of Raf-1 in promoting cell survival (see Section 1.11) has major consequences for the survival of aberrant cells and tumour progression.

1.10.2 The p53 tumour suppressor protein

The p53 gene is mutated in approximately 60% of all human tumours (Hollstein *et al.*, 1991). p53 is an important tumour suppressor protein that serves to maintain genomic integrity by arresting cell growth or inducing apoptosis in response to cellular stress, such as DNA damage (Lakin and Jackson, 1999). The p53 protein has a short half-life and is maintained at low levels in normal cells. Upon stimulation by cellular stress, p53 levels are transiently stabilized and it becomes active as a transcription factor to either promote apoptosis or arrest proliferation to allow DNA repair (Lakin and Jackson, 1999). The mdm2 protein, encoded by a p53-inducible gene, is a critical cellular antagonist of p53, as it binds directly to p53 which blocks its transcriptional activity and also targets p53 for degradation (Momand *et al.*, 1992; Haupt *et al.*, 1997; Kubbutat *et al.*, 1997). p53 itself is responsible for regulating the transcription of *mdm2* thus resulting in a negative feedback in which p53 regulates its own destruction (Barak *et al.*, 1993; Wu *et al.*, 1993c). It was

shown that mdm2 expression was controlled by the Ras/Raf/MEK/ERK cascade as the overexpression of Ras or the activation of ΔB-Raf:ER leads to the induction of *mdm2* transcription. However in wild-type cells, p53 levels were not affected (Ries *et al.*, 2000). The reason for this is that activation of the Ras/Raf/MEK/ERK cascade also induces the expression of $p19^{ARF}$ (Bates *et al.*, 1998; Palmero *et al.*, 1998). $p19^{ARF}$ inhibits mdm2 activity (Pomerantz *et al.*, 1998; Tao and Levine, 1999). Further experiments showed that in cells that lack functional $p19^{ARF}$, the activation of ΔB-Raf:ER leads to the induction of *mdm2* transcription and the subsequent degradation of p53 (Ries *et al.*, 2000). Therefore in normal cells the levels of p53 are determined by a balance between mdm2 and $p19^{ARF}$ expression induced by the Ras/Raf/MEK/ERK cascade. In tumours possessing activated Ras, mdm2 levels will be elevated which may lead to tumour progression via the prevention of p53 mediated apoptosis induction or growth arrest.

1.11 Apoptosis

Apoptosis is also known as programmed cell death. It is an essential physiological process required for the normal development and maintenance of tissue homeostasis. When misregulated, apoptosis can contribute to various diseases including cancer and autoimmune and neurodegenerative diseases. Growth factors, cytokines, and serum provide both mitogenic and anti-apoptotic signals to cells and play an important role in maintaining the homeostatic balance between cell proliferation and cell death.

The actual process of apoptosis involves cytoplasm shrinkage and chromatin condensation with the maintenance of organelle integrity. The plasma membrane blebs but does not rupture, thus preventing the release of cellular compounds into the extracellular medium. Apoptotic cells are then recognised and removed by phagocytes, thereby avoiding inflammation (Cohen, 1997). Most of the morphological changes observed with apoptosis are as a result of a set of cysteine proteases that are specifically activated in apoptotic cells. These cysteine proteases are part of a large family known as caspases and first identified in *C. elegans*. Caspases are highly conserved through evolution and are the central executioners of the apoptotic pathway, as inhibition of caspases can prevent apoptosis (Cohen, 1997). Caspases are synthesized as enzymatically inert zymogens and are activated upon cleavage at specific sites, probably catalysed by other activated caspases

resulting in a caspase cascade giving amplification and integration of pro-apoptotic signals (Cohen, 1997). Caspases selectively cleave a limited set of cellular proteins, usually resulting in the inactivation of the cleaved protein. Examples of caspase substrates include poly (ADP-ribose) polymerase (PARP), DNA-dependent protein kinase (DNA-PK), lamin, and focal adhesion kinase (FAK) (Cohen, 1997). Raf-1 has also been identified as a caspase substrate; the cleavage of Raf-1 results in inhibition of its kinase activity (Widmann *et al.*, 1998).

1.11.1 Death receptor and mitochondria mediated apoptosis

Two major apoptotic pathways exist in mammalian cells: The death receptor pathway and the mitochondrial pathway (Figure 1.6). The death receptor pathway is triggered by members of the death receptor family including CD95/Fas and tumour necrosis receptor I (TNFR1). Binding of the cognate ligand, such as CD95 ligand (CD95L) or agonistic antibodies to the CD95 receptor induces receptor trimerisation and formation of a death inducing signalling complex (Ashkenazi and Dixit, 1998). In the case of CD95, receptor trimerisation results in recruitment of the adapter protein FADD (Fas-associated death domain) whereas in the case of TNFR1, receptor trimerisation results in recruitment of the adapter protein TRADD (TNFR-associated death domain) (Ashkenazi and Dixit, 1998). This allows the engagement of multiple procaspase-8 molecules. This complex is termed the DISC (death-inducing signalling complex), and results in the generation of active caspase-8 by trans-catalysis (Ashkenazi and Dixit, 1998). Caspase-8 is an initiator caspase as it is able to activate all other known caspases *in vitro* (Srinivasula *et al.*, 1996) (Figure 1.6).

The mitochondrial pathway is triggered in response to DNA damage. These diverse response pathways converge on mitochondria, often through the activation of a pro-apoptotic member of the Bcl-2 family. The Bcl-2 family consists of proteins that inhibit (Bcl-2, Bcl-X_L) and promote (Bax, Bad, Bak, Bid) apoptosis (Gross *et al.*, 1999). The different family members interact with each other at the mitochondrial membrane via homodimerisation or heterodimerisation to tightly regulate cytochrome *c* release by an unknown mechanism, although several models have been proposed (Gross *et al.*, 1999). Cytochrome *c* is released from the mitochondria into the cytosol if the pro-apoptotic

Fig. 1.6 Death receptor (CD95 in this example) and mitochondrial mediated apoptosis via the activation of the effector caspases 3, 6 and 7. Also indicated is the potential role of Raf-1 in the prevention of apoptosis by phosphorylation of Bad which leads to the interaction of Bad with 14-3-3 to prevent its pro-apoptotic function.

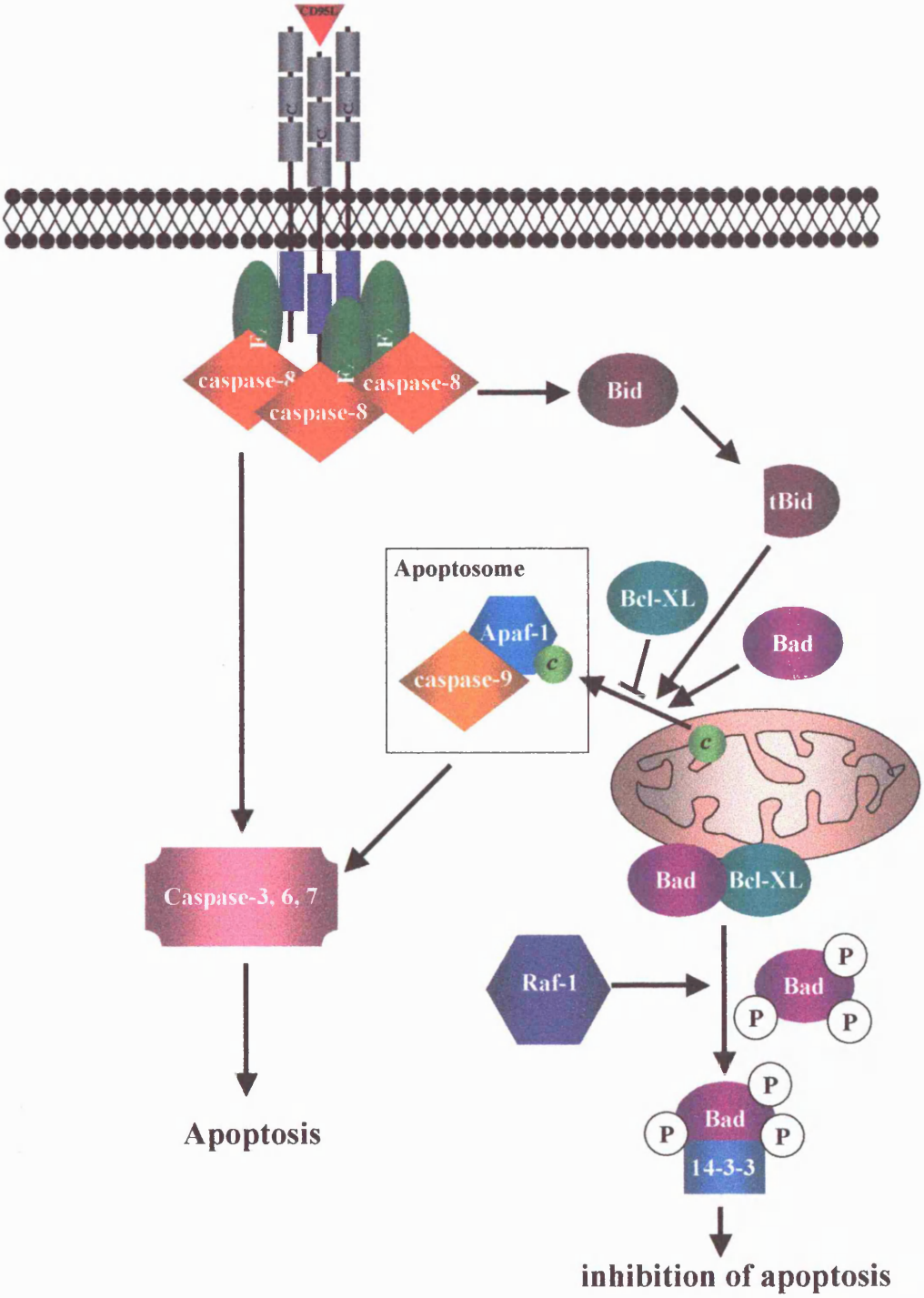

proteins predominate (Gross *et al.*, 1999). Cytochrome *c* then interacts with apoptotic protease activating factor-1 (Apaf-1), dATP/ATP and procaspase-9 to form the apoptosome (Li *et al.*, 1997; Zou *et al.*, 1999). Caspase-9 is also known as an initiator caspase as it sets off a cascade of caspase activation (Figure 1. 6). The activated initiator caspases (caspase-8 and caspase-9) can then activate the effector caspases (caspase-3, caspase-6 and caspase-7), which then initiate a program of cleavage of a limited set of cellular proteins, this results in the ordered dismantling and removal of the cell (Zou *et al.*, 1997).

1.11.2 Linking of the two apoptotic pathways

Bid is a pro-apoptotic protein that has been suggested to link the death receptor pathway to mitochondria. The cleavage of Bid by Caspase-8 releases a truncated protein (tBid) which is translocated to the mitochondria where it promotes cytochrome *c* exit and formation of the apoptosome (Li *et al.*, 1998). The involvement of the mitochondria in CD95-induced apoptosis is controversial, as cytochrome *c* is not always released (Strasser *et al.*, 1995). However, hepatocytes from Bid deficient mice are resistant to CD95 induced apoptosis, and MEFs and thymocytes from these mice display a delay in apoptosis (Yin *et al.*, 1999). This discrepancy has led to the proposal that two different cell types exist; type I in which death ligands induce apoptosis without the involvement of the mitochondria, and type II in which death ligands induce apoptosis with the aid of the mitochondria and cytochrome *c* (Scaffidi *et al.*, 1998). Overall, in CD95-mediated apoptosis it is unclear whether or not Bid significantly contributes to the overall degree of apoptosis.

It has been observed that many DNA damaging agents including etoposide induce apoptosis by inducing the synthesis of CD95-L mediated by the induction of nuclear factor-κB (NF-κB) and AP-1, thereby activating the death receptor pathway (Kasibhatla *et al.*, 1998). However, it is unclear how relevant these findings are as very high drug concentrations are required for the induction of CD95-L synthesis in these experiments (Kaufmann and Earnshaw, 2000).

1.11.3 ERK-dependent role for Raf proteins in apoptosis regulation

The Ras/Raf/MEK/ERK pathway is associated with the inhibition of apoptosis, leading to cell survival in some cell types and it is also associated with the induction of apoptosis in other cell types. The overexpression of constitutively activated MEK, Ras, Raf-1 or B-Raf prevents apoptosis after growth factor deprivation of a variety of cell types including; myeloid cells, PC12 cells and fibroblasts (Cleveland *et al.*, 1994; Xia *et al.*, 1995; Erhardt *et al.*, 1999; Le Gall *et al.*, 2000). Moreover, the removal of NGF from PC12 cells results in apoptosis involving the sustained activation of JNKs and p38MAPKs and inhibition of ERKs. Therefore it appears that whether apoptosis occurs in PC12 cells is dependent upon relative levels of activation/inhibition of the JNK-p38MAPK and ERK pathways (Xia *et al.*, 1995). Activated Ras has been shown to suppress apoptosis through the activation of PKB/Akt. Conversely, a constitutively active Ras mutant is reported to cause c-Myc-induced apoptosis through the activation of Raf-1 (Kauffmann-Zeh *et al.*, 1997). Therefore it is thought that Ras controls both apoptosis induction and suppression by the activation of two different effectors.

Growth factor deprivation induces a mitochondrion-dependent apoptosis pathway that is dependent upon cytochrome *c* release (Green and Reed, 1998). Bcl-2 and Bcl-X_L are inhibitors of apoptosis that act by preventing cytochrome *c* release from mitochondria (Kluck *et al.*, 1997; Yang *et al.*, 1997). The overexpression of B-Raf in serum starved fibroblasts leads to the prevention of apoptosis, after the release of cytochrome *c* (Erhardt *et al.*, 1999). This indicates that constitutive activation of the Ras/Raf/MEK/ERK pathway may activate or upregulate the expression of the caspase inhibitors such as X-linked inhibitor of apoptosis protein (X-IAP) and cellular IAP (cIAP).

The ERKs were found to act in both a transcription-dependent and -independent manner to prevent apoptosis in cerebellar neurones (Bonni *et al.*, 1999). Amongst other substrates, the ERKs phosphorylate and activate $p90^{RSKs}$. At least three Rsk isoforms have been identified in mammals; Rsk-1, Rsk-2 and Rsk-3 (Nebreda and Gavin, 1999). Rsk-2 was shown to directly phosphorylate Bad at Ser 112 (Bonni *et al.*, 1999). Rsks are also able to phosphorylate and activate the transcription factor CREB (cAMP response element-binding protein) which is thought to induce the expression of Bcl-2 (Bonni *et al.*, 1999).

Therefore activation of the RSKs by the ERKs can lead to the prevention of apoptosis through two different mechanisms.

1.11.4 ERK-independent role for Raf proteins in apoptosis regulation

Raf-1 in particular has been implicated in the regulation of apoptotic pathways in an ERK-independent way. Raf-1 has been reported to interact with Bcl-2 *in vitro* and it was shown that these two proteins act synergistically to prevent apoptosis upon withdrawal of interleukin-3 (IL-3) in an IL-3 dependent haematopoietic cell line (Wang *et al.*, 1994). Furthermore, when a mitochondrial membrane localisation signal was fused to the kinase domain of Raf-1, an enhanced resistance to apoptosis in response to IL-3 withdrawal was observed in myeloid cells (Wang *et al.*, 1996a). However, when a mutation which renders Raf-1 inactive was used, this survival effect was abolished (Wang *et al.*, 1996a; Majewski *et al.*, 1999). In a contrasting report, it was shown that Bcl-2 does not stably interact with Raf-1 and that Bcl-2 does not require Raf-1 for its function (Olivier *et al.*, 1997).

Bad is a pro-apoptotic member of the Bcl-2 family. Its function is modulated by phosphorylation at two sites; Ser112 and Ser136 (Datta *et al.*, 1997; Bonni *et al.*, 1999). In the absence of phosphorylation, Bad is thought to induce cell death by binding to the anti-apoptotic protein Bcl-X_L resulting in the translocation of cytochrome c from the mitochondria to the cytosol (Zha *et al.*, 1996). Phosphorylation of Bad leads to binding to 14-3-3 proteins, which may sequester Bad from Bcl-X_L and thus promote cell survival (Zha *et al.*, 1996). Raf-1 has been reported to phosphorylate Bad *in vitro*, independently of the Ras/Raf/MEK/ERK cascade (Wang *et al.*, 1996a). However, the sites of phosphorylation are not those that are required for the inactivation of Bad in response to survival signals (Zha *et al.*, 1996). Therefore Raf-1 may influence the phosphorylation of Bad indirectly (Figure 1.6).

Bag-1 has been reported to interact with and activate Raf-1 *in vitro* (Wang *et al.*, 1996b). However, as Bag-1 is a chaperone, this interaction may simply be required to maintain Raf-1 in an active conformation rather than promoting its activation. Bag-1 has also been reported to bind to Bcl-2 (Takayama *et al.*, 1995) which may provide a mechanism of Raf-1 localisation to the mitochondria where both Bcl-2 and Bad reside.

1.11.5 NFκB

NFκB is a transcription factor that in unstimulated cells is bound to its inhibitor IκB which retains it in the cytosol (Baeuerle and Baltimore, 1988). In response to diverse stimuli, including TNFα, IL-1 and viral RNA, IκB proteins are phosphorylated on two serine residues and rapidly degraded thus freeing NFκB dimers which translocate to the nucleus (Brown *et al.*, 1995; Chen *et al.*, 1995; Traenckner *et al.*, 1995). NFκB is involved in the transcription of genes associated with the inflammatory response, development and cell survival (Beg and Baltimore, 1996; Van Antwerp *et al.*, 1996). The genes induced by NFκB to promote cell survival include the caspase inhibitors c-IAP1 and c-IAP2 (Chu *et al.*, 1997; Wang *et al.*, 1998), BCL-X_L (Chen *et al.*, 2000) and growth arrest and DNA damage45β (Gadd45β) which is involved in cell cycle control and DNA repair (De Smaele *et al.*, 2001).

IκB kinase (IKK) is the kinase responsible for the phosphorylation of IκB (Zandi *et al.*, 1998). IKK is activated by phosphorylation as shown by treatment with PP2A which results in its inactivation (DiDonato *et al.*, 1997). Also, stimulation of cells with TNF results in phosphorylation of all subunits, although it appears that the important sites for activation of IKK are located in the activation loop of IKKβ (Delhase *et al.*, 1999). Two upstream activators of IKK have been identified; NFκB-inducing kinase (NIK) and MEKK1. Overexpression of either results in activation of IKK (Lee *et al.*, 1998; Ling *et al.*, 1998; Nakano *et al.*, 1998). Raf-1 was shown to activate NFκB by inducing the phosphorylation and subsequent degradation of IκB (Li and Sedivy, 1993). More recently it was shown that Raf-1 stimulates the IκB-kinase complex (IKK) which is responsible for phosphorylating and inactivating IκB and that this may be mediated by MEKK1 (Baumann *et al.*, 2000; Figure 1.7).

1.11.6 ASK1

Apoptosis signal-regulating kinase 1 (ASK1) is a MAPKKK (Ichijo *et al.*, 1997) that is activated in response to apoptotic stimuli such as TNFα, CD95L, oxidative stress and DNA damage and relays these signals to JNKs and $p38^{MAPKs}$ (Ichijo *et al.*, 1997; Chang *et al.*, 1998; Nishitoh *et al.*, 1998; Saitoh *et al.*, 1998; Liu *et al.*, 2000).

Fig. 1.7 Activation of NFκB by TNFα resulting in the prevention of apoptosis, and activation of JNK or $p38^{MAPK}$ via ASK1 resulting in the promotion of apoptosis. The potential role of Raf-1 in the prevention of ASK1 function and in the stimulation of the IκB-kinase complex (IKK) is indicated.

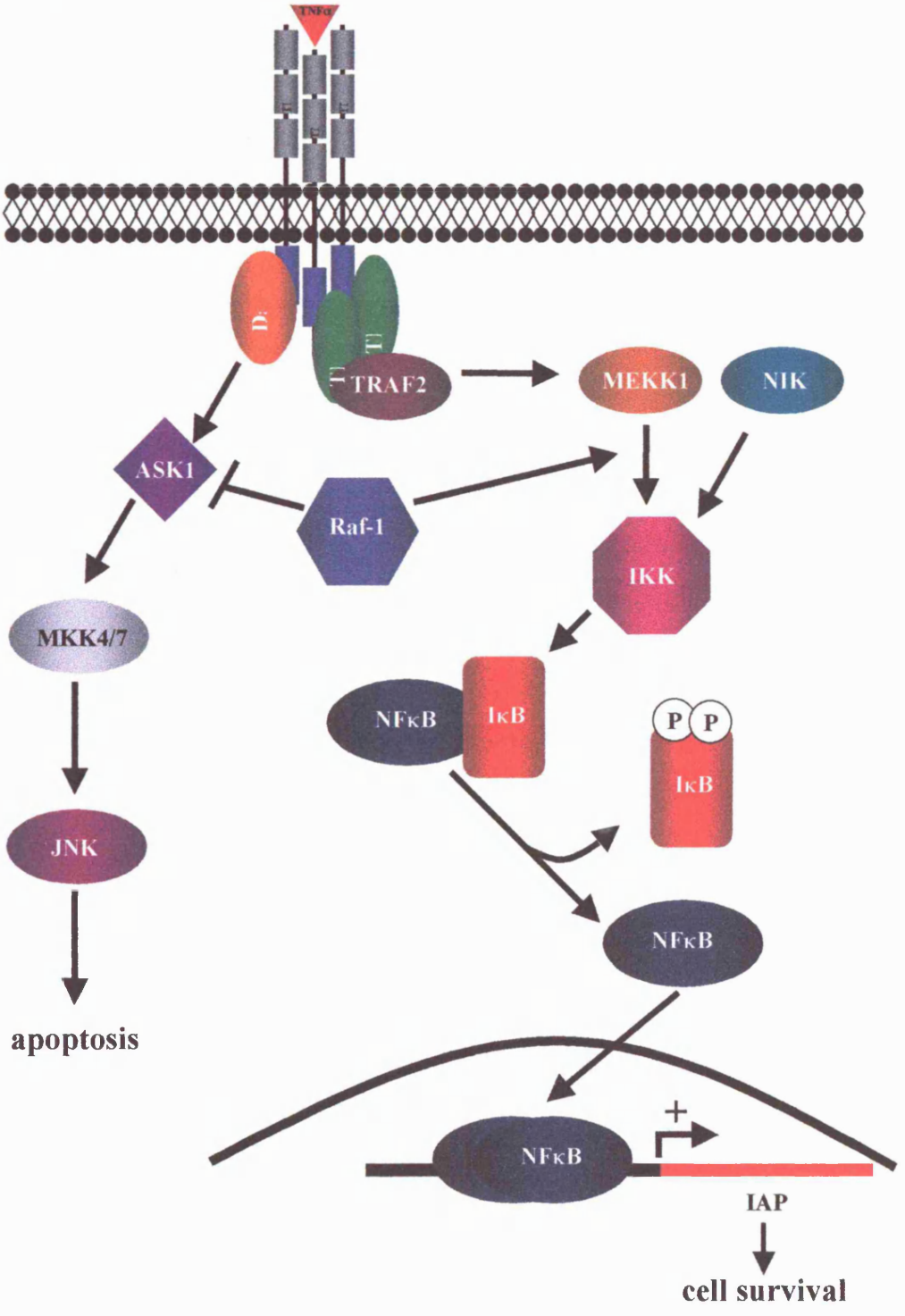

Overexpression of ASK1 induces apoptosis in a variety of cell types by inducing mitochondria-mediated caspase activation (Ichijo *et al.*, 1997; Saitoh *et al.*, 1998; Hatai *et al.*, 2000). Raf-1 was shown to interact with ASK1 *in vivo*, in addition, the overexpression of Raf-1 disrupts ASK1-induced cell death (Chen *et al.*, 2001; Figure 1.7). Use of MEK inhibitors indicate that this function of Raf-1 is independent of its role in activating the MEK/ERK pathway. Moreover, the use of a kinase defective Raf-1 show that this role of Raf-1 is independent of its kinase activity (Chen *et al.*, 2001). These results show that Raf-1 promotes cell survival by interfering with ASK1 function independently of its kinase activity or ability to activate the ERKs.

1.11.7 PI3-K/Akt pathway and cell survival

Phosphoinositide 3-kinase (PI3-K) is involved in the survival of a number of different cell types. A number of PI3-K isoforms exist; the best characterised is a heterodimer that consists of an 85 kDa regulatory subunit (Otsu *et al.*, 1991) and a 110 kDa catalytic subunit (Hiles *et al.*, 1992). Activation of PI3-K involves association of the p85 regulatory subunit with specific phosphotyrosines either on the cytoplasmic domain of growth factor receptors or on receptor-associated adaptor proteins (Rordorf-Nikolic *et al.*, 1995). PI3-K may also interact with and be directly activated by Ras (Rodriguez-Viciana *et al.*, 1994). The result of either of these is the translocation of PI3K from the cytosol to the plasma membrane whereby the p110 subunit catalyses the phosphorylation of phosphoinositides at the D3 position. These PI3-K-generated phospholipids then elicit a diverse set of cellular responses, including the regulation of the Ser/Thr kinase Akt by direct binding to the Akt pleckstrin homology (PH) domain. Activation of Akt is also thought to involve phosphorylation at two major sites Thr308 and Ser473 by phosphoinositide dependent kinase 1 (PDK1) (Currie *et al.*, 1999).

Akt targets several key proteins to keep cells alive, including transcription factors and apoptosis regulators. For example Akt has been shown to phosphorylate Bad *in vitro* and *in vivo* on Ser136 (Datta *et al.*, 1997). Secondly, in human embryonic kidney (HEK293) cells, Akt has been reported to phosphorylate Raf-1 on Ser259 which results in the inhibition of Raf-1 activity by allowing association with 14-3-3 at this site which is thought to maintain Raf-1 in an inactive conformation (Zimmermann and Moelling, 1999). Akt

has also been reported to phosphorylate B-Raf on multiple sites within the amino-terminal regulatory domain including Ser364, the equivalent residue to Ser259 of Raf-1 which similarly acts to inhibit B-Raf activity (Guan *et al.*, 2000). This suggests that the Raf/MEK/ERK pathway is negatively regulated by Akt which may mediate the cell survival effects of Akt.

1.12 Manipulating the mouse genome

1.12.1 Embryonic stem (ES) cells

Embryonic stem (ES) cells are derived from the inner cell mass of mouse blastocyst stage embryos (E3.5). These cells are pluripotent as they can differentiate into all cell types. The isolation of ES cells from mouse blastocysts and their successful culture was first reported in 1981(Evans and Kaufman, 1981; Martin, 1981). ES cells can be successfully cultured to maintain their undifferentiated state by growing them on a feeder layer of mitotically inactivated MEFs which provides a matrix for attachment as well as secreted protein factors whose role is to maintain the cells' pluripotent capacity. ES cells also require the addition of leukaemia inhibitory factor (LIF) to the media which efficiently preserves the cells' pluripotent capacity (Smith *et al.*, 1988). Cultured ES cells can be reintroduced into a mouse blastocyst which are then placed into a surrogate mother. The resulting mouse is termed a chimaera, with some of its cells derived from the host embryo and some of its cells derived from the reintroduced ES cells (Bradley *et al.*, 1984). If the coat colour alleles of the donor ES cells and the recipient blastocyst are distinguishable, the resulting chimaeric mouse will exhibit coat colour mosaicism. ES cells contribute efficiently to the formation of all tissues in a chimaeric mouse, including the germline (sperm or ova). Whether donor ES cells contribute to the germline can then be evaluated by breeding to a suitable mouse with the appropriate coat colour trait (Bradley *et al.*, 1984).

While in culture, ES cells can be manipulated by a number of methods to allow the incorporation of exogenous DNA and they may be passaged many times without losing their pluripotent capacity. Electroporation is technically simple and is the most common method for introducing DNA into ES cells. A high voltage electrical pulse is applied to a suspension of ES cells and DNA, enabling the DNA to enter the ES cells (Joyner, 1999).

The first report on the introduction of exogenous DNA into ES cells followed by the successful transmission of the genetic change through the germline was achieved by the use of retroviral vectors (Robertson *et al.*, 1986).

With an aim to derive an animal model for the Lesch-Nyhan syndrome in humans, hypoxanthine guanine phosphoribosyl transferase (*hprt*) was the first gene to be manipulated in ES cells. This gene is on the X chromosome, therefore disruption of the single copy in male ES cells was sufficient to yield *hprt* null ES cells. One approach was to select for spontaneous mutations that lead to disruption of this gene in ES cells (Hooper *et al.*, 1987). Another approach was by the insertion of retroviral DNA into ES cells to allow random mutagenesis, followed by selection for the loss of HPRT activity (Kuehn *et al.*, 1987). In both cases, the mutant ES cells were used to successfully derive mice deficient for the *hprt* gene.

1.12.2 Gene targeting in ES cells

Gene targeting is the homologous recombination between endogenous DNA sequences and introduced exogenous homologous sequences and this process occurs via a double reciprocal recombination event. A targeting vector is designed to recombine with and mutate a specific chromosomal locus. There are many different kinds of mutations that can be created including: null mutations, point mutations, deletions of specific functional domains, chromosomal translocations and gain-of-function mutations. The general design of a targeting vector includes: homologous DNA sequences, a positive selectable marker and a negative selectable marker. The length of DNA sequence homology is normally in the range of 5-8 kb, separated into a short and a long sequence of homology. Homologous recombination events are very rare, therefore the ES cell population needs to be enriched for cells harbouring such events. Both positive and negative selection procedures are used. A typical positive selection marker is the neomycin resistance gene (neo^R) whose gene product confers resistance to the drug G418 and acts to isolate the rare transfected cells that have stably integrated the targeting vector. The positive selectable marker can also serve as a mutagen by disrupting a coding exon of a gene (Figure 1.8). A typical negative selection marker is the herpes simplex virus thymidine kinase gene (HSV-*tk*) whose gene product converts the drug gancyclovir to a form that is toxic to the cell. Therefore if the

HSV-tk gene is placed outside the targeting event it provides selection for the targeted recombination product (Figure 1.8).

After the targeting vector has undergone homologous recombination with the endogenous sequence, the final recovered product is equivalent to a replacement of the chromosomal homology with all components of the vector which are flanked on both sides by homologous sequences. Any sequences at the ends of the vector homology are excised from the vector, for example the HSV-*tk* gene, and are not recovered as stable genomic sequences in the recombinant allele following targeting (Figure 1.8).

A common way to generate a null allele is to insert a selection cassette into a coding exon and/or replace part of the locus (Figure 1.8). However, exon interruptions and small deletions do not necessarily ablate the function of the target gene to generate a null allele, and in many cases transcripts and truncated proteins are produced from such a mutant allele which may have some function.

The first report of gene targeting in ES cells was the inactivation of the endogenous selectable *hprt* gene in male ES cells. Homologous recombinants could be directly selected for as the *hprt* gene product converts the base analogue 6-thioguanine to a form that is toxic to the cell, therefore only cells that had undergone homologous recombination to disrupt the gene survived treatment with 6-thioguanine (Thomas and Capecchi, 1987). The first report of a targeted non-selectable gene was that of *Int-2* where the targeting vector harboured both positive and negative selectable markers to enrich the ES cell population for homologous recombination events (Mansour *et al.*, 1988).

A relatively new technology has arisen that has many advantages over conventional gene targeting strategies and is explained in more detail in Chapter 3. The Cre/*lox*P site-specific recombination system allows a null allele to be generated in a conditional manner. Firstly, this requires the integration of two 34 bp sequences known as *lox*P sites that flank the gene of interest or part of the gene. Cre is an enzyme that recognises and mediates a site-specific recombination between the two *lox*P sequences and results in deletion of the

Fig. 1.8 Gene targeting to create a null allele. Thick red line represents homologous sequences in vector and locus, thick black line represents sequence of chromosome not homologous to vector sequence, thin black line represents bacterial plasmid not homologous to chromosome sequence. Also indicated is a blue coding exon, the *neo*^{R} gene and the HSV-*tk* gene. (**A**) Positive selectable marker interrupts the coding exon. (**B**) Positive selectable marker replaces the coding exon.

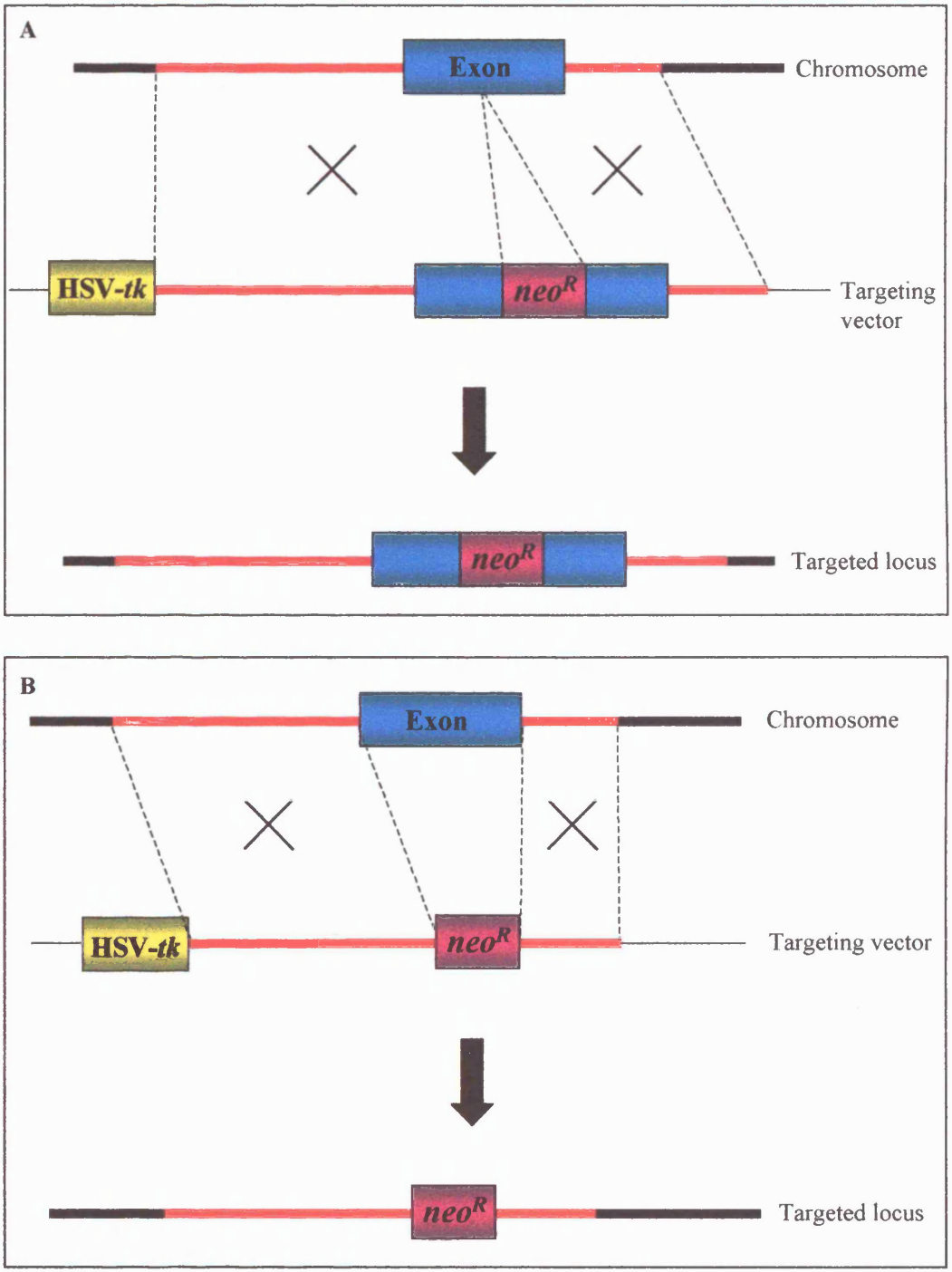

intervening DNA sequence (Hoess and Sternberg, 1982; Hoess and Abremski, 1984). As Cre can be placed under the control of a variety of promoters, this allows both spatial and temporal restriction of the Cre-mediated recombination event by the generation of Cre transgenic mice.

1.12.3 Generation of transgenic mice

The application of gene targeting technology to ES cells in culture followed by the generation of mice enables specific gene function to be studied *in vivo*. Once the required genetic modification has been achieved in ES cells, the next stage is to generate mice from them (Figure 1.9 is a diagram of this process). A timed mating between male and female mice is set up, in this example C57BL6 and CBA strains are used. At E3.5, blastocysts are taken from the female. Normally, between 6 and 12 targeted ES cells are then microinjected into each host blastocyst using micromanipulation techniques. The blastocysts are then transferred into the uterus of a surrogate pseudopregnant female. Approximately 16 days after the transfer, the pups are born. These are referred to as chimaeras, because cells originating from the host blastocyst and the microinjected ES cells contribute to the progeny in a random pattern. The readily apparent genetic marker of chimaerism is coat colour, and the degree of coat colour chimaerism of a particular animal correlates with the degree of germline contribution. Germline transmission of the microinjected ES cells means that they have contributed to the germline of the chimaera. Most ES cells in use were derived from male embryos. The main reason for this is that male mice can be mated many more times than female mice and therefore the ES cell contribution to the germline can be more rapidly assessed. Because the ES cells used are male, it is highly unlikely that female chimaeras will transmit the ES cell genotype through the germline.

To assess whether germline transmission has been achieved, the male chimaeras are mated to wild-type MF-1 mice. Coat colour of the progeny indicates whether germline transmission has been achieved and in the example, albino progeny have originated from the targeted ES cells (which originate from the 129Ola strain) whereas agouti or black progeny have originated from the host blastocyst (Figure 1.10). Once germline

Fig.1.9. Diagram to show the generation of transgenic mice. **(A)** Microinjection of albino coat colour ES cells into an agouti coat colour E3.5 blastocyst. **(B)** Transfer of blastocysts into surrogate female. **(C)** Chimaeras result that harbour a mixture of cells originating from both the injected ES cells and the host blastocyst. **(D)** Mating of the chimaeras with wild-type MF-1 mice. **(E)** The coat colour of the F1 progeny indicates whether germline transmission has been achieved. The albino coloured mice have transmitted the ES cells whereas the agouti coloured mice originate from the host blastocyst cells.

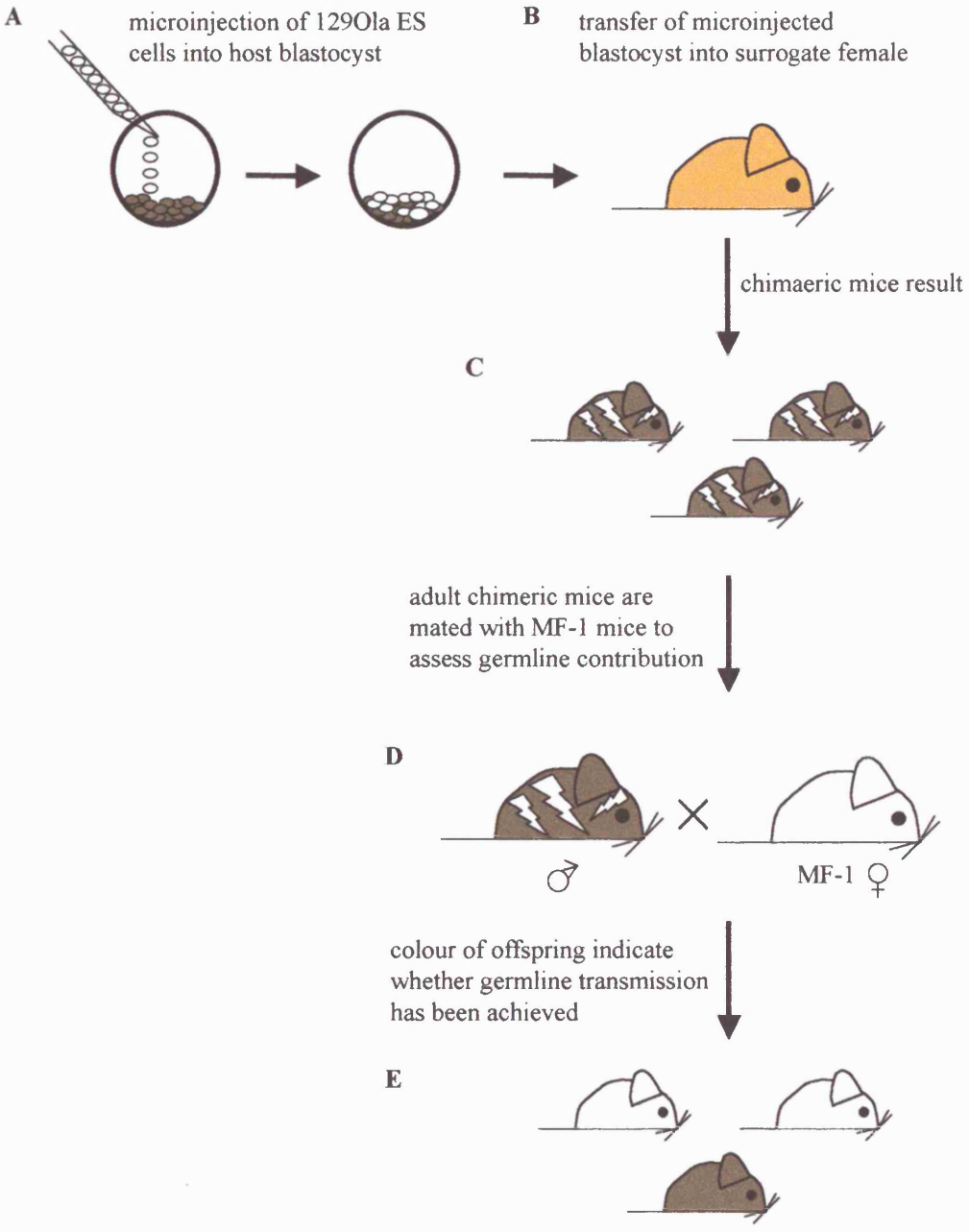

Fig. 1. 10. Germline transmission of ES cells as assessed by coat colour of F1 progeny resulting from mating of a chimaera with a wild-type MF-1. Albino mice in the F1 progeny indicates that the germ cells originated from the microinjected 129Ola ES cells, black coloured mice in the F1 progeny indicates that the germ cells originated from the host blastocyst. A and C are coat colour genes, A is dominant over C.

Dominant coat colour genes: A = agouti, C = black

Recessive coat colour genes: a = nonagouti, c = albino

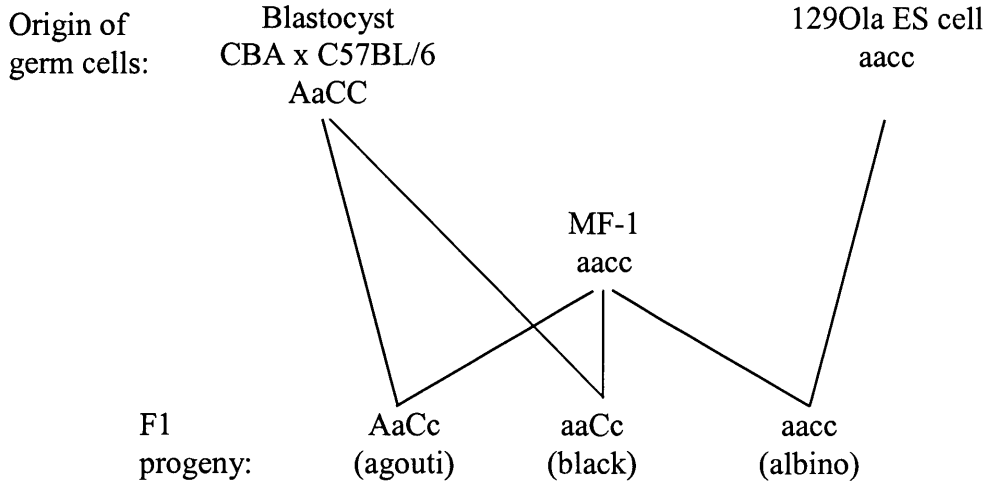

transmission has been achieved, the animals are screened for the presence of the mutation originally introduced into the ES cells in culture. Animals that harbour the mutation are heterozygotes in that every cell of the animal contains the mutation on one chromosome and can be used to form a breeding colony.

1.13 Ras/Raf/MEK/ERK knockouts in mice

A vast number of individual gene knockouts have been accomplished in mice, including many of the signalling components of the Ras/Raf/MEK/ERK signalling cascade. Gene knockouts provide a valuable tool for studying the role of such proteins in comparison to overexpression experiments which often give false information.

1.13.1 Ras

In mammals, there are three functional *ras* genes that encode four highly homologous proteins: H-Ras, N-Ras, K4A-Ras and K4B-Ras. K4A-Ras and K4B-Ras are produced from the same gene.

Mice homozygous for the N-Ras null mutation (N-*ras*$^{-/-}$) are indistinguishable from their wild-type littermates with regards to their development, growth and fertility (Umanoff *et al.*, 1995).

Mice homozygous for the H-Ras null mutation (H-*ras*$^{-/-}$) are also indistinguishable from their wild-type littermates with regards to their development, growth and fertility (Ise *et al.*, 2000).

Mice homozygous for the K-Ras null mutation (K-*ras*$^{-/-}$) on an inbred background strain, die between E12 and E14, with foetal liver defects and anaemia. Therefore K-Ras is the only Ras family member that is essential for embryogenesis. However, the growth and differentiation of many tissues can proceed normally in the absence of K-Ras function through mid-gestation indicating that there is functional compensation from the other Ras proteins (Johnson *et al.*, 1997).

Double H-*ras*$^{-/-}$ and N-*ras*$^{-/-}$ mice were then obtained. These mice grow normally, are fertile and do not show any obvious phenotype. Therefore it appears that H-Ras and N-Ras are dispensable for mouse development and that K-Ras is sufficient for normal mouse development (Esteban *et al.*, 2001).

An overlapping function for K-Ras and N-Ras was revealed, as the K-*ras*$^{-/-}$ phenotype is more severe in combination with just one functional allele of N-*ras*. Also, the N-*ras*$^{-/-}$ phenotype in combination with just one functional K-*ras* allele results in death between E10 and E12. The authors suggest that a critical level of Ras activity is required during development, this is achieved by various combinations of the different Ras proteins (Johnson *et al.*, 1997).

1.13.2 Raf

Mice homozygous for the B-Raf null mutation (*B-raf*$^{-/-}$) die between E10.5 and E12.5, due to vascular defects and endothelial apoptosis. This therefore shows that B-Raf is essential for embryogenesis and has a role in cell survival and the other Raf family members cannot compensate for its loss (Wojnowski *et al.*, 1997).

On the C57 BL/6 and the 129Ola genetic backgrounds, mice homozygous for the A-Raf null mutation (*A-raf*$^{-/Y}$) survive to adulthood and are fertile. However they are much smaller than wild-type littermates, have a feeding ataxia and display a subset of neurological abnormalities. This shows that A-Raf is not essential for mouse development, but it is essential for specific aspects of neurological development (Pritchard *et al.*, 1996).

Raf-1 deficient mice were initially created by Wojnowski et al. (1998). However, the introduced mutation results in the expression of an aberrant 62 kDa Raf-1 protein that has residual kinase activity. Therefore these mice were not null for Raf-1. Despite this, embryos homozygous for this mutation display embryonic lethality with the time-point of death dependent upon genetic background therefore indicating full-length Raf-1 is essential for embryogenesis. Homozygous mutants display a generalised growth retardation which is attributed to the observed defects of the placentas. Other abnormalities are observed in the skin and lungs. MEFs were derived from both homozygous mutant and wild-type

embryos. The homozygous mutant MEFs display a reduced rate of cell proliferation (Wojnowski *et al.*, 1998).

Raf-1 deficient mice were created in our laboratory and is described in Hüser *et al.* (2001). The generation of these mice is described in Chapter 5. The severity of the phenotype of mice homozygous for the Raf-1 null mutation (*raf-1*$^{-/-}$) is dependent upon the genetic background. Mice on a predominantly C57/BL6 background die in embryogenesis at around E9.5 and show vascular defects in the yolk sac and placenta as well as increased apoptosis of embryonic tissues although cell proliferation is not affected. Mice on a mixed MF-1 background survive up until birth but are much smaller than wild-type littermates, are anaemic and the placenta is disorganised (Huser *et al.*, 2001). ERK activation is normal in MEFs derived from the *raf-1*$^{-/-}$ embryos. This indicates that Raf-1 is essential for normal mouse development and it also plays a key role in the prevention of apoptosis.

Our laboratory also reported the generation of knockin transgenic mice that harbour a mutation of the endogenous tyrosine residues 340 and 341 to phenylalanine residues (RafFF) (Huser *et al.*, 2001). These tyrosine residues have previously been found to be essential for Raf-1 activation. Mice homozygous for the RafFF mutation survive to adulthood, are fertile and display a normal phenotype. However, when Raf-1 is immunoprecipitated from MEFs derived from embryos homozygous for the RafFF mutation (*raf-1*$^{FF/FF}$), it has no activity towards MEK. Furthermore, ERK activation is normal in comparison to wild-type MEFs (Huser *et al.*, 2001).

It was therefore concluded that the MEK kinase activity of Raf-1 is not essential for normal mouse development, but that the protein is required, indicating that Raf-1 has a unique role that is independent from its involvement in the Ras/Raf/MEK/ERK cascade.

Raf-1 deficient mice were also created by Mikula *et al.* (2001). They report that the mutant Raf-1 homozygous embryos die during mid-gestation and display growth retardation. Moreover, abnormalities are observed in the mutant placentas and in the foetal liver, with an increase in apoptotic cells. MEFs were derived from mutant and wild-type embryos, and ERK activation is found to be normal in the mutant cells.

1.13.3 MEK

Mice homozygous for the MEK1 null mutation (*mek1*$^{-/-}$) die at around E10.5 due to a reduced level of vascularisation of the placenta. This defect is not due to a defect in differentiation, instead it appears that the vascular endothelial cells are incapable of invading the labyrinthine region which is indicative of a migration defect. Primary mouse embryonic fibroblasts were derived from wild-type and *mek-1*$^{-/-}$ embryos and analysed with regards to their ability to migrate. The migration of *mek-1*$^{-/-}$ MEFs is greatly reduced in comparison to wild-type MEFs and this is not due to a cell adhesion defect. This means that MEK1 has a unique role in the transduction of signals required for vascularisation *in vivo* and cell migration in MEFs. ERK activation was also measured and no differences were found between the *mek-1*$^{-/-}$ MEFs in comparison to wild-type MEFs. This is probably due to compensation by MEK2 or other kinases (Giroux *et al.*, 1999).

1.13.4 ERK

Mice homozygous for the ERK1 null mutation (*erk1*$^{-/-}$) are viable, fertile, and of normal size. However a defect in thymocyte maturation is observed with these mice having half the amount of mature thymocytes. This appears to be due to a proliferation defect. Thus, ERK1 is apparently dispensable for normal mouse development and ERK2 may compensate for its loss, but ERK1 has a specific role in thymocyte development that cannot be compensated for by ERK2 (Pages *et al.*, 1999).

1.14 Aims of the project

The aims of this thesis has been to contribute to the characterisation of the Raf family by:

- The generation of a mouse line where the *raf-1* gene is flanked by *lox*P sites introduced by gene targeting in ES cells with the aim of generating a conditional knockout mouse for *raf-1*.

- The investigation of the use of Cre in ES cells, MEFs and mice to conditionally delete *raf-1*.

- The characterisation of *raf-1*$^{-/-}$ and *raf-1*$^{FF/FF}$ MEFs with regards to growth, proliferation and apoptosis.

- The characterisation of A-*raf* $^{-/Y}$ MEFs with regards to growth, proliferation, differentiation and apoptosis.

2 MATERIALS AND METHODS

2.1 Molecular biology

All chemicals and reagents were supplied by Sigma unless otherwise stated and all restriction endonucleases were supplied by New England Biolabs.

2.1.1 Plasmids

The plasmids used were:

pBluescript KSII$^+$ (Stratagene; Figure 2.1A)

pX53-neo (gift from R. Murray, DNAX Research Institute, California; Figure 2.1B)

pX53-hyg (gift from R. Murray, DNAX, California; Figure 2.1C)

pPGK-puro (gift from R. Fassler, Department of Experimental Pathology, Lund University, Sweden; Figure 2.1D)

pIC-Cre (gift from R. Murray, DNAX, California; Gu *et al.*, 1993)

pCre-Pac (gift from A. Gonzalez-Garcia, The Institute of Cancer Research, London; Figure 2.1E)

pEFm.6, pEFm.6/Raf.1 and pEFm.6/kinase inactive (gifts from R. Marais, The Institute of Cancer Research, London; Marais *et al.*, 1995)

pZIPSVtsA58 (gift from P. Jat, Ludwig Institute for Cancer Research, London; Jat and Sharp, 1989)

Fig. 2. 1. Plasmid maps. **(A)** pBSIIKS^{+} (MCS = multiple cloning site) **(B)** pX53-neo **(C)** pX53-hyg **(D)** pPGK-puro **(E)** pCre-Pac

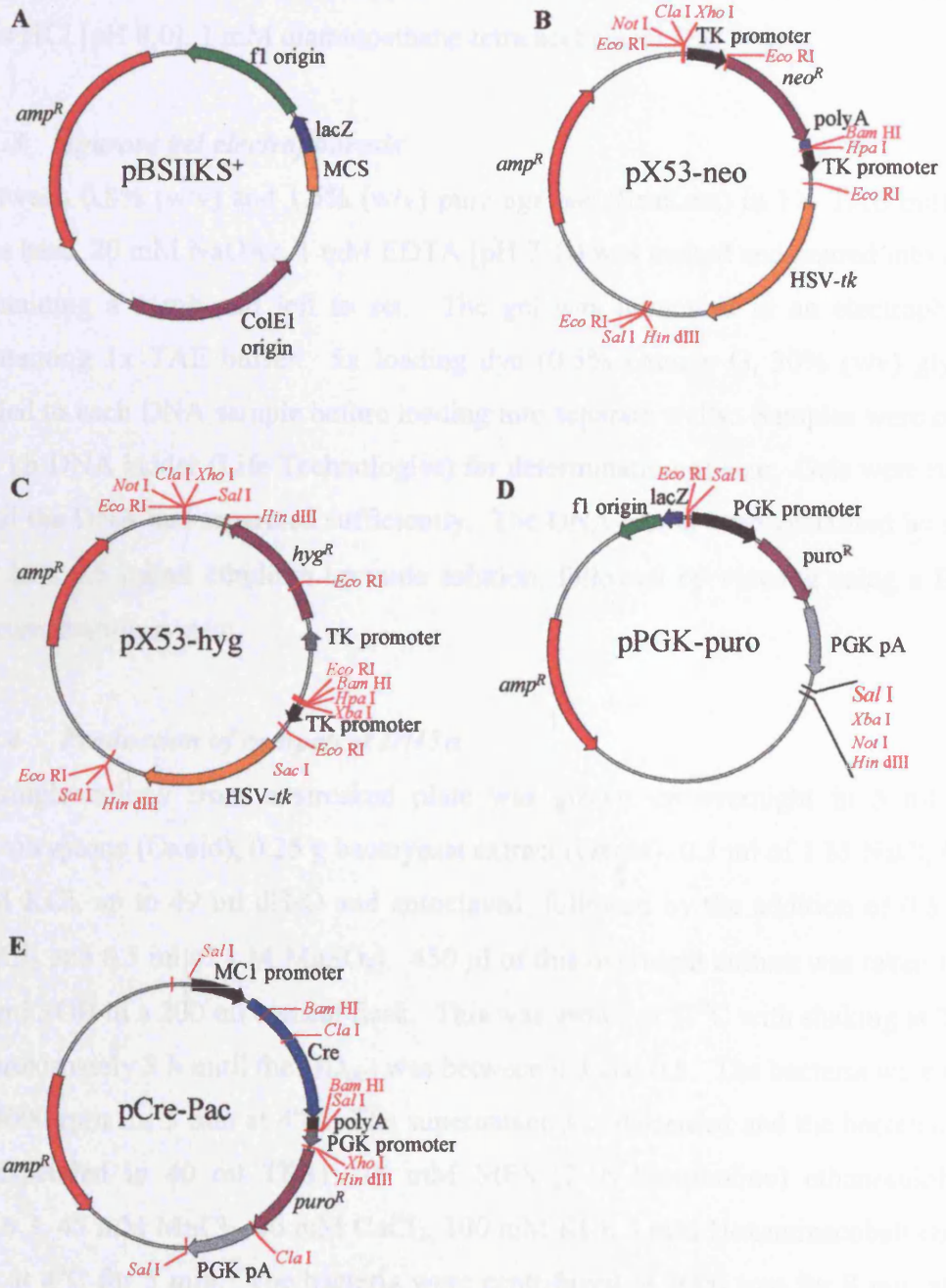

2.1.2 *Ethanol precipitation of DNA*

1/10th volume of 3 M NaOAc pH 5.5 and 2x volumes of 100% ethanol were added to the DNA solution followed by centrifugation at 13000 rpm at 4°C for 10 min. The supernatant was removed by aspiration and the DNA pellet was washed with 70% ethanol. The pellet was left to air dry and resuspended in an appropriate volume of TE (10 mM Tris·HCl [pH 8.0], 1 mM diaminoethane-tetra acetic acid [EDTA]).

2.1.3 *Agarose gel electrophoresis*

Between 0.8% (w/v) and 1.5% (w/v) pure agarose (SeaKem) in 1× TAE buffer (40 mM Tris base, 20 mM NaOAc, 1 mM EDTA [pH 7.4]) was melted and poured into a gel mould containing a comb and left to set. The gel was immersed in an electrophoresis tank containing 1x TAE buffer. 5x loading dye (0.5% Orange G, 30% (v/v) glycerol) was added to each DNA sample before loading into separate wells. Samples were compared to a 1 kb DNA ladder (Life Technologies) for determination of size. Gels were run at 100 V until the DNA had separated sufficiently. The DNA bands were visualised by staining the gel in a 0.5 μg/ml ethidium bromide solution, followed by viewing using a Bio-Rad gel documentation system.

2.1.4 *Production of competent DH5α*

A single colony from a streaked plate was grown up overnight in 5 ml SOB (1 g bactotryptone (Oxoid), 0.25 g bactoyeast extract (Oxoid), 0.5 ml of 1 M NaCl, 0.125 ml of 1 M KCl, up to 49 ml dH_2O and autoclaved, followed by the addition of 0.5 ml of 1 M $MgCl_2$ and 0.5 ml of 1 M $MgSO_4$). 450 μl of this overnight culture was taken to inoculate 45 ml SOB in a 200 ml conical flask. This was grown at 37°C with shaking at 225 rpm for approximately 3 h until the OD_{600} was between 0.3 and 0.5. The bacteria were centrifuged at 4000 rpm for 5 min at 4°C. The supernatant was discarded and the bacterial pellet was resuspended in 40 ml TFB1 (10 mM MES [2-(N-Morpholino) ethanesulphonic acid] pH 6.3, 45 mM $MnCl_2$, 10 mM $CaCl_2$, 100 mM KCl, 3 mM Hexaminecobalt chloride) and left at 4°C for 5 min. The bacteria were centrifuged at 3000 rpm for 8 min at 4°C. The supernatant was discarded and the bacterial pellet was resuspended in 4 mls TFB2 (10 mM MOPS [3-(N-Morpholino) propanesulphonic acid] pH 6.5, 75 mM $CaCl_2$, 10 mM RbCl, 15% (v/v) glycerol) at 4°C. The bacteria were then aliquoted into 50 μl aliquots and snap

frozen in a dry ice/IMS bath and subsequently stored at –80°C. The transforming competency of the DH5α were tested using a known amount of plasmid DNA.

2.1.5 Transformation of DH5α

One aliquot (50µl) of competent DH5α was thawed on ice for each transformation and transferred to a round bottomed tube (Falcon) on ice. 5 µl of ligation mix or 1 µl of plasmid were gently mixed into the competent cells. The tube was left on ice for 30 min followed by heat shock at 42°C for 45 sec and transferred back to ice for 1 min. 900 µl Luria Bertani (LB) medium (10 g bactotryptone, 5 g bactoyeast extract, 10 g NaCl up to 1 litre dH_2O and autoclaved) was added and the tube was shaken at 225 rpm and 37°C for 1 h. 200 µl of this was spread onto a plate containing LB agar (LB with 15 g agar up to 1 litre dH_2O and autoclaved) plus 50 µg/ml ampicillin. The plate was inverted and placed at 37°C overnight to allow the formation of discrete bacterial colonies.

2.1.6 Minipreparation of plasmid DNA from bacteria

5 ml of LB media was inoculated with bacteria and shaken overnight at 225 rpm and 37°C. 1 ml of the culture was placed into 1.5ml eppendorf tubes and centrifuged (Heraeus Biofuge) at 13000 rpm for 30 sec at 4°C. The supernatant was aspirated and the bacterial pellet resuspended in 100 µl buffer P1 (50 mM Tris·HCl [pH 8.0], 10 mM EDTA, 100 µg/ml ribonuclease [RNase]). 200 µl buffer P2 (200 mM NaOH, 1% [w/v] sodium dodecyl sulphate [SDS]) was added and the tubes were inverted 5 times to mix and left at room temp for 5 min. 150 µl ice cold buffer P3 (3 M KOAc [pH 5.5]) was added and the tubes were inverted five times. The tubes were placed on ice for 5 min followed by centrifugation at 13000 rpm for 10 min at 4°C. The supernatant was removed and placed into a new tube. To precipitate the DNA, 400 µl isopropanol was added, tubes were inverted five times, followed by centrifugation at 13000 rpm for 10 min at 4°C. The supernatant was removed by aspiration and the DNA pellet was washed with 70% ethanol. The pellet was left to air dry and resuspended in 50 µl TE.

2.1.7 *Midi scale preparation of plasmid DNA from bacteria*

100 ml of LB media was inoculated with bacteria and shaken overnight at 225 rpm and 37°C. The plasmid midi kit (Qiagen) was used to purify the plasmid DNA from the bacteria following the manufacturer's recommended method.

2.1.8 *Caesium chloride preparation of plasmid DNA from bacteria*

400 ml of LB media was inoculated with bacteria and shaken overnight at 225 rpm and 37°C. The following day the culture was centrifuged at 6000 rpm at 4°C for 10 min (Sorvall RC-5B) and the pellet was resuspended in 10 ml of buffer P1. 20 ml of buffer P2 was added to lyse the cells and the tubes were left on ice for 5 min. 15 ml of buffer P3 was added and the tubes were left on ice for 5 min. Tubes were centrifuged at 9000 rpm for 15 min at 4°C. The supernatant was transferred to a new tube containing 50 ml ice cold isopropanol, mixed and centrifuged at 9000 rpm for 15 min. The pellet was resuspended in 5.5 ml TE. The DNA solution was transferred to a 12 ml tube and 550 µl of a 5 mg/ml ethidium bromide solution was added, 6.0 g CsCl was then added and dissolved before centrifuging at 4000 rpm for 5 min (IEC Centra CL3R) to pellet debris. The clear solution was transferred into two Quickseal centrifuge tubes (Beckman). The tubes were centrifuged at 100000 rpm for 12-16 h overnight at 20°C (Beckman Optima MAX-E ultracentrifuge). The lower plasmid band was removed with a 21G needle and placed into a tube. H_2O saturated isobutanol was added to the DNA solution and the tube was inverted several times, the two layers were allowed to settle, and the top layer was discarded. This step was repeated several more times until the ethidium bromide could no longer be visualised. Twice the volume of water was added and the DNA was precipitated with twice the volume of 100% ethanol. The tubes were centrifuged at 11000 rpm for 15 min at 4°C and the pellet was washed with 70% ethanol and left to air dry. The pellet was resuspended in 500 µl TE and the DNA quantitated using a spectrophotometer (LKB Biochrom Ultrospec 4050) to measure OD_{260}.

2.1.9 *Restriction digestion of miniprep plasmid DNA*

For analytical purposes, 1 unit of the appropriate 10x restriction digestion buffer (supplied by the manufacturer of the enzyme) was added to the miniprep DNA with 1 unit of the enzyme in a total volume of 10 µl. The reactions were incubated at 37°C for one hour.

2.1.10 Restriction digestion of genomic DNA

In a total volume of 200 µl, 20 µl of the appropriate 10x restriction digestion buffer was added to the DNA with 10 units of the enzyme, 2.5 mM spermidine, and 100 µg/ml RNase. The reactions were incubated at 37°C for at least 16 h.

2.1.11 Fill-in of 5' overhangs resulting from restriction digestion

In a total volume of 10 µl, 1 µl of 10x klenow buffer (supplied by the manufacturer), 0.5 mM of each dNTP and 5 units of klenow DNA polymerase I was added to the DNA. The reaction was incubated at 37°C for 15 min. The enzyme was inactivated by heating to 75°C for 10 min.

2.1.12 Removal of 5' phosphate groups from linear plasmid DNA

After restriction digestion of the DNA sample, 5 units of shrimp alkaline phosphatase (United States Biochemical) was added to the reaction and placed at 37°C for 30 min. The sample was run through an agarose gel for purification.

2.1.13 Purification of gel fragments

The DNA fragment to be purified was excised from the agarose gel using a scalpel blade. The QIAquick gel extraction kit (Qiagen) was used to purify the DNA from the gel slice following the manufacturer's recommended method.

2.1.14 Ligation of DNA fragments

A molar ratio of 1:4 of vector:insert plus 1 unit of T4 DNA ligase (Boehringer Mannheim) and 2 µl 10x T4 DNA ligase buffer (supplied by the manufacturer) up to a total volume of 20 µl was placed at 16°C overnight.

2.1.15 DNA sequencing and primer synthesis

The Protein and Nucleic Acid Laboratory (PNACL) at the University of Leicester performed all DNA sequencing and primer synthesis. Sequencing was analysed by the Applied Biosystems program Factura™.

2.1.16 Lysis of cells to extract DNA

Attached cells were washed twice with PBS and an appropriate volume of DNA lysis buffer (50 mM Tris·HCl [pH 7.6], 1 mM EDTA, 100 mM NaCl, 0.2% [w/v] SDS, 100 µg/ml fresh proteinase K) was added, and the mixture was incubated at 37°C overnight. DNA was precipitated the next day by placing the DNA solution into an eppendorf tube and adding an equal volume of 100% ethanol. The tube was inverted several times until the DNA was visible. The tube was centrifuged at 13000 rpm for 1 min, the supernatant was discarded and 1 ml of 70% ethanol was added to wash the DNA pellet. The ethanol was removed and the pellet was left to air dry and then resuspended in an appropriate volume of TE.

2.1.17 Lysis of mouse tail samples to extract DNA

A 2 mm tail sample was lysed in 100 µl of PCR buffer with non-ionic detergent (50 mM KCl, 10 mM Tris·HCl [pH 8.3], 0.1 mg/ml gelatin, 0.45% [v/v] Nonidet P-40, 0.45% [v/v] polyoxyethylene sorbitan monolaurate [Tween 20], 100 µg/ml fresh proteinase K) at 56°C until the tissue had completely digested. Samples were heat inactivated at 95°C for 10 min.

2.1.18 Polymerase chain reaction (PCR)

PCR beads (Amersham Pharmacia Biotech) were hydrated in 25 µl milliQ H_2O plus primers (Table 1) at a final concentration of 1 pmol/µl. 8 µl of this PCR mix was placed in 0.5 ml PCR tubes and 1 µl sample DNA was added. Each PCR reaction was overlaid with 10 µl mineral oil. PCR was performed on a Biometra TRIO-thermoblock. The conditions for PCR were the following:

Initial denaturation of DNA at 94°C for 5 min followed by 35 cycles consisting of three steps:

step 1 94°C for 30 sec

step 2 X°C for 30 sec (Table 1)

step 3 72°C for 1 min per kb of product

A final extension at 72°C for 10 min

Table 1. List of primers used and their corresponding optimal annealing temperature.

Primer name	Sequence 5' to 3'	Annealing temperature of PCR reaction ($X^{o}C$)
Ocp10	GAT GTA GCT GTG AAA GTG	60
Ocp26	GAC TAG ACA TGT CTT AAC ATC TGT CC	65
Ocp27	CCT ATT GCA TGG ACT GCA GCT TAT G	65
Ocp52	CAG ATT ATA TCT GTA CCT GAC CTG	52
Ocp56	ACA GAA AGT GTA GCT GCA GTG A	60
Ocp59	TTA CAT GTC CAC AAG ACT CCT TAC	52
Ocp66	CGT GCA ATC CAT CTT GTT CA	60
Ocp67	GGC AGC AGC TAG GAT GAT TT	60
Ocp68	GCA GGT AGC AAA CAC CCA CT	60
Ocp69	AGG GGA TCG GCA ATA AAA AG	60
Ocp77	GTC CAG AGT GCC GTG TGA TA	62
Ocp78	ATT GAT TTG ATT GCC AGG TAT GAT	60
Ocp82	TAA GCC CAA CCA GCT CTG TC	60
Ocp83	CAA CCC CTG GCA TCT TTT TA	60
Ocp84	GTT CGC AAG AAC CTG ATG GAC A	62
Ocp85	CTA GAG CCT GTT TTG CAC GTT C	62
Ocp86	GGC AAC TGG CCT CAG ACA CCA T	62
Ocp87	TGT GGA GCC TCT GGA TCA GGA C	62
Ocp90	GCT CAG AGG AGA AAG GGT CA	60
Ocp100	GTT TGC CTC CAG AGC ATC TT	60
Ocp106	GCT TAC ATT TGC TTC TGA CA	60
Ocp107	GTG ATA CTT GTG GGC CAG G	60
3'pgk	CCA GAA AGC GAA GGA GCA AAG C	60

2.1.19 Southern blot analysis

DNA was electrophoresed at 15 V through 0.8% (v/v) agarose gels overnight. Gels were then placed in a bath of 0.25 M HCl for 15 min to depurinate the DNA and in a bath of 0.4 M NaOH (transfer buffer) for 30 min on a moving platform. Sponges were placed in a deep container and were flooded with transfer buffer until the sponges were immersed up to half way. A piece of gel blot paper (Schleicher and Schuell) cut to the same size as the gel was placed on top of the sponges. The agarose gel was inverted and placed on top of the paper, flooded with transfer buffer and any bubbles removed. A piece of Zeta-probe GT genomic tested blotting membrane (Bio-Rad) was cut to size and placed on top of the gel followed by another piece of gel blot paper. More transfer buffer was added to the stack and all bubbles were removed. Paper towels to a height of 15 cm were stacked on top of the structure and a 100 g weight was placed on top to compress the towels. Blotting was left to take place for at least 6 h. The Zeta-probe membrane was then orientated and soaked in 1x SSC (made from diluting stock 20x SSC; 3 M NaCl, 0.3 M trisodium citrate [pH 7.0]) for 10 min. The membrane was baked at 80°C for 30 min after which it was ready for hybridisation with a probe.

2.1.20 Probe radiolabelling

10 ng of probe DNA was boiled and rapidly cooled on ice. To the boiled probe DNA 5 units Klenow DNA polymerase I (United States Biochemical), 200 μg/ml BSA, 10 μl 5x Oligo labelling buffer (Table 2), 1 μl [α-^{32}P] dCTP (Perkin Elmer Life Sciences) was added in a total volume of 50 μl. The reaction was incubated at 37°C for two hours. The labelled probe was then recovered by centrifugation through a spin column containing Sephadex G50 saturated with TE buffer. The probe was boiled for 5 min followed by rapid cooling on ice and then added to the Zeta-probe membranes that had been prehybridised with Church buffer (0.5 M sodium phosphate [pH 7.2], 7% [w/v] SDS, 0.5 mM EDTA [pH 8.0]) for at least 1 hour at 65°C. Hybridisation was allowed to proceed in a rotating Hybaid oven at 65°C overnight. The membranes were washed 3 times with 2x SSC and 0.1% (w/v) SDS at 65°C in the Hybaid oven, and 2 times with 0.5x SSC and 0.1% SDS at 65°C in the Hybaid oven, with each wash lasting for 10 min. They were then wrapped in Saranwrap, placed in a cassette and exposed to autoradiography film (Kodak) at –80°C for varying amounts of time depending upon the strength of the signal.

Table 2. Oligo labelling buffer.

Solutions were mixed in the ratio A:B:C 100:250:150

	Ingredients
Solution O	1.25 M Tris-HCl (pH 8.0), 0.125 M $MgCl_2$
Solution A	1 ml solution O, 18 µl β-mercaptoethanol, 5 µl 100 mM dATP, dTTP, dGTP (Amersham/Pharmacia Biotech)
Solution B	2 M HEPES (pH 6.6 titrated with 4M NaOH and filter sterilised)
Solution C	Hexadeoxyribonucleotides $pd(N)_6$ (Amersham/Pharmacia Biotech)

2.1.21 Stripping Southern blots for re-probing

Blots were incubated with 0.1x SSC, 0.5% (w/v) SDS at 95°C for 2 washes. Prehybridisation in Church buffer was repeated before freshly labelled probe was added.

2.2 Cell culture

All cell culture reagents were supplied by Life Technologies and plasticware was supplied by Nunc unless otherwise stated.

2.2.1 Media and maintenance of mouse embryonic fibroblast (MEF) cell lines

Cell lines were maintained in Dulbecco's modified Eagle's medium (DMEM) with 4500 mg/litre D-glucose, supplemented with:

15% (v/v) foetal calf serum (FCS; Globefarm)
20 mM L-glutamine
100 U/ml penicillin
100 µg/ml streptomycin

Cells were incubated at 37°C and 10% CO_2 in a humidifying incubator. Cells were passaged once they became 100% confluent by aspiration of the media followed by the addition of an appropriate volume of phosphate buffered saline (PBS; 137 mM NaCl, 8.1

mM Na_2HPO_4, 2.7 mM KCl, 1.5mM KH_2PO_4 and autoclaved) depending upon the plate size. The PBS was aspirated and an appropriate volume of 0.5 mg/ml trypsin in PBS was added depending on the size of the dish. The cells were placed at 37°C for 5 min to generate a single cell suspension, followed by addition of media to neutralise the trypsin.

2.2.2 Production of primary MEFs from E14.5 mouse embryos

The uterus was dissected from the pregnant mouse and placed into sterile PBS at 4°C. The uterus was torn using forceps and each embryo was dissected from the placenta and amniotic fluids followed by removal of the liver. The embryos were washed in several changes of PBS. They were then chopped into small pieces using a sterilised scalpel and placed into a tube containing 4 ml of 2.5 mg/ml trypsin in PBS. The tubes were placed at 4°C overnight to allow dissociation of the tissues. The next day the tubes were placed at 37°C for 30 min. The trypsin was removed carefully, then 1 ml media was added and the dissociated embryo was pipetted up and down until the cell suspension was complete. This was then plated out onto a 15 cm plate containing 15 ml media. The cells were left to grow until confluent. They were then passaged to make stocks for freezing and for genotyping.

2.2.3 Freezing down stocks of cell lines

Cells to be frozen were trypsinised, pelleted by centrifugation and resuspended in an appropriate volume of media. An equal volume of 2x Freezing mix (1 ml dimethylsulphoxide, 2 ml foetal calf serum, 2 ml growth media) was added and the cells were transferred to cryovials and placed at -80°C.

2.2.4 Immortalisation of primary MEFs with a temperature sensitive version of the SV40 large T antigen

5 x 10^6 Bosc23 cells (Pear *et al.*, 1993) were cultured in MEF media and were plated out onto a 10 cm plate the evening prior to transfection. The next morning, 12.5 μg pZIPSVtsA58 was mixed with 1 ml OPTI-MEM 1 containing no supplements. 90 μl lipofectamine was mixed with 1 ml OPTI-MEM 1 medium containing no supplements. The two solutions were mixed with gentle vortexing. The mixture was incubated at room temperature for 15 min. The Bosc23 cells were washed twice with 5 ml OPTI-MEM 1 medium containing no supplements and the DNA/lipofectamine mixture was gently laid

onto the cells. The plate was agitated gently to distribute the liquid over the monolayer. Plates were placed at 37°C for 5 h, with gentle agitation every hour to ensure proper coverage of the cells. 10 ml of OPTI-MEM 1 medium, supplemented with 20% (v/v) FCS was added to the cells and the incubation was continued for a further 19 h. The media was removed and replaced with 6 ml of DMEM containing 15% (v/v) FCS. 12 h later the viral supernatant was removed, polybrene was added to a final concentration of 8 μg/ml and filtered through a 0.2 μm filter to remove cell debris. The viral supernatant was then either aliquoted and placed at –80°C or used immediately. 2 ml of viral supernatant was added to each 6 cm dish of primary MEFs that had been plated out at a density of 1 x 10^5 cells the previous evening for 8 h. The virus was removed and replaced with fresh media containing 20% FCS for 24 h. Once the cells became confluent, they were trypsinised into media containing 500 μg/ml G418.

2.2.5 Transfection of MEFs with Lipofectamine

6 x 10^5 MEFs were plated onto each 10cm plate the day before transfection. An appropriate amount of caesium chloride prepared plasmid DNA was added to 800 μl OPTI-MEM 1 media. 36 μl Lipofectamine was added to 800 μl OPTI-MEM 1 media. The two solutions were mixed and left at room temperature for 15 min. MEFs to be transfected were washed with media containing no supplements. 4.4 ml media was added to tubes containing complexes. The DNA/lipofectamine mixture was gently laid onto the MEFs and they were placed at 37°C in a humidifying incubator for 5 h. 6 ml media plus 1.5 ml serum was added and the cells were left at 37°C overnight. Selection for resistant cells was applied the following day.

2.2.6 Mitomycin C treatment of primary MEFs

When primary MEFs containing the bacterial neomycin phosphotransferase gene (neo) were 80% confluent on 10 cm plates, Mitomycin C in H_2O was added to the growth media to a final concentration of 2 μg/ml, and incubated at 37°C for 2 h. MEFs were washed three times with 10 ml PBS, and the cells harvested by trypsinisation. MEFs were counted using a haemocytometer. MEFs were then either aliquoted and frozen down or plated out onto the appropriate sized tissue culture plate that had been pretreated with 0.1% (w/v) gelatin to ensure a confluent monolayer of MEFs (Table 3).

Table 3. Number of Mitomycin C treated MEFs to be plated out for different sized tissue culture plates to ensure a confluent monolayer.

Size of plate	Number of MEFs
10 cm	1×10^6
6 cm	6×10^5
6-well	4×10^5
12-well	2.5×10^5
24-well	1×10^5
48-well	4×10^4

2.2.7 Media and maintenance of embryonic stem cell (ES) cells

The E14.1a ES cell line was derived from the 129Ola strain and was maintained in Dulbecco's modified Eagle's medium (DMEM) with 4500 mg/litre D-glucose, supplemented with:

15% (v/v) embryonic stem cell qualified foetal bovine serum (Labtech International)
20 mM L-glutamine
100 U/ml penicillin
100 μg/ml streptomycin
1 mM non-essential amino acids
10 mM sodium pyruvate
115 μM β-mercaptoethanol
1 ml recombinant LIF

Leukaemia inhibitory factor (LIF) was made by a calcium phosphate transient transfection of COS7 cells with a LIF expression vector, followed by harvesting the supernatant after 48 h. LIF was provided by S. Figgit, Department of Biochemistry, University of Leicester.

ES cell lines were incubated at 37°C and 10% CO_2 in a humidifying incubator. Cell lines were grown on dishes pretreated with 0.1% (w/v) gelatin in H_2O alone or containing a confluent layer of mitomycin C treated MEFs. Cells were passaged once they became

70% confluent, by aspiration of the media, followed by the addition of an appropriate volume of PBS depending upon the plate size. The PBS was aspirated and an appropriate volume of 0.5 mg/ml trypsin in PBS was added depending on the size of the dish. The cells were placed at 37°C for 5 min to generate a single cell suspension, followed by addition of media to neutralise the trypsin.

2.2.8 Electroporation of ES cells

ES cells were harvested by trypsinisation and counted using an improved neubauer haemocytometer (Marienfeld, Germany). Depending upon the particular experiment, either 1 x 10^8 or 1 x 10^7 cells were taken and washed with 20 ml PBS to remove any remaining media. The cells were resuspended in 1.6 ml PBS and the appropriate amount of caesium chloride prepared DNA to be electroporated was added. The mixture was placed into two Bio-Rad electroporation cuvettes and cells were electroporated with a Bio-Rad Gene Pulser equipped with a capacitance extender at 0.25 V and 500 μFD. The cells were left at room temperature for 5 min. They were then pooled and plated out onto an appropriate number of 10 cm plates containing mitomycin C treated MEFs. The day after the electroporation, the appropriate selection was applied. After one week, ES cell clones were visible. The media was aspirated and the ES cells were washed two times with PBS followed by the addition of 10 ml PBS. Using a pipette, each clone was individually picked into a single well of a 96 well plate containing 100 μl of 0.5 mg/ml trypsin in PBS. After 24 clones had been picked, the 96 well plate was transferred to 37°C for 5 min. Each clone was dissociated to a single cell suspension and transferred into a single well of a 48 well plate containing a confluent monolayer of Mitomycin c treated MEFs and ES cell media. Media was aspirated and replaced with fresh media daily minus selection. Once the ES cells became 60% confluent, they were harvested by trypsinisation, 100 μl was transferred to a single well of a 96 well plate containing 2x freezing mix and placed at –80°C, and 50 μl was transferred to a single well of a 12 well plate that had been pre-treated with 0.1% (w/v) gelatin. The ES cells on the 12 well plate were left until they were 100% confluent and were then lysed for DNA extraction to be used to screen for the detection of homologous recombinants by PCR and Southern blot analysis.

2.2.9 Selection of resistant ES cell/MEF clones

24 h after the introduction of exogenous DNA the appropriate selection was added in normal growth media and selection continued until distinct cell clones could be identified and picked (Table 4). The concentrations for selection had been previously established.

Table 4. Selections applied to transfected cells.

	Concentration used for selection of ES cells	**Concentration used for selection of MEFs**
G418	250 μg/ml	500 μg/ml
Hygromycin B	100 μg/ml	200 μg/ml
Gancyclovir (Roche)	0.6 μg/ml	Not applicable
Puromycin	0.9 μg/ml	1.2 μg/ml

2.2.10 Generation of transgenic mice

ES cells to be injected were grown in wells of a 12 well plate containing a confluent layer of Mitomycin c treated MEFs until they were 70% confluent. The ES cells were harvested by trypsinisation and the cells collected by centrifugation at 1250 rpm for 4 min. The ES cell pellet was resuspended in 500 μl Connaught Medical Research Labs (CMRL) media supplemented with 15% (v/v) embryonic stem cell qualified foetal bovine serum, 100 U/ml penicillin, 100μg/ml streptomycin, 20 mM L-glutamine and 10 mM sodium pyruvate. ES cells were injected into host blastocysts and implanted into surrogate female mice by J. Brown, Transgenic Unit, University of Leicester, following Home Office regulations under project licence number: 80/1260 held by C. Pritchard.

2.3 Protein Analysis

2.3.1 Standard cleared lysis of cells for protein analysis

Plates were placed on ice and the media was aspirated. Cells were washed twice with ice cold PBS and, dependent upon plate size, an appropriate volume of Gold lysis buffer (20 mM Tris·HCl [pH 7.9], 137 mM NaCl, 5 mM EDTA, 10% [v/v] glycerol, 1% [v/v] Triton X-100, 1 mM phenylmethylsulfonyl fluoride, 1 mM aprotinin, 1 mM leupeptin, 1

mM sodium orthovanadate) was added. The plates were placed on a moving platform at 4°C for 20 min. Using a cell scraper, the plates were scraped to ensure any unlysed cells were obtained, and the mixture was placed into an eppendorf on ice for 15 min. Tubes were centrifuged at 13000 rpm for 10 min at 4°C, and the supernatants were placed into fresh eppendorf tubes on ice. Tubes were centrifuged for a second time at 13000 rpm for 15 min at 4°C, and the supernatants were placed into fresh eppendorf tubes on ice. Protein concentrations were measured with the bicinchoninic acid (BCA) protein assay kit (Pierce). On a 96 well plate, different amounts of bovine serum albumin (BSA) were aliquoted in duplicate to provide a protein range of 0, 2, 5, 6, 8, 10, 15 and 20 μg. 5μl of the cell lysates were aliquoted into individual wells in duplicate. 200 μl of the BCA mix was added for each test and the plate was incubated at 37°C for 30 min. Using a plate reader (EL340 Microplate Biokinetics Reader), the OD_{630} was determined. A standard curve was plotted and using linear regression, the protein concentrations of the cell lysates were calculated. Each cell lysate was prepared for electrophoresis by the addition of 25 μl 4x laemmli loading buffer (250 mM Tris·HCl [pH 6.8], 8% [w/v] SDS, 20% [v/v] β-mercaptoethanol, 40% [v/v] glycerol, 0.004% [w/v] pyronin Y) made up to 100 μl with H_2O to give a final protein concentration of 1 μg/μl. Each sample was boiled at 100°C for 5 min.

2.3.2 Lysis of cells for protein analysis over a timecourse of stimulation

Attached cells were washed once with PBS and between 50 to 100 μl 1x laemmli loading buffer (62.5 mM Tris·HCl pH 6.8, 2% [w/v] SDS, 5% [v/v] β-mercaptoethanol, 10% [v/v] glycerol, 0.001% [w/v] pyronin Y) was added. Using a pipette and a swirling motion to ensure that all of the cells had been lysed, the mixture was removed from the well and placed into an eppendorf tube. The samples were boiled at 100°C for 5 min.

2.3.3 SDS-polyacrylamide gel electrophoresis (SDS-PAGE)

Either 6% or 10% separating polyacrylamide gels, depending upon the size of the protein of interest, were made with a 4% stacking gel (Table 5). Gels were placed in the mini-protean II container (BioRad) and were immersed in SDS-PAGE running buffer (192 mM glycine, 25 mM Tris-base, 0.1% [w/v] SDS). Between 10 μg and 20 μg of each protein sample were loaded per well. The protein samples were electrophoresed at 100 mA

through the 4% stacking gel and 200 mA through the separation gel using a Bio-Rad Power pac 300.

Table 5. Composition of SDS-PAGE gels.

	6% separation gel	**10% separation gel**		**4% Stacking gel**
H_2O	8.0ml	6.0ml	**H_2O**	3.6ml
1.5 M Tris·HCl (pH 8.8)	3.75ml	3.75ml	**0.5 M Tris·HCl (pH 6.8)**	1.5ml
30% acrylamide, 0.8% Bisacrylamide (National Diagnostics)	3.0ml	5.0ml	**30% acrylamide, 0.8% Bisacrylamide (National Diagnostics)**	0.8ml
10% SDS (w/v)	150µl	150µl	**10% SDS (w/v)**	60µl
10% APS (w/v)	150µl	150µl	**10% APS (w/v)**	60µl
N, N, N', N'-tetramethylethylenediamine	15µl	15µl	**N, N, N', N'-tetramethylethylenediamine**	6µl

2.3.4 Western blot analysis

SDS-PAGE gels were soaked in gel transfer buffer (192 mM glycine, 25 mM Tris, 0.01% [w/v] SDS) for 30 min. The proteins were electroblotted onto either 0.2 µm or 0.45 µm nitrocellulose filters (Schleicher and Schuell) pre-soaked in membrane transfer buffer (192 mM glycine, 25 mM Tris-base, 0.01% [w/v] SDS, 10% [v/v] methanol) at 1 mA/cm^2 for 90 min using a semi-dry blotting apparatus. After transfer, Western blots were stained with Ponceau S stain (0.5% (w/v) Ponceau S made in 5% (w/v) trichloroacetic acid), and protein loadings were compared. After three washes at 15 min intervals in Tris-buffered saline (10 mM Tris·HCl [pH 7.6], 150 mM NaCl) containing 0.05% (v/v) Tween 20 (TBS/Tween), non-specific sites were blocked by incubation of the blots at room temperature with gentle shaking in 5% (w/v) non-fat milk powder (Marvel) in TBS/Tween for 1 h. However, if the blots were to be subsequently incubated with anti phospho-p38 MAPK, they were incubated with 3% (w/v) BSA overnight at 4°C with gentle shaking. After three washes at 15 min intervals in TBS/Tween, the blots were incubated with an

appropriate dilution of primary antibody (Table 6) in TBS/Tween, or in 0.5% (w/v) BSA in TBS/Tween if using anti phospho-p38 MAPK overnight at 4°C with gentle shaking. The filters were washed three times at 15 min intervals in TBS/Tween and incubated with a 1:3500 dilution in TBS/Tween of the appropriate (Table 6) secondary antibody coupled to horseradish peroxidase for 1 h with gentle shaking at room temperature. After washing three times at 15 min intervals with TBS/Tween, the enhanced chemiluminescence detection system (Pierce) was used to visualise antigen-antibody complexes by placing the blots onto plastic wrap, mixing an equal ratio of the two solutions, and adding 1 ml of the mixture to each blot ensuring an even distribution for 3 min. Excess liquid was removed from the blots, they were then wrapped in Saranwrap and placed into a cassette and various times of exposure to photographic film (Fuji) were performed at room temperature.

Table 6. Details of primary antibodies used for Western blot analysis.

	Size of protein (kDa)	Dilution	Type and secondary	Company
Raf-1	74	1:1000	mouse monoclonal	Transduction Laboratories
A-Raf	68	1:1000	rabbit polyclonal	Santa Cruz Biotechnology, Inc
phospho-ERK	42 + 44	1:2000	mouse monoclonal	New England Biolabs
ERK	42 + 44	1:1000	rabbit polyclonal	Zymed Laboratories, Inc.
Vinculin	116	1:1000	mouse monoclonal	Gift from Dr. V. Koteliansky, CNRS, Paris
SV40 Large T	85	1:5000	Mouse polyclonal	PharMingen
phospho-p38 MAPK	38	1:1000	rabbit polyclonal	New England Biolabs
p38 MAPK	38	1:1000	goat polyclonal	Santa Cruz Biotechnology, Inc

2.3.5 Stripping Western blots

Western blots were incubated in 0.5 M Glycine, 1% (w/v) SDS pH 2.8 with HCl on a shaking platform for 15 min at room temperature. The blots were blocked again before incubation with a different antibody.

2.4 Proliferation, apoptosis and differentiation analysis

2.4.1 Cell growth profiles

Each MEF cell line was seeded onto a 24 well tissue culture plate at a density of 1 x 10^4 cells per well in triplicate in MEF media. At 24 hourly intervals, the cells were trypsinised and resuspended in 1 ml of media. The cells were transferred to eppendorf tubes and centrifuged at 2000 rpm for 5 min. The supernatant was aspirated and the cell pellets resuspended in 100 µl media. 100 µl of a 0.4% (v/v) Trypan Blue solution (Sigma) was added, and the viable cells that did not take up the dye were counted using a haemocytometer.

2.4.2 BrdU proliferation analysis

MEFs were plated out onto 3.5 cm dishes at a density of 2 x 10^4 cells. The plates were allowed to become 60% confluent and then serum free MEF media was added to the cells and they were left overnight. The next day MEF media containing 15% serum plus 10 µM Bromodeoxyuridine (BrdU; Amersham/Pharmacia Biotech) was added and the cells were left for 18 h at 37°C. The next day, the cells were washed once with PBS and then fixed by the addition of 4% (w/v) paraformaldehyde in PBS for 20 min at room temp. After three washes at 15 min intervals with PBS, cells were permeabilised by the addition of 0.2% (v/v) Triton X 100 in PBS for 20 min. After three washes at 15 min intervals with PBS, DNA was denatured by the addition of 1.5 M HCl for 10 min. After three washes at 15 min intervals with PBS, Non-specific sites were blocked by the addition of 10% (v/v) FCS in PBS for 30 min. After three washes at 15 min intervals with PBS, a 1:10 dilution in PBS of a monoclonal rat anti-BrdU antibody (gift from H. Paterson, Institute of Cancer Research, London) was added for 1 h at 37°C in a humidified chamber. After three washes at 15 min intervals with PBS, 1:50 dilution in PBS of a goat-anti-Rat IgG FITC coupled secondary antibody (Southern Biotechnology Associates) was added to the cells for 1 h at 37°C in a humidified chamber. After three washes at 15 min intervals with PBS, mounting solution (80% [v/v] glycerol in PBS) was added and a coverslip placed on top. This was sealed using nail varnish. A minimum total of 100 cells per dish was counted and scored for whether or not the nuclei were fluorescent using a fluorescence microscope (Zeiss Axiophot). Data were analysed by using the two-tailed unpaired *t*-test.

2.4.3 Annexin V FITC staining of cells

MEFs were plated out onto 6 cm dishes at a density of 1.5 x 10^5 cells. These were placed in a humidifying incubator at 37°C. The next day, fresh media was added to the plates and they were returned to 37°C, or, if the cells harboured the tsSV40T antigen they were placed at the restrictive temperature of 39.5°C. The day after, the plates were either left untreated, placed in serum free MEF media or 50 μM etoposide or 50 ng/ml anti-CD95 monoclonal antibody (PharMingen) plus 0.5 μM cycloheximide and placed in a humidifying incubator at 37°C (or 39.5°C) for 20 h. The media was removed and placed in a tube. 1 ml PBS was added, removed and placed into the tube. 1 ml of 0.125 mg/ml trypsin in PBS was added and the cells were placed at 37°C for 5 min. 1 ml media was added to neutralise the trypsin, and the cells were placed into the tubes containing the suspension cells. The tubes were centrifuged for 5 min at 1500 rpm to collect both suspension and attached cells in a pellet. The supernatant was removed and discarded. The cell pellets were resuspended in 1 ml media and were placed in a humidifying incubator at 37°C for 20 min to allow the phosphatidyserine groups to re-equilibrate. 500 μl was removed from the tubes and was discarded. The tubes were centrifuged for 5 min at 1500 rpm to collect the cells. The supernatant was removed and discarded. Phosphatidylserine externalisation was quantified by resuspending the cell pellets in 500 μl 1x Annexin binding buffer (Bender MedSystems; 10 mM HEPES/NaOH [pH 7.4], 140 mM NaCl, 2.5 mM CaCl) plus 5 μl Annexin V-FITC (Bender MedSystems) followed by incubation at room temp for 10 min. 1 μg/ml propidium iodide in H_2O was added to allow the measurement of membrane integrity. Cells were analysed by fluorescence activated cell sorting (Becton Dickinson) in conjunction with CELLQuest software, with 5000 events recorded per assay. Data were analysed by using the two-tailed unpaired *t*-test.

2.4.4 Hoechst staining

Live cells were stained with 5 μg/ml Hoechst 33258 in PBS for 1 h at 37°C. Apoptotic cells were identified as those with brightly stained, condensed nuclei. Images were recorded using a Leica TC54D confocal microscope.

2.4.5 Teratoma formation

ES cells were cultured, trypsinised, and washed with PBS and 5 x 10^6 cells in PBS were injected subcutaneously into the flank of 8-week-old syngeneic 129Ola male mice. After 3 weeks, tumours were dissected, weighed, fixed in 4% (w/v) paraformaldehyde in PBS, embedded in paraffin and 5 μm sections were prepared and stained with haematoxylin and eosin and viewed using a Leica DMLB light microscope. The sections were prepared by S. Giblett, Department of Biochemistry, University of Leicester.

3 GENERATION OF A CONDITIONAL RAF-1 KNOCKOUT MOUSE

3.1 Introduction

3.1.1 Cre/loxP technology and its use in knockouts

The general approach to embryonic stem (ES) cell mediated gene targeting has been to create null mutations in the gene of interest by deleting part of the target gene and replacing it with an antibiotic resistance gene. However, this approach is limited by the fact that the alteration is present in the germline and is thus present in all cells at all times during development. Therefore, if the genetic change results in an early lethal phenotype, later phenotypes cannot be assessed. An example of an early lethal phenotype is that of the targeted disruption of the *talin* gene, as the mutant embryos die at the gastrulation stage of embryonic day (E) 8.5-9.5 (Monkley *et al.*, 2000). An even earlier lethal phenotype is observed with the targeted disruption of the *cadherin* gene, as the mutant embryos die at around the time of implantation (Larue *et al.*, 1994). Gene disruptions that result in such early lethal phenotypes limit studies even further as even primary mouse embryonic fibroblasts (MEFs) cannot be generated. Also, tumour studies cannot be performed as these studies utilise older animals. Moreover, a genetic change that produces a complex multi-component phenotype could be more easily analysed if the alteration were restricted to one tissue or cell type. By combining the Cre/*lox*P site-specific recombination system with transgenic technologies, it has become possible to introduce conditional genome alterations that are spatially and temporally restricted.

Cre is the 38kDa product of the *cre* (cyclization recombination) gene of bacteriophage P1 that recognises and mediates site-specific recombination between 34 bp sequences referred to as *lox*P (locus of crossover (x) in P1). The *lox*P sequence consists of two 13 bp inverted repeats interrupted by an 8 bp non-palindromic spacer sequence. It is the spacer that determines the orientation of the *lox*P sequence (Figure 3.1; Hoess and Sternberg, 1982; Hoess and Abremski, 1984).

Fig. 3. 1. Sequence of a *lox*P site.

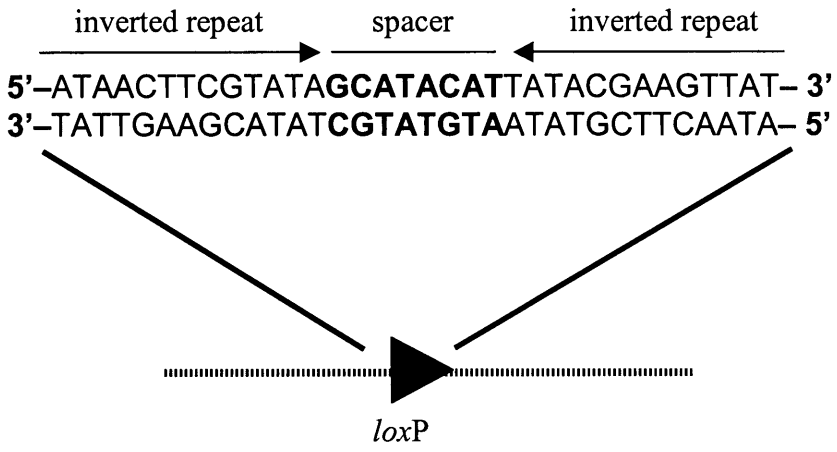

When two *lox*P sites are placed in the same orientation on a linear DNA molecule, including a mammalian chromosome, and Cre is added, a Cre-mediated intramolecular recombination event occurs, resulting in the excision of the *lox*P flanked, or 'floxed' sequence (Figure 3.2; Sauer and Henderson, 1989).

Fig. 3. 2. Cre-mediated deletion of a floxed gene upon addition of Cre.

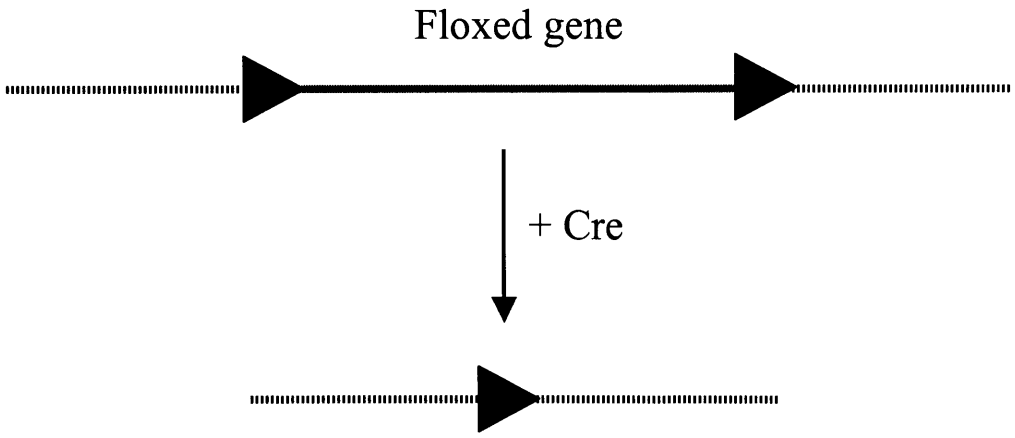

Cre/loxP mediated gene deletion in mice and mammalian cells is accomplished in two steps. The first is the incorporation of *lox*P sites via homologous recombination into the genome of mouse ES cells, flanking the gene of interest, to generate a 'floxed' allele via corresponding targeting vectors and the identification of these homologous recombinant

clones. The final genetic modification is obtained by a Cre-mediated deletion event, either by transient or stable transfection of a plasmid expressing Cre in cultured ES cells, which can then be used to make mice. Alternatively the Cre-mediated deletion event can be achieved in a conditional manner, in mice by the expression of Cre as a transgene. Expression of the Cre transgene can be restricted by placing it under the control of a tissue-specific promoter or an inducible promoter resulting in spatial and temporal specificity of Cre-mediated deletion. Alternatively, a chimeric Cre protein can be created such that Cre is only active when the corresponding synthetic ligand is administered such as by fusing Cre to a ligand binding domain of a receptor (discussed in Section 3.1.2). This will result in temporal specificity of Cre mediated deletion. Moreover, it can also be placed under the control of a tissue-specific promoter (Torres and Kühn, 1997). A website exists that lists the different available Cre transgenic mice (http://www.mshri.on.ca/nagy/default.htm).

3.1.2 Previous reported uses of the Cre/loxP recombination system

The first reported use of the Cre/*lox*P recombination system in the generation of a conditional knockout in mice was by Gu *et al.* (1994). They flanked a segment of the DNA polymerase β gene (*polβ*) with *lox*P sites ($polβ^{flox}$). The *lox*P sites were introduced into introns to prevent disruption of the gene. Animals homozygous for the $polβ^{flox}$ mutation survived and were healthy, in contrast to the homozygous *polβ* knockout mice that died during embryogenesis. This indicates that the presence of the *lox*P sites does not severely affect *polβ* expression *in vivo*. A mouse line expressing Cre under control of the *lck* proximal promoter (cre^{lck}), which means it is selectively expressed in T lineage cells, was used to selectively delete the *polβ* gene. Mice homozygous for $polβ^{flox}$ and harbouring cre^{lck} were assessed and the development of these mice was normal. However, 38% of $CD4^+$ and $CD8^+$ thymocytes had deleted the *polβ* gene, and no detectable deletion was observed in B lymphocytes as assessed by Southern blot analysis. The reasons for incomplete deletion of the *polβ* gene in T cells could be due to the fact that the *lck* proximal promoter is only transiently active early on in T cell development and therefore this limited the time for completion of recombination. In addition, the particular *cre* gene that was used has subsequently been found not to be expressed as optimally as other *cre* genes (Gu *et al.*, 1994).

Kühn *et al.* (1995) reported on the use of an inducible Cre recombinase, that of an inducible promoter of the mouse *Mx1* gene. The *Mx1* gene is part of the defence to viral infections and is silent in healthy mice. However, upon the administration of interferon-α (IFN-α) or IFN-β, the *Mx1* promoter can be transiently activated to high amounts of transcription in many tissues. A mouse line expressing Cre under control of the *Mx1* promoter (*Mx-cre*) were crossed to $pol\beta^{flox}$ mice. Offspring at 8 weeks old and homozygous for $pol\beta^{flox}$ and harbouring *Mx-cre* were assessed following the injection of recombinant human IFN-α. Excision of the floxed target genes occurred in all organs. However, the only complete deletion occurred in the liver and a nearly complete deletion occurred in lymphocytes as assessed by Southern blot analysis. The least amount of deletion occurred in the brain which is probably due to lack of transport of IFN across the blood-brain barrier. A reason for the tissue variation in Cre-mediated deletion could be due to the differing availability of IFN in the different tissues or the different responsiveness of particular cell types to IFN. Also the proliferation rates of different tissues varies considerably which may affect Cre-mediated recombination (Kuhn, 1995).

Feil *et al.* (1996) reported the use of ligand-activated site-specific recombination in mice. They created transgenic mice expressing Cre-ER, representing a fusion protein between Cre and a mutated ligand-binding domain of the human estrogen receptor. Cre-ER was placed under the control of a cytomegalovirus (CMV) promoter. These mice were crossed to reporter mice harbouring a floxed target gene. The gene that was floxed in the reporter mice was a modified retinoid X receptor α (RXRα) allele carrying a floxed neomycin resistance gene integrated by homologous recombination. When 4-hydroxytamoxifen was injected intraperitoneally into 4 week old offspring, excision of the floxed target gene in all organs except in the thymus occurred. No excision of the floxed target gene was observed in control mice. Semi-quantitative PCR was used to estimate the extent of gene excision. These results indicate that Cre-ER is a tightly regulated recombinase that displays undetectable activity in the absence of ligand and can be activated in mice by 4-hydroxytamoxifen treatment. Excision of the floxed target gene was most efficient in skin, tail, kidney and spleen where it occurred in 40-50% of cells. 30% excision was achieved in the liver and stomach. 15% excision was achieved in other tissues. An explanation for the differing efficiencies of excision could be due to the fact that CMV-driven transgene

expression varies considerably between different cell types. It could also be due to differences in accessibility of particular tissues to hydroxytamoxifen. Also, the proliferation rates of tissues varies considerably which may affect Cre-mediated recombination (Feil *et al.*, 1996).

Schwenk *et al.* (1995) generated a Cre transgenic mouse line that carries several copies of the Cre gene under control of a human CMV minimal promoter and is referred to as a deleter strain. These mice were crossed to the $pol\beta^{flox}$ mice and Southern blot analysis of homozygous offspring showed that complete deletion of the floxed gene in all cell lineages including germ cells had occurred, indicating that Cre is ubiquitously expressed from very early in development. This particular Cre transgenic mouse line is useful for generating null alleles through the germline.

Therefore, as described, deletion of a floxed target sequence can be successfully restricted to specific cell types and/or at a specific time during development, or in all cell types ranging from very early on in embryogenesis to adulthood. Currently this is only limited by the availability of Cre expresssing transgenic mice. This means that once a floxed mouse line has been generated, the function of the floxed target gene can be assessed independently in a large number of different tissues and at different times during development.

Other uses of Cre/*lox*P technology include; chromosome translocations which are useful for modelling human diseases that are associated with chromosomal rearrangements (Smith *et al.*, 1995; Van Deursen *et al.*, 1995) and conditional knockins, which are particularly useful for tumour studies. For example, two groups reported on the generation of mice that harbour oncogenic K-Ras that only becomes activated upon the expression of Cre. They used a recombinant adenovirus that expressed Cre in lung epithelial cells and once the adenovirus was delivered it resulted in the rapid onset of tumorigenesis. This allowed the development of a new model for human lung cancer progression due to control over the time of tumour initiation (Jackson *et al.*, 2001; Meuwissen *et al.*, 2001).

Fig. 3. 3 Knockout targeting event for the *raf-1* gene; Hüser *et al.* (2001).
(A) Restriction map of the targeted part of the wild-type *raf-1* gene indicating exons 10 to 13. **(B)** Targeting vector that contains a short and a long arm of homology to the *raf-1* gene separated by the neo^R gene, and also containing the herpes simplex virus-thymidine kinase (*HSV-tk*) gene for a negative selection marker. **(C)** *raf-1* targeted allele after homologous recombination with the targeting vector results in the replacement of exons 10 to 13 with the neo^R gene.

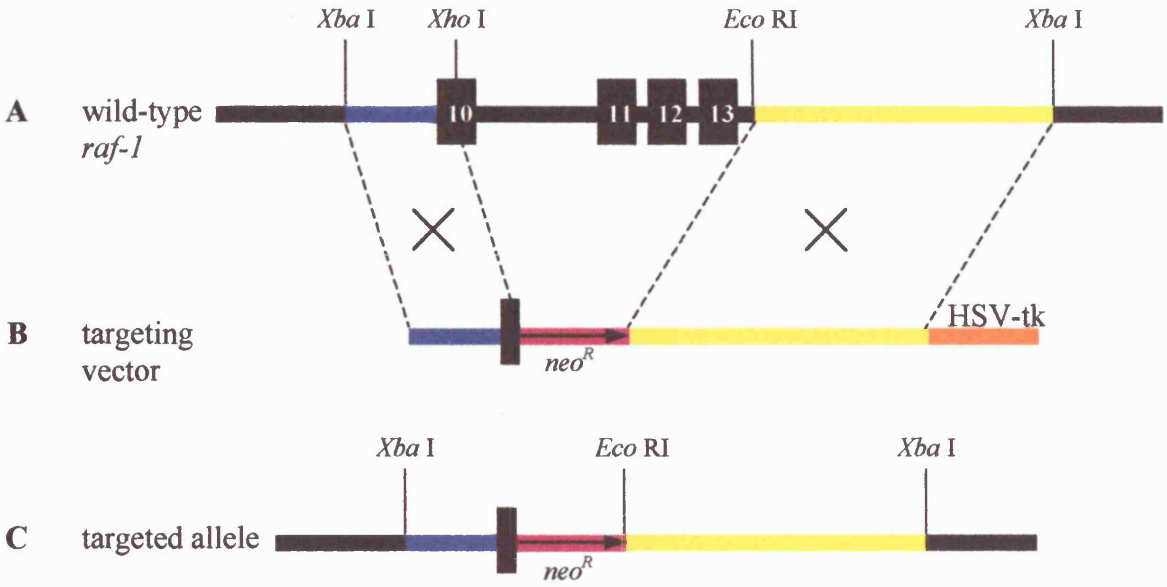

3.1.3 Conventional knockout of raf-1

A knockout of the *raf-1* gene in mice was previously accomplished in our laboratory and is described in Hüser *et al.* (2001). This was achieved by construction of a targeting vector that resulted in the introduction of a neomycin resistance (neo^R) gene to replace approximately 6 kb of *raf-1* genomic DNA encoding exons 10 to 13 that encodes amino acids 338 to 472 (Figure 3.3). No Raf-1 protein or N-terminal Raf-1 fragment was expressed in protein lysates prepared from mice homozygous for this mutation as detected by Western blot analysis or Raf-1 kinase assays.

The phenotype of the homozygous Raf-1 deficient mice differs depending upon genetic background. On the C57/BL6 inbred background embryos survived to E9.5. However on the MF-1 outbred background a few survived up to birth. These results indicated that *raf-1* is an essential gene for development. Therefore, the only way to study the function of Raf-1 in adult tissues was to generate a conditional allele for Raf-1 in mice. With the ever-expanding database of new Cre expressing transgenic mice, the generation of such a conditional *raf-1* knockout has many implications for further analysis of Raf-1 function.

3.2 Aims

The aim of this part of the project was to flank the *raf-1* gene with *lox*P sites generating a 'floxed' *raf-1* allele in mouse ES cells and to consequently produce a mouse line harbouring these sites. The reason for flanking the whole *raf-1* gene with *lox*P sites was because Wojnowski *et al.* (1998) targeted exon 3 of *raf*-1 with an aim to produce a null, but instead this resulted in the generation of a truncated Raf-1 protein that had residual kinase activity. Moreover, the generation of the Raf-1 knockout described in Hüser *et al.* (2001) had not been completed by the time that this project began. Therefore it was not known whether the deletion of exons 10 to 13 would result in no Raf-1 protein being produced.

The *raf-1* gene is too large to be able to use just one targeting vector to introduce two *lox*P sites. Therefore, to flank the *raf-1* gene with two *lox*P sites required the generation of two targeting constructs harbouring *lox*P sites and performing two independent targeting events

in ES cells, with one being targeted to the 5' end of *raf-1* within intron 2 and the other being targeted to the 3' end of *raf-1* after the 3' untranslated region. The *lox*P sites were placed approximately 26.8 kb apart with the intervening sequence containing exons 3 to 17. Once ES cells were identified that had homologously recombined both targeting events, the aim was to generate mice.

3.3 Results

The gene for *raf-1* had previously been isolated by screening a Stratagene mouse genomic library made from mouse strain 129Sv DNA cloned into the *Xba* I site in the Lambda vector Lambda-FIX. *raf-1* phages were isolated by screening with the full length *raf-1* cDNA and eight phages were isolated. These were restriction mapped. Two of these λ clones (λ1 and λ13) were used in construction of the two targeting vectors (Figure 3.4). The aim was to produce two targeting vectors, each with a 5' arm and a 3' arm separated by a *lox*P sequence and a selectable marker. Therefore homologous recombination between the arms and the endogenous *raf-1* gene will result in the incorporation of the *lox*P sequence and the selectable marker. Two more vectors were to be constructed that would act as a positive control for PCR to test primers that would be used to screen ES cell clones for homologous recombination events. The reason for this is because homologous recombination events are very rare, and as the PCR is specific for the homologous recombination event (i.e. one primer outside the targeting event in the gene of interest and one primer unique to the targeting event such as a neo^R sequence), the only way to work out optimal PCR conditions is to generate a vector that has these sequences adjacent to each other.

3.3.1 Construction of the 5' loxP targeting vector

The 3' arm of the 5' targeting construct was derived from λ clone 1. This was a 4.4 kb *Xba* I fragment subcloned from pSP/*raf-1*/4.4 kb/*Xba* I (Figure 3.4 and 3.5A; provided by Dr. C. Pritchard) into *Xba* I digested pBluescript II KS^+ (pBS II KS^+) containing a single *lox*P sequence (Figure 3.5B; pBS II KS^+-*lox*P). The resulting vector, confirmed by *Hin*d III restriction digestion analysis was named pBS II KS^+-*lox*P-4.4 kb *raf-1* (Figure 3.6A).

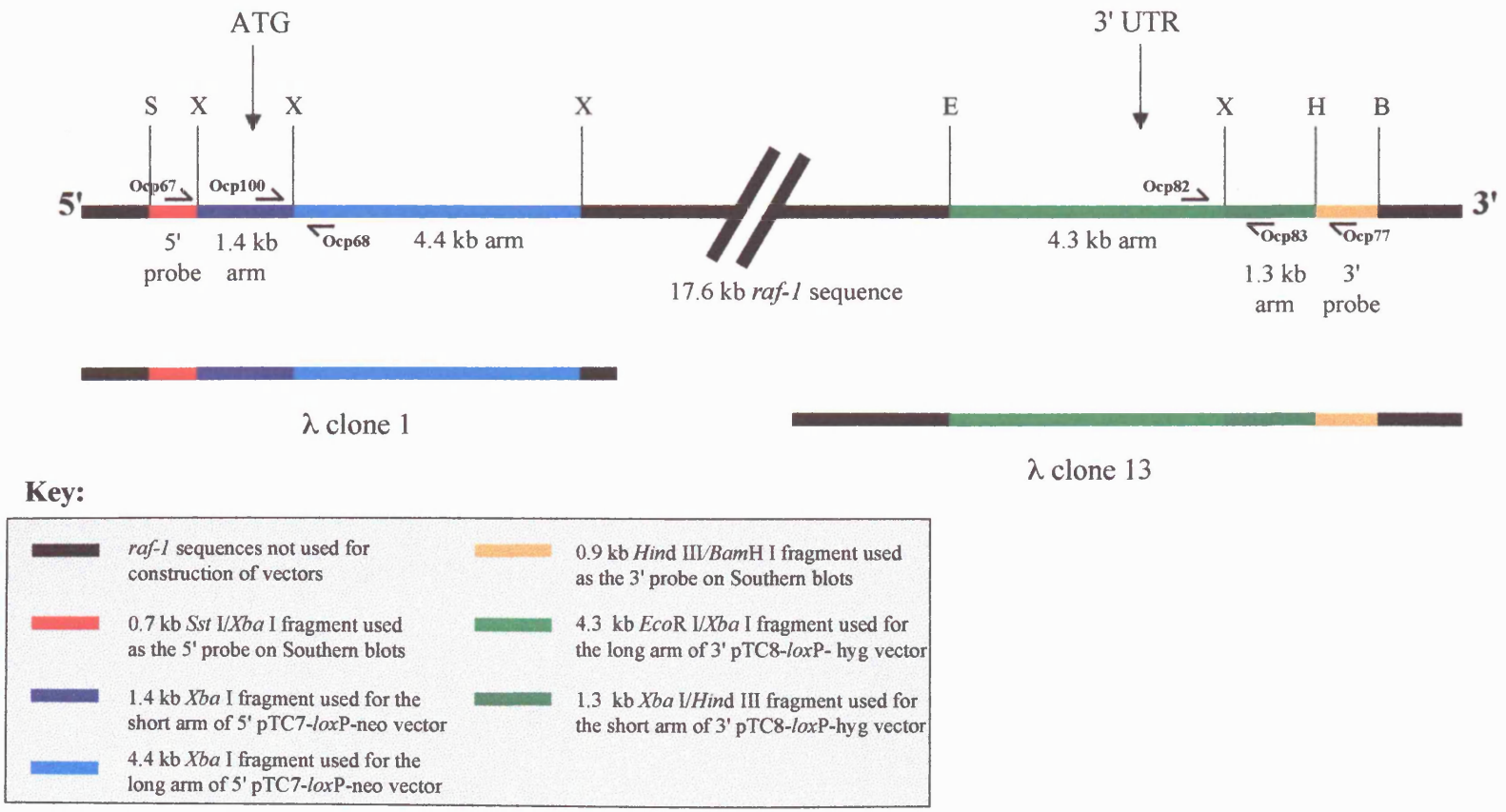

Fig. 3. 4. Restriction map of *raf-1* showing the restriction fragments used for construction of the arms of the 3' and 5' *loxP* targeting constructs and the fragments used as probes for Southern blot analysis of targeted ES cell clones. The λ clones that contain the restriction fragments used for cloning are also shown. The positions of primers Ocp67, Ocp100, Ocp68, Ocp82, Ocp83 and Ocp77 are indicated. Single letter key: S = *Sst* I X = *Xba* I E = *Eco*R I H = *Hind* III B = *Bam*H I

Fig. 3.5 First part of the construction of the 5' pTC7-*lox*P-neo targeting construct. **(A)** Restriction map of pSP72/*raf-1*/4.4 kb/*Xba* I, highlighting the *Xba* I sites used for cloning. **(B)** Restriction map of pBS II KS^{+}/*lox*P, highlighting the *Xba* I site used for cloning. **(C)** Restriction map of pSP/*raf-1*/ 1.4 kb *Xba* I, highlighting the *Xba* I sites used for cloning. **(D)** Restriction map of pX53-neo, highlighting the *Hpa* I site used for cloning.

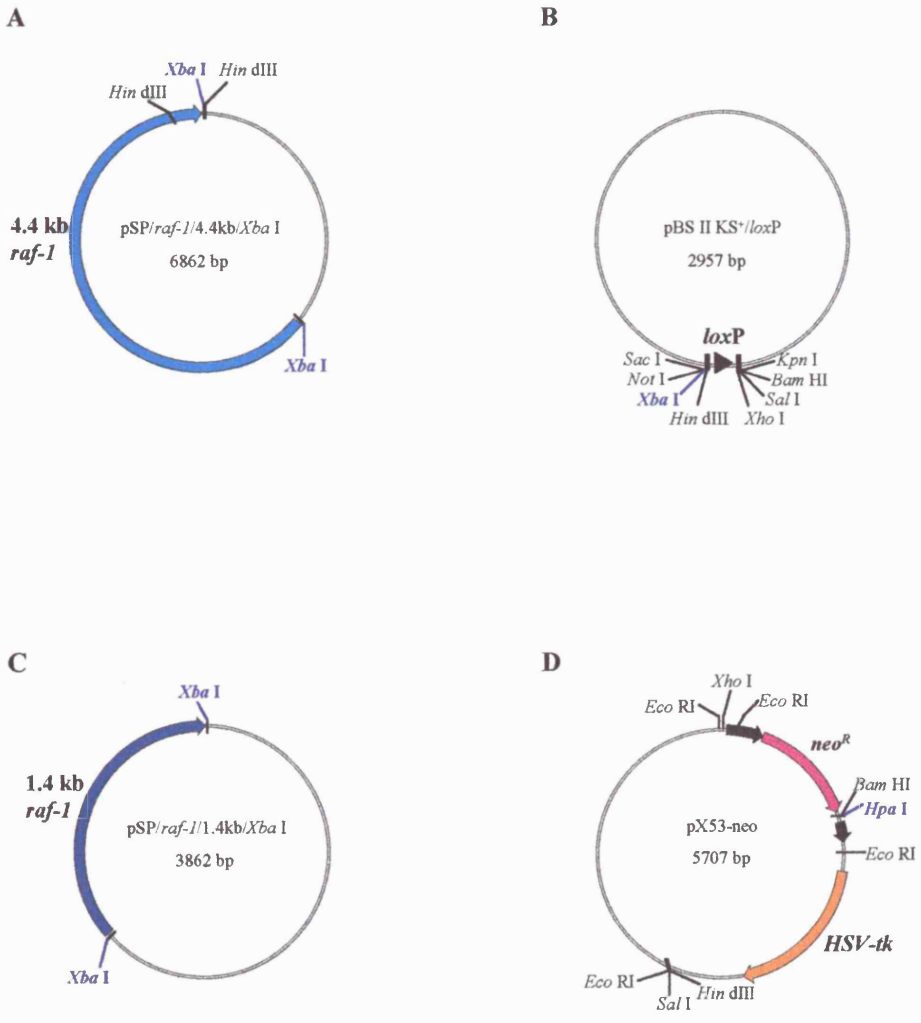

Fig. 3.6 Second part of the construction of the 5' pTC7-*lox*P-neo targeting construct. **(A)** Restriction map of pBS II KS$^+$ *lox*P-4.4 kb *raf-1*, highlighting the *Sal* I site used for cloning. **(B)** Restriction map of pX53-neo-1.4 kb *raf-1*, highlighting the *Sal* I and *Xho* I sites used for cloning. **(C)** Restriction map of pTC7-*lox*P-neo, highlighting the *Not* I and site used to linearise the vector before electroporation into ES cells. **(D)** Restriction digestion of pTC7-*lox*P-neo with various enzymes followed by agarose gel electrophoresis. M = 1 kb DNA marker.

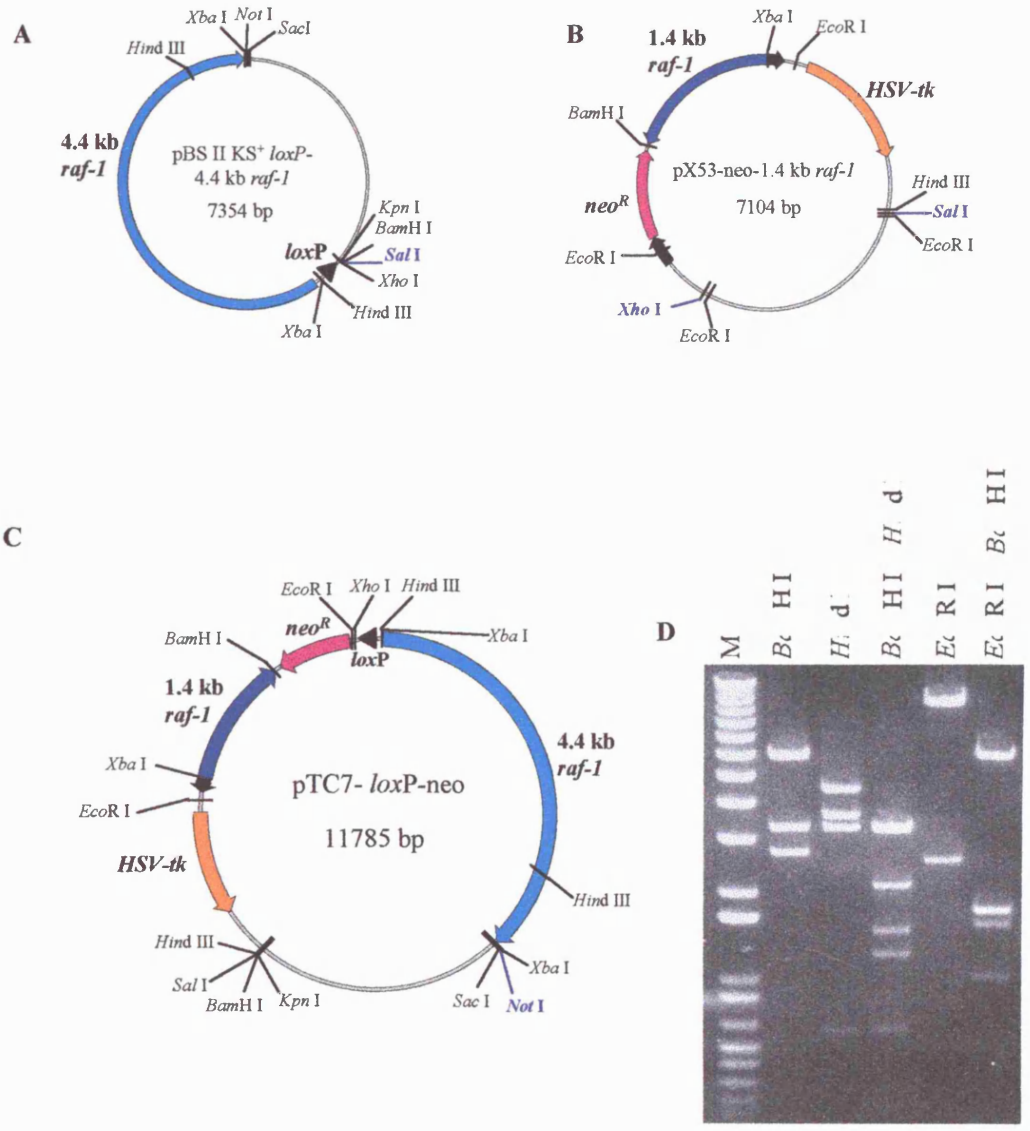

The 5' arm of the 5' targeting construct was also derived from λ clone 1. This was a 1.4 kb *Xba* I fragment subcloned from pSP-*raf-1*-1.4 kb-*Xba* I (Figure 3.4 and 3.5C; provided by Dr. C. Pritchard) that was subsequently filled in and blunt end ligated with the *Hpa* I digested pX53-neo plasmid (Figure 3.5D). This plasmid harbours a neomycin resistance (*neo*^{R}) gene that allows for positive selection and a Herpes Simplex Virus (HSV) *thymidine kinase* (*tk*) gene that allows for negative selection; both of these genes are driven by the *tk* promoter. The resulting vector was confirmed by *Sst* I restriction digestion analysis and was named pX53-neo-1.4 kb *raf-1* (Figure 3.6B).

The final stage in construction of this targeting vector was to digest pX53-neo-1.4 kb *raf-1* with *Xho* I and *Sal* I, followed by gel purification of the fragment and ligation to *Sal* I digested pBS II KS$^+$-*lox*P-4.4 kb *raf-1*. The resulting vector was named pTC7-*lox*P-neo (Figure 3.6C). Restriction mapping using several restriction enzymes was performed to confirm the vector obtained was correct (Figure 3.6D).

3.3.2 Construction of a positive control vector for PCR detection of the 5' targeting event

A positive control vector was constructed with an aim to establish optimum PCR conditions with the primers to be used for the detection of the pTC7-*lox*P-neo homologous recombination event in ES cells. A 0.7 kb *Sst* I/ *Xba* I fragment was derived from λ clone 1 and subcloned from pSP-*raf-1*-7 kb-*Eco*R I/*Hin*d III (Figure 3.4 and 3.7A; provided by Dr. C. Pritchard) into pBS II KS$^+$ (Figure 3.7B). This vector was confirmed by restriction digestion analysis with *Eco*R I and *Hin*d III and was named pBS II KS$^+$ 0.7 kb *raf-1* (Figure 3.7C).

A 2561 bp *Eco*R I fragment was gel purified from pX53-neo-1.4 kb *raf-1* (created in construction of pTC7-*lox*P-neo). This fragment contained the *neo*^{R} gene and the 1.4 kb *raf-1 Xba* I fragment (Figure 3.7D).

The final stage in construction of the PCR vector was to ligate the 2561 bp *Eco*R I fragment to *Eco*R I digested pBS II KS$^+$ 0.7 kb *raf-1*. This vector was named positive control PCR vector (Figure 3.7E). A single diagnostic restriction digestion with *Bam*H I

Fig. 3.7 Construction of the positive control PCR vector. (**A**) Restriction map of pSP/*raf-1*/ 7 kb /RI/H3 highlighting the *Sst* I and *Xba* I sites used for cloning. (**B**) Restriction map of pBS II KS$^+$ highlighting the *Sst* I and *Xba* I sites used for cloning. (**C**) Restriction map of pBS II KS$^+$ 0.7 kb *raf-1* highlighting the *Eco*R I site used for cloning. (**D**) Restriction map of pX53-neo-1.4 kb *raf-1* highlighting the *Eco*R I sites used for cloning. (**E**) Restriction map of PCR vector highlighting the positions of primers Ocp67 and Ocp69. (**F**) Restriction digestion with *Bam*H I and agarose gel electrophoresis to screen bacterial clones 1-6 for presence of the positive control PCR vector. (**G**) PCR of bacterial clones 1, 3 and 6 using Ocp67 and Ocp69 to ensure that the PCR is specific. M = 1 kb DNA marker.

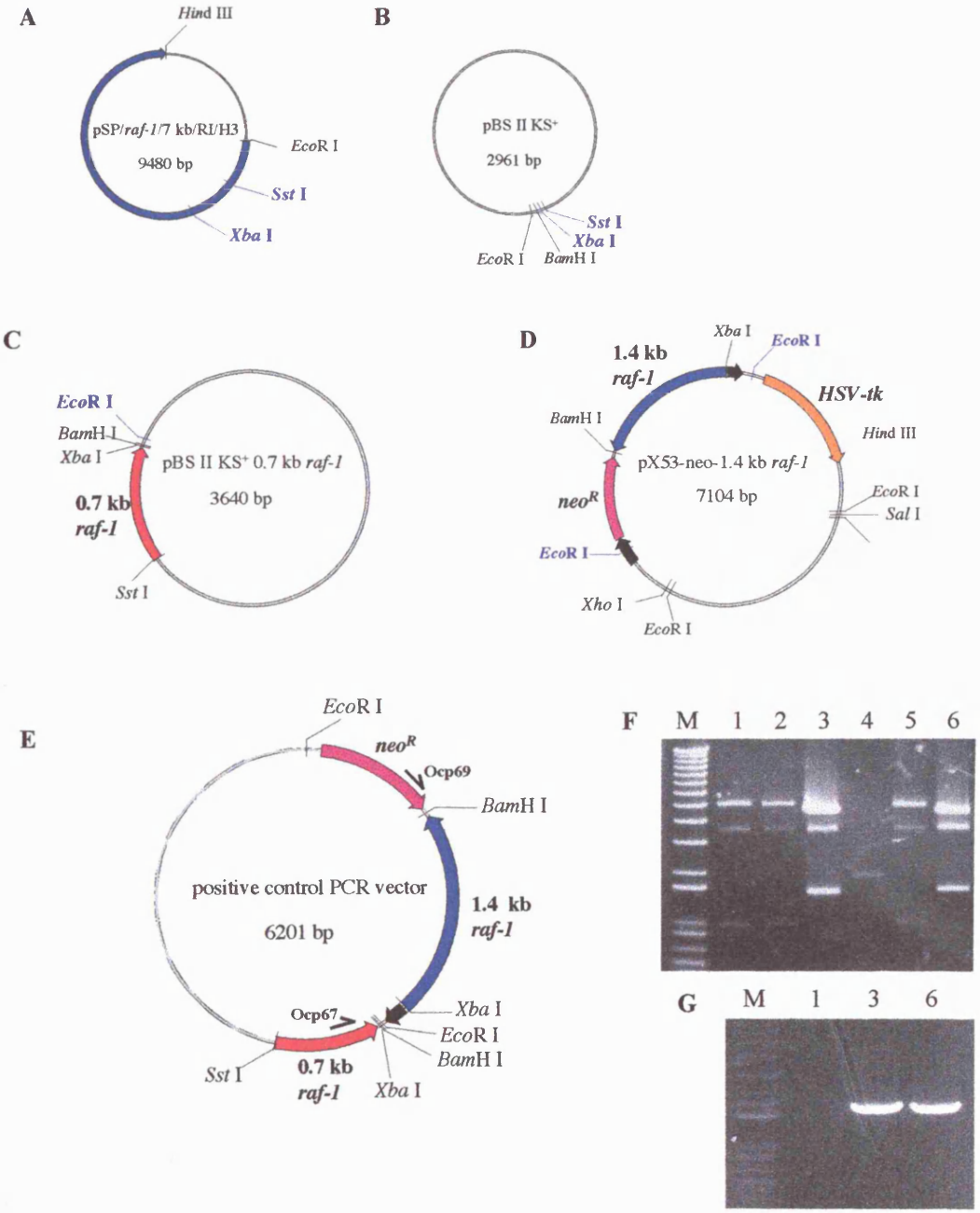

was used to confirm that the *Eco*R I insert ligated in the correct orientation, yielding fragments of sizes 4763 bp and 1598 bp. Clone numbers 3 and 6 were found to be correct; the others were incorrect (Figure 3.7F). Clones 3 and 6 were then used in a PCR reaction with Ocp67 and Ocp69, and a product of the correct size (1815 bp) was visualised in these two clones (Figure 3.7G). These primers could now be used to screen ES cell clones for the 5' homologous recombination event with pTC7-*lox*P-neo.

3.3.3 Construction of the 3' loxP targeting vector

The 5' arm of the 3' targeting construct was derived from λ clone 13. This was a 4.3 kb *raf-1 Eco*R I/*Sal* I fragment subcloned from pSP-*raf-1*-4.3 kb-*Eco*R I/*Xba* I (Figure 3.4 and 3.8A; provided by Dr. C. Pritchard) that was subsequently filled in at the *Eco*R I site only and ligated with *Sal* I and *Bam*H I digested pBS II KS$^+$/*lox*P that had also been filled in at the *Bam*H I site (Figure 3.8B). The resulting vector was confirmed by restriction digestion analysis with *Hin*d III and *Kpn* I and was named pBS II KS$^+$-*lox*P-4.3 kb *raf-1* (Figure 3.9A).

The 3' arm of the 3' targeting construct was also derived from λ clone 13. This was a 1.3 kb *Xba* I/ *Hin*d III fragment subcloned from pBS II KS$^+$-1.3 kb-*raf-1*-X/H (Figure 3.4 and 3.8C) that was subsequently filled in and blunt end ligated with the *Hpa* I digested pX53-hyg plasmid (Figure 3.8D). This plasmid harbours the hygromycin resistance (*hyg*^{R}) gene that allows for positive selection and the HSV-*tk* gene; both of these genes are driven by the *tk* promoter. The resulting vector was confirmed by restriction digestion analysis with *Sst* I and was named pX53-hyg-1.3 kb *raf-1* (Figure 3.9B).

The final stage in construction of this targeting vector was to digest pX53-hyg-1.3 kb *raf-1* with *Hin*d III, gel purification of the fragment and ligation to *Hin*d III digested pBS II KS$^+$-*lox*P-4.3 kb *raf-1*. The resulting vector was named pTC8-*lox*P-hyg (Figure 3.9C). Restriction mapping using several restriction enzymes was performed to confirm the vector obtained was correct (Figure 3.9D).

The design of both targeting vectors was such that the transcriptional direction of the antibiotic resistance genes (*neo*^{R} gene and *hyg*^{R} gene) were in the opposite orientation to

Fig. 3.8 First part of the construction of the 3' pTC8-*lox*P-hyg targeting construct. (**A**) Restriction map of pSP/*raf-1*/4.3/E/X, highlighting the *Eco*R I and *Sal* I sites used for cloning. (**B**) Restriction map of pBS II KS$^+$ *lox*P, highlighting the *Sal* I and *Bam*H I sites used for cloning. (**C**) Restriction map of pBS II KS$^+$ -1.3kb-*raf-1*-X/H, highlighting the *Xba* I and *Hin*d III sites used for cloning. (**D**) Restriction map of pX53-hyg, highlighting the *Hpa* I site used for cloning.

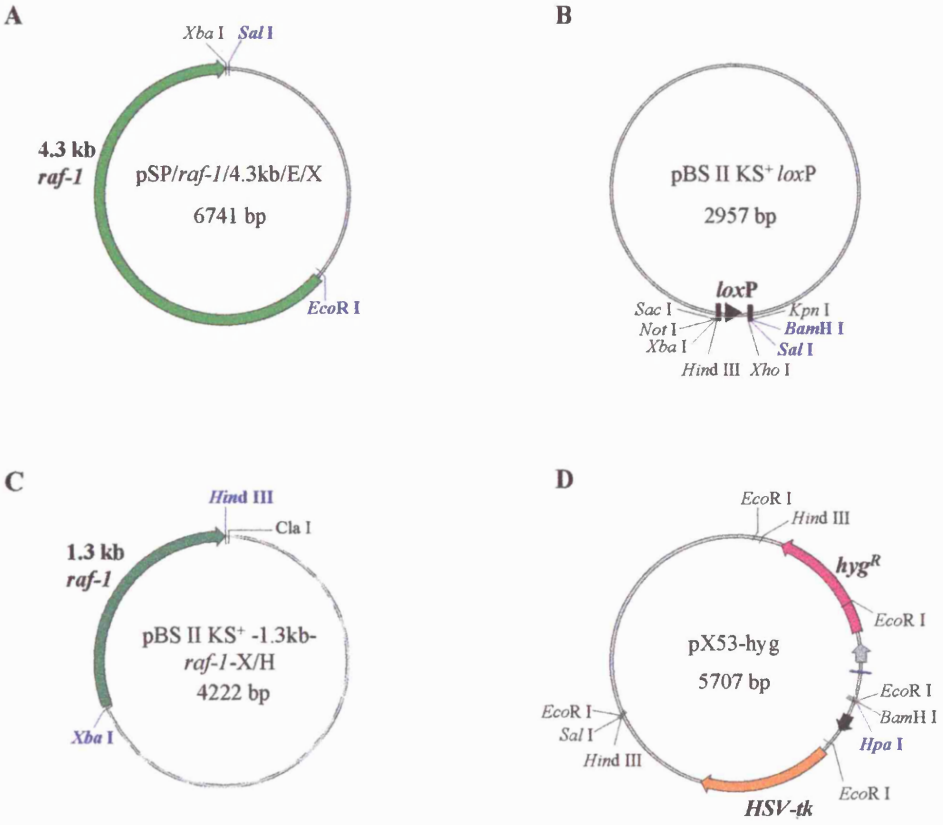

Fig. 3.9 Second part of the construction of the 3' pTC8-*lox*P-hyg targeting construct. **(A)** Restriction map of pBS II KS$^+$ *lox*P-4.3 kb *raf-1*, highlighting the *Hin*d III site used for cloning. **(B)** Restriction map of pX53-hyg-1.3 kb *raf-1*, highlighting the *Hin*d III sites used for cloning. **(G)** Restriction map of pTC8-*lox*P-hyg, highlighting the *Not* I site used to linearise the vector before electroporation into ES cells. **(H)** Restriction digestion of pTC8-*lox*P-hyg with various enzymes followed by agarose gel electrophoresis. M = 1 kb DNA marker.

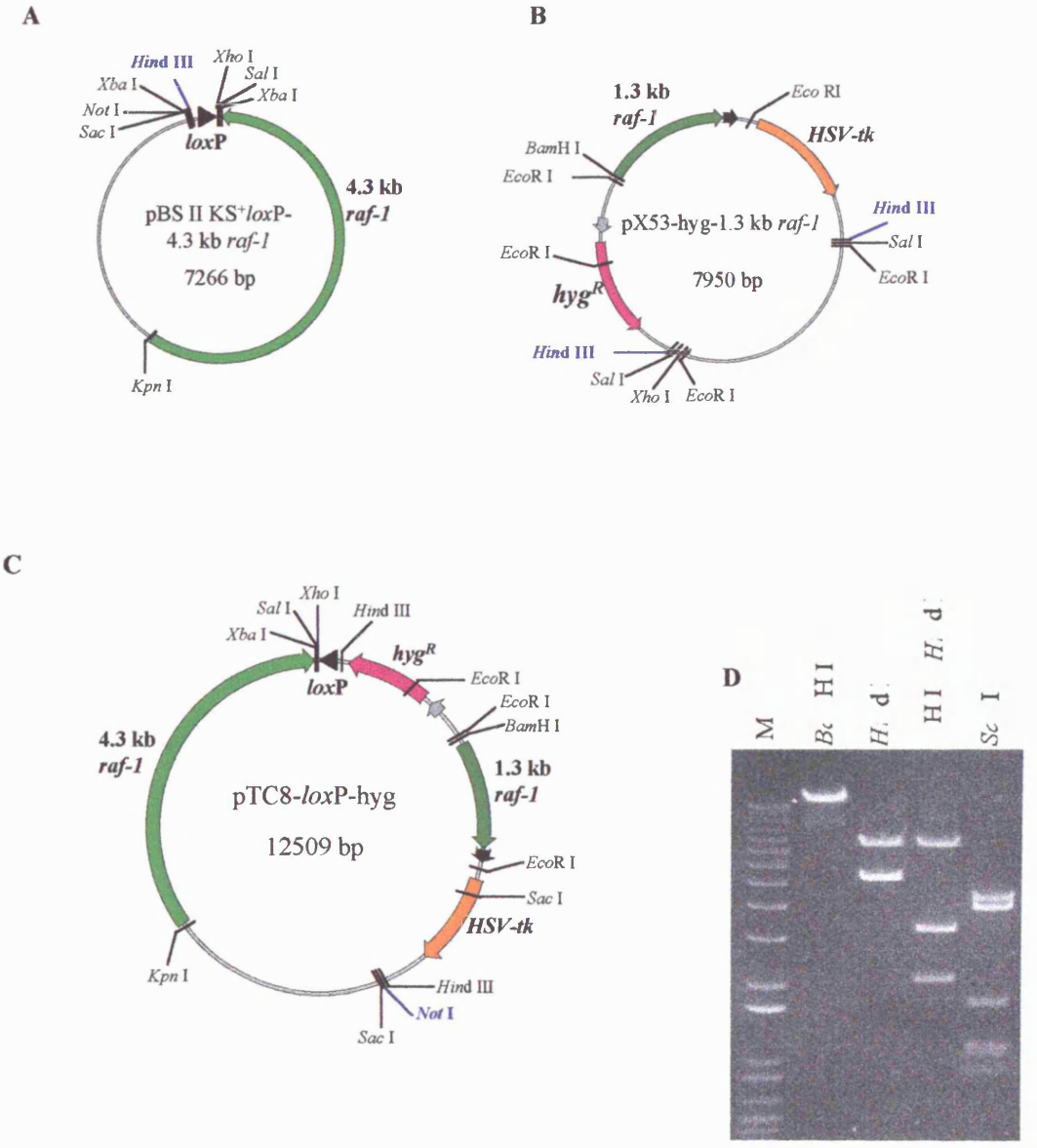

raf-1 so that they would be transcribed in the opposite direction to *raf-1* transcription with the aim that the polyadenylation signals would not interfere with *raf-1* transcription of the floxed allele. The *lox*P sites were placed in the same orientation as each other, but were in the opposite orientation to the *raf-1* gene. Also, the antibiotic resistance genes and the *lox*P sequence were placed within *raf-1* introns to prevent any possible disruption to *raf-1* gene expression from the floxed allele. Sequencing information was obtained for the sites of integration and BLAST searches were performed to confirm that the insertion sites for both targeting vectors were within introns and did not disrupt splice sites.

3.3.4 Electroporation of positive control PCR vector into ES cells

1μg of PCR vector was linearised by restriction digest with *Hind* III. It was then electroporated into 1 x 10^6 E14.1a ES cells as described in Chapter two. After seven days of G418 selection, one single clone was picked and grown up. This was used to establish PCR conditions for screening clones from the pTC7-*lox*P-neo targeting event for homologous recombinants.

3.3.5 Electroporation of 5' pTC7-loxP-neo targeting construct into ES cells

60 μg of pTC7-*lox*P-neo was linearised by restriction digest with *Not* I and then electroporated into 1 x 10^8 E14.1a ES cells as described in chapter two. After seven days of G418 selection, 288 G418 resistant clones were picked and grown up. A portion of each cell culture was frozen and the remaining cells were lysed for DNA analysis.

3.3.6 Detection of homologous recombination with pTC7-loxP-neo by PCR

Three primers, Ocp67, Ocp68 and Ocp69 were designed. Ocp67 is located within the 0.7 kb *Sst* I/*Xba* I fragment which lies outside of the targeting event, with extension occurring towards the 3' end of the *raf-1* gene (Figure 3.4 and 3.10A+C). Ocp68 is located within the 4.4 kb *Xba* I/*Xba* I fragment used as one of the arms of pTC7-*lox*P-neo, with extension occurring towards the 5' end of the *raf-1* gene (Figure 3.4 and 3.10A-C). Ocp69 is located at the 3' end of neo^R gene with extension occurring towards the 5' end of the *raf-1* gene (Figure 3.10B+C). Ocp67 and Ocp68 amplified a 1625 bp product from the wild-type allele and were used as a control to confirm that the DNA samples were of a high enough quality to be used in a PCR reaction. All samples analysed amplified the

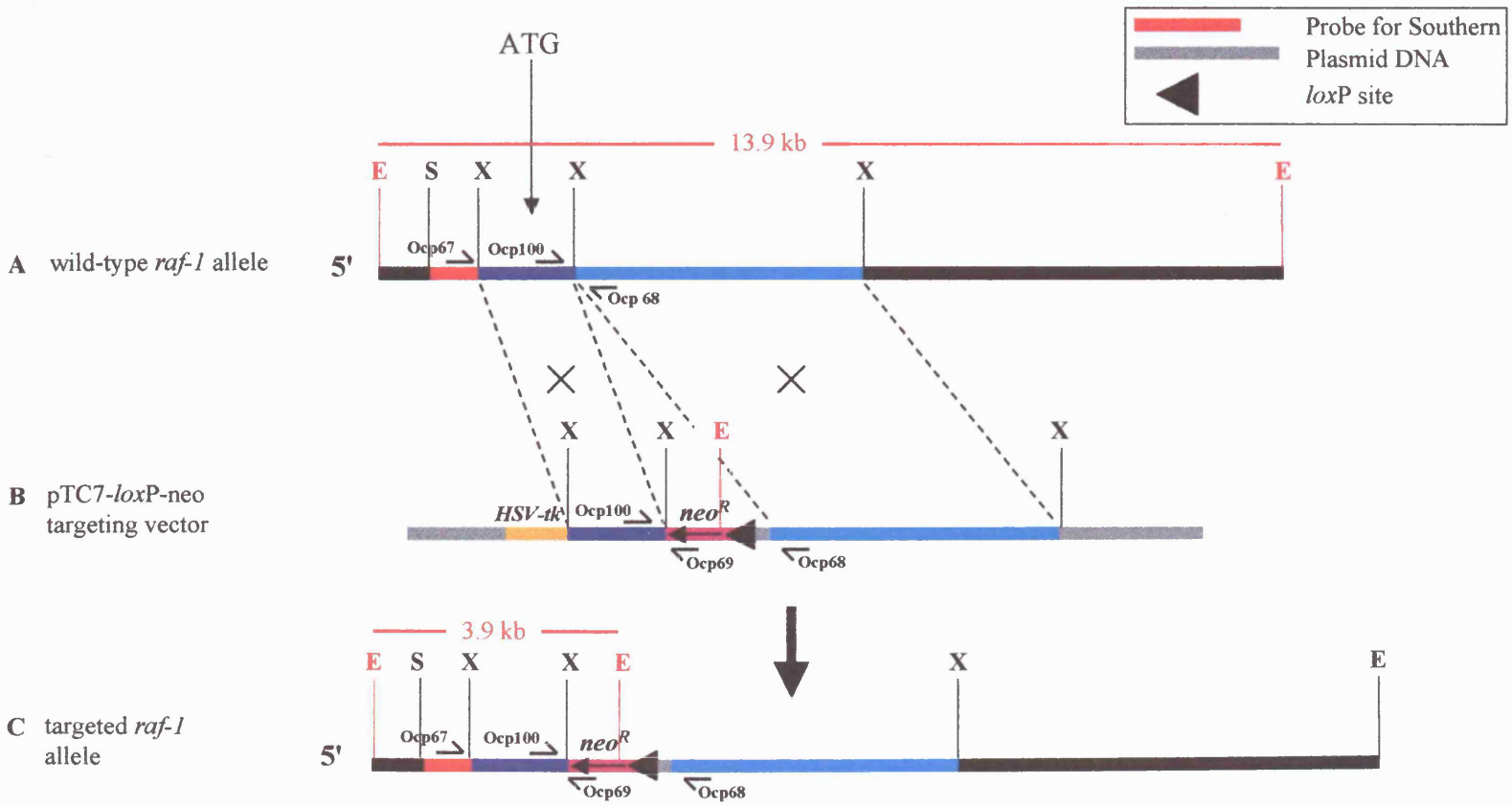

Fig. 3.10 5' targeting event highlighting the positions of homologous arms used in the construction of pTC7, restriction enzyme sites, positions of primers, the position of the probe for Southern blot analysis and the size of the restriction fragment that hybridises to the probe. **(A)** Wild-type *raf-1* gene. **(B)** Restriction map of pTC7-*lox*P-neo. **(C)** 5' *Eco* RI restriction fragment of *raf-1* after homologous recombination with pTC7. Single letter key: E = *Eco*R I, S = *Sst* I, X = Xba I.

Fig. 3.11 Screening for homologous recombination in ES cell clones electroporated with pTC7-*lox*P-neo. (**A**) PCR using control primers Ocp67 and Ocp68 amplified the wild-type PCR product of 1625 bp in all ES cell clones. (**B**) PCR using Ocp67 and Ocp69 to amplify the 5' targeted allele. A 1623 bp product was amplified from ES cell clone numbers 2, 8 and 9, and a 1815 bp product from the positive control PCR vector. (**C**) Southern blot analysis using the 0.7 kb *raf-1* Sst I/Xba I fragment to probe *Eco*R I digested DNA. Hybridisation to the targeted 3.9 kb fragment was observed with ES cell clones 2, 8, 9, 19, 24 and 28. (**D**) Southern blot analysis using the neo^R gene to probe *Eco*R I digested DNA. Hybridisation to the targeted 3.9 kb fragment was observed with ES cell clones 2, 8, 9, 19, 24, 28, but clone 12 harbours a random integration (RI) event. M = 1 kb DNA marker.

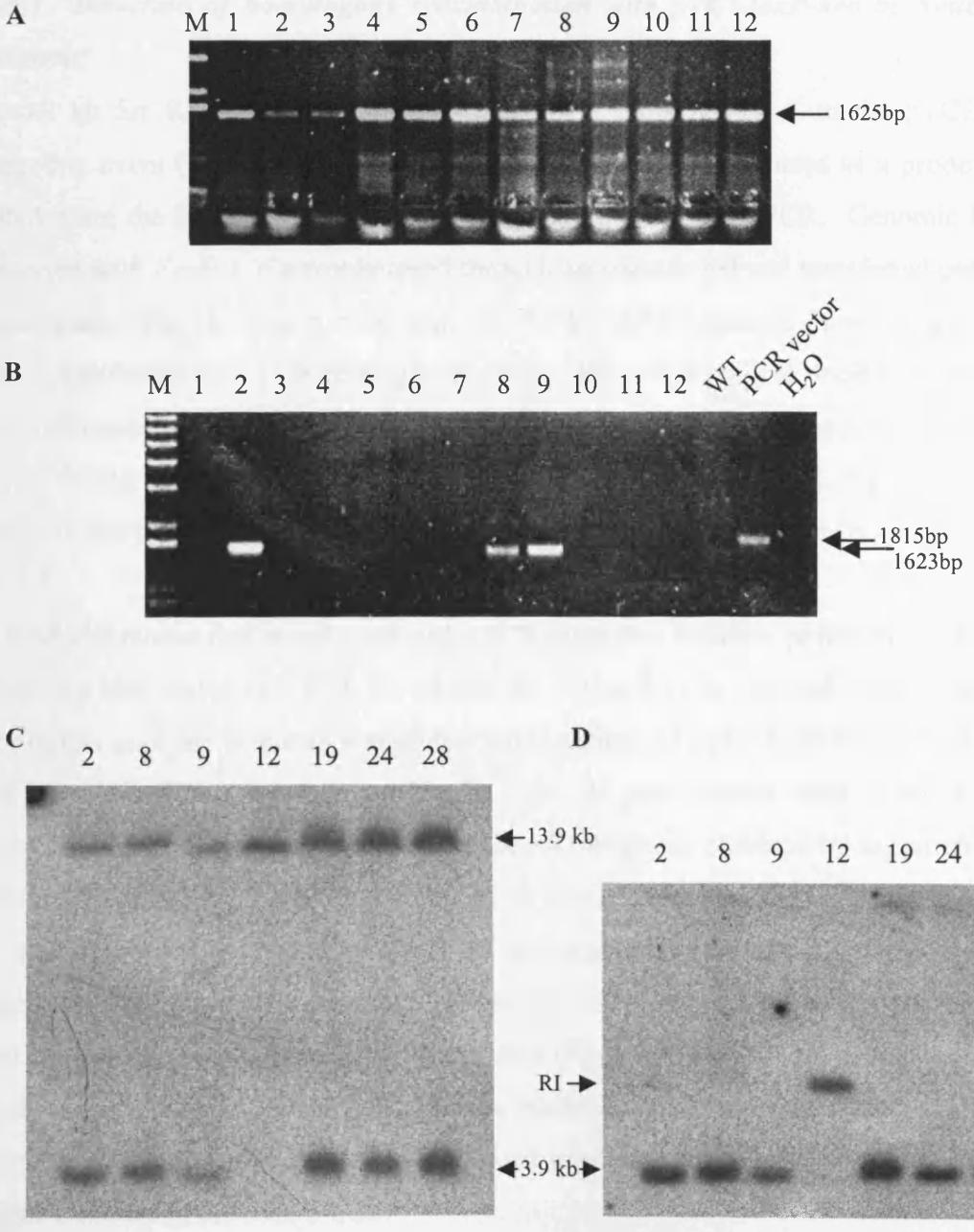

wild-type PCR product (clone numbers 1 to 12 inclusive; Figure 3.11A). Ocp67 and Ocp69 amplified a 1623 bp PCR product from the targeted allele as well as a 1815 bp PCR product from the positive control PCR vector. Several positive clones were identified via PCR screening (clone numbers 2, 8, 9 were positive and clone numbers 1, 3, 4, 5, 6, 7, 10, 11, 12 were negative; Figure 3.11B). Of 70 clones analysed by PCR, 18 had undergone homologous recombination with pTC7-*lox*P-neo, representing a targeting frequency of 1:3.9.

3.3.7 Detection of homologous recombination with pTC7-loxP-neo by Southern blot analysis

A 0.7 kb *Sst I/Xba* I fragment obtained from λ clone 1 lies 5' to the pTC7-*lox*P-neo targeting event (Figure 3.4 and 3.10A+C). This fragment was used as a probe to screen DNA from the ES cell clones that gave a positive result with PCR. Genomic DNA was digested with *Eco*R I, electrophoresed through an agarose gel and transferred onto a nylon membrane. The blot was probed with this 0.7 kb *raf-1* fragment. In wild-type DNA this probe hybridises to a 13.9 kb fragment. If the ES cell clone had undergone homologous recombination with pTC7-*lox*P-neo, hybridisation to a 3.9 kb fragment of the targeted allele would also be detected. This reduction in size of the *Eco*R I fragment occurs as a result of the introduction of an additional *Eco* RI site in the neo^R gene (Figure 3.10C).

All ES cell clones that tested positive by PCR were also found to be positive as assessed by Southern blot analysis (2, 8, 9, 19, 24 and 28; Figure 3.11C). Several clones were selected for further analysis to ensure that multiple integrations of pTC7-*lox*P-neo had not occurred. ES genomic DNA was digested with *Eco* RI and probed with a short sequence corresponding to the neo^R gene (963 bp *Eco* RI fragment obtained by digestion of pX53-neo). Hybridisation to a 3.9 kb fragment of the targeted allele was visualised with all ES clones selected showing the presence of the targeting event and no extra hybridisations were observed except for clone 12 which had not undergone homologous recombination but had randomly integrated pTC7-*lox*P-neo (Figure 3.11D). This indicated that pTC7-*lox*P-neo had only integrated once in the homologously recombined clones. Six clones were selected to undergo the next round of targeting with pTC8-*lox*P-hyg. These were clone numbers 2, 8, 9, 19, 24, 28.

3.3.8 Electroporation of 3' pTC8-loxP-hyg targeting construct into ES cells containing the pTC7-loxP-neo targeting event

50 μg of pTC8-*lox*P-hyg was linearised by restriction digest with *Not* I and was then electroporated separately into each of the six ES cell clones positive for the first targeting event (clone numbers 2, 8, 9, 19, 24, 28). After seven days of hygromycin B selection, a total of 260 resistant clones were picked and grown up with at least 40 picked from each of the six parental ES cell clones. A portion of each cell culture was frozen and the remaining cells were lysed for DNA analysis.

3.3.9 Detection of homologous recombination with pTC8-loxP-hyg by PCR

An attempt to construct a positive control vector for PCR detection of the 3' targeting event was unsuccessful. Therefore conditions for PCR had to be established using the electroporated ES cell clones. Two primers 3'pgk and ocp77 were used. Ocp77 is located within the 0.9 kb *Hin*d III/*Bam*H I fragment which lies outside of the targeting event, with extension occurring towards the 5' end of the *raf-1* gene (Figure 3.4 and 3.12A+C). 3'pgk is located at the 5' end of the hyg^R gene, with extension occurring towards the 3' end of the *raf-1* gene (Figure 3.12B+C). Ocp77 and 3'pgk amplify a 1758 bp PCR product from the targeted allele. Eight positive clones out of 270 were identified via PCR screening. These were clone numbers 7, 9, 18, 26, 29, 38, 55 and 166 (Figure 3.13A).

3.3.10 Detection of homologous recombination with pTC8-loxP-hyg by Southern blot analysis

A 0.9 kb *Hin*d III/*Bam*H I fragment obtained from λ clone 13 lies 3' to the pTC8-*lox*P-hyg targeting event (Figure 3.4 and 3.12A+C). This was used as a probe to screen DNA from the eight ES cell clones that gave a positive result with PCR. Genomic DNA was digested with *Bam*H I, electrophoresed through an agarose gel and transferred onto a nylon membrane. The blot was probed with this 0.9 kb *raf-1* fragment. In wild-type DNA this probe hybridises to a 15.2 kb fragment of the wild type allele. If the ES cell clone had undergone homologous recombination with pTC8-*lox*P-hyg, hybridisation to a 2.3 kb fragment of the targeted allele would also be detected. This reduction in size of the *Bam*H I fragment occurs as a result of the introduction of an additional *Bam*H I site in the hyg^R gene (Figure 3.12B). 8 clones out of 270 were identified as having undergone homologous

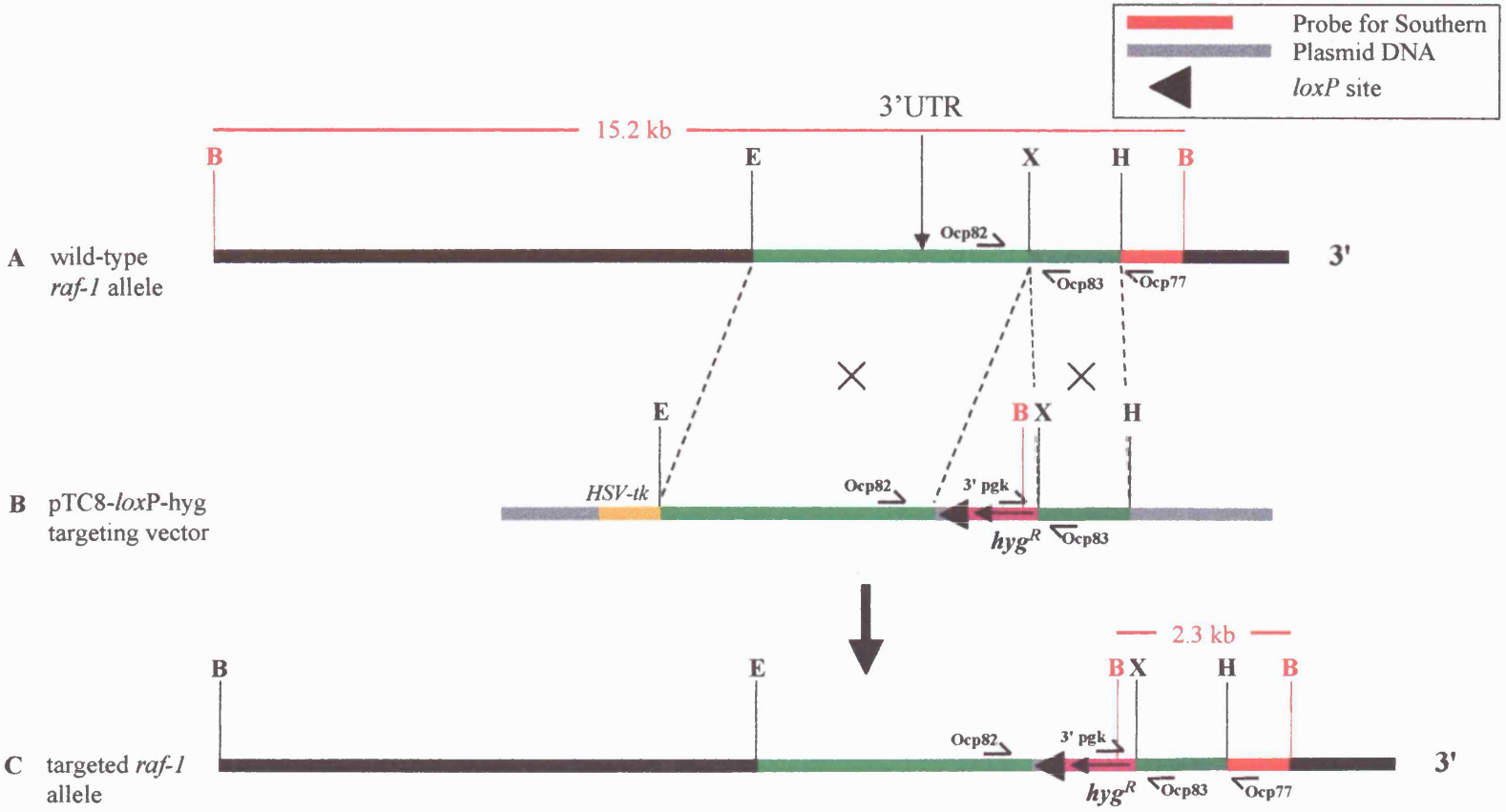

Fig. 3.12 3' targeting event highlighting the positions of homologous arms used in the construction of pTC8, restriction enzyme sites, positions of primers, the position of the probe used for Southern blot analysis and the size of the restriction fragment that hybridises to the probe. **(A)** Wild-type *raf-1* gene. **(B)** Restriction map of pTC8-*lox*P-hyg. **(C)** 3' *Bam*H I restriction fragment of *raf-1* gene after homologous recombination with pTC8. Single letter key: E = *Eco*R I, S = *Sst* I, X = Xba I, H = *Hin*d III.

Fig. 3.13 Screening for homologous recombination in pTC7-*lox*P-neo targeted ES cell clones electroporated with pTC8-*lox*P-hyg. (**A**) PCR using ocp77 and 3'pgk to amplify the 3' targeted allele. A 1758 bp product was amplified from ES cell clone numbers 9, 18, 29, 38 and 55 but not from ES cell clone number 54 (upper panel). A 1758 bp product was amplified from ES cell clone numbers 7, 166 and 26 but not from ES cell clone number 156 (lower panel). (**B**) Southern blot analysis using the 0.9 kb *raf-1 Hin*d III/*Bam*H I fragment to probe *Bam*H I digested DNA. Hybridisation to the targeted 2.3 kb fragment was observed with ES cell clones 7, 9, 18, 26, 29, 38, 55 and 166. (**C**) Southern blot analysis using the hyg^R gene to probe *Bam*H I digested DNA. Hybridisation to the targeted 15.2 kb fragment was observed with ES cell clones 9, 18, 26, 29, 38, 55 and 166 but an extra insertion of pTC8-*lox*P-hyg was observed with clone 7. Also clones 12 and 54 harbour random integration events. M = 1 kb DNA marker.

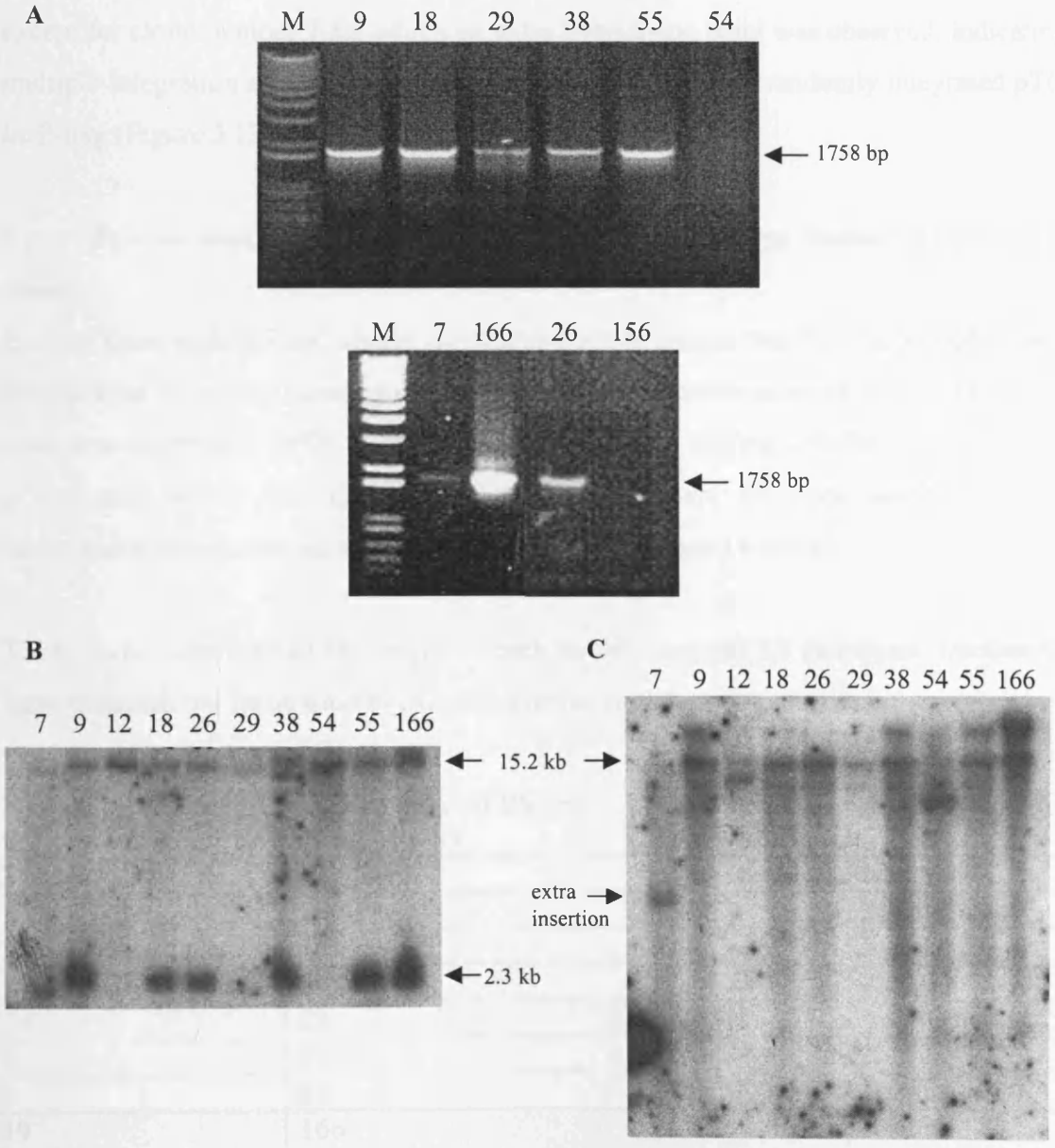

recombination with pTC8-*lox*P-hyg (clones 7, 9, 18, 26, 29, 38, 55, 166; Figure 3.13B) representing a targeting frequency of 1:33. Therefore, all 8 ES cell clones that tested positive by PCR were also found to be positive as assessed by Southern blot analysis.

The parental pTC7-*lox*P-neo ES cell clones of each of these clones are indicated in Table 3. 1. All eight clones were selected for further analysis to ensure that multiple integrations of pTC8-*lox*P-hyg had not occurred. ES genomic DNA was digested with *Bam*H I, Southern blotted and probed with a short sequence corresponding to the hyg^R gene (1109 bp *Eco*R I/*Hin*d III fragment obtained by digestion of pX53-hyg). Hybridisation to the expected 15.2 kb fragment of the targeted allele was visualised with all ES clones except for clone number 7 for which an extra hybridising band was observed, indicating a multiple integration event. Clone numbers 12 and 54 had also randomly integrated pTC8-*lox*P-hyg (Figure 3.13C).

3.3.11 Further analysis of pTC7-loxP-neo and pTC8-loxP-hyg double targeted ES cell clones

Each of these eight ES cell clones was karyotyped to ensure that they harboured a normal complement of chromosomes to allow for germline transmission of the ES cells. This work was undertaken by Dr. E. P. Evans (Department of Zoology, Oxford University). All clones were 40XY with no abnormal karyotype except for clone number 29 which harboured a reciprocal translocation between chromosomes 14 and 18.

Table 3. 1. Summary of the origin of each double targeted ES cell clone, whether they harbour additional integration events and whether their karyotype is normal.

Parental pTC7-*lox*P-neo clone number	Double targeted ES cell clone number	Additional integrations	Karyotype
19	7	Yes	Normal
28	9	No	Normal
19	18	No	Normal
9	26	No	Normal
24	29	No	translocation 14:18
9	38	No	Normal
2	55	No	Normal
19	166	No	Normal

To ensure that the integration events had not interfered with the production of Raf-1 protein, protein lysates were prepared from these double targeted ES cell clones, followed by SDS-PAGE and electro-transfer of the proteins onto nitrocellulose. The blots were incubated with an anti-Raf-1 antibody. The amount of Raf-1 in the double targeted ES cell clones appeared to be similar to the amount of Raf-1 in wild-type cells (Figure 3.14A). A vinculin antibody was used as a control for protein loading (Figure 3.14B).

Each of the clones that were frozen down at the earliest stage were expanded and a portion lysed for DNA and re-checked by PCR using Ocp67 and Ocp69 for detection of the 5' targeting event, and using Ocp77 and 3'pgk for detection of the 3' targeting event. This was to ensure that the presence of both targeting events had been maintained. Figure 3.14C shows data for double targeted ES cell clones 9, 38 and 55 plus ES cell clone 54 which has only been targeted with pTC7-*lox*P-neo.

It had not been established at this stage which, if any, of the eight clones had acquired both targeting events on the same chromosome. It was decided that due to the length of time needed to generate mice, it was not feasible to delay the blastocyst microinjections. Therefore, all clones were microinjected into blastocysts, except clone number 7 since this also harboured a random integration of pTC8-*lox*P-hyg. Further analysis of the clones was undertaken in the meantime to establish which clones had acquired both targeting events on the same chromosome. This work is described in Chapter 4. Segregation of the two targeting events in mice could also address whether both alleles are on the same chromosome.

3.3.12 Generation of mice from pTC7-loxP-neo and pTC8-loxP-hyg targeted ES cell clones

Each of the ES cell clones positive for both targeting events, except number 7, were microinjected into E3.5 blastocysts (C57BL/6 x CBA F1) by standard micromanipulation techniques followed by implantation into the uterine tract of pseudopregnant surrogate mothers to generate chimeric mice. This work was undertaken by Ms. J. Brown (Division of Biomedical Services, University of Leicester). 19 chimeric mice from both sexes were produced from these microinjections (Table 3.2). The targeted E14.1a ES cells originate

Fig. 3.14 Further analysis of double targeted ES cell clones. (**A**) Western blot analysis for detection of Raf-1 levels. (**B**) Western blot analysis for detection of Vinculin levels as a control for protein loading. (**C**) Reconfirmation of both *lox*P targeting events by PCR. PCR using primers Ocp67 and Ocp69 amplified the 5' *lox*P targeted PCR product of 1623 bp from ES cell clones 9, 38, 54 and 55 but not from the wild-type sample (WT). PCR using primers Ocp77 and 3'pgk amplified the 3' *lox*P targeted PCR product of 1758 bp from ES cell clones 9, 38 and 55 but not from 54 or the WT sample. M = 1 kb DNA marker.

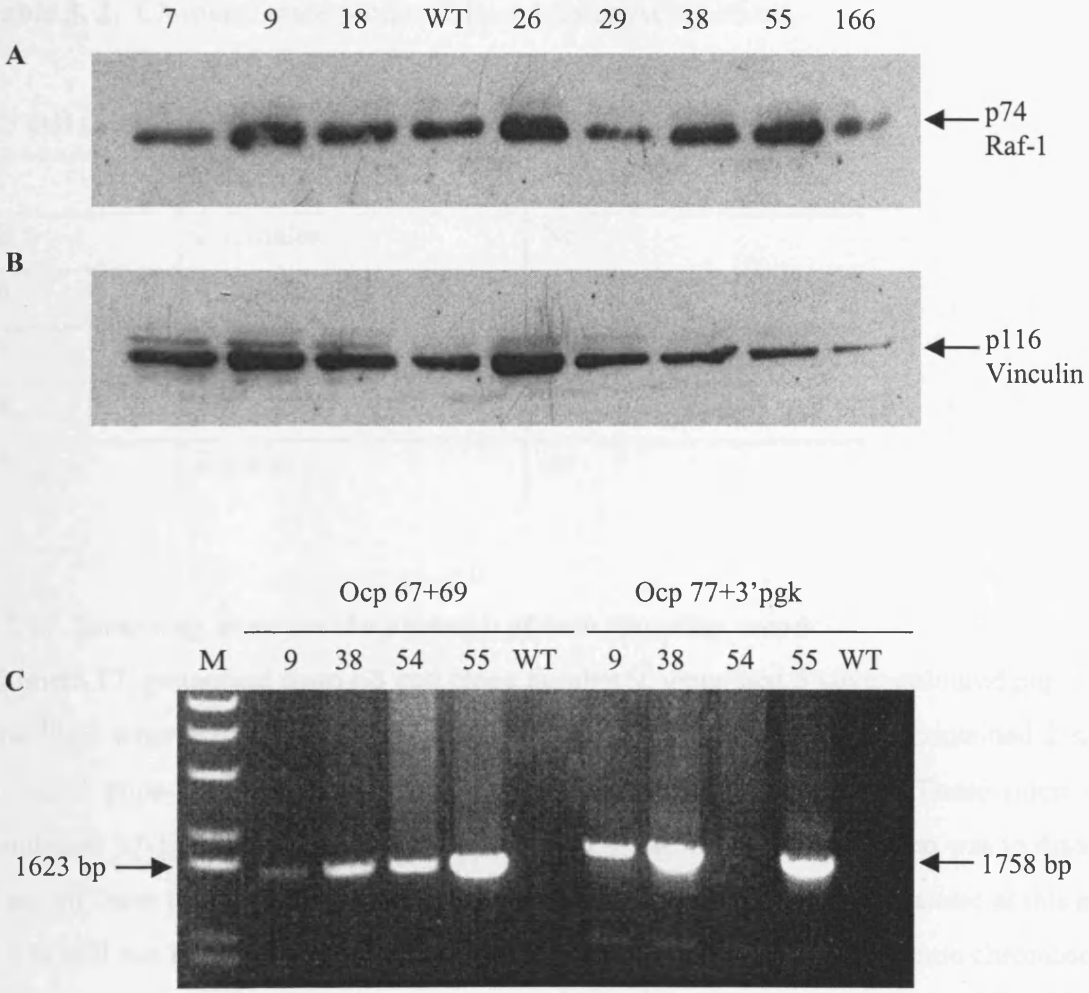

from the 129Ola strain. Therefore, these chimeras were each mated to wild-type animals from the MF-1 background in order to screen for germline transmission which was indicated by the presence of albino coloured pups in the offspring (see Chapter 1 for the genetics to explain this). Germline transmission was obtained from only one of the male chimeras (17); this chimera had originated from the microinjection of ES cell clone number 9.

Table 3. 2. Chimeric mice produced from blastocyst injections.

ES cell clone	chimeras produced	germline transmission
9	2 female 3 male	Yes
18	2 females	No
26	3 females 3 males	No
29	1 male	No
38	3 females	no
55	2 males	no

3.3.13 Screening mice for the presence of both targeting events

Chimera 17, generated from ES cell clone number 9, generated 5 silver coloured pups in its first litter when mated to a wild-type MF-1 female. The second litter contained 2 silver coloured pups and the third litter contained 1 silver coloured pup. These mice were numbered 17-1, 17-2, 17-3, 17-4, 17-5, 17-6, 17-7 and 17-8. The next step was to discover if any of these mice harboured both the 3' and 5' *lox*P targeting events, because at this stage it was still not known whether the targeting events were present on the same chromosome. Segregation would have occurred in these mice and this would therefore give proof of the presence or absence of both targeting events on the same chromosome. Different primers for genotyping the mice with respect to the presence of both targeting events were designed, as the primers that were originally used to genotype ES cell clones produce a PCR product too large to reliably reproduce from mouse tail DNA (Figure 3.15).

Fig. 3.15 Diagram to show the positions of primers used to genotype progeny from germline transmitting chimera. (**A**) Restriction map of the 5' end of *raf-1* highlighting the two fragments used for the targeting construct. (**B**) Restriction map of the 3' end of *raf-1* highlighting the two fragments used for the targeting construct.

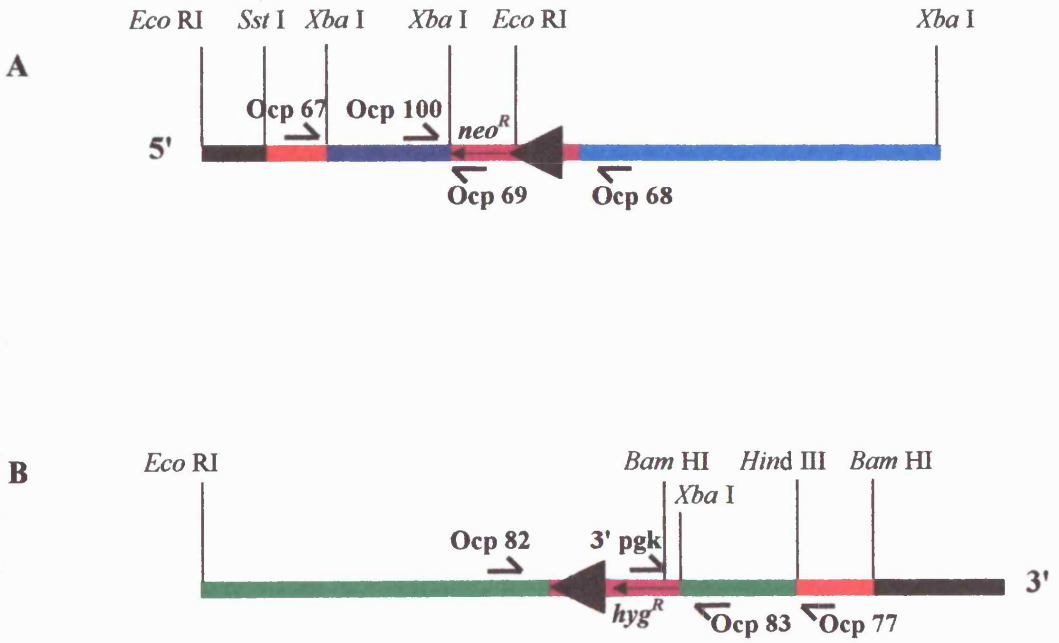

Primers Ocp100 and Ocp68 were used to amplify a 286 bp PCR product from the wild type allele which was used as a control for all other PCRs (Figure 3.16A). Ocp100 and Ocp68 amplified a product in each of the silver mice; samples 17-2, 17-4, 17-5, 17-6, 17-7 and 17-8 are shown in Figure 3.16A. This indicated that the DNA was of a high enough quality for PCR. 17-1 and 17-3 samples are not shown in this figure.

Primers Ocp83 and 3'pgk were used to amplify a 788 bp PCR product from the 3' targeted allele. Ocp83 and 3'pgk amplified a product in 3 of the 6 silver mice; samples 17-2, 17-5 and 17-8 (Figure 3.16B). 17-1 and 17-3 samples are not shown in this figure. However, 17-1 was negative for the 3' targeting event and 17-3 was positive for the 3' targeting event. Therefore from a total of 8 silver coloured mice, 4 harboured the 3' *lox*P targeting event which is the expected frequency of transmission.

Primers Ocp100 and Ocp69 were used to amplify a 290 bp PCR product from the 5' targeted allele. However, the 5' targeting event could not be detected in any of the silver mice. As a control for this PCR, a product was successfully amplified from DNA obtained from ES cell clone number 9 as these were the cells injected that generated the transmitting male chimera (Figure 3.16C).

To confirm the PCR data suggesting the presence of the 3' targeting event, mouse numbers 17-4 (negative by PCR for the 3' targeted allele) and 17-5 (positive by PCR for the 3' targeted allele) were culled and used to make a large amount of DNA for Southern blot analysis. To detect the 3' targeting event, tail DNA was digested with *Bam*H I, electrophoresed through an agarose gel and transferred onto a nylon membrane. The blot was probed with the 0.9 kb *raf-1 Hin*d III/*Bam*H I 3' fragment. This showed hybridisation to a 15.2 kb fragment from the wild type allele in both 17-4 and 17-5 samples as expected (Figure 3.16D). A 2.3 kb fragment corresponding to the targeted allele in sample 17-5 was also observed (Figure 3.16D). This provided firm evidence that germ-line transmission had been achieved with respect to the 3' pTC8-*lox*P-hyg targeting event. To detect the 5' targeting event, tail DNA was digested with *Bam*H I, electrophoresed through an agarose gel and transferred onto a nylon membrane. The blot was probed with a short sequence

Fig. 3.16 Evidence for germline transmission of the *raf-1* targeted allele. (**A**) PCR using control primers Ocp100 and Ocp68 to amplify the wild-type PCR product of 286 bp from all of the silver coloured mice. (**B**) PCR using primers Ocp83 and 3' pgk to amplify the 3' *lox*P targeted PCR product of 788 bp from 17-2, 17-5 and 17-8. No PCR product was amplified from 17-4, 17-6 or 17-7. (**C**) PCR using primers Ocp100 and Ocp69 to amplify the 5' *lox*P targeted PCR product. No PCR product was amplified from any of the silver coloured mice or the wild-type sample, but a product was observed in ES cell DNA from number 9. (**D**) Southern blot analysis using the 0.9 kb *raf-1 Hin*d III/*Bam*H I fragment to probe *Bam*H I digested DNA from 17-4 and 17-5. Hybridisation to the targeted 2.3 kb fragment was observed with 17-5 only. (**E**) Southern blot analysis using the neo^R gene to probe *Bam*H I digested DNA from 17-4 and 17-5. No hybridisation was observed from either of the DNAs. M = 1 kb DNA marker.

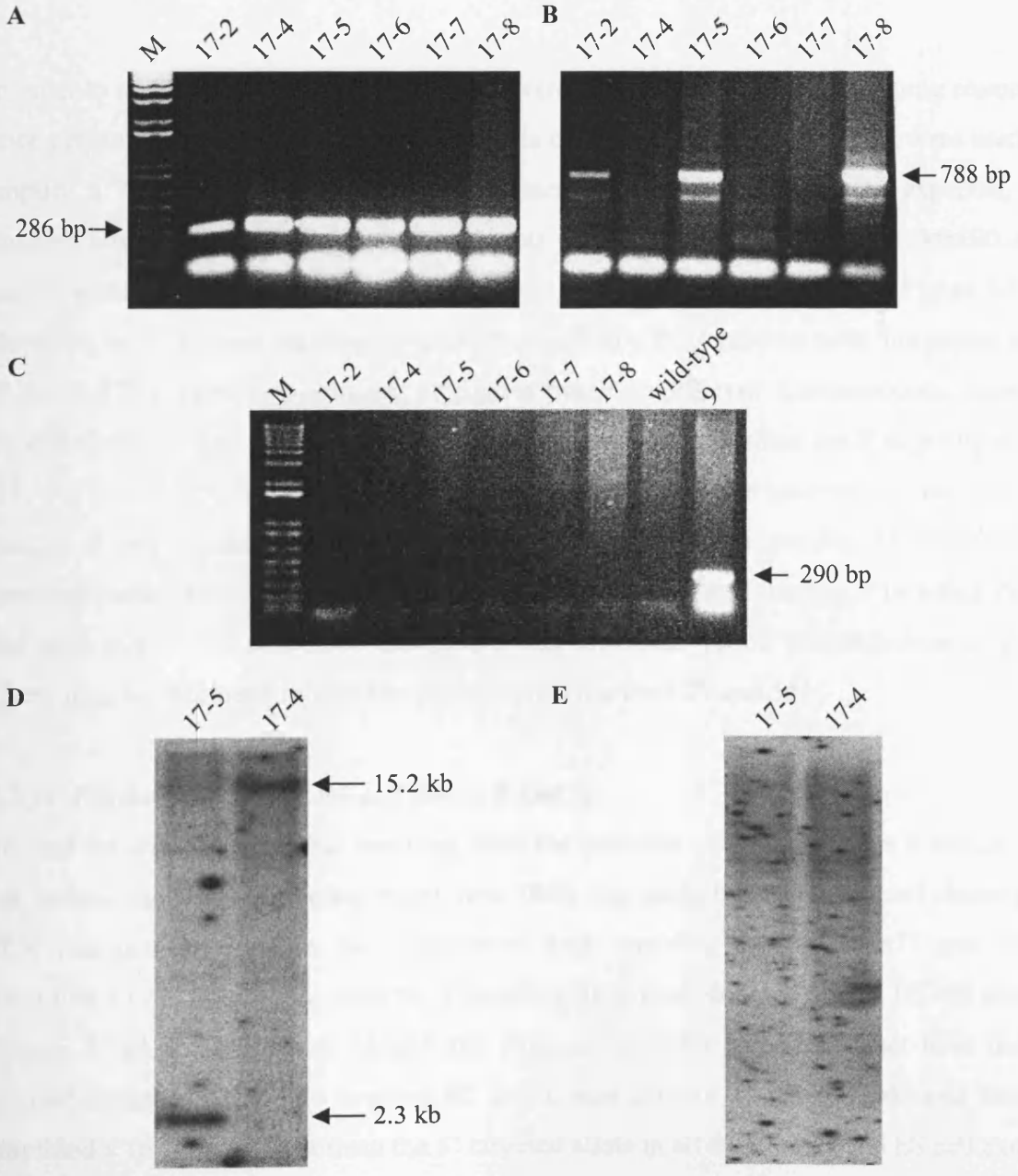

corresponding to the *neo*^{R} gene. A smear of hybridisation and no specific hybridisation was observed in either of the samples 17-4 or 17-5 (Figure 3.16E).

Together with the PCR data it therefore appeared that neither of the samples 17-5 or 17-4 harboured the 5' pTC7-*lox*P-neo targeting event. An explanation for this could have been that the two targeting events were on different chromosomes and had segregated during meiosis resulting in each of the silver offspring having either one or the other of the targeting events. However, this can not be the case as all mice negative for the 3' event were also negative for the 5' event.

In order to analyse this further, tail samples were taken from all of the remaining chimeric mice generated including the transmitting male chimera 17. Ocp83 and 3'pgk were used to amplify a 788 bp product from the 3' targeted allele (Figure 3.15). As expected, all samples amplified the PCR product with this primer pair (Figure 3.17A). Ocp100 and Ocp69 were used to amplify a 290 bp product from the 5' targeted allele (Figure 3.15). However, only chimera numbers 10 and 12 amplified a PCR product with this primer pair (Figure 3.17B). These two chimeras originated from two different microinjections, those of ES cell clones 55 and 29. All the other chimeras that did not contain the 5' targeting event (13, 16, 17, 18, 19, 20, 21, 22, 23, 24, and 25) arose from the microinjections of clone number 9 and number 26, which includes the male chimera number 17 from which germline transmission had been achieved. Therefore it appeared that the 5' targeting event had been lost in ES cell clone numbers 9 and 26 either before microinjection or soon afterwards, but had been retained in ES cell clone numbers 29 and 55.

3.3.14 Further analysis of ES cell clones 9 and 26

To find out why the chimeras resulting from the injection of ES cell clones 9 and 26 did not harbour the 5' *lox*P targeting event, new DNA was made from these ES cell clones and PCR was used to confirm the presence of both targeting events. Ocp77 and 3'pgk amplified a 1758 bp product from the 3' targeted allele in all double targeted ES cell clones (Figure 3.18A). In addition, Ocp83 and 3'pgk amplified a 788 bp product from the 3' targeted allele in all double targeted ES cell clones (Figure 3.18B). Ocp67 and Ocp69 amplified a 1623 bp product from the 5' targeted allele in all double targeted ES cell clones

Fig. 3.17 PCR analysis of DNA from 13 chimera tail samples (numbered 10, 12, 13, 16, 17, 18, 19, 20, 21, 22, 23, 24, 25). **(A)** PCR using primers Ocp83 and 3' pgk amplified the 3' *lox*P targeted PCR product of 788 bp from all samples except the wild-type (WT) sample. **(B)** PCR using primers Ocp100 and Ocp69 amplified the 5' *lox*P targeted PCR product from 10, 12 and ES cell clone number 9. No PCR product was amplified from 13, 16, 17, 18, 19, 20, 21, 22, 23, 24, 25 or WT. M = 1 kb DNA marker.

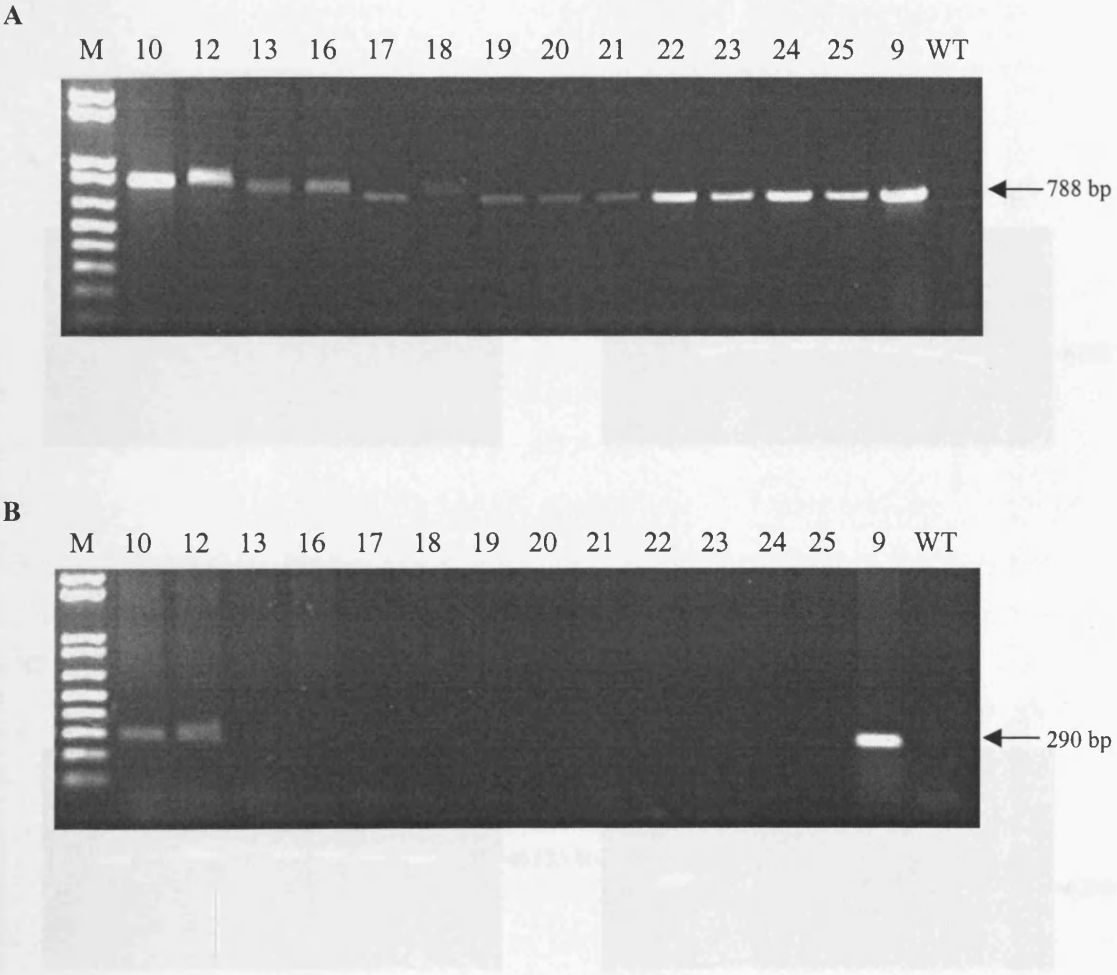

Fig. 3.18 PCR analysis of DNA from ES cell clones **(A)** PCR using primers Ocp77 and 3'pgk amplified the 3' *lox*P targeted PCR product of 1758 bp from all clones. **(B)** PCR using primers Ocp83 and 3' pgk amplified the 3' *lox*P targeted PCR product of 788 bp from all clones. **(C)** PCR using primers Ocp67 and Ocp69 amplified the 5' *lox*P targeted PCR product of 1623 bp from all clones. **(D)** PCR using primers Ocp100 and Ocp69 amplified the 5' *lox*P targeted PCR product of 290 bp from all clones. WT = wild-type, M = 1 kb DNA marker.

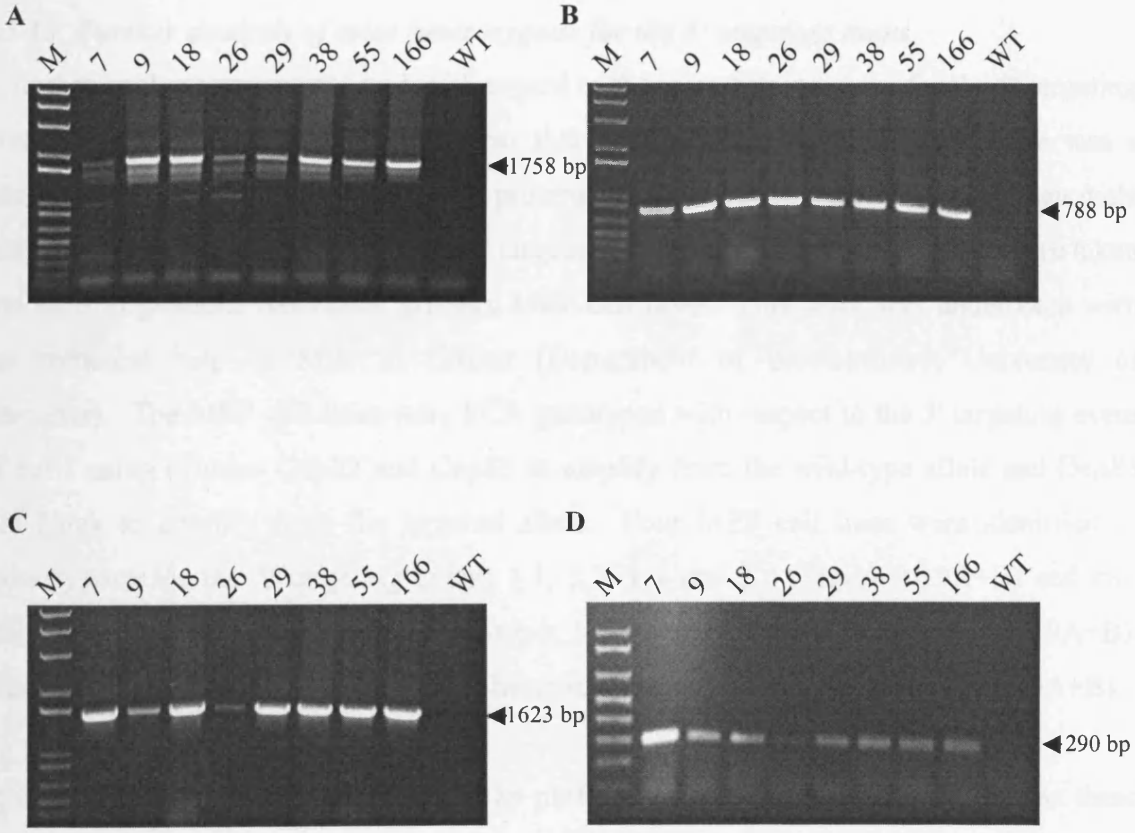

(Figure 3.16C). However, ES cell clone numbers 9 and 26 produced a much weaker band than the other clones, indicating loss of the pTC7-*lox*P-neo targeting event in a portion of these cells. In addition, Ocp100 and Ocp69 amplified a 290 bp product from the 5' targeted allele in all double targeted ES cell clones. However, ES cell clone number 26 produced a much weaker band than the other clones (Figure 3.18D).

The only possible explanation for the loss of the 5' *lox*P targeting event in ES cell clone numbers 9 and 26 is that the 5' *lox*P targeting event is unstable in these two clones.

3.3.15 Further analysis of mice heterozygous for the 3' targeting event

A further analysis was performed with regard to the mice heterozygous for the 3' targeting event, because even though it was clear that they had lost the neo^R gene, there was a possibility that the 5' *lox*P site was still present. A timed mating was set up between male and female mice heterozygous for the 3' targeting event. At E14.5, the embryos were taken and used to generate individual primary MEF cell lines. This work was undertaken with the technical help of Mrs. S. Giblett (Department of Biochemistry, University of Leicester). The MEF cell lines were PCR genotyped with respect to the 3' targeting event of *raf-1* using primers Ocp82 and Ocp83 to amplify from the wild-type allele and Ocp83 and 3'pgk to amplify from the targeted allele. Four MEF cell lines were identified as homozygous for the 3' targeting event; 1.1, 1.3, 1.4 and 2.4 (Figure 3.19A+B) and five MEF cell lines were identified as wild-type; 1.6, 1.8, 2.1, 2.2 and 2.3 (Figure 3.19A+B). Three MEF cell lines were identified as heterozygotes; 1.7, 1.9 and 1.5 (Figure 3.19A+B).

PCR analysis of the 5' end of *raf-1* was performed using Ocp68 and Ocp100, as these primers span the region of insertion of the neo^R gene and the *lox*P site. It seemed feasible that if extra sequences were present, then the PCR product from the homozygous targeted MEFs would be larger than the PCR product from the wild-type MEFs. However, it appeared that the size of the bands from the targeted allele were exactly the same size as those from the wild-type allele (Figure 3.19C). As a definite way to identify if the *lox*P site was present at the 5' end of the *raf-1* gene, sequencing across where the neo^R gene and *lox*P site should have been was then performed using primer Ocp100 on the PCR product resulting from primers Ocp67 and Ocp68 (Figure 3.15A). Sequencing was performed on

Fig. 3.19 Further analysis of germline transmitting mice. (**A**) Genotyping primary MEFs generated from a timed mating between mice heterozygous for the 3' targeting event. PCR using primers Ocp82 and Ocp83 amplified the wild-type PCR product of 514 bp from the 3' targeted end of *raf-1* from 1.7, 1.9, 2.1, 2.3 (left panel), ES cell clone number 9, 1.5, 1.6, 1.8 and 2.2 (right panel). No PCR product was amplified from 1.1, 1.3, 1.4 and 2.4 (left panel) except a non-specific PCR product (NS) which is amplified from all samples except from the H_2O control. (**B**) PCR using primers Ocp83 and 3' pgk amplified the 3' *lox*P targeted PCR product of 788 bp from 1.1, 1.3, 1.4, 1.7, 1.9, 2.4, ES cell clone number 9 and 1.5. No PCR product was amplified from 2.2, 2.3, 1.8 and 2.2. (**C**) PCR using primers Ocp68 and Ocp100 amplified the wild-type PCR product of 286 bp from the 5' targeted end of *raf-1* from 1.1, 1.6, wild-type (WT), 1.5, 1.6, 1.8 and 2.2. M = 1 kb DNA ladder.

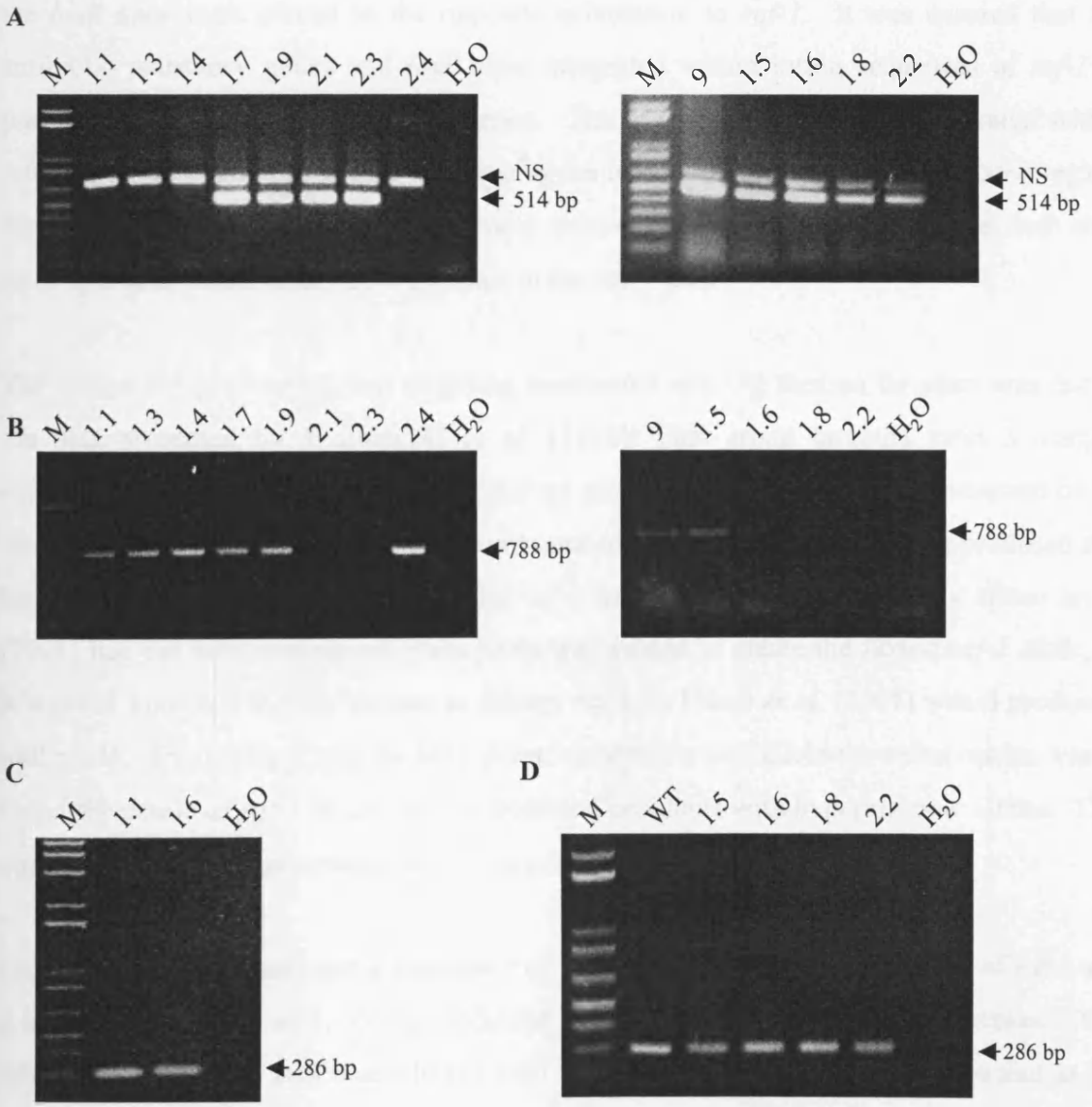

both a wild-type sample (1.6) and a homozygote sample (1.1). The sequence of the homozygote sample was identical to that of the wild-type sequence and a *lox*P sequence could not be identified (data not shown). This led to the conclusion that a *lox*P site did not exist at the 5' end of the *raf-1* gene in these transgenic mice that harboured a *lox*P site at the 3' end of *raf-1*. Hence these animals were of no further use.

3.4 Conclusions

This chapter describes the successful generation of two different targeting constructs that involved multiple complex cloning stages. The vectors were arranged so that two different selectable markers were used that were transcribed in the opposite orientation to *raf-1* and the *lox*P sites were placed in the opposite orientation to *raf-1*. It was ensured that the antibiotic resistance genes and *lox*P sites integrated within intron sequences of *raf-1* to prevent disruption to the coding sequence. The 5' *lox*P and neo^R gene integrated within intron 2 of *raf-1* and the 3' *lox*P and hyg^R gene integrated after the 3' untranslated region. Therefore when both targeting constructs were homologously integrated, the *lox*P sites were spaced approximately 26.8 kb apart in the *raf-1* gene.

The reason for performing two targeting events and spacing then so far apart was due to the data presented by Wojnowski *et al.* (1998). This group targeted exon 3 using a conventional approach with an aim to disrupt gene transcription by the introduction of the neo^R gene. However, a null allele was not created as a truncated protein was produced that had residual kinase activity. Also, the *raf-1* knockout mice generated by Hüser *et al.* (2001) had not been completed when work was started to create the floxed *raf-1* allele, so it was not known if the site chosen to disrupt *raf-1* by Hüser *et al.* (2001) would produce a null allele. Therefore, it was decided that to generate a null allele the safest option was to target the whole of *raf-1* to circumvent potential problems with hypermorphic alleles. This strategy required the generation of two targeting vectors.

Gene targeting was used and a frequency of 1: 3.9 was obtained for the 5' end of *raf-1* and a targeting frequency of 1: 33 was obtained for the 3' end of *raf-1*. A possible reason that the 3' targeting event was much lower than the 5' targeting frequency could be that as the cells had already been electroporated once, the chance of a second homologous

recombination may be reduced. Other groups have previously targeted the *raf-1* gene; Hüser *et al.* (2001) observed a frequency of 1 in 60 when exons 10 to 13 were targeted, Mikula *et al.* (2001) observed a frequency of 1 in 35 when exon 3 was targeted and Wojnowski *et al.* (1998) observed a frequency of 1 in 34.5 when exon 3 was targeted.

Eight ES cell clones were positive for having undergone homologous recombination with both pTC7-*lox*P-neo and pTC8-*lox*P-hyg. One ES cell clone was not used any further as it had multiple integrations of the 3' pTC8-*lox*P-hyg vector. The remaining 7 ES cell clones were microinjected into blastocysts and 19 chimeras were obtained. It was not known which, if any, of the ES cell clones had *lox*P sites present on the same chromosome but segregation in the mice would address this.

Germline transmission was achieved from ES cell clone 9. It was subsequently determined that these mice harboured the 3' pTC8-*lox*P-hyg targeting event but they did not harbour the 5' pTC7-*lox*P-neo targeting event. It became evident through DNA analysis of tail samples, that all chimeras arising from the injections of ES cell clone numbers 9 and number 26 did not have the 5' *lox*P targeting event, even though PCR analysis of the cells that were injected did screen positive for this particular targeting event. The only possible explanation for the loss is that the 5' *lox*P targeting event is unstable alone or that the integration of the 3' *lox*P targeting event has made the 5' *lox*P targeting event become unstable and a proportion of the cells have lost it. Other groups using this new technology have not previously reported this phenomenon probably because the general trend for producing floxed alleles is to use just one targeting vector.

Subsequent analysis of the 8 double targeted ES cell clones (described in chapter four), indicate that ES cell clone 29 acquired both *lox*P targeting events on the same chromosome, but that clones 7, 9, 18, 26, 38, 55 and 166 acquired both targeting events on separate chromosomes. The 5' *lox*P targeting event appears to be stable in ES cell clone number 29 as reflected by the presence of this event in a chimera created from injection of these ES cells (Figure 3.15B). Furthermore, it appears to efficiently delete the *raf-1* gene upon the expression of Cre (described in chapter four). Therefore this clone may prove useful for the generation of mice. However, there is a problem with this clone as it

harbours a reciprocal translocation between chromosomes 14 and 18. This would mean that litter numbers resulting from a mating between the chimeras generated from these ES cells and wild-type mice will be approximately halved due to the production of unbalanced products at meiosis, thus reducing the possibility of obtaining germline transmission of the *raf-1* floxed allele.

The Baccarini group has recently reported the generation of mice in which exon 3 of *raf-1* is flanked by *lox*P sites. These mice were crossed to mice expressing Cre under the control of the *Mx1* promoter. Upon induction of Cre by the administration of polyinosinic: cytidyllic acid, exon 3 was deleted in the liver and bone marrow. The deletion of exon 3 in other tissues was not reported upon. Macrophages were derived from these mice and *raf-1* was not detected by Western blot analysis indicating that the deletion of exon 3 resulted in a null *raf-1* allele (Jesenberger *et al.*, 2001). However, this does not fit in with the data observed by Wojnowski *et al.* (1998). This group also targeted exon 3 using a conventional approach but they did not generate a null allele as a truncated protein was produced that had residual kinase activity.

It is now evident that the *raf-1* null mice previously generated in our laboratory survive postnatally on the MF-1 background strain. This may possibly circumvent the need for a conditional *raf-1* knockout. However, if tumour studies are to be performed on animals that lack *raf-1*, they require older animals, and at this stage the *raf-1* knockout animals would not survive long enough. Also, tissue-specific deletion of *raf-1* is a desirable tool, as it overcomes the influence of surrounding cells/tissues that would also lack *raf-1* from interfering with the interpretation of Raf-1 function. Therefore if *raf-1* floxed mice could be generated from clone number 29 they would be invaluable for these reasons.

Unfortunately, it was recently discovered that the gene encoding for makorin RING zinc-finger 2 (MKRN2), overlaps, in an antisense orientation with the 3' UTR of the mouse *raf-1* gene (Gray *et al.*, 2001). MKRN2 belongs to a family that has a characteristic zinc-finger composition. The function of the protein family to which MKRN2 belongs is unknown. Comparison of intron and exon boundaries showed that the 3' *lox*P targeting event has integrated between exons 6 and 7 of MKRN2 (Figure 3.20). MKRN2 has a total

Fig. 3.20. Diagram showing the intron/exon structures of the 3' end of the *raf-1* gene and the 3' end of the *Mkrn2* gene. The *Mkrn2* gene is antisense to the *raf-1* gene and overlaps by 91 bp indicated by the broken parallel lines. The *raf-1* gene is coloured red and the *Mkrn2* gene is coloured green. The *lox*P and hyg^R introduced by homologous recombination with the 3' targeting vector integrated at the Xba I site. Therefore following Cre-mediated recombination between the two *lox*P sites (the other *lox*P site being present at the 5' end of *raf-1*) will result in the the deletion of exons 7 and 8 of *Mkrn2* in addition to the deletion of exons 3 to 17 of *raf-1*.

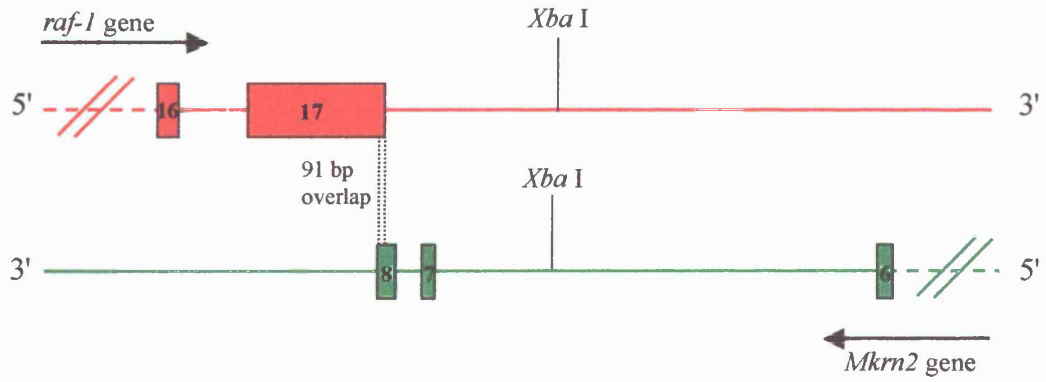

of 8 exons, therefore upon Cre-mediated recombination between the two *lox*P sites, this would result in the deletion of exons 7 and 8 of *Mkrn2* in addition to the deletion of *raf-1*. In hindsight therefore, the 3' *lox*P site should have been placed within intron 16 of *raf-1* between exons 16 and 17 as this region does not overlap with the *Mkrn2* gene. The deletion of exons 7 and 8 of *Mkrn2* will probably result in a truncated protein which may or may not function as the native protein. Therefore the future analysis of the phenotypes of the Raf-1 floxed mice when they have been made will have to be considered in light of this fact.

4 CRE-MEDIATED DELETION OF A FLOXED DNA SEQUENCE

4.1 Introduction

4.1.1 Expression of Cre in vitro and in vivo

Once a floxed allele for a given gene has been generated in ES cells, Cre-mediated deletion can be achieved by transfection of the ES cells with a vector expressing Cre under the control of a suitable promoter. Alternatively, once a floxed allele has been generated *in vivo*, the mutant mouse can be crossed with a corresponding Cre transgenic mouse that exhibits the desired spatial or temporal specificity of Cre expression resulting in the generation of a double transgenic mouse line. As discussed in chapter three, to achieve spatial restriction, the *cre* coding sequence can be placed under the regulation of a variety of tissue-specific promoters and to achieve temporal restriction, *cre* can be placed under the regulation of an inducible promoter, or a ligand regulated Cre protein can be used.

4.1.2 Potential role of Raf-1 in cardiac myocyte hypertrophy

Cardiac hypertrophy occurs in response to an increased workload. It is a compensatory response which results in an increase in myocyte size in the absence of cell division as these cells are terminally differentiated. Changes in gene expression occur in order to maintain the function of the heart. With the use of cardiomyocytes in primary culture, a variety of extracellular stimuli that induce the hypertrophic response have been identified including; mechanical stretch, cytokines, growth factors, hormones, catecholamines and vasoactive peptides (Yamazaki *et al.*, 1998). The exposure of ventricular myocytes to such stimuli activates a series of genetic changes that leads to cell hypertrophy including the induction of early response genes such as c-*jun*, c-*fos* and c-*myc*. Many of these hypertrophic agonists have also been shown to activate MEK and ERK in these cells and suggest that the Ras/Raf/MEK/ERK cascade may play a role in the transcriptional changes associated with hypertrophy (Sadoshima and Izumo, 1993; Yamazaki *et al.*, 1993; Bogoyevitch *et al.*, 1994; Thorburn *et al.*, 1994a;). Direct support for this hypothesis is provided by studies using neonatal rat ventricular myocytes where the introduction of RasV12 and constitutively activated forms of MEK induce changes in gene expression that are associated with hypertrophy (Thorburn *et al.*, 1993). A-Raf and Raf-1 are expressed in

cultured ventricular myocytes and hypertrophic stimuli differentially activate these two isoforms (Bogoyevitch *et al.*, 1995). A role for Raf-1 in the regulation of cardiac myocyte hypertrophy was demonstrated by using an estradiol-inducible Raf-1 and dominant negative Raf-1 mutants. The activation of Raf-1 results in ERK activation and subsequent expression of the atrial natriuretic factor (ANF) and myosin light chain-2 (MLC-2) genes, indicating that Raf-1 can induce expression of genes that are involved in the hypertrophic response in the absence of other stimuli. However, active Raf-1 alone is not sufficient to induce the morphological changes associated with the hypertrophic response (Thorburn *et al.*, 1994b).

To further study the role of Raf-1 specifically in the hypertrophic response, it is possible to achieve the specific deletion of Raf-1 in the heart by crossing a Raf-1 floxed mouse, described in Chapter 3, with a Cre expressing transgenic mouse line where Cre is expressed under control of the myosin light chain 2v (MLC-2v) promoter (Chen *et al.*, 1998). This promoter is only active in the ventricular chamber of the heart. Therefore the deletion of *raf-1* would be restricted to these cells only.

4.1.3 MLC2v-Cre knock-in mice

Expression of the *MLC-2v* gene at E8.75 is the earliest ventricular restricted marker during mammalian cardiogenesis. The *MLC-2v* gene is an abundant transcript in all ventricular muscle cell lineages, even at the earliest stages of ventricular chamber specification, which acts to assist in achieving high levels of efficiency of recombination. Use of *MLC2v*-Cre transgenic mice to generate a conditional knockout has previously been reported by Chen *et al.* (1998). As a test for the efficiency of Cre expression, a conditional allele of one of the retinoic acid receptors, RXRα, in which *lox*P sites flanked an essential exon, was established in the mouse germline. Mice homozygous for the floxed RXRα allele and carrying the MLC2v-Cre knock-in gene demonstrate a conditional mutation of the RXRα gene exclusively in the ventricular chamber of the heart as early as E8.75, with an efficiency of approximately 80%. These results show that this is a highly efficient method for generating a conditional knockout of a floxed gene in the ventricular chamber of the embryonic heart (Chen *et al.*, 1998).

In order to study Raf-1 function in heart and the role of Raf-1 in cardiac myocyte hypertrophy, the aim was to cross the Raf-1 floxed mice generated in chapter three with the MLC2v-Cre knock-in mice.

4.2 Aims

The aim of this part of the project was to firstly develop conditions for using Cre in tissue culture cells since it had not been used previously in the laboratory. Conditions for this purpose were developed for the deletion of the *neo*^{R} gene in *raf-1*$^{FF/FF}$ MEFs. The second aim was to use Cre to confirm whether or not that the two *lox*P sites introduced by homologous recombination with two separate targeting vectors (generated in Chapter 3) had integrated on the same chromosome by the expression of Cre. The third aim was to establish a colony of MLC2vCre mice obtained from Dr. K. Chien (Department of Medicine and Center for Molecular Genetics, University of California, San Diego) that would eventually be mated with the *raf-1* floxed mice with an aim to delete *raf-1* specifically in the heart.

4.3 Results

4.3.1 Derivation of immortalised MEFs from raf-1$^{FF/FF}$ *mice*

It is thought that full activation of Raf-1 requires the phosphorylation of two tyrosine residues 340 and 341 as mutation of these two tyrosine residues to phenyalanine residues, creating RafFF, prevents activation of Raf-1 by oncogenic Ras and v-Src, or by ligand stimulation (Fabian *et al.*, 1993; Marais *et al.*, 1995). A 'knockin' strategy was employed to mutate these two residues to phenylalanine residues creating RafFF. The generation of *raf-1*$^{FF/FF}$ mice was reported by Hüser et al. (2001) and Figure 4.1 provides details of the targeting event. In order to generate *raf-1*$^{FF/FF}$ MEFs, *raf-1*$^{+/FF}$ male and *raf-1*$^{+/FF}$ female mice were mated and embryos were harvested at E14.5. MEFs were derived from the embryos by standard procedures and the genotypes were confirmed by PCR. This work was undertaken by Dr. M. Hüser (Department of Biochemistry, University of Leicester). Sibling *raf-1*$^{+/+}$ MEFs were named A2 and A8 and *raf-1*$^{FF/FF}$ MEFs were named A6 and A7. These four cell lines were immortalised with virus expressing the SV40 large T antigen by Dr. M. Hüser.

Protein lysates were prepared from these immortalised MEFs, followed by SDS-PAGE and electro-transfer of the proteins onto nitrocellulose. The blots were incubated with an anti-Raf-1 antibody. The western blot data showed a decreased amount of Raf-1 protein in the *raf-1*$^{FF/FF}$ cells in comparison to *raf-1*$^{+/+}$ cells (Figure 4.2A). An anti-vinculin antibody was used as a control for protein loading (Figure 4.2B). This decreased level of Raf-1 protein was probably due to a decrease in *raf-1* transcription as a result of the presence of the *neo*^{R} gene. Since two *lox*P sites flank the *neo*^{R} gene, the expression of Cre in these cells would result in deletion of the *neo*^{R} gene, possibly leading to the restoration of expression of Raf-1 protein levels.

4.3.2 In vitro Cre-mediated deletion of the neo^{R} *gene in immortalised MEFs from raf-1*$^{FF/FF}$ *mice*

A plasmid containing the gene for Cre recombinase driven by the HSV-tk promoter, named pIC-Cre was obtained (Gu *et al.*, 1993). This pIC-Cre plasmid also contains the *neo*^{R} gene. Therefore in order to introduce it into *raf-1*$^{FF/FF}$ MEFs that also harboured the *neo*^{R} gene, a co-electroporation with the pX53-hyg plasmid was performed as this confers resistance to hygromycin B. It was assumed that a high proportion of resistant clones that grew through after selection with hygromycin B would also have acquired the pIC-Cre plasmid. 15 μg pIC-Cre was linearised with *Hin*d III and 1.5 μg pX53-hyg was linearised with *Bam*H I. These were electroporated into two *raf-1*$^{FF/FF}$ immortalised lines (A6 and A7). After 7 days of hygromycin B selection, 40 clones from each electroporated cell line were picked and grown up for DNA analysis.

In order to screen for the deletion of the *neo*^{R} gene, two primers were designed that flanked the *neo*^{R} gene in the *raf-1*$^{FF/FF}$ MEFs. Ocp52 is located within the *Xba* I/*Xba* I *raf-1* fragment used for one of the arms of the targeting construct with extension occurring towards the 3' end of the *raf-1* gene (Figure 4.1). Ocp59 is located within the *Xba* I/*Eco* RI *raf-1* fragment used for the other arm of the targeting construct with extension occurring towards the 5' end of the *raf-1* gene (Figure 4.1).

PCR was performed on the *raf-1*$^{FF/FF}$ MEFs before and after they were transfected with pIC-Cre plus *raf-1*$^{+/+}$ MEF control samples. PCR with Ocp52 and Ocp59 amplified a

Fig. 4.1 Diagram showing homologous recombination between RafFF targeting vector and the *raf-1* gene and the consequences of a Cre-mediated recombination event. The positions of PCR primers used for detection of both the wild-type and targeted alleles are indicated. **(A)** Restriction map of the wild-type *raf-1* gene highlighting the positions of homologous arms used in the construction of the RafFF targeting vector. **(B)** RafFF targeting vector. In this vector, the neo^R gene is flanked by *lox*P sequences. **(C)** Restriction map of the *raf-1* gene following homologous recombination with the RafFF targeting vector. **(D)** Restriction map of the *raf-1* gene after Cre mediated recombination.

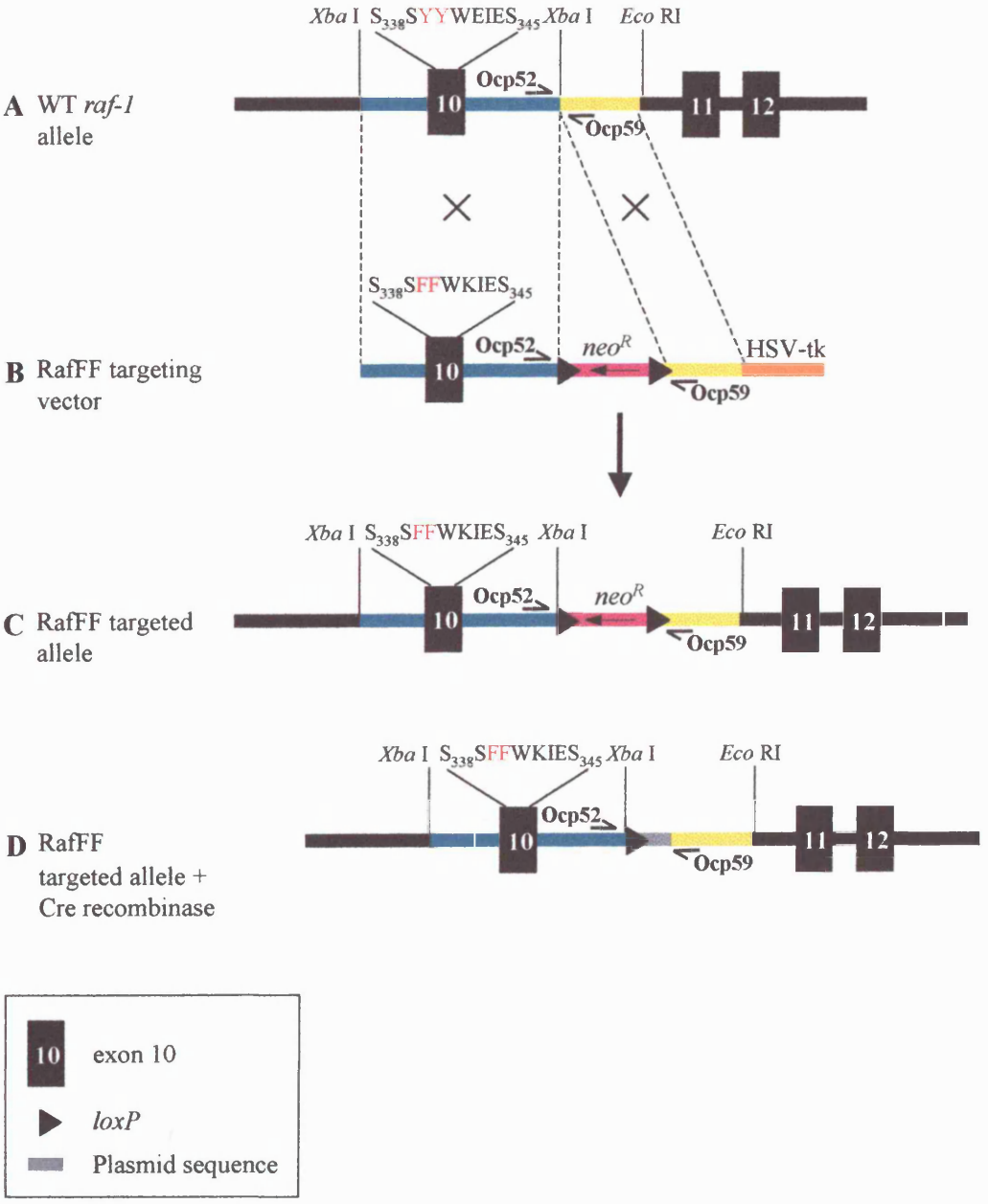

Fig. 4.2 Screening immortalised *raf-1*$^{FF/FF}$ MEFs transfected with the pIC-Cre plasmid to detect excision of the *neo*^{R} gene. (**A**) Western blot analysis to detect levels of Raf-1 in the *raf-1*$^{+/+}$, *raf-1*$^{FF/FF}$ and in the MEFs transfected with pIC-Cre. (**B**) Western blot analysis to detect levels of vinculin as a control for protein loadings. (**C**) PCR using Ocp52 and Ocp59 to amplify both the wild-type allele, the targeted allele, and the cre-mediated deleted allele from the *raf-1*$^{+/+}$, *raf-1*$^{FF/FF}$ and in the MEFs transfected with pIC-Cre. M = 1 kb DNA marker.

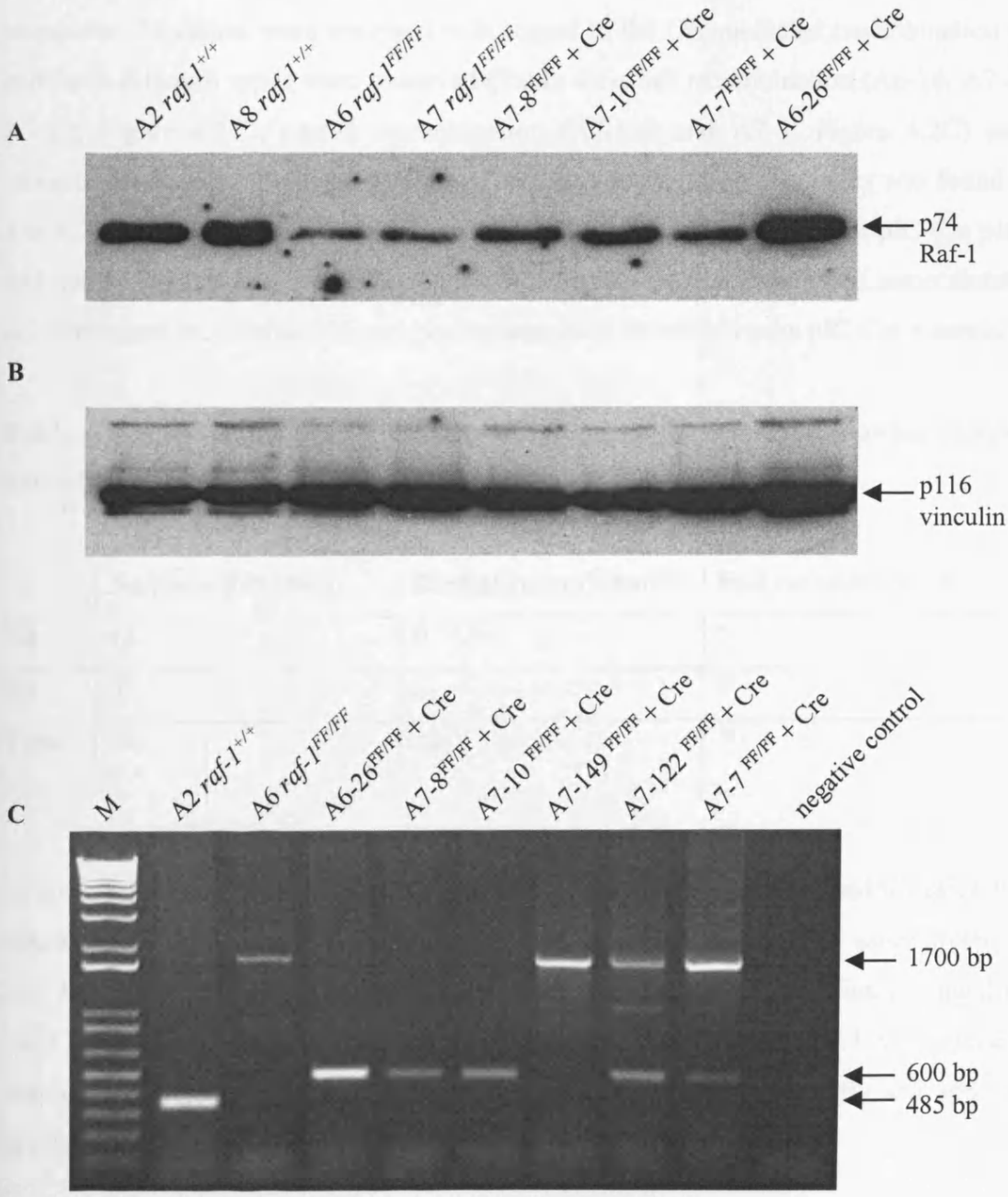

485 bp product from *raf-1*$^{+/+}$ MEFs (A2; Figure 4.2C) and a 1700 bp product from *raf-1*$^{FF/FF}$ MEFs (A6; Figure 4.2C). Following the introduction of Cre into the *raf-1*$^{FF/FF}$ MEFs, a smaller product of around 600 bp was observed from clones that had undergone cre-mediated deletion of the *neo*^{R} gene (A6-26, A7-8, A7-10, A7-122 and A7-7; Figure 4.2C). This PCR product represents the Cre-recombined allele lacking the *neo*^{R} gene with the retention of a single *lox*P site (Figure 4.1D). It is important to note that the product arising from the Cre-recombined allele is larger than that arising from the wild-type allele which is presumably due to the presence of the remaining *lox*P site and extra plasmid sequence. 33 clones were analysed with regard to the Cre-mediated recombination event and three different types were observed (Table 4.1); full recombination (A6-26, A7-8 and A7-10; Figure 4.2C), partial recombination (A7-122 and A7-7; Figure 4.2C) and no recombination (A7-149; Figure 4.2C). The full recombination efficiency was found to be 1 in 4.7. However, the clones were not screened for the integration of the pIC-Cre plasmid and due to the fact that a co-transfection was performed, the reason that some clones had not undergone recombination could be because they do not have the pIC-Cre plasmid.

Table 4.1 Number of clones with different recombination products following transfection with pIC-Cre as assessed by PCR with Ocp52 and Ocp59.

	No recombination	**Partial recombination**	**Full recombination**
A6	11	6	0
A7	3	6	7
Total	14	12	7

In order to confirm that Cre-mediated deletion of the *neo*^{R} gene had lead to restoration of expression of Raf-1 protein levels, a Raf-1 western blot was performed using protein from A2, A8, A6, A7, A7-8, A7-10, A7-7 and A6-26 (Figure 4.2C). Detection of vinculin was used as a control for protein loading (Figure 4.2B). In all cases, Raf-1 from clones that amplified the cre-recombined allele by PCR had increased significantly and approached levels similar to wild type.

4.3.3 In vitro Cre mediated deletion of raf-1 in ES cells containing 5' and 3' loxP targeting events

Of major importance in the generation of the floxed *raf-1* allele described in Chapter 3 was knowledge of whether the two *lox*P targeting events (pTC7-*lox*P-neo and pTC8-*lox*P-hyg) had occurred on the same chromosome. Since conditions for Cre-mediated deletion had been established (see Section 4.3.2), the simplest approach was to introduce Cre into ES cells containing the two *lox*P targeting events and assess whether or not the intervening DNA had been deleted. For these experiments, a different Cre expression vector containing the gene for Cre driven by the MC1 promoter named pCre-Pac (Chapter 2, Figure 2. 1) was used. This plasmid contains a puromycin resistance ($puro^R$) gene and is advantageous to use as it can be electroporated without a co-selectable plasmid. 10 μg of the pCre-Pac plasmid was electroporated separately into each of the eight ES cell clones positive for pTC7-*lox*P-neo and pTC8-*lox*P-hyg targeting events (ES cell clones 7, 9, 18, 26, 29, 38, 55 and 166). After 7 days of puromycin and G418 selection, 12 resistant colonies from each ES cell clone and 24 clones from ES cell clone numbers 9 and 26 were picked and grown up for DNA analysis and a portion was frozen down. The reason for selecting using G418 along with puromycin was because of the problem encountered with loss of the neo^R gene in ES cell clone 9 and 26 discussed in chapter three.

4.3.4 Detection of Cre-mediated deletion of raf-1 in ES cells

To assess whether Cre-mediated deletion of *raf-1* had occurred in any of the ES cell clones, PCR using Ocp66 and Ocp83 was attempted that spanned the region of deletion i.e. from the hyg^R gene to the neo^R gene, but unfortunately this PCR was unsuccessful. Also, there were no suitable restriction enzymes that could be used to perform diagnostic Southern blot analysis.

The only other way to easily assess whether Cre-mediated deletion of *raf-1* had occurred was to perform a PCR that gave a negative result if *raf-1* had been deleted. Two primers were used for this purpose. Ocp100 is located within the 1.4 kb *Xba* I *raf-1* fragment used as one of the arms for pTC7-*lox*P-neo with extension occurring towards the 3' end of *raf- 1* (Figure 4.3A and B). Ocp68 is located within the 4.4 kb *Xba* I *raf-1* fragment used as one of the arms for pTC7-*lox*P-neo with extension occurring towards the 5' end of *raf-1*

(Figure 4.3A and B). Ocp100 and Ocp68 amplified a 286 bp PCR product from the wild-type allele and a 1430 bp PCR product from the targeted allele. All of the untransfected ES cell clones amplified both PCR products because they were all heterozygous for the pTC7-*lox*P-neo targeting event (shown for ES cell clones 9 and 26 in Figure 4.4A).

Following Cre-mediated deletion of *raf-1*, if the 1430 bp product disappears then this would indicate that both *lox*P targeting events were on the same chromosome as Ocp68 would be deleted. The wild-type PCR product of 286 bp was amplified in all clones analysed that had been transfected with pCre-Pac and this conveniently served as a control for the larger PCR product (Figure 4.4A). The 1430 bp PCR product was amplified from all clones originating from 7, 18, 38, 55 and 166 (Figure 4.4A). However, 5 out of 6 clones that originated from ES cell clone number 29 did not amplify the 1430 bp PCR product (clones 29-1, 29-2, 29-3, 29-4, 29-6; Figure 4.4A). Also, 5 out of 8 clones that originated from ES cell clone number 9 (9-13, 9-14, 9-15, 9-17 and 9-18; Figure 4.4A) and 2 out of 5 clones that originated from ES cell clone number 26 (26-10 and 26-14; Figure 4.4A) did not detectably amplify the 1430 bp PCR product.

To further confirm these results, another PCR was set up using primers Ocp66 and Ocp68 that again was reliant on the lack of a PCR product to indicate Cre-mediated deletion of *raf-1*. These primers amplified a 450 bp PCR product from the targeted allele in all clones analysed (shown for 26-14, 9-14 and 38-5 in Figure 4.4B) except from clone 29-1 (Figure 4.4B). The data for 29-1 is consistent with the other PCR result obtained from primers Ocp68 and Ocp100. However, the data from 9-14 and 26-14 is not consistent with the other PCR results obtained from primers Ocp68 and Ocp100. Therefore it is clear that ES cell clone 29 consistently gives results to show that Cre-mediated deletion of the *raf-1* gene has occurred, but the results for ES cell clones 9 and 26 are not so clear.

A final PCR was set up using Ocp69 and Ocp100 as a further control to confirm that the reason for the loss of PCR product described for clones originating from ES cell clone 29 with the two previous PCRs were not as a result of a loss of the 5' targeting event. A PCR product was amplified with sample 29-1 indicating that the 5' targeting event was still present (Figure 4.4C).

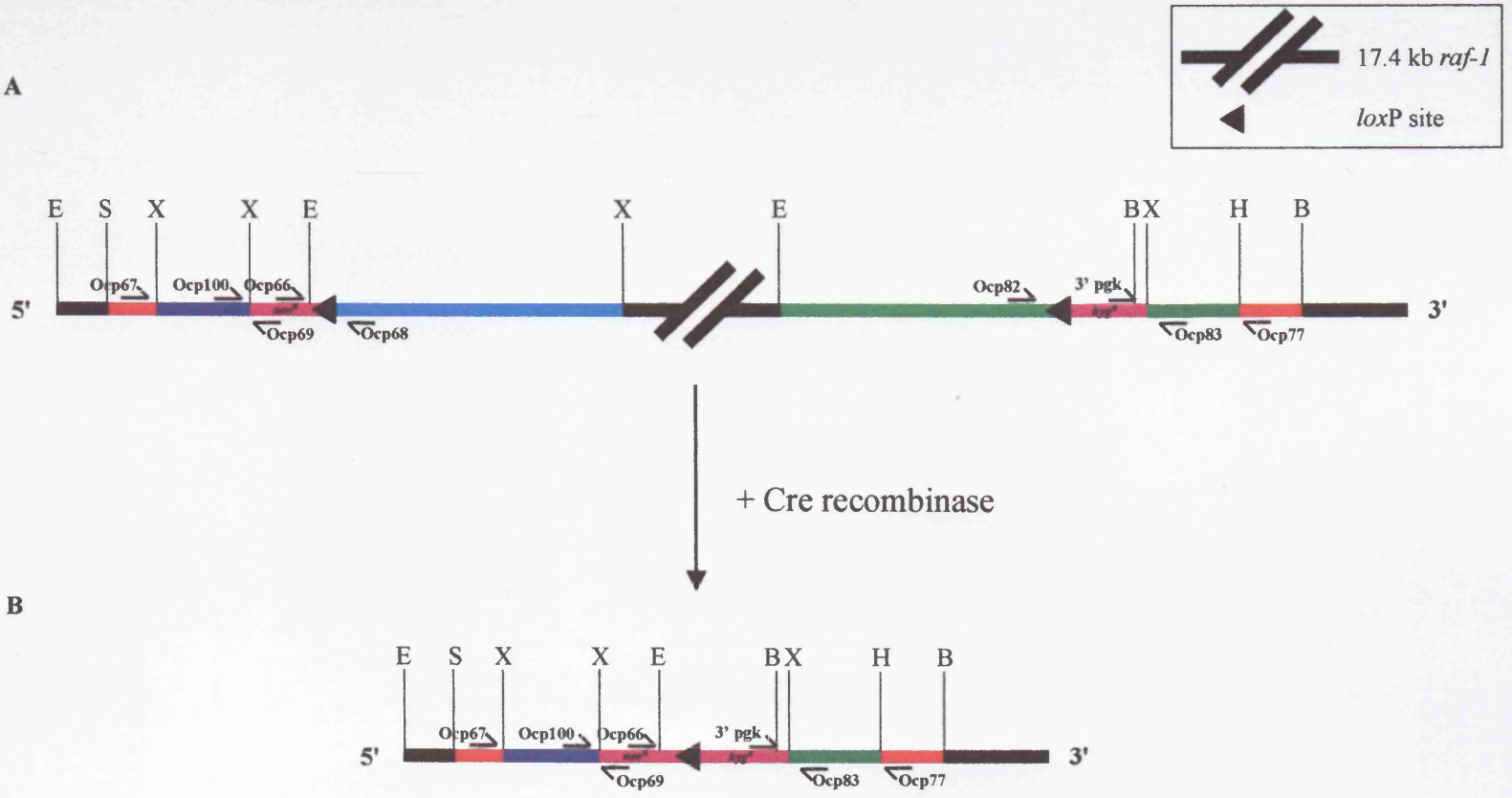

Fig. 4.3 Diagram showing the *raf-1* gene before and after Cre-mediated deletion if *lox*P sites are present on the same chromosome, highlighting restriction sites and positions of PCR primers. **(A)** *raf-1* targeted gene containing 5' and 3' *lox*P targeting events prior to Cre-mediated deletion, highlighting the positions of homologous arms used in the construction of the targeting vectors. **(B)** *raf-1* gene following Cre-mediated recombination between *lox*P sites. Single letter key: E = *Eco* RI, S = *Sst* I, X = *Xba* I, B = *Bam*H I and H = *Hin*d III.

Fig. 4.4 PCR analysis of eight ES cell clones electroporated with pCre-Pac. (**A**) PCR using Ocp68 and Ocp100 amplified the wild-type PCR product of 286 bp from all samples and the 5' *lox*P targeted PCR product of 1430 bp from all samples except from 29-1, 29-2, 29-3, 29-4 and 29-6. (**B**) PCR using Ocp66 and Ocp68 amplified the 5' *lox*P targeted PCR product of 450 bp from 26-14, 9-14, 38-5 and 29 but not from 29-1 and wild-type (WT). (**C**) PCR using Ocp69 and Ocp100 amplified the 5' *lox*P targeted PCR product of 290 bp from 29-1 and 38-5 but not from WT. M = 1 kb DNA marker.

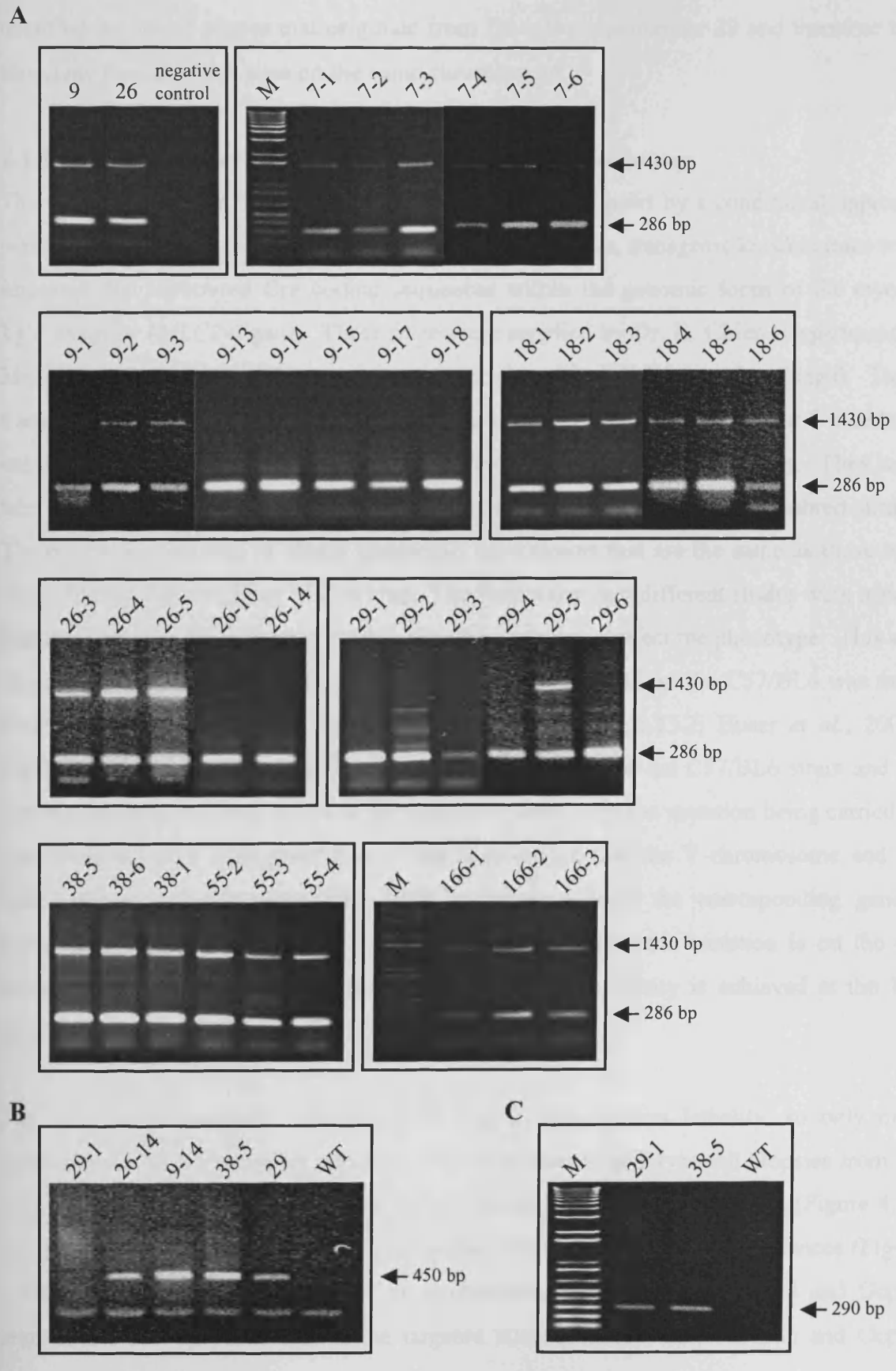
A
9
26
negative control
M
7-1
7-2
7-3
7-4
7-5
7-6
1430 bp
286 bp
9-1
9-2
9-3
9-13
9-14
9-15
9-17
9-18
18-1
18-2
18-3
18-4
18-5
18-6
1430 bp
286 bp
26-3
26-4
26-5
26-10
26-14
29-1
29-2
29-3
29-4
29-5
29-6
1430 bp
286 bp
38-5
38-6
38-1
55-2
55-3
55-4
M
166-1
166-2
166-3
1430 bp
286 bp
B
29-1
26-14
9-14
38-5
29
WT
450 bp
C
M
29-1
38-5
WT
290 bp

These PCR results provide strong evidence that Cre-mediated deletion of *raf-1* had occurred in these 5 clones that originate from ES cell clone number 29 and therefore that this clone contains *lox*P sites on the same chromosome.

4.3.5 Maintenance of a Cre expressing transgenic mouse colony

The ultimate goal was to analyse the role of Raf-1 in the heart by a conditional approach using mice harbouring a floxed *raf-1* gene. For this purpose, transgenic knockin mice were imported that harboured Cre coding sequences within the genomic locus of the myosin light chain 2v (*MLC2v*) gene. These mice were supplied by Dr. K. Chien (Department of Medicine and Center for Molecular Genetics, University of California, San Diego). These transgenic mice were imported from California and kept in an isolated unit for 6 months to ensure that they did not pose a health risk to the other animals in the facility. They were bred onto 2 different background strains; the MF-1 outbred and C57/BL6 inbred strains. The reason for this was to obtain genetically pure strains that are the same as those onto which the *raf-1* floxed mice will be bred. The reason that two different strains were used is that the particular strain used to establish a mutation on can affect the phenotype. This was observed with the *raf-1* knockout phenotype, as the mutation on the C57/BL6 was more severe than on the MF-1 background strains (see Section 1.13.2; Huser *et al.*, 2001). Figure 4.5 shows the breeding strategy that was followed for the C57/BL6 strain and the breeding strategy that was followed for the MF-1 strain with the mutation being carried on alternating sexes at each generation. This is to ensure that the Y chromosome and the maternally inherited mitochondrial DNA is inherited from the corresponding genetic background that the mice are being bred onto. At present the mutation is on the 6th generation on both genetic backgrounds. Virtual genetic purity is achieved at the 10^{th} generation.

The *MLC2v*-Cre knock-in mutation gives rise to homozygous lethality, so only mice heterozygous for the mutation survived. PCR was used to genotype tail biopsies from the mice. Primers Ocp84 and Ocp85 are located within Cre specific sequences (Figure 4.6B and C). Primers Ocp86 and Ocp87 are located within *MLC2v* specific sequences (Figure 4.6A). All four primers were used in combination for each PCR. Ocp84 and Ocp85 amplified a 350 bp product from the targeted allele (Figure 4.6D). Ocp86 and Ocp87

Fig. 4.5 Breeding strategy for obtaining the MLC2vCre knock-in mutation on the MF-1 outbred strain and on the C57/BL6 inbred strain. At present, breeding has been achieved up to the 6th generation. At each generation, the males and females were alternated as shown.

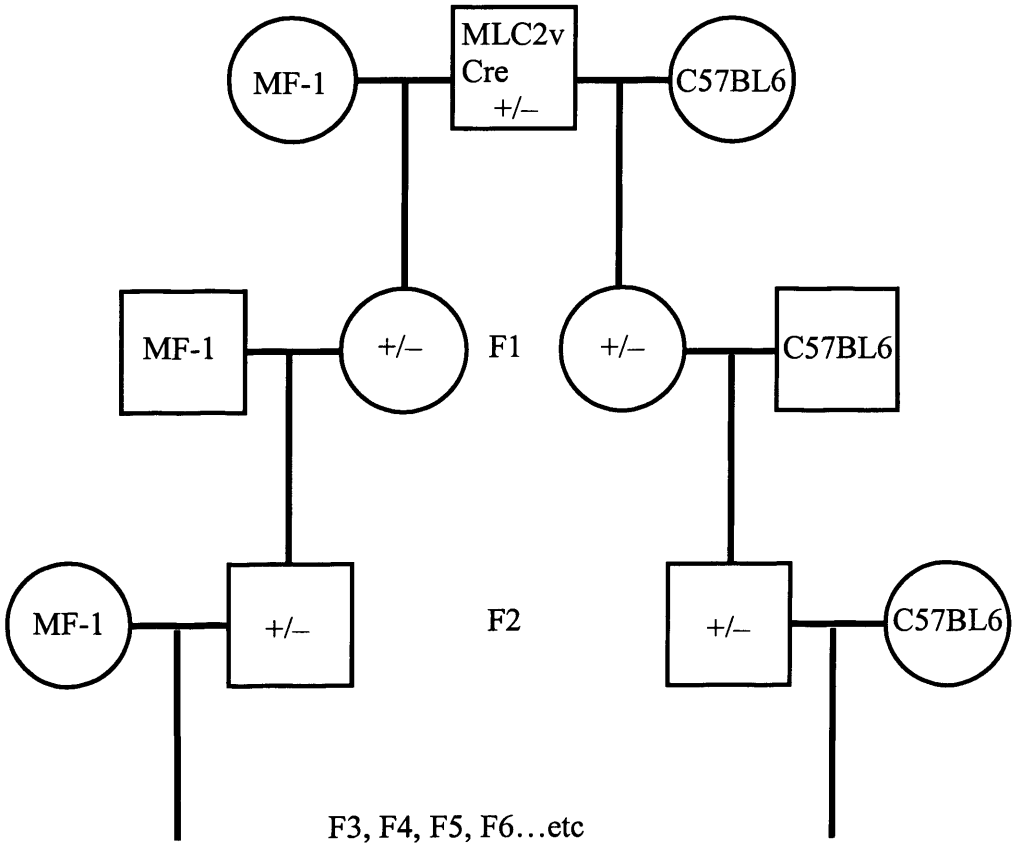

Fig. 4.6 Generation and PCR genotyping of MLC2v Cre transgenic mice (Chen *et al.*, 1998). **(A)** MLC2v wild-type allele indicating positions of primers Ocp86 and Ocp87. **(B)** Targeting construct to replace MLC2v coding sequence with Cre recombinase coding sequence by homologous recombination. The positions of primers Ocp84 and Ocp85 are indicated. **(C)** Targeted allele indicating positions of primers Ocp84 and Ocp85. **(D)** PCR genotyping of MLC2v mice using Ocp84, Ocp85, Ocp86 and Ocp87 to amplify both the wild-type allele and the targeted allele. M = 1 kb DNA marker.

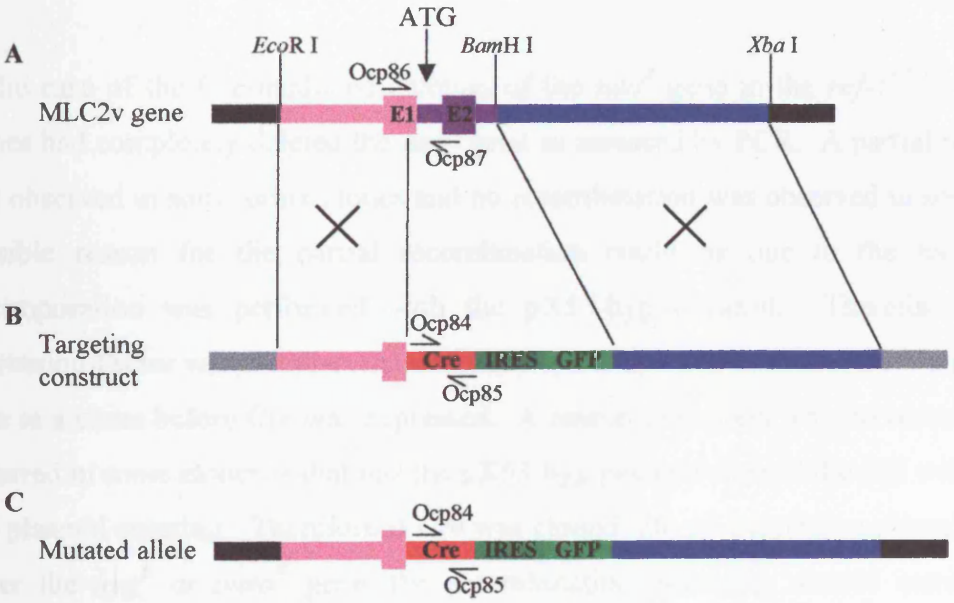

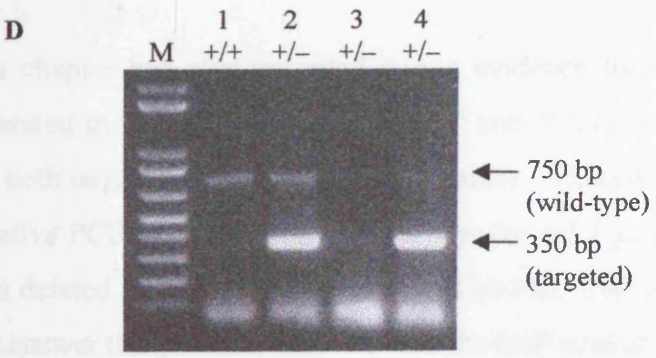

amplified a 750 bp product from the wild type allele (Figure 4.6D). Therefore 2, 3 and 4 are heterozygous mice and could be used for future breeding with the *raf-1* floxed mice. 1 is a wild-type mouse.

4.4 Conclusions

This chapter describes the successful use of Cre expressing plasmids for two purposes: Firstly, the deletion of the neo^R gene from an intron of the *raf-1* gene in immortalised $raf\text{-}1^{FF/FF}$ MEFs, and secondly, the determination of which of the ES cell clones generated in Chapter 3 contain two *lox*P sites on the same chromosome.

In the case of the Cre-mediated deletion of the neo^R gene in the $raf\text{-}1^{FF/FF}$ MEFs, some clones had completely deleted the neo^R gene as assessed by PCR. A partial recombination was observed in some other clones and no recombination was observed in some others. A possible reason for the partial recombination could be due to the fact that a co-electroporation was performed with the pX53-hyg plasmid. Therefore, as the Cre expression vector was not directly selected for, it may have been lost from a portion of the cells in a clone before Cre was expressed. A reason to explain why no recombination had occurred in some clones is that just the pX53-hyg plasmid entered the cell without the pIC-Cre plasmid entering. Therefore if Cre was cloned into an expression plasmid harbouring either the hyg^R or $puro^R$ gene, the recombination efficiency should increase, as each resistant clone would have taken up the plasmid. Nonetheless these results have shown that Cre efficiently deletes a floxed gene in tissue culture cells and that this deletion is stable.

This chapter has also provided strong evidence by PCR that ES cell clone number 29 generated in chapter 3 contains both 5' and 3' targeting events on the same chromosome and both targeting events appear to be stable. This conclusion is based on two independent negative PCR results which suggest that the *raf-1* gene in between the two *lox*P sites has been deleted after the introduction of pCre-Pac. The generation of mice is in progress and will answer the question as to whether the *lox*P sites are on the same chromosome.

An interesting observation was discovered with ES cell clone numbers 9 and 26 transfected with pCre-Pac. The targeted PCR product (1430 bp) that arises from Ocp100 and Ocp68 was not detectably amplified from several ES cell clones derived from numbers 9 and 26. However, when Ocp66 and Ocp68 were used, the intensity of the targeted PCR product was similar to that from a sample that had not been transfected with pCre-Pac. Therefore the only reasonable explanation for the difference is that the low intensity of the targeted PCR product is simply as a result of sub-optimal PCR due to the large size (1430 bp) in comparison to the smaller wild-type PCR product (286 bp) from Ocp68 and Ocp100 and the targeted PCR product (450 bp) from Ocp66 and Ocp68. However, even if ES cell clones 9 and 26 do prove to have both *lox*P sites on the same chromosome, they could not be used to generate mice as it is evident from experiments conducted in Chapter 3 that the 5' *lox*P targeting event is unstable in these ES cell clones.

Finally, a colony of mice expressing Cre specifically in the heart has been imported and bred. The mutation has been established onto the MF-1 outbred and C57/BL6 inbred genetic backgrounds and are available to cross to the *raf-1* floxed mice once they have been made from ES cell clone 29. The specific deletion of Raf-1 in the heart would give information on the role of Raf-1 in cardiac hypertrophy as it has been shown that Raf-1 is expressed in cultured ventricular myocytes and is differentially activated by hypertrophic stimuli (Bogoyevitch *et al.*, 1995). Moreover, it appears that the Ras/Raf/MEK/ERK cascade has a role in the transcriptional changes associated with hypertrophy including induction of expression of the ANF and MLC-2 genes (Thorburn *et al.*, 1994b). Therefore the specific deletion of Raf-1 in the ventricular cells would give valuable information to its role in the hypertrophic response. Analysis of the *raf-1* null mice previously generated in our laboratory indicated that there was no obvious problem with heart function in E9.5 embryos and is probably not the cause of death, therefore the specific deletion of Raf-1 in the heart is postulated to result in healthy mice.

4.5 Further work

It would be desirable to further analyse ES cell clone 29 to be able to confirm the PCR data suggesting that that the two *lox*P sites at the 3' and 5' end of *raf-1* are on the same chromosome. For example, a Western blot to detect Raf-1 could be performed, as there

may be a reduction in the amount of Raf-1 expressed if one *raf-1* allele has been deleted, as this is observed with cells heterozygous for the conventional Raf-1 knockout. In the meantime mice are being generated from these ES cells.

Once, mice have been generated and a colony of *raf-1* floxed mice has been established on the C57/BL6 and MF-1 background strains, they can then be crossed with the *MLC2v*–Cre mice with an aim to analyse Raf-1 function in the heart. The aim would be to isolate cardiac myocytes and investigate the activation of the Ras/Raf/MEK/ERK cascade in response to hypertrophic stimuli.

The *raf-1* floxed mice can be used to generate primary MEFs. Each primary floxed line could then be transfected with a Cre-ER expressing plasmid whereby Cre is only active upon the addition of 4-hydroxytamoxifen (see Chapter 3). This therefore means that experiments can be performed with genetically identical cells with the only difference being that one population is treated with 4-hydroxytamoxifen resulting in the deletion of the *raf-1* gene and the other is not treated and retains *raf-1*. This therefore should eliminate problems often observed with inconsistency between cell lines derived from different siblings. The MEFs would be used primarily to investigate the role of Raf-1 in apoptosis since Chapter 5 uncovered a specific role of Raf-1 in the prevention of apoptosis in MEFs.

A major advantage of using conditional technology rather than to generate null alleles in the conventional way is the recent discovery that cells can adapt to the loss of a particular protein and respond by altering the regulation of other proteins (Sage *et al.* [abstract at Genes and Cancer meeting, Warwick, 2001]). This makes the analysis of the role of the protein in question more difficult to interpret and hence *lox*P technology could eliminate this unwelcome complication.

5 CHARACTERISATION OF PROLIFERATION AND APOPTOSIS IN *raf-1*$^{-/-}$ AND *raf-1*$^{FF/FF}$ MUTANT MOUSE EMBRYONIC FIBROBLASTS

5.1 Introduction

5.1.1 Potential involvement of Raf-1 in proliferation and apoptosis

Raf-1 is the most studied of the three Raf proteins and abundant levels of Raf-1 transcript can be detected in all tissues (Storm *et al.*, 1990). The best characterised role for Raf-1 is as a key component in the Ras/Raf/MEK/ERK cascade. It was shown to bind to activated Ras (Koide *et al.*, 1993; Van Aelst *et al.*, 1993; Vojtek *et al.*, 1993; Warne *et al.*, 1993; Zhang *et al.*, 1993) which results in the translocation of Raf-1 to the plasma membrane (Traverse *et al.*, 1993; Leevers *et al.*, 1994; Stokoe *et al.*, 1994) where additional signals are received to allow full activation including phosphorylation events (Leevers *et al.*, 1994; Marais *et al.*, 1995). Raf-1 has been shown to phosphorylate and activate MEK-1 and MEK-2 when the kinase domain of Raf-1 is overexpressed *in vitro* and *in vivo* (Dent *et al.*, 1992; Howe *et al.*, 1992; Kyriakis *et al.*, 1992; Pritchard *et al.*, 1995; Marais *et al.*, 1997). However, in comparison to B-Raf, the kinase domain of Raf-1 is much weaker in its ability to phosphorylate and activate MEK as assessed by overexpression studies of the kinase domains and by measuring the ability of coimmunoprecipitated endogenous Raf proteins to phosphorylate and activate MEK and ERK, but it is a much better activator of MEK than A-Raf (Pritchard *et al.*, 1995; Marais *et al.*, 1997; Papin *et al.*, 1998; Huser *et al.*, 2001). Therefore, Raf-1 is able to participate in the Ras/Raf/MEK/ERK cascade, although its effect on this signalling pathway is less significant than the effect of activated B-Raf. The differing abilities of the Raf isoforms to activate MEK may have profound implications for the cell, with low levels of Raf activity eliciting cell cycle progression and high levels of Raf activity eliciting cell cycle arrest. Therefore, the specific Raf protein that becomes activated at a certain time may determine cell fate (Woods *et al.*, 1997).

A direct connection between activation of the Ras/Raf/MEK/ERK cascade and transcriptional changes that are believed to induce cell proliferation has been demonstrated. The ERKs have been shown to phosphorylate transcription factors including Elk-1. This

particular transcription factor, in combination with the SRF is responsible for the transcription of the prominent early response gene *c-fos* (Treisman, 1996). c-Fos is one of the components of AP-1 which promotes the transcription of many genes including cyclin D1 which is responsible for promoting the G1 to S phase transition (Angel and Karin, 1991; Albanese *et al.*, 1995;).

A connection between the Ras/Raf/MEK/ERK cascade and the inhibition of apoptosis was demonstrated by the overexpression of constitutively activated MEK, Ras, Raf-1 or B-Raf, which resulted in the prevention of apoptosis following growth factor deprivation of various cell types (Cleveland *et al.*, 1994; Erhardt *et al.*, 1999; Le Gall *et al.*, 2000). Also, the removal of nerve growth factor from PC12 cells results in apoptosis involving the sustained activation of JNKs and p38MAPKs and inhibition of ERKs (Xia *et al.*, 1995). The ERKs were found to act in both a transcription-dependent or -independent manner to prevent apoptosis in cerebellar neurones via the phosphorylation and activation of p90RSKs. Rsk-2 has been shown to directly phosphorylate Bad on Ser112 (Bonni *et al.*, 1999). RSKs are also able to phosphorylate and activate the transcription factor CREB which is thought to induce the expression of Bcl-2 (Bonni *et al.*, 1999). Therefore activation of the RSKs by the ERKs leads to the prevention of apoptosis through two different mechanisms.

There are numerous reports of the localisation of Raf-1 to the mitochondria (Wang *et al.*, 1996a; Salomoni *et al.*, 1998; Nantel *et al.*, 1999; Peruzzi *et al.*, 2001). As a result of these findings a role for Raf-1 in the prevention of apoptosis has been proposed that is independent from its role in the Ras/Raf/MEK/ERK cascade. Raf-1 has been reported to interact with Bcl-2 in myeloid cells, which results in its translocation to the mitochondrial membrane and leads to an increased resistance to apoptosis in response to IL-3 withdrawal (Wang *et al.*, 1994). Furthermore, when the kinase domain of Raf-1 was fused to a mitochondrial membrane localisation signal it resulted in enhanced resistance to apoptosis in response to IL-3 withdrawal. However, when a kinase inactive Raf-1 was used, this survival effect was abolished (Wang *et al.*, 1996a; Majewski *et al.*, 1999). However, in a contrasting report, it was shown that Bcl-2 does not stably interact with Raf-1, and Bcl-2 does not require Raf-1 for its death protective function (Olivier *et al.*, 1997).

Raf-1 has been reported to phosphorylate the pro-apoptotic protein Bad *in vitro* (Wang *et al.*, 1996a). However, the sites of phosphorylation are not those that are required for the inactivation of Bad in response to survival signals (Zha *et al.*, 1996). Therefore Raf-1 may influence the phosphorylation of Bad indirectly. Raf-1 has been reported to interact with Bag-1 *in vitro* and Bag-1 has also been reported to bind to Bcl-2 which means that Bag-1 may function to translocate Raf-1 to the mitochondria where both Bcl-2 and Bad reside (Wang *et al.*, 1996b).

NFκB is a transcription factor that in unstimulated cells, is bound to its inhibitor IκB which retains it in the cytosol (Baeuerle and Baltimore, 1988). In response to diverse stimuli, including TNF, IL-1 and viral RNA, IκB proteins are phosphorylated on two serine residues and rapidly degraded thus freeing NFκB dimers which translocate to the nucleus (Brown *et al.*, 1995; Chen *et al.*, 1995; Traenckner *et al.*, 1995). The genes induced by NFκB to promote cell survival include the caspase inhibitors c-IAP1 and c-IAP2 (Chu *et al.*, 1997; Wang *et al.*, 1998), BCL-X_L (Chen *et al.*, 2000) and Gadd45β which is involved in cell cycle control and DNA repair (De Smaele *et al.*, 2001). IKK is the kinase responsible for the phosphorylation of IκB (Zandi *et al.*, 1998). NIK and MEKK1 are able to activate IKK when overexpressed (Lee *et al.*, 1998; Ling *et al.*, 1998; Nakano *et al.*, 1998). Raf-1 has been shown to induce the phosphorylation and subsequent degradation of IκB which leads to the activation of NFκB (Li and Sedivy, 1993). It appears that Raf-1 stimulates IKK which is responsible for phosphorylating and inactivating IκB and this is mediated by MEKK1 (Baumann *et al.*, 2000).

ASK1 is activated in response to apoptotic stimuli such as TNFα, Fas (CD95), oxidative stress and DNA damage and relays these signals to JNKs and p38MAPKs (Ichijo *et al.*, 1997; Chang *et al.*, 1998; Nishitoh *et al.*, 1998; Saitoh *et al.*, 1998; Liu *et al.*, 2000). Overexpression of ASK1 induces apoptosis in a variety of cell types by inducing mitochondria-mediated caspase activation (Ichijo *et al.*, 1997; Saitoh *et al.*, 1998; Hatai *et al.*, 2000). Recently, Raf-1 has been shown to interact with ASK1 in cells and the overexpression of Raf-1 disrupts ASK1-induced cell death that is not dependent on Raf-1 kinase activity and results in the promotion of cell survival (Chen *et al.*, 2001). Therefore

it is evident that Raf-1 could influence apoptosis through its potential involvement in multiple pathways.

5.1.2 *Raf-1 knockout*

As reported earlier, gene targeting was used previously in the laboratory to generate Raf-1 deficient mice by a conventional approach. The severity of the phenotype of mice homozygous for the mutation (*raf-1*$^{-/-}$) is dependent upon the genetic background. Mice on a predominantly C57/BL6 background died in embryogenesis at around E9.5 and showed vascular defects in the yolk sac and placenta as well as increased apoptosis of embryonic tissues as detected by terminal deoxynucleotidyl transferase-mediated dUTP nick end labelling (TUNEL) assay, although cell proliferation was not affected as assessed by α-Ki67 staining which is a marker for cells in S phase. Therefore, Raf-1 is essential for normal mouse development and it also plays a key role in the prevention of apoptosis. Mice on a mixed MF-1 background survived up until birth but were much smaller than wild-type littermates, were anaemic and the placenta was disorganised (Huser *et al.*, 2001). It has recently been observed that *raf-1*$^{-/-}$ mice on the MF-1 strain survive to 2-3 days postpartum although they are much smaller than wild-type littermates. Therefore genetic modifiers of the MF-1 strain appear to be compensating for the lack of Raf-1.

One of the main aims for producing mice deficient in Raf-1 is to generate primary MEFs which can be used for a variety of biochemical and biological experiments. Primary *raf-1*$^{-/-}$ MEFs could not be cultured from embryos on the C57BL6 background which is indicative of an inherent spontaneous apoptotic phenotype, but they could be cultured from embryos on the MF-1 background. In these cells, ERK activation was similar to wild-type levels in response to a variety of treatments (Huser *et al.*, 2001). The biological characteristics of these cells is investigated in this chapter.

5.1.3 *RafFF mutation*

Previous studies in COS7 cells have shown a requirement for the phosphorylation of the two tyrosine residues 340 and 341 for Raf-1 activation as mutation of these residues to phenylalanine residues (RafFF) blocks activation of Raf-1 by oncogenic Ras and v-Src, or by ligand stimulation (Marais *et al.*, 1995; Marais *et al.*, 1997; Barnard *et al.*, 1998). A

knockin strategy was employed to generate transgenic mice harbouring the RafFF mutation (Huser *et al.*, 2001). During the generation of these RafFF mutant mice, Mason *et al.* (1999) identified that the phosphorylation of tyrosine 341 was a critical event in the activation of Raf-1 whereas the phosphorylation of tyrosine 340 was not essential (Mason *et al.*, 1999). When Raf-1 was immunoprecipitated from MEFs derived from embryos homozygous for the RafFF mutation (*raf-1*$^{FF/FF}$), it had no activity towards MEK. However, the *raf-1*$^{FF/FF}$ mice survived to adulthood, were fertile and displayed a normal phenotype which is in stark contrast to the Raf-1 knockout phenotype (Huser *et al.*, 2001). It was therefore concluded that the MEK kinase activity of Raf-1 is not essential for normal mouse development, but that the protein is required, indicating that Raf-1 has a unique role that is independent from its involvement in the Ras/Raf/MEK/ERK cascade.

5.2 Aims

The aims for this chapter were to characterise the role of Raf-1 with respect to cell growth and apoptosis. This was achieved by the derivation of MEFs that were deficient for Raf-1 (*raf-1*$^{-/-}$) and the derivation of MEFs that harboured a mutation of the two endogenous tyrosine residues 340 and 341 to phenylalanine residues (*raf-1*$^{FF/FF}$). Further analysis of the apoptosis phenotype of the *raf-1*$^{-/-}$ primary MEFs was performed as well as ERK phosphorylation and p38 phosphorylation in response to apoptosis induction. Finally, the primary MEFs were immortalised by using a virus encoding a temperature sensitive version of the SV40T antigen, followed by assessment of apoptosis upon induction with α-CD95 to ensure that they exhibited similar sensitivities to undergo apoptosis as the primary MEFs. These cells were transfected with an empty vector, full-length Raf-1 and a kinase inactive version of Raf-1 to assess if the increased sensitivity to undergo apoptosis could be restored to levels similar to that observed with wild-type cells with these expression vectors.

5.3 Results

5.3.1 Derivation of raf-1$^{-/-}$ primary MEFs

The production of mice with a complete knockout of Raf-1 was reported by Hüser *et al.* (2001) and is described in Chapter 3. A breeding colony of these mice is maintained at the University of Leicester. Primary MEFs were derived from E14.5 embryos on the MF-1

background strain resulting from a timed mating between a male *raf-1*$^{+/-}$ and female *raf-1*$^{+/-}$. Each MEF line was generated from a single embryo and was genotyped using a combination of three primers; Ocp56, Ocp66 and Ocp78 in one PCR reaction. Ocp56 and Ocp78 amplified a 355 bp product of the wild-type allele and Ocp56 and Ocp66 amplified a 450 bp product of the targeted allele (Figure 5.1A). Both PCR products were present in heterozygous MEFs. Of the MEF cell lines tested; 34-2, 33-6, 121-3 and 121-6 were identified as *raf-1*$^{-/-}$ and 34-3, 33-3, 121-2, 121-7 and 121-8 were identified as *raf-1*$^{+/+}$. 121-1, 121-4, 121-5, 121-9, 121-10, 121-11 and 121-12 were identified as *raf-1*$^{+/-}$.

To confirm the PCR results, protein lysates were prepared from the MEFs, followed by SDS-PAGE and electro-transfer of the proteins onto nitrocellulose. The blots were incubated with an anti-Raf-1 antibody, and as expected, the *raf-1*$^{-/-}$ primary MEFs lacked Raf-1 protein (Figure 5.1B). An antibody against vinculin was used as a control for protein loading (Figure 5.1B). MEF cell lines 34-2, 33-6, 121-3 and 121-6 were shown to be deficient in Raf-1 (*raf-1*$^{-/-}$). MEF cell lines 34-3, 33-3, 121-2, 121-7 and 121-8 were identified as wild-type (*raf-1*$^{+/+}$). Only primary MEFs originating from *raf-1*$^{-/-}$ and *raf-1*$^{+/+}$ embryos were used for subsequent experiments.

5.3.2 Derivation of raf-1$^{FF/FF}$ primary MEFs

The production of mice harbouring a mutation of Raf-1 where the endogenous tyrosine residues 340 and 341 have been mutated to phenylalanine residues (RafFF) is described in Chapter 4. A breeding colony of these mice are maintained at the University of Leicester. Primary MEFs were derived from MF-1 E14.5 embryos resulting from a timed mating between a male *raf-1*$^{+/FF}$ and female *raf-1*$^{+/FF}$. The derivation of these MEFs was undertaken by Dr. M. Hüser (Department of Biochemistry, University of Leicester). Each MEF line was generated from a single embryo and was genotyped using a combination of three primers, Ocp52, Ocp59 and Ocp69. Ocp59 and Ocp69 amplified a 245 bp product of the targeted allele (Figure 5.2A). Ocp52 and Ocp59 amplified a 350 bp product of the wild-type allele and a 1700 bp product of the targeted allele (Figure 5.2B). As an example, only cell lines B1, B3, B4, B5 and B7 are shown in Figure 5.2A+B. Of these MEF cell lines; B1 and B5 were identified as *raf-1*$^{FF/FF}$ and B3 was identified as *raf-1*$^{+/+}$. B4 and B7 were identified as *raf-1*$^{+/FF}$.

Fig. 5.1 Derivation of *raf-1*$^{-/-}$ MEFs. (**A**) PCR using Ocp56, Ocp66 and Ocp78 to amplify both the wild-type allele (355 bp) and the *raf-1* targeted allele (450 bp). (**B**) Western blot analysis to detect Raf-1 (upper panel) and vinculin (lower panel).

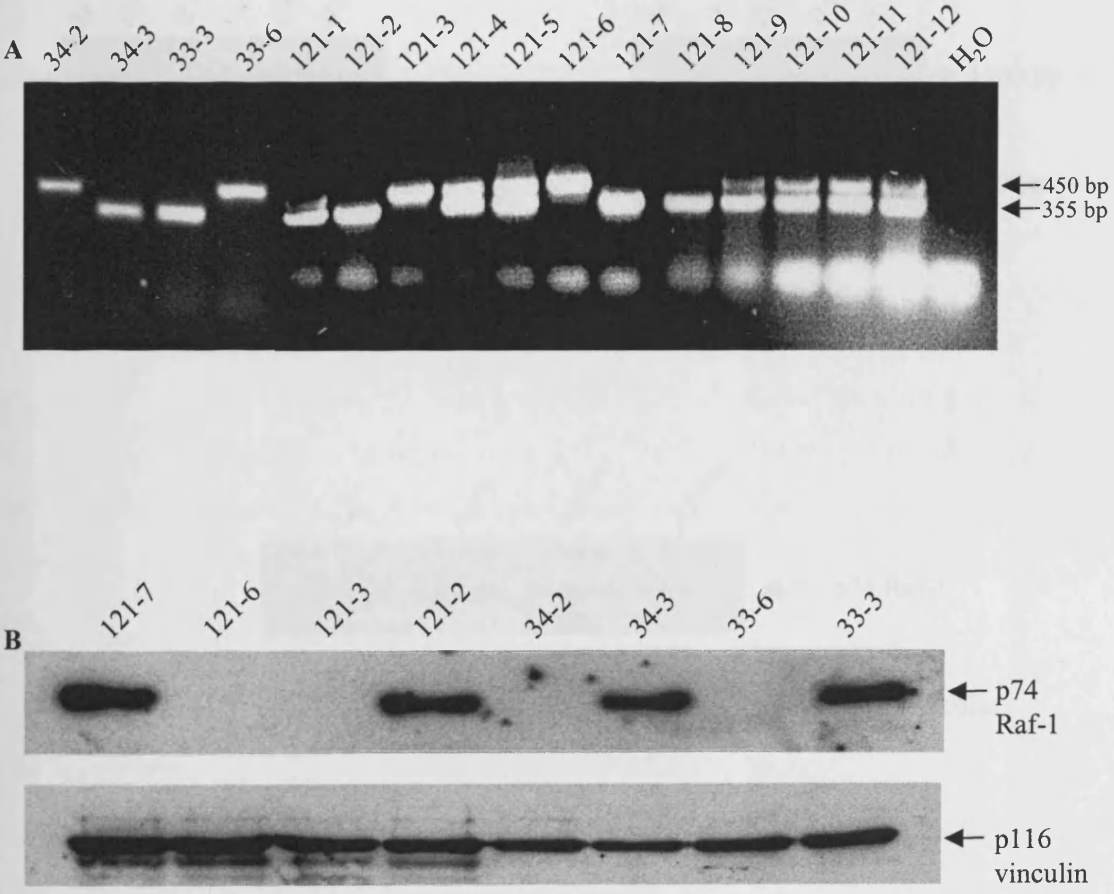

Fig. 5.2 Derivation of *raf-1*$^{FF/FF}$ MEFs. (**A**) PCR using Ocp59 and Ocp69 to amplify the RafFF targeted allele (245 bp) (**B**) PCR using Ocp52 and Ocp59 to amplify both the wild-type allele (485 bp) and the RafFF targeted allele (1700 bp). A non-specific (NS) product was amplified from B1. (**C**) Western blot analysis to detect Raf-1 (upper panel) and vinculin (lower panel) in the MEFs. M = 1 kb DNA marker.

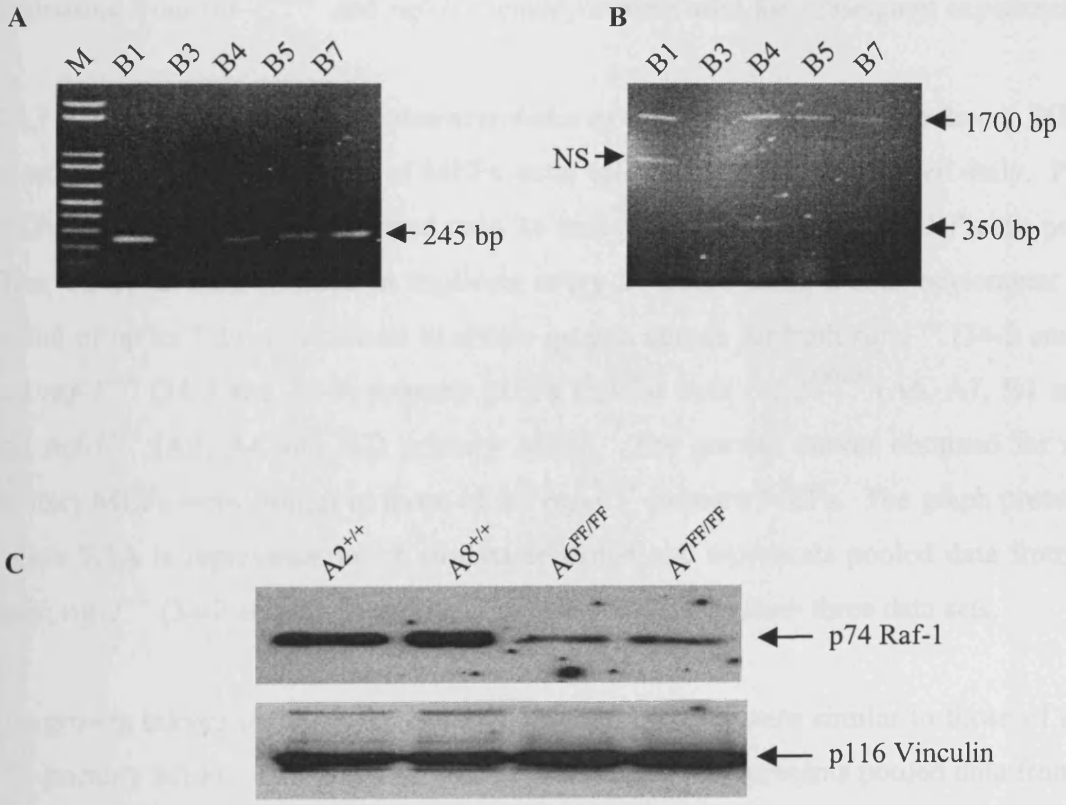

Western blot analysis using a Raf-1 antibody was performed to check levels of expression of Raf-1. A reduced amount of Raf-1 protein was detected in the *raf-1*$^{FF/FF}$ primary MEFs. Only cell lines A2, A8, A6 and A7 are shown in Figure 5.2C. An antibody against vinculin was used as a control for protein loading (Figure 5.2C). Cell lines A6, A7, B1 and B5 were identified as being homozygous for the RafFF mutation (*raf-1*$^{FF/FF}$). Cell lines A2, A4, A8 and B3 were identified as wild-type (*raf-1*$^{+/+}$). Only primary MEFs originating from *raf-1*$^{FF/FF}$ and *raf-1*$^{+/+}$ embryos were used for subsequent experiments.

5.3.3 Analysis of the growth characteristics of raf-1$^{-/-}$ *and raf-1*$^{FF/FF}$ *primary MEFs*

In order to analyse the growth of MEFs, total cell numbers were measured daily. Primary MEFs of all genotypes were plated onto 24 well plates at a density of $1x10^4$ cells per well. Then the cells were counted in triplicate every 24 hours using a haemocytometer over a period of up to 7 days in culture to obtain growth curves for both *raf-1*$^{-/-}$ (34-2 and 33-6) and *raf-1*$^{+/+}$ (34-3 and 33-3) primary MEFs and for both *raf-1*$^{FF/FF}$ (A6, A7, B1 and B5) and *raf-1*$^{+/+}$ (A2, A4 and B3) primary MEFs. The growth curves obtained for *raf-1*$^{-/-}$ primary MEFs were similar to those of the *raf-1*$^{+/+}$ primary MEFs. The graph presented in Figure 5.3A is representative of all data recorded and represents pooled data from 2 cell lines; *raf-1*$^{-/-}$ (34-2 and 33-6) and *raf-1*$^{+/+}$ (34-3 and 33-3) from three data sets.

The growth curves obtained for *raf-1*$^{FF/FF}$ primary MEFs were similar to those of the *raf-1*$^{+/+}$ primary MEFs. The graph presented in Figure 5.3B represents pooled data from 2 cell lines of each genotype; *raf-1*$^{FF/FF}$ (A6 and A7) and *raf-1*$^{+/+}$ (A2 and A4) from three data sets. In general, the growth curves obtained were occasionally variable between different experiments. However this was not reflective of the genotype.

5.3.4 Analysis of proliferation of raf-1$^{-/-}$ *and raf-1*$^{FF/FF}$ *primary MEFs*

In order to analyse the ability of MEFs to progress through the cell cycle, DNA synthesis was measured. MEFs were made quiescent and then stimulated with 10% foetal calf serum in media containing bromodeoxyuridine (BrdU). Cell proliferation was measured by detection of cells that had incorporated BrdU by the addition of an anti-BrdU antibody, followed by addition of a FITC-conjugated secondary antibody. A minimum of 100 cells per experiment were analysed using a fluorescent microscope and scored for whether or

Fig. 5.3 Analysis of the growth characteristics of primary MEFs. (**A**) Growth profiles of *raf-1*$^{-/-}$ primary MEFs (closed circles) compared to *raf-1*$^{+/+}$ primary MEFs (open circles) over seven days in culture. The data represent pooled data from 2 cell lines of each geneotype (34-2, 34-3, 33-3, 33-6) from three data sets. (**B**) Growth profiles of *raf-1*$^{FF/FF}$ (closed grey circles) primary MEFs compared to *raf-1*$^{+/+}$ (open circles) primary MEFs over six days in culture. The data represent pooled data from 2 cell lines of each genotype (A2, A4, A6, A7) from three data sets. Standard deviation bars are shown.

A

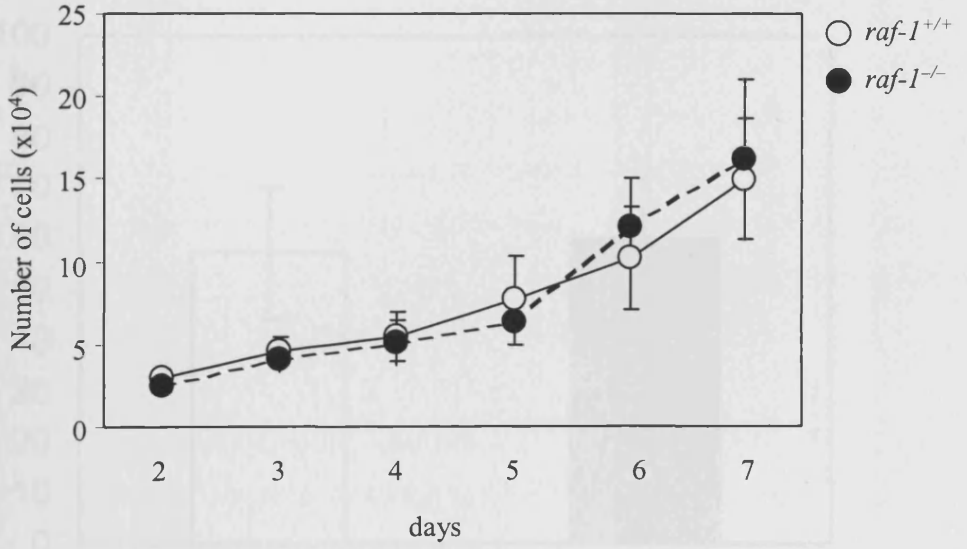

B

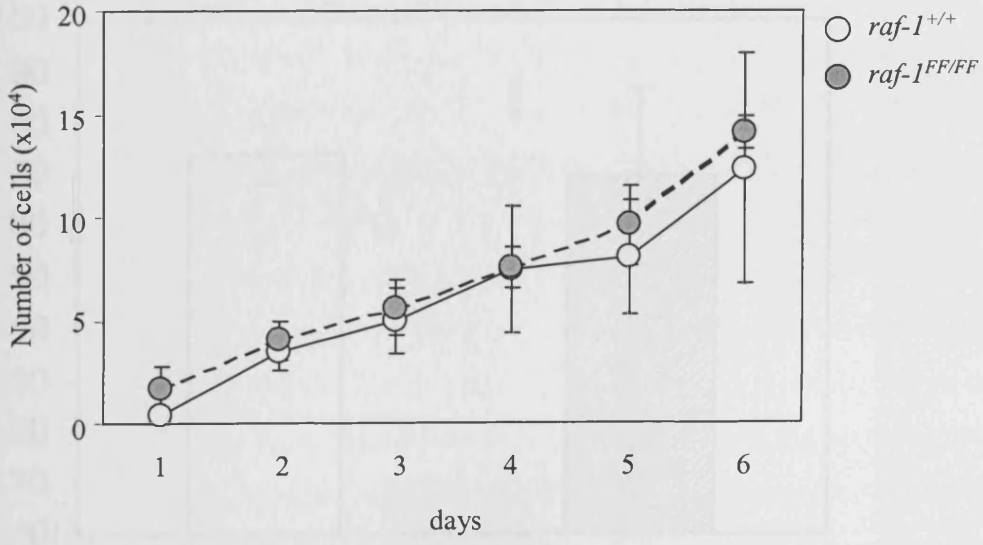

Fig. 5.4 DNA synthesis analysis of primary MEFs by the addition of 10% serum. (**A**) Percentage of BrdU positive *raf-1*$^{-/-}$ primary MEFs compared to *raf-1*$^{+/+}$ primary MEFs. The data represent pooled data from 2 cell lines of each genotype (34-2, 34-3, 33-3, 33-6) from 5 experiments. (**B**) Percentage of BrdU positive *raf-1*$^{FF/FF}$ primary MEFs compared to *raf-1*$^{+/+}$ primary MEFs. The data represent pooled data from 2 cell lines of each genotype (A2, A4, A6, A7) from 3 experiments. Standard deviation bars are shown.

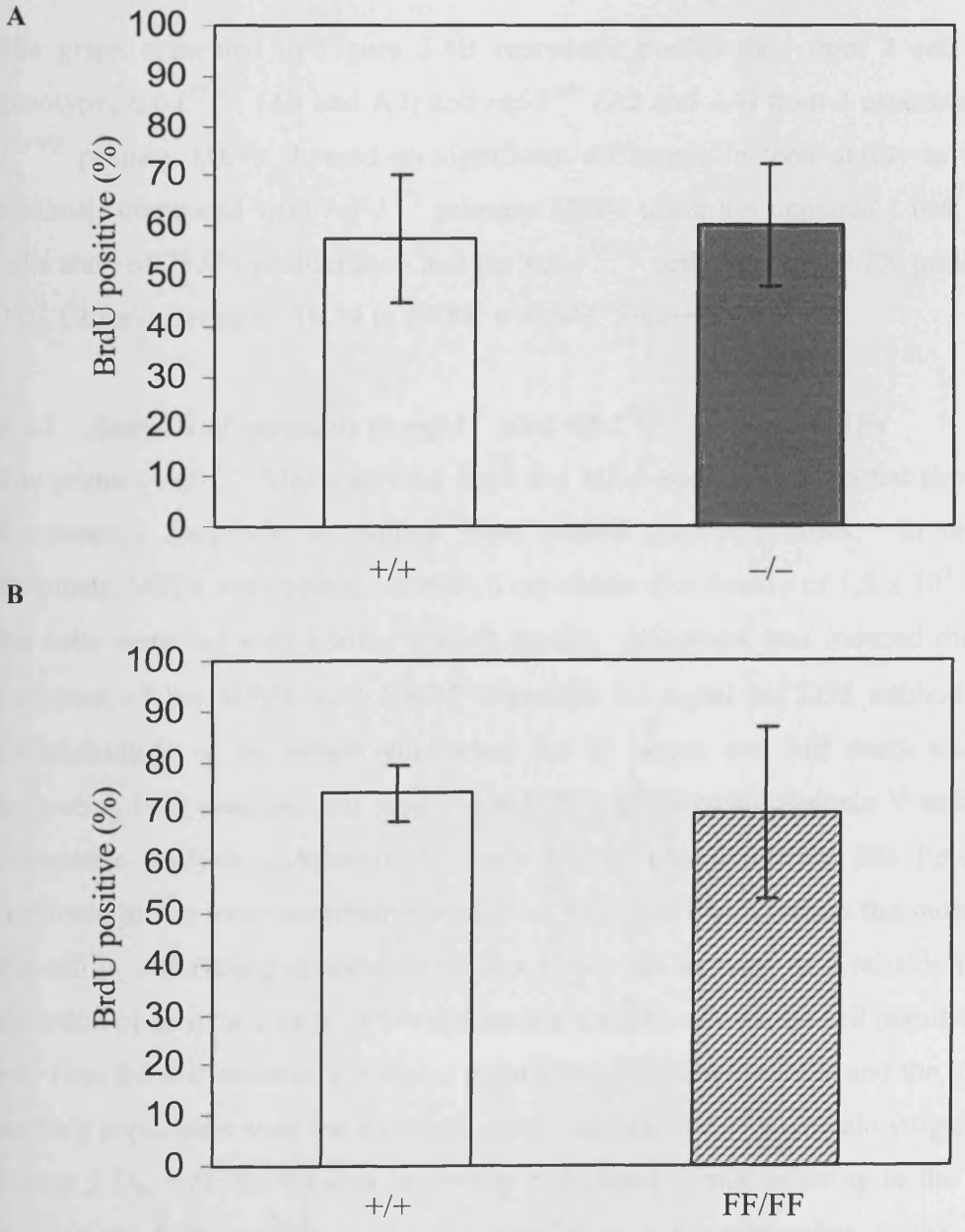

not they had fluorescent nuclei. The graph presented in Figure 5.4A represents pooled data from 2 cell lines of each genotype; *raf-1*$^{-/-}$ (34-2 and 33-6) and *raf-1*$^{+/+}$ (34-3 and 33-3) from 5 experiments. The *raf-1*$^{-/-}$ primary MEFs showed no significant difference in their ability to undergo DNA synthesis compared with *raf-1*$^{+/+}$ primary MEFs using the unpaired t test. The *raf-1*$^{+/+}$ cells showed 63.06% proliferation and the *raf-1*$^{-/-}$ cells showed 63.43% proliferation (n=5; 95% CI for difference –21.06 to 20.31, p=0.968; Figure 5.4A).

The graph presented in Figure 5.4B represents pooled data from 2 cell lines of each genotype; *raf-1*$^{FF/FF}$ (A6 and A7) and *raf-1*$^{+/+}$ (A2 and A4) from 3 experiments. The *raf-1*$^{FF/FF}$ primary MEFs showed no significant difference in their ability to undergo DNA synthesis compared with *raf-1*$^{+/+}$ primary MEFs using the unpaired t test. The *raf-1*$^{+/+}$ cells showed 73.9% proliferation and the *raf-1*$^{FF/FF}$ cells showed 69.7% proliferation (n=3; 95% CI for difference –19.34 to 27.84, p=0.643; Figure 5.4B).

5.3.5 Analysis of apoptosis in raf-1$^{-/-}$ and raf-1$^{FF/FF}$ primary MEFs

The primary *raf-1*$^{-/-}$ MEFs derived from the MF-1 background did not show evidence of spontaneous apoptosis as evident from normal growth profiles. In order to assess apoptosis, MEFs were plated out onto 6 cm dishes at a density of 1.5 x 10^5. The next day the cells were fed with normal growth media. Apoptosis was induced the day after by treatment of the MEFs with 50μM etoposide, 50 ng/ml α-CD95 antibody plus 0.5μM cycloheximide or by serum withdrawal for 20 hours, and cell death was assessed by harvesting both attached and suspension MEFs followed by annexin V staining and flow cytometric analysis. Annexin V binds to phosphatidylserine; this lipid is normally restricted to the inner-membrane leaflet but becomes displayed on the outer leaflet when the cell is undergoing apoptosis and as a result can be used as a reliable marker for the detection of apoptotic cells. Flow cytometric analysis allows the cell population to be split into two; the low annexin V staining population were the live cells and the high annexin V staining population were the apoptotic cells. An example of a typical cytogram is shown in Figure 5.5A, with the number in the top right hand corner referring to the percentage of cells in the high annexin V staining population and hence refers to the percentage of apoptotic cells in the sample.

Fig. 5.5 Analysis of primary MEFs with respect to apoptosis induced by either serum free media, 50 μM etoposide or 50 ng/ml α-CD95 antibody plus 0.5 μM cycloheximide. (**A**) Percentage of annexin positive staining cells as assessed by flow cytometric analysis of *raf-1*$^{-/-}$ primary MEFs compared to *raf-1*$^{+/+}$ primary MEFs with the number in the top right corner representing the percentage of cells in the high annexin staining population. (**B**) Hoechst 33258 staining of *raf-1*$^{-/-}$ and *raf-1*$^{+/+}$ primary MEFs after no treatment or after treatment with 50 ng/ml α-CD95 antibody plus 0.5 μM cycloheximide.

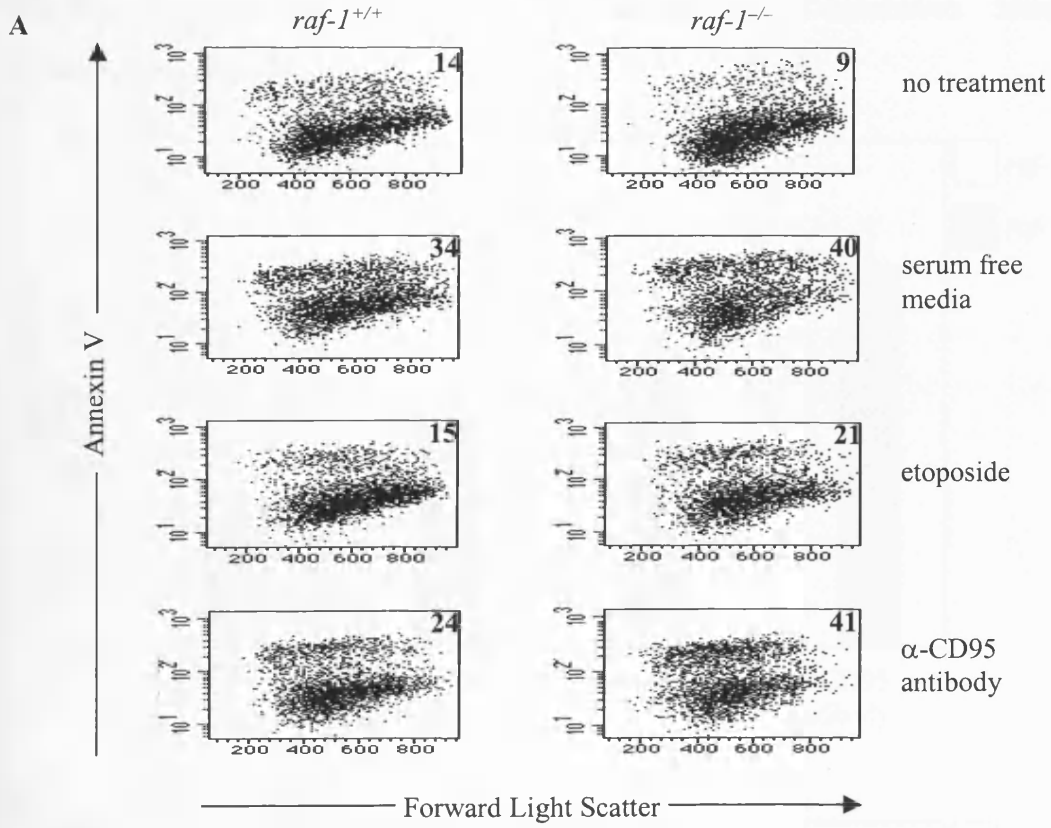

Fig. 5.6 Analysis of primary MEFs with respect to apoptosis induced by either serum free media, 50 μM etoposide or 50 ng/ml α-CD95 antibody plus 0.5 μM cycloheximide. **(A)** Percentage of annexin positive staining cells as assessed by flow cytometric analysis of *raf-1*$^{-/-}$ primary MEFs compared to *raf-1*$^{+/+}$ primary MEFs. The data represent pooled data from 2 cell lines of each genotype (34-2, 34-3, 33-3 and 33-6) from 7 experiments. **(B)** Percentage of annexin positive staining cells as assessed by flow cytometric analysis of *raf-1*$^{FF/FF}$ primary MEFs compared to *raf-1*$^{+/+}$ primary MEFs. The data represent pooled data from 7 cell lines (A2, A6, A8, A7, B1, B3 and B5) from 11 experiments. Standard deviation bars are shown.

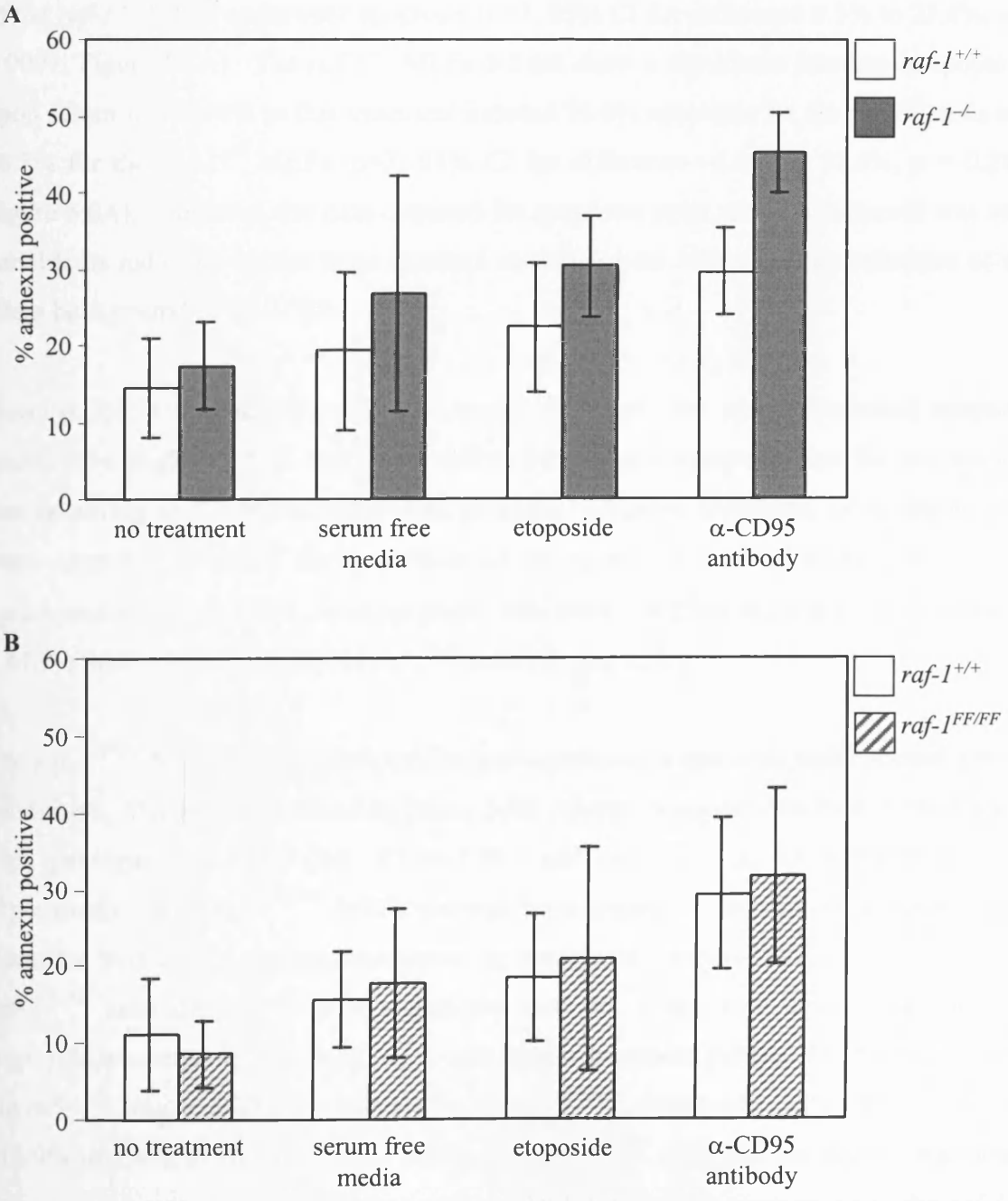

The graph presented in Figure 5.6A represents pooled data from 2 cell lines of each genotype; *raf-1*$^{-/-}$ (34-2 and 33-6) and *raf-1*$^{+/+}$ (34-3 and 33-3) from 7 experiments. The *raf-1*$^{-/-}$ MEFs showed a significant increase in apoptosis in response to both etoposide and α-CD95 antibody plus cycloheximide in comparison to the *raf-1*$^{+/+}$ cells. Upon treatment with etoposide, 21.1% of the *raf-1*$^{+/+}$ MEFs compared with 30% of the *raf-1*$^{-/-}$ MEFs underwent apoptosis (n=7; 95% CI for difference 0.5% to 17.2%, p = 0.04; Figure 5.6A). Upon treatment with α-CD95 antibody, 29.9% of the *raf-1*$^{+/+}$ MEFs compared with 48.3% of the *raf-1*$^{-/-}$ MEFs underwent apoptosis (n=7; 95% CI for difference 9.5% to 27.4%, p = 0.0007; Figure 5.6A). The *raf-1*$^{-/-}$ MEFs did not show a significant increase in apoptosis upon serum withdrawal as this treatment induced 26.0% apoptosis for the *raf-1*$^{-/-}$ cells and 18.7% for the *raf-1*$^{+/+}$ MEFs (n=7; 95% CI for difference –6.8% to 21.4%, p = 0.284; Figure 5.6A). However, the data obtained for apoptosis upon serum withdrawal was very variable as indicated by the large standard deviation bars. This may be reflective of the strain background of the MEFs.

Hoechst 33258 is a nuclear stain that stains all nuclei, but stains condensed apoptotic nuclei very brightly. This stain was used to confirm that apoptosis was the process that was occurring in the MEFs rather than necrosis. Upon no treatment, no apoptotic cells were identified, whereas upon addition of 50 ng/ml α-CD95 antibody plus 0.5 μM cycloheximide for 20 hours, more apoptotic cells were identified in the population of *raf-1*$^{-/-}$ MEFs than in the population of *raf-1*$^{+/+}$ cells (Figure 5.5B).

The *raf-1*$^{FF/FF}$ MEFs did not show evidence of spontaneous apoptosis under normal growth conditions. The graph presented in Figure 5.6B represents pooled data from 3 cell lines of each genotype; *raf-1*$^{FF/FF}$ (A6, A7 and B1) and *raf-1*$^{+/+}$ (A2, A8 and B3) from 11 experiments. The *raf-1*$^{FF/FF}$ MEFs showed no increase or decrease in apoptosis upon treatment with any of the apoptotic inducing treatments compared to *raf-1*$^{+/+}$ MEFs. The *raf-1*$^{FF/FF}$ cells did not show a significant increase in apoptosis upon treatment with etoposide in comparison to the *raf-1*$^{+/+}$ cells as this treatment induced 18.1% apoptosis for the *raf-1*$^{+/+}$ cells and 20.8% apoptosis for the *raf-1*$^{FF/FF}$ cells (n=11; 95% CI for difference –12.9% to 7.4%, p =0.581; Figure 5.6B). The *raf-1*$^{FF/FF}$ cells did not show a significant increase in apoptosis upon treatment with α-CD95 antibody in comparison to the *raf-1*$^{+/+}$

cells as this treatment induced 29.4% apoptosis for the *raf-1*$^{+/+}$ cells and 31.6% apoptosis for the *raf-1*$^{FF/FF}$ cells (n=11; 95% CI for difference -11.3% to 6.9%, p =0.616; Figure 5.6B). The *raf-1*$^{FF/FF}$ cells did not show a significant increase in apoptosis upon serum withdrawal as this treatment induced 17.6% apoptosis for the *raf-1*$^{FF/FF}$ cells and 15.5% for the *raf-1*$^{+/+}$ cells (n=11; 95% CI for difference –9.1% to 4.8%, p =0.53; Figure 5.6A).

5.3.6 Analysis of raf-1$^{-/-}$ primary MEFs in comparison to wild-type primary MEFs with respect to ERK phosphorylation

To measure ERK activation, phosphorylation of ERK in response to apoptosis induction by treatment with α-CD95 antibody plus cycloheximide was assessed since this particular treatment gave the largest difference in apoptosis between *raf-1*$^{+/+}$ and *raf-1*$^{-/-}$ MEFs. In order to achieve this, primary *raf-1*$^{+/+}$ (34-3, 121-2 and 121-8) and *raf-1*$^{-/-}$ MEFs (34-2, 121-3 and 121-6) were plated out at a density of 2 x 10^4 cells on each well of a 24 well plate. The next day they were fed with normal growth media. Then the following day they were stimulated with 50 ng/ml α-CD95 antibody plus 0.5 μM cycloheximide for different times. Cells were lysed at timepoints of 0, 2, 5, 10, 20, 40 and 60 minutes of stimulation. Protein lysates were prepared from these MEFs, followed by SDS-PAGE and electro-transfer of the proteins onto nitrocellulose. The blots were incubated with an α-phosphoERK antibody to detect levels of phospho-ERK (Figure 5.7). Total ERK levels were analysed using an α-ERK2 antibody as a control for protein loading and to ensure that any differences in phospho-ERK were not due to differences in the relevant amounts of ERK protein (Figure 5.7). The levels of phospho-ERK in the *raf-1*$^{-/-}$ MEFs was similar to that in the *raf-1*$^{+/+}$ MEFs with phospho-ERK levels increasing following 2 min treatment and continuing to increase up to 10 min of treatment and beginning to decrease after this timepoint (Figure 5.7). However there was a degree of variability between experiments. This was repeated at least three times for three different cell lines of each genotype. No consistent difference between *raf-1*$^{-/-}$ and *raf-1*$^{+/+}$ MEFs was observed.

5.3.7 Analysis of Raf-1 deficient primary MEFs in comparison to wild-type primary MEFs with respect to p38MAPK phosphorylation

To measure p38MAPK activation, phosphorylation of p38MAPK in response to apoptosis induction was assessed. In order to achieve this, primary *raf-1*$^{+/+}$ (34-3, 121-2 and 121-8)

Fig. 5.7 ERK phosphorylation in *raf-1*$^{+/+}$ and *raf-1*$^{-/-}$ primary MEFs over a timecourse of stimulation (0 to 40 or 60 min) with 50 ng/ml α-CD95 antibody plus 0.5 μM cycloheximide. (**A**) Protein lysates were prepared from primary MEF cell lines 34-2 and 34-3 followed by western blot analysis and detection of phospho-ERK (upper panel) and detection of total ERK protein as a control for protein loading (lower panel). (**B**) Protein lysates were prepared from primary MEF cell lines 121-2 and 121-3 followed by western blot analysis and detection of phospho-ERK (upper panel) and detection of total ERK protein as a control for protein loading (lower panel). (**C**) Protein lysates were prepared from primary MEF cell lines 121-6 and 121-7 followed by Western blot analysis and detection of phospho-ERK (upper panel) and detection of total ERK protein as a control for protein loading (lower panel).

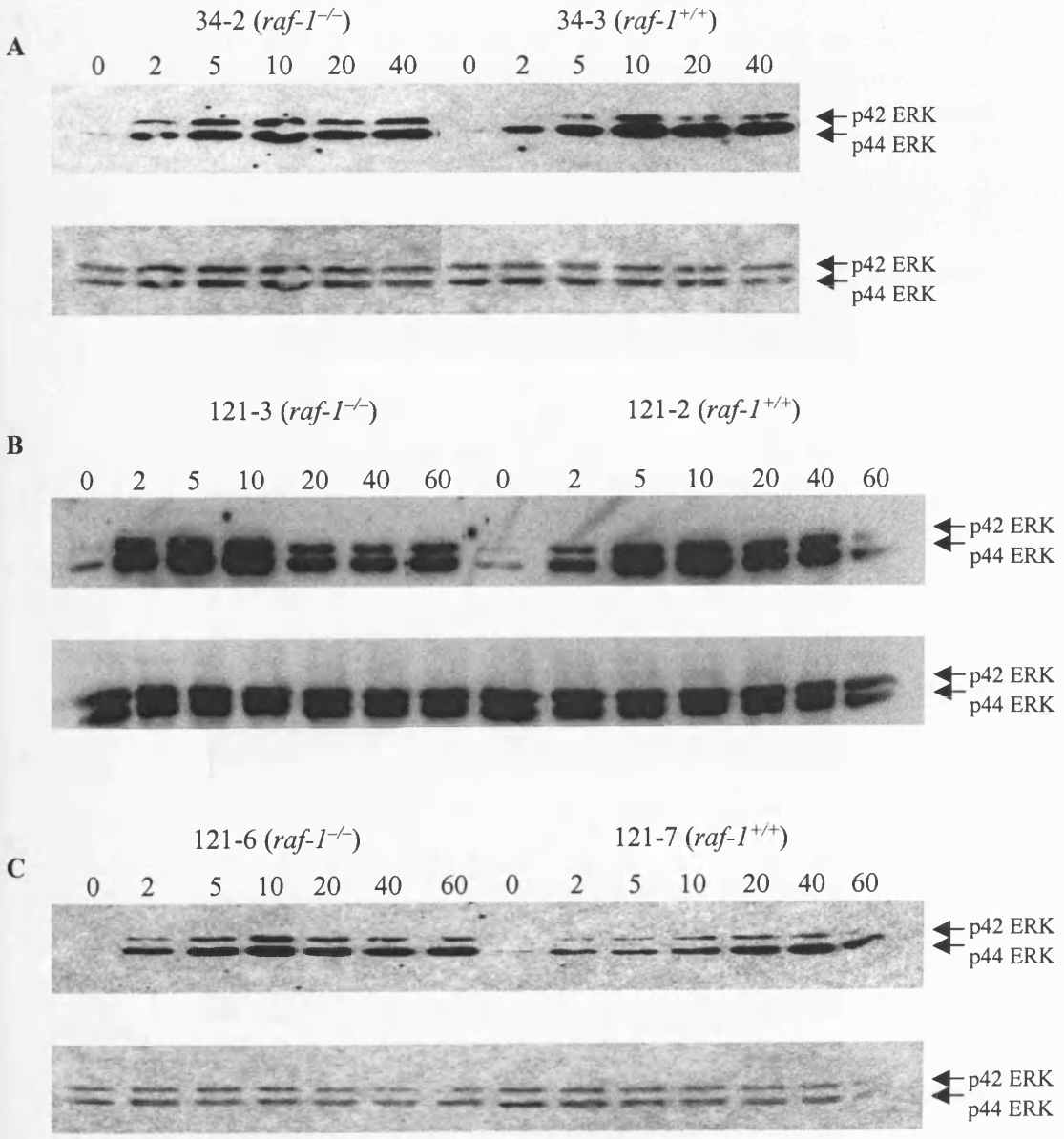

Fig. 5.8 p38MAPK phosphorylation in *raf-1*$^{+/+}$ and *raf-1*$^{-/-}$ primary MEFs over a timecourse of stimulation with 50 ng/ml α-CD95 antibody plus 0.5 μM cycloheximide. Treatment of *raf-1*$^{+/+}$ MEFs with 500 mM sorbitol for 30 min was used as a control for phospho-p38MAPK. (**A**) Protein lysates were prepared from primary MEF cell lines 34-2 and 34-3 followed by western blot analysis and detection of phospho-p38MAPK (upper panel)and detection of total p38MAPK protein as a control for protein loading (lower panel). (**B**) Protein lysates were prepared from primary MEF cell lines 121-2 and 121-3 followed by western blot analysis and detection of phospho-p38MAPK (upper panel) and detection of total p38MAPK protein as a control for protein loading (lower panel). (**C**) Protein lysates were prepared from primary MEF cell lines 121-6 and 121-7 followed by western blot analysis and detection of phospho-p38MAPK (upper panel) and detection of total p38MAPK protein as a control for protein loading (lower panel).

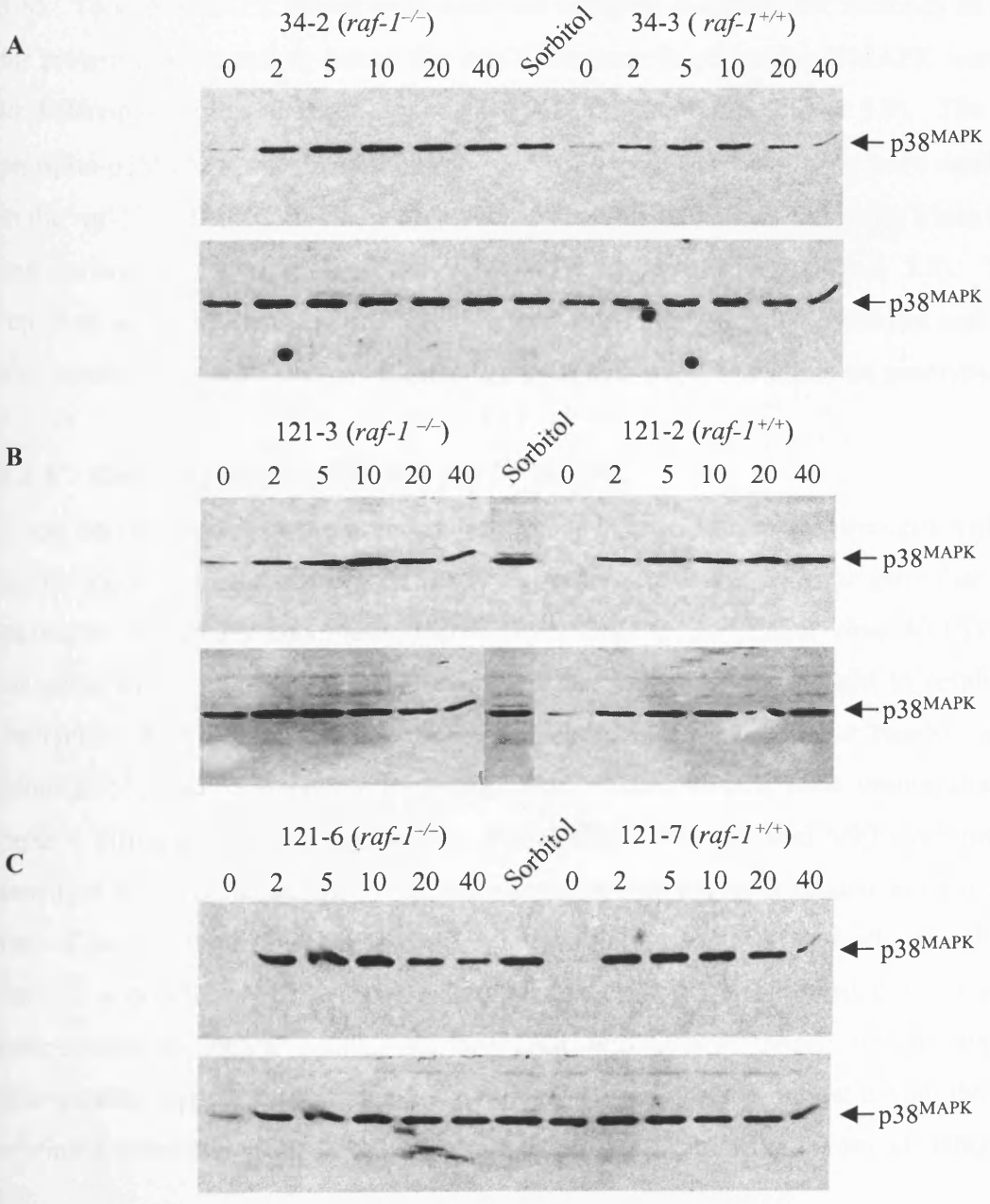

and *raf-1*$^{-/-}$ MEFs (34-2, 121-3 and 121-6) were plated out at a density of 2 x 10^4 cells on each well of a 24 well plate. The next day they were fed with normal growth media. Then the following day they were stimulated with 50 ng/ml α-CD95 antibody plus 0.5 μM cycloheximide for different times. Cells were lysed at timepoints of 0, 2, 5, 10, 20, 40 and 60 minutes of stimulation. As a control for phospho-p38MAPK, MEFs were treated with 500 mM sorbitol for 30 min. Protein lysates were prepared from these MEFs, followed by SDS-PAGE and electro-transfer of the proteins onto nitrocellulose. The blots were incubated with an α-phospho-p38MAPK antibody to detect levels of phospho-p38 (Figure 5.8). Total p38MAPK levels were analysed using an α-p38MAPK antibody as a control for protein loading and to ensure that any differences in phospho-p38MAPK were not due to differences in the relevant amounts of p38MAPK protein (Figure 5.8). The levels of phospho-p38MAPK induced in the *raf-1*$^{-/-}$ MEFs by α-CD95 antibody were similar to that in the *raf-1*$^{+/+}$ MEFs, with phospho-p38MAPK levels increasing following 2 min treatment and staying at the same level following 40 min of treatment (Figure 5.8). This was repeated at least two times for three different cell lines of each genotype and although slight differences were observed, they did not appear to be dependent on genotype.

5.3.8 Generation of immortalised raf-1$^{-/-}$ *MEFs*

It was necessary to generate immortalised MEFs in order to transfect the cells with vectors, as the transfection of primary MEFs is extremely difficult. A viral gene that has been shown to be capable of immortalising rodent cells is the simian virus 40 (SV40) gene encoding the large T antigen. This immortalisation ability is thought to result from its interaction with a number of cellular gene products, including the tumour suppressor proteins p53 and pRb family members. As a result of this, such immortalised MEFs behave differently to primary MEFs. For example immortalised MEFs are much more sensitive to DNA damaging agents such as etoposide which is related to their increased rate of proliferation. For this reason, a reversible system was used whereby the SV40T antigen is present at the permissive temperature of 33°C and degraded at the restrictive temperature of 39.5°C. The plasmid used was pZIPSVtsA58, which contains the thermolabile large T antigen encoded by the SV40 early region mutant tsA58, the Moloney murine Leukaemia virus (M-MuLV) transcriptional unit derived from an integrated M-

MuLV provirus, pBR322 sequences necessary for the propagation of the vector DNA in *E. coli* and the *neo*^{R} gene (Jat and Sharp, 1989; Figure 2.1).

Using a Lipofectamine transfection, pZIPSVtsA58 was transfected into Bosc23 cells. This cell line contains integrated copies of an M-MuLV provirus genome that provides all the *trans* functions necessary for the encapsidation of a recombinant genome, yet it is defective in the ability to encapsidate its own RNA (Pear *et al.*, 1993). 24 hours after transfection, the Bosc23 culture fluid was harvested and used to infect two *raf-1*$^{+/+}$ (34-3 and 33-3) and two *raf-1*$^{-/-}$ (34-2 and 33-6) primary MEF cell lines. G418 selection was applied to the primary MEFs until colonies were visible at which point the colonies were pooled, passaged and a portion of the cells frozen down. To determine levels of SV40 T antigen expression, the four cell lines were split onto two 6 cm plates at a density of 3 x 10^5 and placed at 33°C overnight. The next day, one plate from each cell line was placed at 33°C and the other plates were placed at 39.5°C for 24 hours. Protein lysates were prepared from these 8 plates of MEFs, followed by SDS-PAGE and electro-transfer of the proteins onto nitrocellulose. The blots were incubated with an α-large T antigen antibody to analyse the presence of this antigen (Figure 5.9A). The SV40 T antigen was expressed in all cell lines at the permissive temperature of 33°C. However in cell line 34-3 it was not expressed as highly as it was in the other three cell lines. Unexpectedly, at 39.5°C, the antigen was present in all of the cell lines except 34-3, but at reduced levels in comparison to the levels of expression at 33 °C. Therefore it had not fully degraded. It was expressed most highly in 33-6. This particular cell line had a different morphology to the other cell lines as the cells were smaller and had a spindle-like appearance reminiscent of transformed cells. Despite these findings, all tsSV40T immortalised cell lines were analysed with respect to apoptosis to assess if they could reproduce similar susceptibilities as the primary MEFs upon α-CD95 and cycloheximide addition.

5.3.9 Analysis of apoptosis in immortalised raf-1$^{-/-}$ MEFs

In order to assess apoptosis, tsSV40T immortalised MEFs were plated out onto 6 cm dishes at a density of 1.5 x 10^5 at the permissive temperature of 33°C. The next day the cells were fed with normal growth media and the cells were shifted to the restrictive temperature of 39.5°C in order to allow at least some degradation of the large T antigen.

Fig. 5.9 Analysis of tsSV40T MEFs. **(A)** Western blot analysis to detect levels of SV40 large T antigen in *raf-1*$^{+/+}$ and *raf-1*$^{-/-}$ MEFs after they had been placed at either 33°C or at 39.5°C for 24 hours. **(B)** Percentage of annexin V positive staining cells as assessed by flow cytometric analysis of *raf-1*$^{-/-}$ MEFs (34-2 and 33-6) compared to *raf-1*$^{+/+}$ MEFs (34-3 and 33-3) when apoptosis was induced by 50 ng/ml α-CD95 antibody plus 0.5 μM cycloheximide or with no treatment. The data represents three experiments. Standard deviation bars are shown. **(C)** Bar chart showing the same data from **B** split up into the individual MEF cell lines. Standard deviation bars are shown.

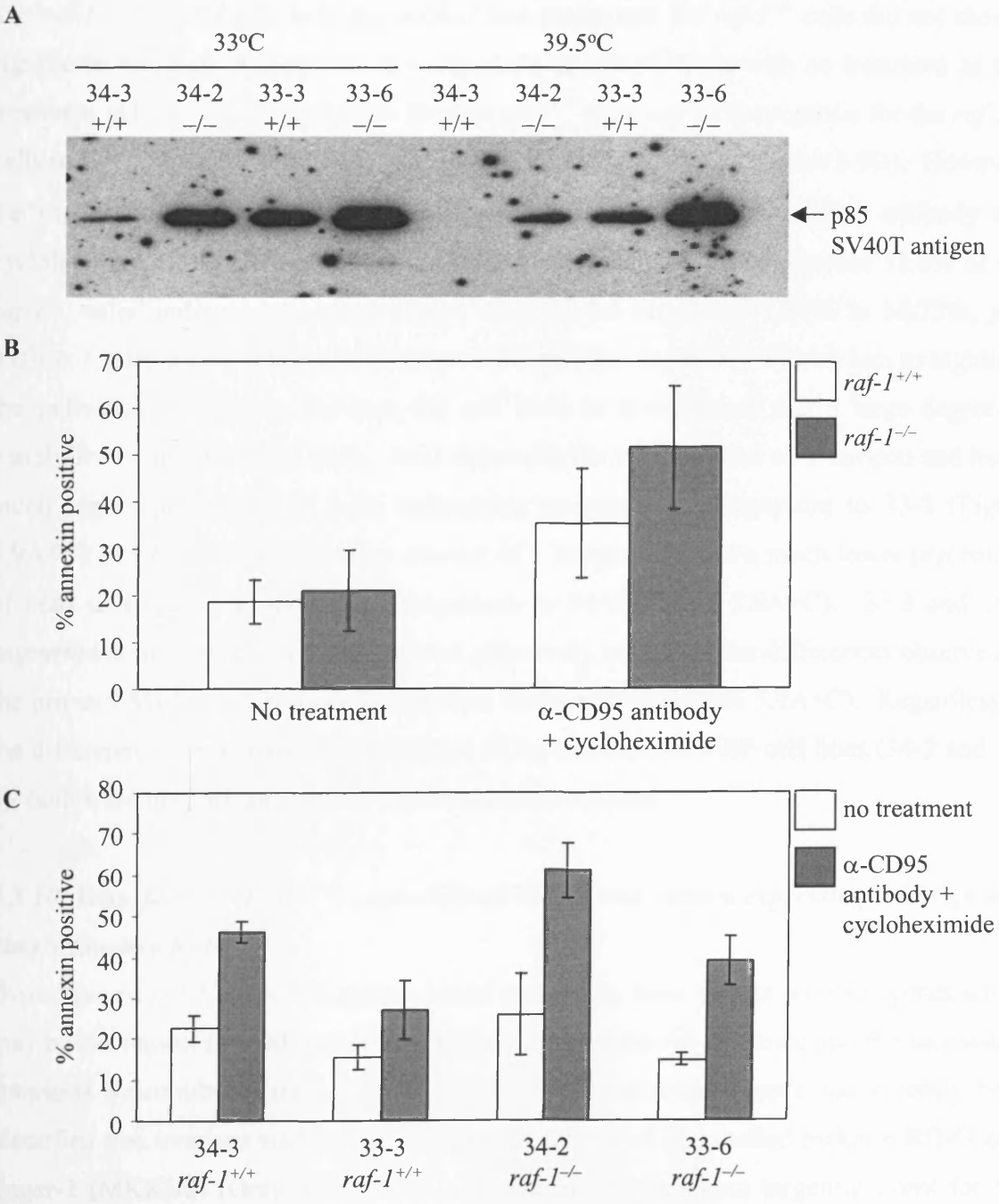

Apoptosis was induced the following day by treatment of the MEFs with 50 ng/ml α-CD95 antibody plus 0.5 μM cycloheximide for 20 hours, and cell death was assessed by harvesting both attached and suspension MEFs followed by annexin V staining and flow cytometric analysis.

The graphs presented in Figure 5.9B+C represent the data from 3 experiments on each of the 4 cell lines (34-2, 34-3, 33-3, 33-6). Figure 5.9B shows the data pooled for *raf-1*$^{+/+}$ and *raf-1*$^{-/-}$ cells. Analysis of the pooled data shows that the *raf-1*$^{-/-}$ cells did not show a significant increase in apoptosis in comparison to *raf-1*$^{+/+}$ cells with no treatment as this treatment induced 18.6% apoptosis for the *raf-1*$^{+/+}$ cells and 21% apoptosis for the *raf-1*$^{-/-}$ cells (n=7; 95% CI for difference –6.13% to 10.99%, $p = 0.5479$; Figure 5.9B). However, the *raf-1*$^{-/-}$ cells showed a significant increase in apoptosis with α-CD95 antibody and cycloheximide, as 35.3% of the *raf-1*$^{+/+}$ cells underwent apoptosis whereas 51.6% of the *raf-1*$^{-/-}$ cells underwent apoptosis (n=7; 95% CI for difference 1.84% to 30.73%, $p = 0.0302$; Figure 5.9B). Figure 5.9C shows each cell line separately with an aim to highlight the individual differences between the cell lines as it was clear that a large degree of variability existed between them. 34-3 expressed the least amount of T antigen and had a much higher percentage of cells undergoing apoptosis in comparison to 33-3 (Figure 5.9A+C). 33-6 expressed the most amount of T antigen and had a much lower percentage of cells undergoing apoptosis in comparison to 34-2 (Figure 5.9A+C). 33-3 and 34-2 expressed similar levels of T antigen and effectively replicated the differences observed in the primary MEFs with respect to apoptosis susceptibility (Figure 5.9A+C). Regardless of the difference in apoptosis susceptibilities of the two *raf-1*$^{-/-}$ MEF cell lines (34-2 and 33-6), both were used for subsequent transfection experiments.

5.3.10 Transfection of raf-1$^{-/-}$ *immortalised MEFs with vectors expressing wild-type and kinase inactive Raf-1*

Disruption of *raf-1* by gene targeting could potentially have effects on other genes which may be the reason for both the observed phenotype of the *raf-1*$^{-/-}$ mice and the increase in apoptosis susceptibility of the *raf-1*$^{-/-}$ MEFs. In particular, a gene has recently been identified that overlaps with and is antisense to *raf-1* by 91 bp, called makorin RING zinc finger-2 (MKRN2) (Gray *et al.*, 2001). However, the knockout targeting event for the

raf-1 gene was achieved by the deletion of exons 10 to 13, therefore the MKRN2 gene was not disrupted. The authors suggest that *raf-1* and *MKRN2* mRNA may be co-regulated as the expression patterns are similar in a variety of tissues and cell lines (Gray *et al.*, 2001). This means that the *raf-1* knockout may have an effect on MKRN2 mRNA. In order to rule this out, the ability of the expression of wild-type Raf-1 to rescue the increase in susceptibility to undergo apoptosis observed with the immortalised *raf-1*$^{-/-}$ MEFs was assessed. In addition, the use of a kinase inactive Raf-1 mutant where the critical ATP binding site of lysine 375 has been mutated to methionine was used to provide information as to whether the kinase function of Raf-1 is necessary for its role in cell survival.

The *raf-1*$^{-/-}$ tsSV40T immortalised MEFs (clones 34-2 and 33-6) were plated out onto three 10 cm plates at a density of 6 x 10^5. The next day they were fed with normal growth media. The following day both cell lines were transfected with three different vectors; a vector expressing wild-type human Raf-1 (pEFm.6/Raf-1), a vector expressing a kinase inactive version of human Raf-1 where lysine 375 is mutated to methionine (pEFm.6/kinase inactive) and the empty backbone vector (pEFm.6). Using Lipofectamine, 8 μg of each expression vector was co-transfected with 0.8 μg pPGKpuro (a plasmid harbouring the *puro*^{R} gene driven by the PGK promoter; Figure 2.1D). The reason for the co-transfection was that the expression vectors have the *neo*^{R} gene and the immortalised MEFs already harbour a copy of this gene. After 10 days of puromycin selection, resistant clones were picked (Table 5.1).

DNA was harvested from clones transfected with the pEFm.6 vector and the samples were analysed by PCR to discover if they contained the construct. Primers Ocp106 and Ocp107 were used to amplify a 200 bp product from the pEFm.6 vector as a control (Figure 5.10). Ocp106 and Ocp107 amplified a 200 bp product in 4 out of 15 clones from 34-2 (1, 11, 23 and 35; Figure 5.10) and 6 out of 9 clones from 33-6 (43, 48, 49; Figure 5.10A and not shown 70, 83 and 85). Therefore these clones contained the pEFm.6 vector. This gave a mean frequency of integration of 1 in 2.4. Therefore, the co-transfection technique used for pEFm.6 was very effective.

In order to confirm levels of expression of Raf-1 in all clones transfected with wild-type Raf-1 and kinase inactive Raf-1, protein lysates were prepared followed by SDS-PAGE and electro-transfer of the proteins onto nitrocellulose. The blots were incubated with an α-Raf-1 antibody. An α-vinculin antibody was used as a control for protein loading. Proteins from *raf-1*$^{+/+}$ MEFs (34-3 and 33-3), *raf-1*$^{-/-}$ MEFs (34-2 and 33-6) and *raf-1*$^{-/-}$ MEFs transfected with pEFm-6 (1, 23 and 35) were used as controls (Figure 5.11A, B and C). 2 clones out of 17 from 34-2 (58 and 72) and 3 clones out of 9 from 33-6 (46, 47 and 62) were identified that expressed the wild-type Raf-1 construct (Figure 5.11A, B and C). 3 clones out of 26 from 34-2 (37, 56 and 68) and no clones out of 16 from 33-6 were identified that expressed the kinase inactive Raf-1 construct (Figure 5.11A and C). This gave a mean frequency of expression of both of the Raf-1 constructs of 1 in 8.5. Therefore a restoration of Raf-1 expression was observed in these clones. However the expression levels of Raf-1 were highly variable between them. Table 5. 1 gives a summary of the clones identified that either harbour pEFm.6 or expressed Raf-1 and from which clones they originated.

Table 5. 1. Number of puromycin resistant clones picked from each parental MEF line for each transfection. Clones that were positive for PCR in the case of pEFm.6 or expressed Raf-1 protein as assessed by Western blot analysis and from which parental MEF line they originated from.

	Total number of clones picked		**Clones positive for pEFm.6 PCR or Raf-1 expression**	
Parental MEF line	**34-2**	**33-6**	**34-2**	**33-6**
pEFm.6	15	9	1, 11, 23, 35	43, 48, 49, 70, 83, 85
Wild-type Raf-1	17	9	58, 72	46, 47, 62
Kinase inactive Raf-1	26	16	37, 56, 68	None

Fig. 5.10 Screening *raf-1*$^{-/-}$ clones transfected with the pEFm.6 vector by PCR using primers Ocp106 and Ocp107. Amplification of a PCR product of 200 bp was observed from the pEFm.6 vector in 10 out of 14 clones.

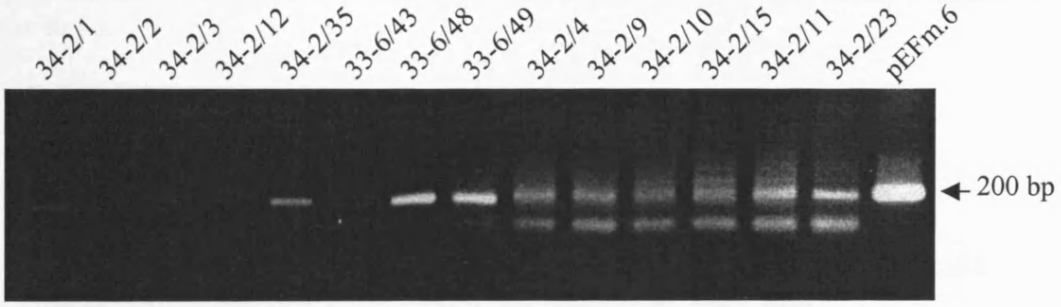

Fig. 5.11 Screening *raf-1*$^{-/-}$ transfected clones for Raf-1 expression. (**A**) Western blot analysis to detect Raf-1 expression in transfected clones (upper panel). Western blot analysis to detect vinculin levels as a control for protein loading (lower panel). (**B**) Western blot analysis to detect Raf-1 expression in transfected clones (upper panel). Western blot analysis to detect vinculin levels as a control for protein loading (lower panel). (**C**) Western blot analysis to detect Raf-1 expression (upper panel). Longer exposure of same blot in upper panel to visualise the faint band of clone number 58 (middle panel). Western blot analysis to detect vinculin levels as a control for protein loading (lower panel). Abbreviations; pEFm.6 = empty backbone vector, WT = wild-type human Raf-1, KI = kinase inactive mutant of human Raf-1.

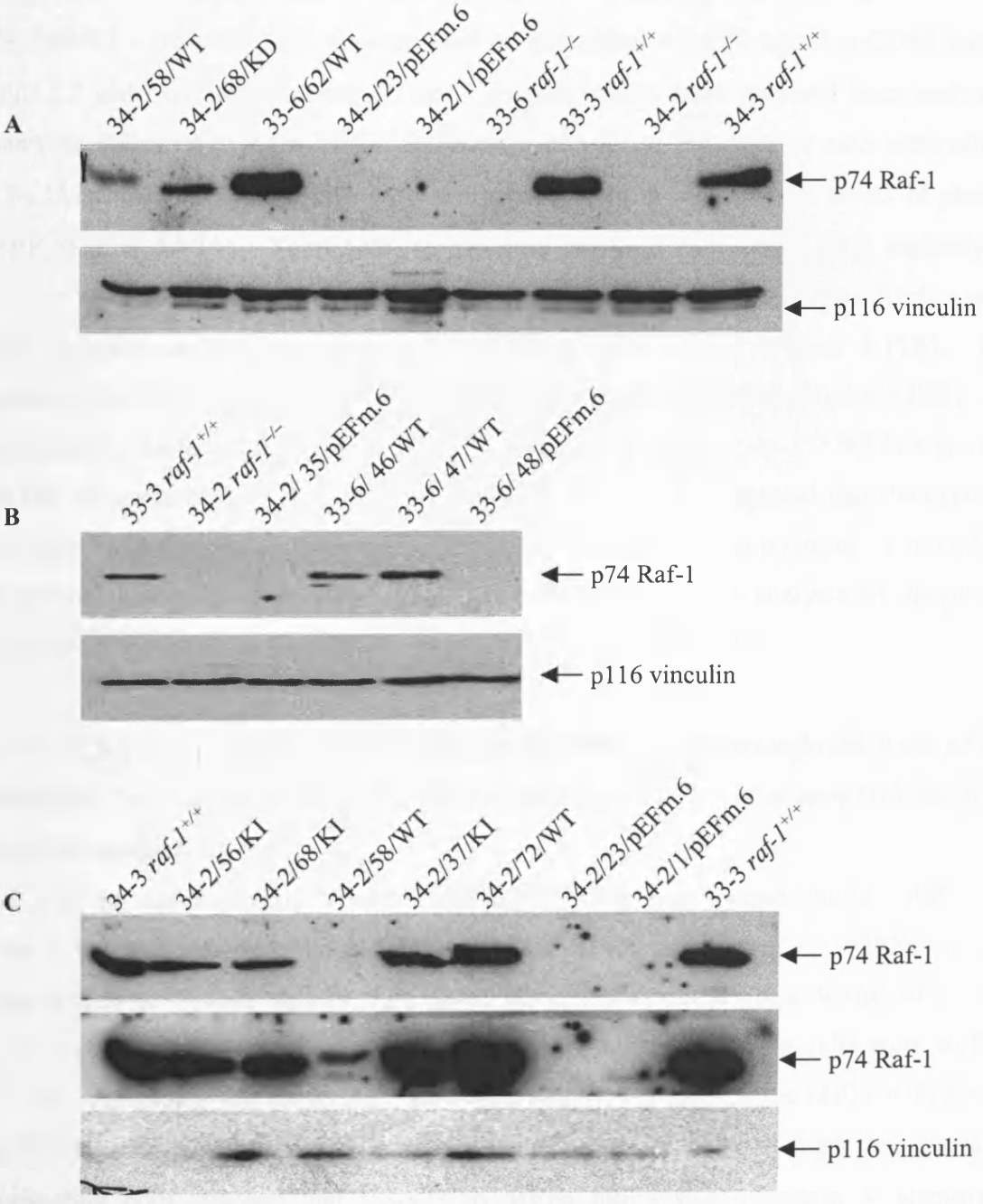

5.3.11 Characterisation of Raf-1 deficient tsSV40T MEFs transfected with pEFm.6, wild-type Raf-1 and kinase inactive Raf-1 with respect to ERK phosphorylation

Previous reports have suggested that the expression of dominant negative mutants of Raf-1 inhibit the phosphorylation of ERK and suppress cell growth (Kolch *et al.*, 1991; Schaap *et al.*, 1993). Therefore the kinase inactive mutant used for these experiments may also act in a dominant negative fashion. In order to determine whether the unregulated expression of kinase inactive Raf-1 had any effect on the phosphorylation of ERK, the following clones; 33-3/*raf-1*$^{+/+}$, 34-2/1/pEFm.6, 34-2/23/pEFm.6, 34-2/72/WT, 34-2/58/WT, 34-2/37/KIand 34-2/68/KI were either left unstimulated or stimulated with 50 ng/ml α-CD95 antibody plus 0.5 μM cycloheximide for 10 min. Protein lysates were prepared from each of the samples, followed by SDS-PAGE and electro-transfer of the proteins onto nitrocellulose. The blots were incubated with an α-phosphoERK antibody to detect levels of phospho-ERK (Figure 5.12A). Total ERK levels were analysed using an α-ERK antibody as a control for protein loading and to ensure that any differences in phospho-ERK were not due to differences in the relevant amounts of ERK protein (Figure 5.12B). In all unstimulated MEFs, levels of phospho-ERK were barely detectable (Figure 5.12B). After stimulation, the levels of phospho-ERK in all of the transfected *raf-1*$^{-/-}$ MEFs was similar to that observed in the *raf-1*$^{+/+}$ MEFs (Figure 5.12A). This suggested that the expression of kinase inactive Raf-1 does not significantly disrupt ERK activation. The cells that expressed kinase inactive Raf-1 could then be used for the analysis of apoptosis in response to α-CD95 antibody.

5.3.12 Characterisation of Raf-1 deficient tsSV40T MEFs transfected with pEFm.6, wild-type Raf-1 and kinase inactive Raf-1 with respect to levels of apoptosis induced by α-CD95 antibody

In order to assess whether the expression of wild-type or kinase inactive Raf-1 could rescue the increase in apoptosis susceptibility observed with *raf-1*$^{-/-}$ MEFs, apoptosis assays were performed. MEFs were plated out onto 6 cm dishes at a density of 1.5 x 10^5. The next day the cells were fed with normal growth media and the cells were shifted to 39.5°C. Apoptosis was induced the following day by treatment of the MEFs with 50 ng/ml α-CD95 antibody plus 0.5 μM cycloheximide for 20 hours, and cell death was assessed by harvesting both attached and suspension MEFs followed by annexin V staining and

Fig. 5.12 Analysis of transfected tsSV40T MEFs with respect to ERK phosphorylation induced by 50 ng/ml α-CD95 antibody plus 0.5 μM cycloheximide and with no treatment. (**A**) Western blot analysis to detect phospho-ERK after no treatment (NT) or after 10 min stimulation with 50 ng/ml α-CD95 antibody plus 0.5 μM cycloheximide. (**B**) Western blot analysis to detect total ERK levels as a control for protein loading. Abbreviations; pEFm.6 = empty backbone vector, WT = wild-type human Raf-1, KI = kinase inactive mutant of human Raf-1.

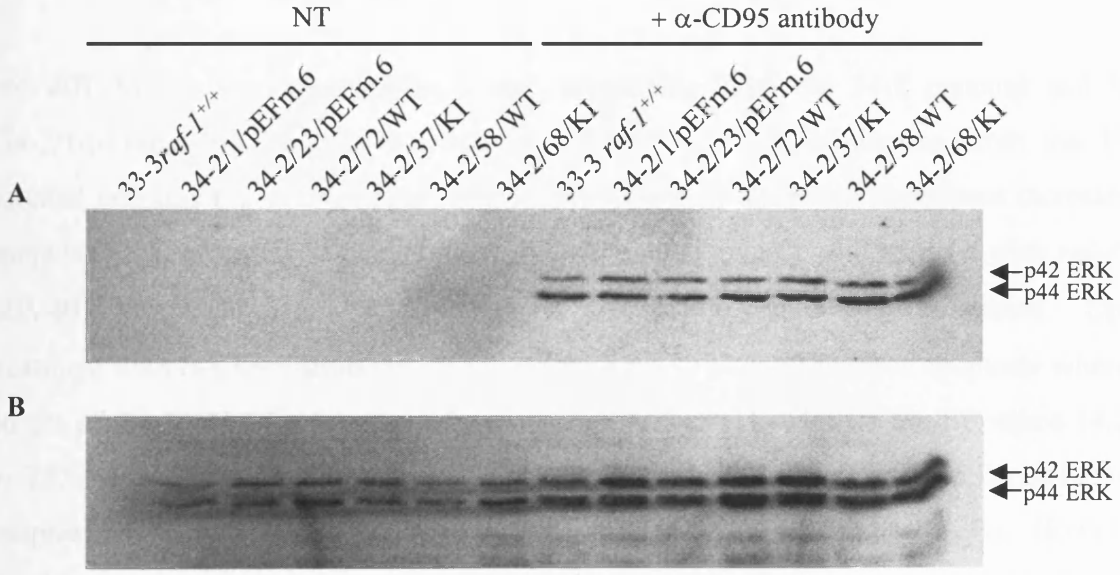

FACScan analysis. Each individual apoptosis experiment was performed with varying combinations of the following cell clones due to number limits for the assay; 34-3 and 33-3 *raf-1*$^{+/+}$ MEFs, three clones of 34-2 with pEFm.6 (1, 23 or35), two clones of 33-6 with pEFm.6 (49 or 48) two clones of 34-2 expressing wild-type Raf-1 (72 and 58) three clones of 34-2 expressing kinase inactive Raf-1 (37, 56 and 68) and three clones of 33-6 expressing wild-type Raf-1 (46, 47 or 62). Cell clones originating from each of the two parental *raf-1*$^{-/-}$ tsSV40T MEF cell lines (34-2 and 33-6) were analysed separately as it was found that results differed greatly between them.

tsSV40T MEFs containing pEFm.6 both originating from the 34-2 parental cell line (34-2/1/pEFm.6, 34-2/23/pEFm.6 and 34-2/35/pEFm.6) and originating from the 33-6 parental cell line (33-6/49/pEFm.6 and 33-6/48/pEFm.6) showed a significant increase in apoptosis in response to α-CD95 antibody plus cycloheximide as compared with *raf-1*$^{+/+}$ tsSV40T MEFs (34-3 and 33-3) when all data sets obtained were combined. Upon treatment with α-CD95 antibody, 26.9% of the *raf-1*$^{+/+}$ cells underwent apoptosis whereas 46.5% of the 34-2/pEFm.6 cells underwent apoptosis (n=11; 95% CI for difference 14.2% to 25%, p = <0.0001; Figure 5.13A) and 44.3% of the 33-6/pEFm.6 cells underwent apoptosis (n=3; 95% CI for difference 5% to 30%, p = 0.0096; Figure 5.13A). However, the data obtained from 33-6 MEFs transfected with pEFm.6 upon treatment with α-CD95 antibody plus cycloheximide was very variable as indicated by the large standard deviation. This limits the usefulness of this clone for the rescue experiments especially in light of the observed high expression levels of the T antigen.

tsSV40T MEFs originating from the 33-6 parental cell line and expressing wild-type Raf-1 (46/WT/33-6, 47/WT/33-6 and 62/WT/33-6) showed a significant increase in apoptosis in response to α-CD95 antibody plus cycloheximide as compared with *raf-1*$^{+/+}$ tsSV40T MEFs (34-3 and 33-3). This treatment induced 73.5% apoptosis for 46/WT/33-6, 64% apoptosis for 47/WT/33-6 and 48.7% apoptosis for 62/WT/33-6 (Figure 5.14B). When these three data sets are combined they induced 60.1% apoptosis whereas the *raf-1*$^{+/+}$ cells induced 26.9% apoptosis (n=7; 95% CI for difference 21.8% to 44.8%, p = <0.0001; Figure 5.14A). This indicated that the expression of Raf-1 in these cells did not rescue the apoptotic phenotype resulting from a lack of Raf-1. In fact, significantly more death was

Fig. 5.13 Analysis of tsSV40T immortalised MEFs transfected with pEFm.6 with respect to apoptosis induced by 50 ng/ml α-CD95 antibody plus 0.5μM cycloheximide (α-CD95 antibody; grey bars) and with no treatment (NT; white bars). Apoptosis is measured by the percentage of cells that have high annexin V staining as assessed by flow cytometric analysis. Graph of pooled data from *raf-1*$^{+/+}$, three clones of 34-2 with pEFm.6 (1, 23 and 35) and two clones of 33-6 with pEFm.6 (48 and 49). Standard deviation bars are shown.

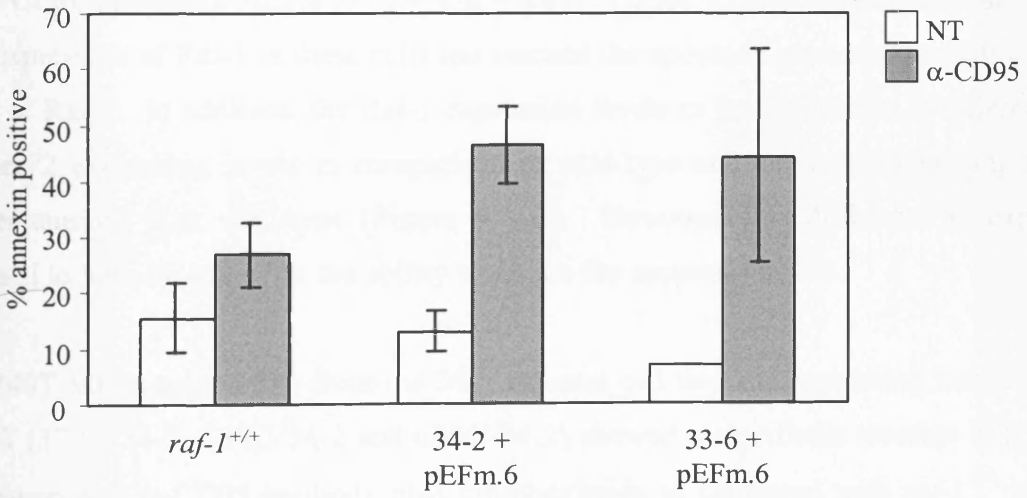

observed with these clones transfected with wild-type Raf-1 than clones transfected with pEFm.6.

However, tsSV40T MEFs originating from the 34-2 parental cell line and expressing wild-type Raf-1 (72/WT/34-2 and 58/WT/34-2) did not show a significant increase in apoptosis in response to α-CD95 antibody plus cycloheximide as compared with *raf-1*$^{+/+}$ tsSV40T MEFs (34-3 and 33-3). This treatment induced 34.25% apoptosis for 58/WT/34-2 and 19.2% apoptosis for 72/WT/34-2 (Figure 5.14C). When these two data sets are combined they induced 25.9% apoptosis whereas the *raf-1*$^{+/+}$ cells induced 26.9% apoptosis (n=8; 95% CI for difference –0.5% to 10.4%, $p = 0.071$; Figure 5.14A). This result indicates that the expression of Raf-1 in these cells has rescued the apoptosis phenotype resulting from a lack of Raf-1. In addition, the Raf-1 expression levels in the two clones is different, with clone 72 expressing levels in comparison to wild-type and clone 58 expressing a much lower amount than wild-type (Figure 5.11C). However, this difference in expression seemed to have no effect on the ability to rescue the apoptosis defect.

tsSV40T MEFs originating from the 34-2 parental cell line and expressing kinase inactive Raf-1 (37/KI/34-2, 56/KI/34-2 and 68/KI/34-2) showed a significant increase in apoptosis in response to α-CD95 antibody plus cycloheximide as compared with *raf-1*$^{+/+}$ tsSV40T MEFs. This treatment induced 52.5% apoptosis for 37/KI/34-2, 40.8% apoptosis for 56/KI/34-2 and 16.7% apoptosis for 68/KI/34-2 (Figure 5.15B). When these three data sets are combined they induced 38.5% apoptosis whereas the *raf-1*$^{+/+}$ cells induced 26.9% (n=11; 95% CI for difference 1.6% to 21.62%, $p = 0.025$; Figure 5.15A). This indicated that the expression of kinase inactive Raf-1 in these cells did not rescue the apoptotic phenotype resulting from a lack of Raf-1. However when one of the clones expressing kinase inactive Raf-1 (68/KI/34-2) is analysed alone, the *raf-1*$^{+/+}$ cells showed 26.9% apoptosis whereas the 34-2 *raf-1*$^{-/-}$ cells showed 16.7% apoptosis (n=3; 95% CI for difference 1.79% to 18.57%, $p = 0.021$; Figure 5.15B). This means that not only has the kinase inactive Raf-1 rescued the apoptosis phenotype in this clone, but it has reduced the amount of cells undergoing apoptosis to even less than that observed with wild-type MEFs. The Raf-1 expression levels in the three clones are all similar to each other and to wild-

Fig. 5.14 Analysis of tsSV40T immortalised MEFs expressing human wild-type Raf-1 with respect to apoptosis induced by 50 ng/ml α-CD95 antibody plus 0.5 μM cycloheximide (α-CD95 antibody; grey bars) and with no treatment (NT; white bars). Apoptosis is measured by the percentage of cells that have high annexin V staining as assessed by flow cytometric analysis. (**A**) Graph of pooled data from *raf-1*$^{+/+}$ and clones 34-2 and 33-6 expressing WT Raf-1. (**B**) Graph of pooled data from *raf-1*$^{+/+}$ and clones 33-6 transfected with pEFm.6 and the three 33-6 clones expressing WT Raf-1 (46, 47 and 62). (**C**) Graph of pooled data from *raf-1*$^{+/+}$ and 34-2 transfected with pEFm.6 and the two 34-2 clones expressing WT Raf-1 (58 and 72). Standard deviation bars are shown.

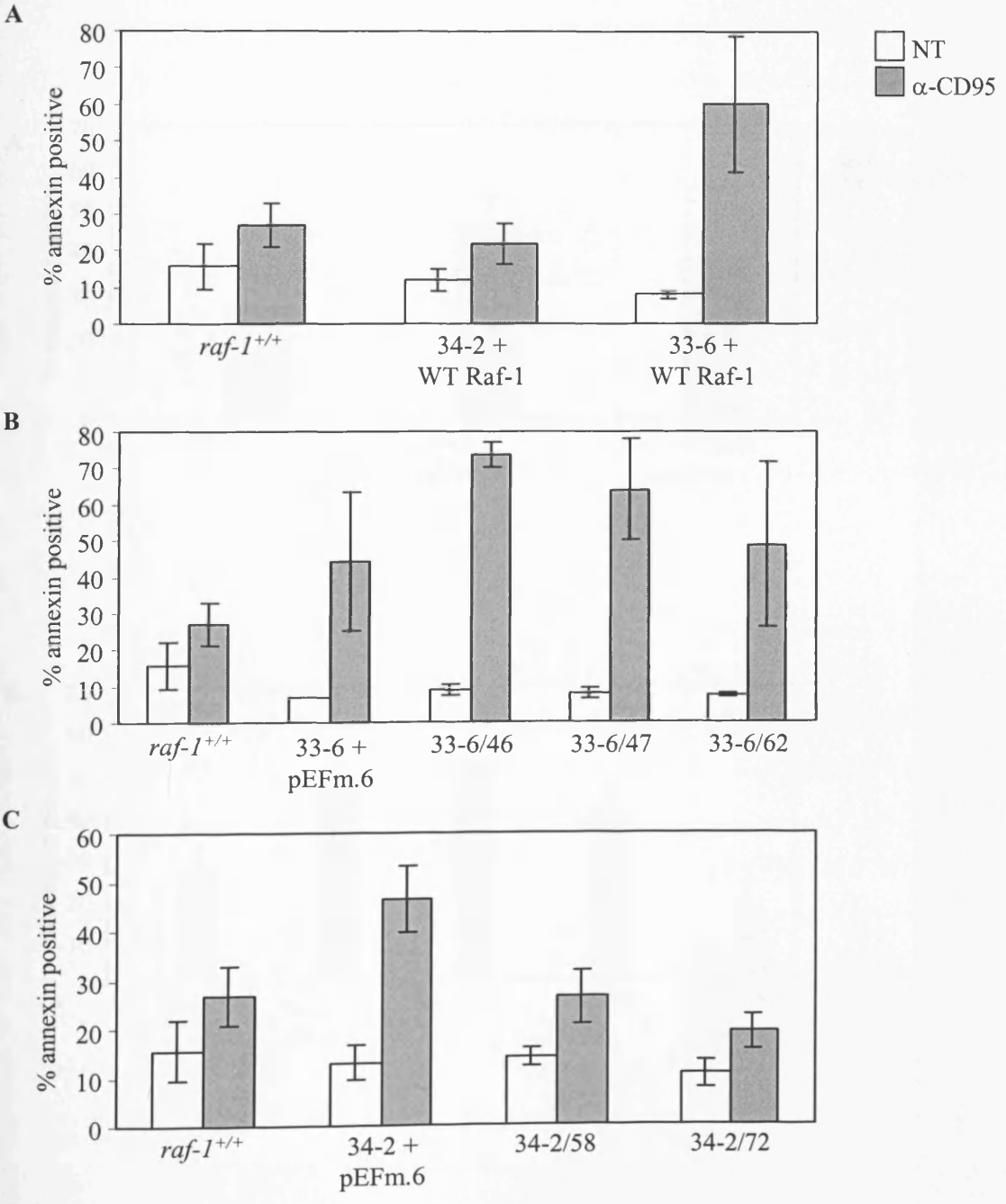

Fig. 5.15 Analysis of tsSV40T immortalised MEFs transfected with kinase inactive human Raf-1 with respect to apoptosis induced by 50 ng/ml α-CD95 antibody plus 0.5 μM cycloheximide (α-CD95 antibody; grey bars) and with no treatment (NT; white bars). Apoptosis is measured by the percentage of cells that have high annexin V staining as assessed by flow cytometric analysis. (**A**) Bar chart of pooled data from *raf-1*$^{+/+}$, 34-2 transfected with pEFm.6 and 34-2 clones expressing kinase inactive Raf-1. (**B**) Bar chart of pooled data from, 34-2 transfected with pEFm.6 and the three 34-2 clones expressing kinase = inactive Raf-1 (37,56 and 68). Standard deviation bars are shown.

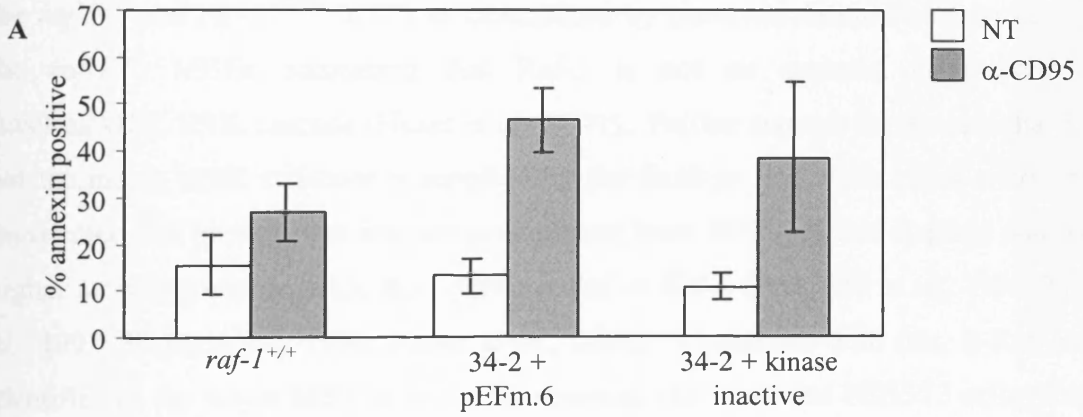

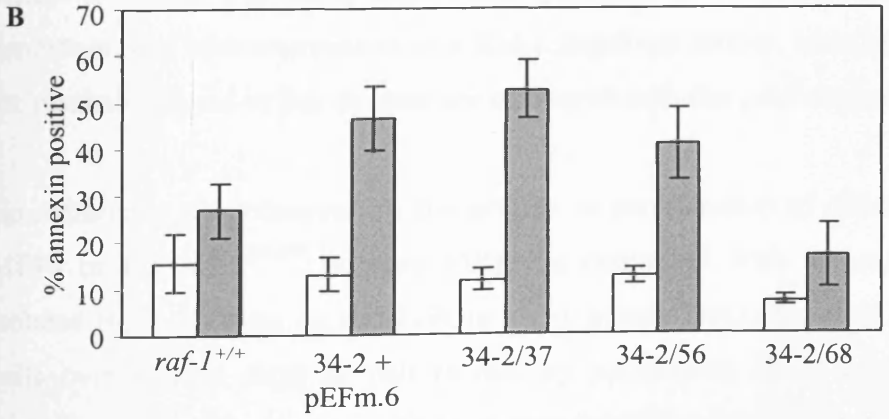

type levels (Figure 5.11C). Therefore a difference in expression levels cannot explain the differences on the ability to rescue the apoptosis defect.

5.4 Conclusions

This chapter describes the derivation of MEFs that lack Raf-1 (*raf-1*$^{-/-}$) and MEFs that harbour a mutation of the endogenous tyrosine residues 340 and 341 to phenylalanines (*raf-1*$^{FF/FF}$). These MEFs were used to analyse the role of Raf-1 in growth, proliferation and apoptosis. Raf-1 immunoprecipitated from the *raf-1*$^{FF/FF}$ MEFs has previously been confirmed as having no detectable kinase activity towards MEK. It was also previously discovered that after stimulation with various growth factors, levels of ERK activation in the *raf-1*$^{-/-}$ and *raf-1*$^{FF/FF}$ MEFs as determined by phosphorylation status are identical to the *raf-1*$^{+/+}$ MEFs, indicating that Raf-1 is not an essential component of the Ras/Raf/MEK/ERK cascade (Huser *et al.*, 2001). Further support for the idea that Raf-1 is not the major MEK activator is supplied by the findings that when either endogenous or transfected Raf proteins are immunoprecipitated from MEFs, B-Raf displays considerably higher activity towards MEK than either A-Raf or Raf-1 (Pritchard *et al.*, 1995; Marais *et al.*, 1997; Papin *et al.*, 1998; Huser *et al.*, 2001). Consistent with this, B-Raf has been identified as the major MEK activator in neuronal cell types and NIH3T3 cells (Catling *et al.*, 1994; Jaiswal *et al.*, 1994; Moodie *et al.*, 1994; Traverse and Cohen, 1994; Reuter *et al.*, 1995).

Whilst this work was being undertaken, Mikula et al. (2001) also published work on the generation and characterisation of a Raf-1 knockout mouse, and therefore where relevant the results obtained in this chapter are compared with the published results from this group.

No difference was observed in the growth or proliferation of either the *raf-1*$^{-/-}$ primary MEFs or the *raf-1*$^{FF/FF}$ primary MEFs as compared with the *raf-1*$^{+/+}$ primary MEFs isolated from embryos on the 129Ola/MF-1 genetic background as assessed by counting cells over several days in culture and by performing BrdU assays. These data are consistent with Mikula et al. (2001) as they determined the DNA content of synchronised populations of primary MEFs and found no cell cycle anomalies with the *raf-1*$^{-/-}$ primary MEFs. However, when primary MEFs were isolated from embryos on the

129Ola/C57BL6 genetic background they failed to grow which meant that they either had a cell proliferation defect or an apoptosis defect. These data are consistent with those shown by Mikula *et al.* (2001), as they found that their *raf-1*$^{-/-}$ primary MEFs, which were obtained from embryos on the 129Sv/C57BL6 genetic background, grew significantly slower than wild-type MEFs although they were able to culture them. They came to the conclusion that the reason for the defective growth of their *raf-1*$^{-/-}$ primary MEFs was due to an apoptosis defect rather than a proliferation defect, as the flow cytometric analysis highlighted a significantly larger sub-2N DNA content in the *raf-1*$^{-/-}$ primary MEFs in comparison to the *raf-1*$^{+/+}$ primary MEFs. Therefore this chapter describes the lack of a requirement for Raf-1 specifically in MEFs with respect to cell growth and proliferation. However this does not exclude the possibility that Raf-1 is essential for these processes in other cell types.

No defect in spontaneous apoptosis was observed in the *raf-1*$^{-/-}$ primary MEFs in comparison to the *raf-1*$^{+/+}$ primary MEFs on the 129Ola/MF-1 genetic background. However the fact that primary MEFs on the 129Ola/C57BL6 could not be cultured indicates that on this particular genetic background, the lack of Raf-1 results in spontaneous apoptosis. Furthermore, spontaneous apoptosis was observed by Mikula *et al.* (2001) on the 129Sv/C57BL6 genetic background. This indicates the presence of genetic modifiers in different strains. The nature of these modifiers is presently unknown but it is clear that they have profound effects on Raf-1 function in different strains.

This chapter describes a role for Raf-1 in the prevention of apoptosis in response to etoposide and α-CD95 antibody plus cycloheximide, because a lack of Raf-1 results in an increased susceptibility to these agents, with the largest susceptibility to α-CD95 antibody plus cycloheximide. This data is supported by Mikula *et al.* (2001) who found that their *raf-1*$^{-/-}$ primary MEFs were more susceptible to undergo apoptosis in comparison to the *raf-1*$^{+/+}$ primary MEFs in response to serum deprivation, actinomycin D treatment and α-CD95 antibody plus actinomycin D treatment. The only contradiction is that they observed an increase in susceptibility to undergo apoptosis following serum deprivation. However the difference between the *raf-1*$^{-/-}$ primary MEFs and *raf-1*$^{+/+}$ primary MEFs was very small in comparison to the other treatments. This difference in response to serum

deprivation is probably due to the genetic strain difference, with the 129Ola/MF-1 genetic background having a genetic modifier that resists an increase in apoptosis under these conditions.

It appears that this function of Raf-1 is independent of its MEK kinase function, as the *raf-1*$^{FF/FF}$ primary MEFs do not exhibit the same susceptibility as the *raf-1*$^{-/-}$ primary MEFs to these apoptosis inducers, even though Raf-1 in the *raf-1*$^{FF/FF}$ primary MEFs has no detectable kinase activity towards MEK. It therefore appears that Raf-1 has a unique role in cell survival that cannot be compensated for by A-Raf or B-Raf, and that is probably independent of its function as a component of the Ras/Raf/MEK/ERK cascade.

The largest difference in apoptosis between *raf-1*$^{-/-}$ primary MEFs and *raf-1*$^{+/+}$ primary MEFs was observed with α-CD95 antibody plus cycloheximide treatment. Therefore ERK activation and p38MAPK phosphorylation was assessed over a timecourse of stimulation with this apoptosis inducer. No obvious differences were observed in the phosphorylation profile of ERK or p38MAPK between the *raf-1*$^{-/-}$ MEFs and the *raf-1*$^{+/+}$ MEFs. Mikula et al. (2001) also investigated ERK phosphorylation over a timecourse of stimulation with α-CD95 antibody and observed a similar ERK phosphorylation profile. This shows that the apoptosis susceptibility of the *raf-1*$^{-/-}$ MEFs in response to α-CD95 antibody plus cycloheximide treatment is not due to effects mediated by either the Ras/Raf/MEK/ERK cascade, which is in agreement with the RafFF data, or the p38MAPK stress pathway.

This chapter also describes the derivation of MEFs immortalised with a temperature sensitive version of the SV40 large T antigen for the first time in MEFs. The reason that the primary MEFs were immortalised was to allow the successful transfection of *raf-1*$^{-/-}$ MEFs with various Raf-1 expressing constructs as primary MEFs are very difficult to transfect. The reason for the use of a reversible system was because large T antigen has many effects on the cell, including interference with the cell cycle control machinery that may interfere with the interpretation of results. By placing cells that express a temperature sensitive SV40 large T antigen at the permissive temperature of 33°C, the protein is active, but when the same cells are placed at the restrictive temperature of 39.5°C, the T antigen is degraded (Jat and Sharp, 1989). However, it was found that after placing cells expressing

the temperature sensitive version of the large T antigen for 24 hours at 39.5°C, western blot analysis showed that in three out of four cell lines, the large T antigen was still present but at reduced levels. Therefore it had not fully degraded. In spite of this, the tsSV40T transformed *raf-1*$^{-/-}$ MEFs showed similar characteristics to the *raf-1*$^{-/-}$ primary MEFs at 39.5°C with respect to apoptosis upon induction with α-CD95 antibody plus cycloheximide when data was pooled. However, the degree of apoptosis appeared to be dependent on the levels of expression of the T antigen.

Nevertheless, these tsSV40T transformed *raf-1*$^{-/-}$ MEFs were transfected with two Raf-1 expressing constructs to ensure that the observed apoptosis susceptibility was both specifically due to the lack of Raf-1 rather than disruption of a different gene such as MKRN2 (Gray *et al.*, 2001) and to determine whether the kinase function of Raf-1 was required for its postulated role in apoptosis suppression. However, only 8 out of 68 puromycin resistant clones were obtained that expressed Raf-1. The reason for this low frequency was probably because it was necessary to perform a co-transfection as the expression plasmids could not be directly selected for. This therefore highlighted a major drawback to this approach as clonal variation is observed from analysing too few clones that each express different levels of Raf-1. An improvement to this technique would be to subclone the Raf-1 cDNAs into a plasmid harbouring the *Puro*^{R} gene so that integration of the plasmid could be directly selected for.

Each of the five tsSV40T transformed *raf-1*$^{-/-}$ MEF clones expressing wild-type Raf-1 were then analysed with respect to apoptosis induced by treatment with α-CD95 antibody in order to assess whether they could rescue the observed increased susceptibility to undergo apoptosis. The two clones originating from the 34-2 parental cell line (58 and 72) rescued the apoptosis phenotype with the response being similar to that of tsSV40T transformed *raf-1*$^{+/+}$ MEFs and lower than the control tsSV40T transformed *raf-1*$^{-/-}$ MEFs harbouring the backbone vector (pEFm.6). However, clones originating from the 33-6 parental cell line (46, 47 and 62) did not rescue the apoptosis phenotype, with the response being greater than that of tsSV40T transformed *raf-1*$^{+/+}$ MEFs and even greater than the control tsSV40T transformed *raf-1*$^{-/-}$ MEFs harbouring the backbone vector (pEFm.6). These differences between clones derived from the two different parental cell lines in

ability to rescue the apoptosis defect is possibly due to the fact that the 33-6 parental cell line expressed higher levels of SV40 large T antigen in comparison to the 34-2 parental cell line, as it clearly had an effect on the morphology of these cells with them having a much smaller and spindle-like appearance reminiscent of transformed cells. It would be preferable to generate more cell lines before a confident conclusion can be made as to whether wild-type Raf-1 can rescue the observed apoptosis defect.

Three tsSV40T transformed *raf-1*$^{-/-}$ MEF clones expressing kinase inactive Raf-1 were obtained from the parental cell line 34-2 (37, 56 and 68) and were then analysed with respect to apoptosis induced by treatment with α-CD95 antibody in order to assess whether they could rescue the observed increased susceptibility to undergo apoptosis. When all data was pooled from each of these clones the apoptosis phenotype was not rescued, with the response being greater than that of tsSV40T transformed *raf-1*$^{+/+}$ MEFs. However when each clone was analysed separately, clone number 68 did rescue the apoptosis phenotype, with the response being even lower than that of tsSV40T transformed *raf-1*$^{+/+}$ MEFs. Therefore due to too few clones and just one out of three rescuing the apoptosis defect, it cannot be confirmed that the kinase activity of Raf-1 is not required for its role in cell survival as more cell lines need to be analysed.

The data presented in this chapter suggest a MEK/ERK independent role for Raf-1 in apoptosis in response to α-CD95 antibody and etoposide which were originally thought to mediate apoptosis through two separate pathways; the death receptor pathway and the mitochondrial pathway correspondingly. However, links between these two pathways have been identified. It has been observed that many DNA damaging agents including etoposide, induce apoptosis by the inducing the synthesis of CD95-L mediated by induction of NF-κB and AP-1 thus activating the death receptor pathway (Kasibhatla *et al.*, 1998). However, it is unclear how relevant these findings are, as very high drug concentrations were required for induction of CD95-L protein (Kaufmann and Earnshaw, 2000). Also, death receptors such as CD95, can activate caspase-8 which can then cleave and activate Bid which has been shown to stimulate cytochrome c release from mitochondria and induce formation of the apoptosome (Scaffidi *et al.*, 1998). Therefore the analysis of Bid cleavage and cytochrome c release in *raf-1*$^{-/-}$ MEFs in comparison to

raf-1$^{+/+}$ MEFs could reveal whether Raf-1 is involved in mediating this process. It would also be interesting to further address whether Raf-1 is involved in the control of susceptibility to other apoptosis inducers that act through these different pathways.

Raf-1 has been reported to interact with several proteins involved in the regulation of apoptosis independent from its role in the Ras/Raf/MEK/ERK cascade. Raf-1 has been reported to activate the transcription factor NF-κB by inducing the phosphorylation and degradation of IκB (Li and Sedivy, 1993). It appears that Raf-1 stimulates IKK which is responsible for phosphorylating and inactivating IκB and this is mediated by MEKK1 (Baumann *et al.*, 2000). Once released from IκB, NF-κB is free to translocate to the nucleus where it is involved in the transcription of genes involved in the prevention of apoptosis such as c-IAP1 and c-IAP2 (Chu *et al.*, 1997; Wang *et al.*, 1998), BCL-X_L (Chen *et al.*, 2000) and Gadd45β which is involved in cell cycle control and DNA repair (De Smaele *et al.*, 2001). However Mikula *et al.* (2001) analysed IκB degradation in response to TNF-α and α-CD95 antibody. They reported no difference in the degradation of this protein upon α-CD95 antibody or TNF-α treatment between *raf-1*$^{+/+}$ and *raf-1*$^{-/-}$ MEFs.

Raf-1 has also been reported to interact with the chaperone Bag-1 (Wang *et al.*, 1996b) and the anti-apoptotic protein Bcl-2 (Wang *et al.*, 1994) either of which may enable its translocation to the mitochondrial membrane where it may promote resistance to apoptosis by promoting the phosphorylation of the pro-apoptotic protein Bad (Wang *et al.*, 1996a). In this respect it would be useful to analyse whether mitochondrial targeted Raf-1 can rescue the apoptosis susceptibility of these cells.

Raf-1 has also been reported to interact with the MAPKKK, ASK1 *in vivo*. Furthermore, the overexpression of Raf-1 disrupted ASK1-induced cell death (Chen *et al.*, 2001). ASK1 is activated in response to apoptotic stimuli such as TNFα, CD95-L, oxidative stress and DNA damage and relays these signals to JNKs and p38MAPKs (Ichijo *et al.*, 1997; Chang *et al.*, 1998; Nishitoh *et al.*, 1998; Saitoh *et al.*, 1998; Liu *et al.*, 2000). ASK1 is thought to induce apoptosis in a variety of cell types by inducing mitochondria-mediated caspase activation (Ichijo *et al.*, 1997; Saitoh *et al.*, 1998; Hatai *et al.*, 2000). Therefore, this interaction with ASK1 would explain the results obtained as both CD95-L and DNA

damage activate ASK1, therefore if Raf-1 is normally required to suppress ASK1 activity, a lack of Raf-1 would result in increased susceptibility to apoptosis. In light of these findings, it is important to assess ASK1 activity in the *raf-1*$^{-/-}$ MEFs in response to apoptosis induction. However, the p38MAPK data suggests that ASK1 activity may not be deregulated in these cells.

In conclusion, it is now important to obtain firm evidence for the rescue of the apoptosis defect. This can be achieved by isolating more tsSV40T transformed cell lines and, from these, more stable clones transfected with various Raf-1 constructs need to be generated. This might be better done by using an expression vector that harbours the *puro*^{R} rather than using a non-selectable plasmid. Another improvement may be to perform transient transfections so that a mixed population of cells expressing different levels of Raf-1 is analysed for each experiment which should eliminate the clonal variation that has been observed in this study. The mechanism for the role of Raf-1 in the prevention of apoptosis needs to be explored by analysis of each of the pathways mentioned above in which Raf-1 has been reported to act. This could be done by comparing the activity or levels of expression of proteins that are either upregulated or downregulated in response to α-CD95 antibody in *raf-1*$^{-/-}$ versus *raf-1*$^{+/+}$ MEFs.

6 CHARACTERISATION OF A-RAF DEFICIENT PRIMARY MOUSE EMBRYONIC FIBROBLASTS AND EMBRYONIC STEM CELLS

6.1 Introduction

6.1.1 Potential involvement of A-Raf in growth and proliferation and apoptosis

A-Raf protein is abundant in all cell types (Luckett *et al.*, 2000) and has been shown to bind to activated Ras (Vojtek *et al.*, 1993) which results in the translocation of A-Raf to the plasma membrane (Marais *et al.*, 1997). A-Raf binds to MEK and can phosphorylate MEK in immunecomplex kinase assays (Pritchard *et al.*, 1995; Marais *et al.*, 1997; Huser *et al.*, 2001). However one report suggests that, upon EGF stimulation, A-Raf only phosphorylates and activates MEK1 but not MEK2 (Wu *et al.*, 1996). In comparison to Raf-1 and B-Raf, the kinase domain of A-Raf is much weaker in its ability to phosphorylate and activate MEK as assessed by overexpression studies (Pritchard *et al.*, 1995; Marais *et al.*, 1997; Papin *et al.*, 1998). Also, when endogenous A-Raf is immunoprecipitated from growth factor stimulated MEFs, its ability to phosphorylate and activate MEK using the kinase cascade assay is negligible (Huser *et al.*, 2001). In fact, endogenous A-Raf activity towards MEK has only been observed in primary rat ventricular myocytes upon stimulation with strong hypertrophic agonists such as 12-O-tetradecanoylphorbol-13-acetate (TPA) (Bogoyevitch *et al.*, 1995). Therefore, although A-Raf is able to participate in the Ras/Raf/MEK/ERK cascade, its effect on this signalling pathway is less significant than the effect of activated Raf-1 and B-Raf. These differing abilities of the Raf isoforms to activate MEK could have profound implications on cell proliferation and cell cycle arrest, as low levels of Raf activity elicit cell cycle progression and high levels of Raf activity elicit cell cycle arrest due to the induction of $p21^{WAF1/Cip1}$ as a result of high levels of ERK activation (Woods *et al.*, 1997). Therefore, as activation of A-Raf leads to weak signalling through the Ras/Raf/MEK/ERK cascade, this may implicate a specific role for A-Raf in cell proliferation.

Besides Ras and MEK, A-Raf specifically has been reported to interact with the β regulatory subunit of casein kinase 2 (CK2) using yeast two-hybrid assays (Boldyreff and

Issinger, 1997; Hagemann *et al.*, 1997). CK2 is a ubiquitously expressed serine/threonine protein kinase that has a wide range of substrates, many of which are involved in cell cycle regulation and as such it is thought to be involved in proliferation and tumourigenesis (Allende and Allende, 1995). A-Raf was also shown to interact with hTOM and hTIM. These are novel proteins that are thought to be involved in mitochondrial transport implicating their involvement in the transport of A-Raf to the mitochondria where it was shown to be localised (Yuryev *et al.*, 2000). This mitochondrial localisation may implicate a role for A-Raf in apoptosis or other mitochondrial functions such as the citric acid cycle. However no evidence has been shown for its involvement in apoptosis except for its possible role in regulation of the ERKs which have been shown to both promote and inhibit apoptosis.

6.1.2 A-Raf knockout in mice

A knockout of the X-linked *A-raf* gene in ES cells and mice has previously been described (Pritchard *et al.*, 1996). The 5' arm of the targeting construct was a 5 kb Sac I fragment that spanned the promoter and sequences encoding the initiator ATG and the amino-terminal 84 amino acids of the mouse A-Raf protein. The 3' arm of the targeting construct was a 4.5 kb Stu I-Sac I fragment that contained sequences encoding amino acids 349 to 500 of the mouse A-Raf protein. The *neo*^{R} gene separated the two arms of the targeting construct. Homologous recombination between this targeting construct and the *A-raf* gene in E14.1a ES cells resulted in deletion of sequences encoding 263 amino acids of *A-raf* that encompass the cysteine finger of the CR1 domain, the entire CR2 domain and the ATP binding site of the CR3 domain (Pritchard *et al.*, 1996; Figure 6.1A).

E14.1a ES cells are male. Therefore the clones obtained that had undergone homologous recombination were null for A-Raf as determined by Western blot analysis as the *A-raf* gene is located on the X chromosome. Two of the ES cell clones (89 and 99) were used to generate knockout mice by standard procedures and a breeding colony of these mice is maintained at the University of Leicester. The A-Raf knockout mice survive postnatally but have a distinct phenotype on the C57/BL6 genetic background, exhibiting both neurological and intestinal abnormalities, although on the 129/Ola genetic background,

Fig. 6.1 *A-raf* targeting event. (**A**) Restriction map of the targeted part of the wild-type *A-raf* gene indicating CR1, CR2 and CR3. (**B**) Targeting vector that contains a short and a long arm of homology to the *A-raf* gene separated by the *neo*^{R} gene, and also containing the herpes simplex virus-thymidine kinase gene (*HSV-tk*) for a negative selection marker. (**C**) *A-raf* targeted allele after homologous recombination with the targeting vector results in the replacement of the whole of CR2 and part of CR1 and CR3 with the *neo*^{R} gene.

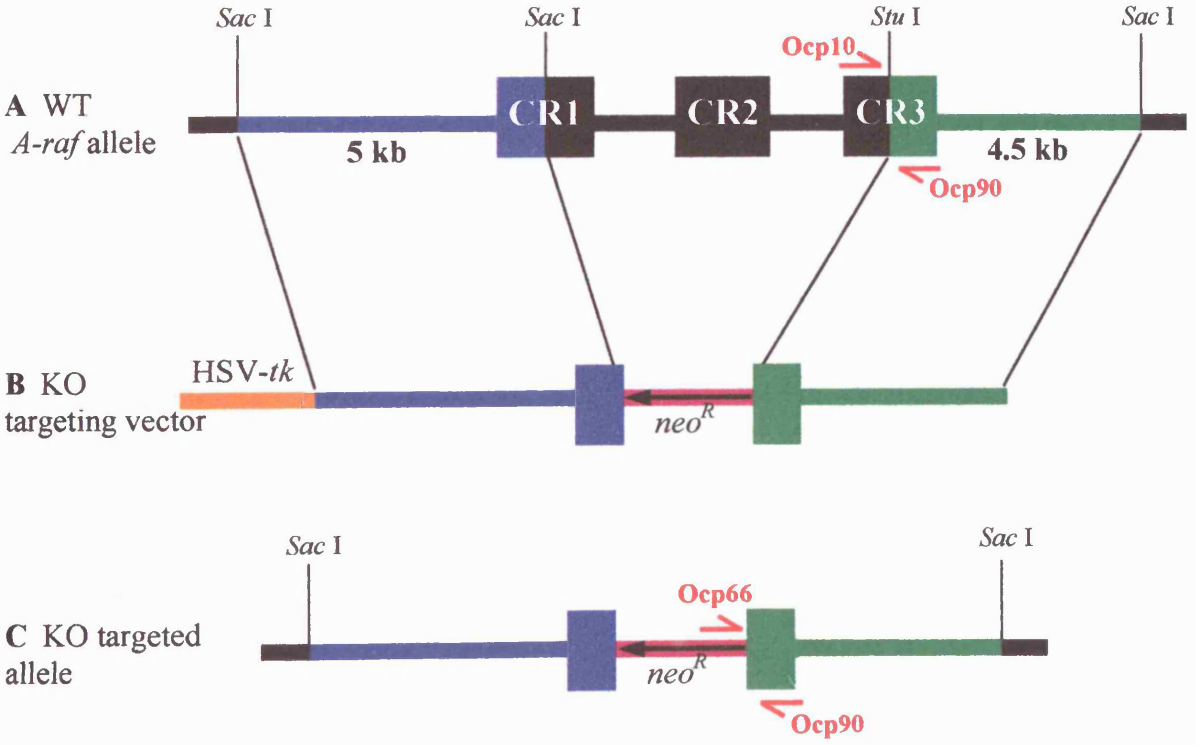

they only display a subset of the neurological abnormalities. This indicates that A-Raf has a role specifically in neurological development that is not compensated for by Raf-1 or B-Raf. A-Raf knockout mice also suffer from progressive wasting post-partum which indicates that they have a feeding ataxia (Pritchard *et al.*, 1996).

6.2 Aims

The aims for this chapter were to characterise the role of A-Raf with respect to cell growth and proliferation, differentiation and apoptosis by the derivation and analysis of MEFs and ES cells that were null for A-Raf.

6.3 Results

6.3.1 Derivation of A-Raf$^{-/Y}$ primary MEFs

Primary MEFs were derived from C57BL/6 E14.5 embryos resulting from a timed mating between C57BL/6 male animals and *A-raf* $^{+/-}$ female animals. The derivation of these MEFs was undertaken by Dr. C. Pritchard (Department of Biochemistry, University of Leicester). Each primary MEF line was generated from a single embryo and was genotyped by PCR using primers Ocp66 and Ocp90 (Figure 6.1C) to amplify a 500 bp product from the targeted allele and Ocp10 and Ocp90 (Figure 6.1A) to amplify a 250 bp product from the wild type allele (only A3-4, A3-12 and A3-14 are shown; Figure 6.2A). An extra PCR was performed using primers Ocp26 and Ocp27 corresponding to the *sry* gene to amplify a 150 bp product of this Y specific allele (only A3-4, A3-12 and A3-14 are shown; Figure 6.2B). Western blot analysis using an α-A-Raf antibody was performed to confirm PCR results (only MEFs A3, A4, A5, A6, A8 and A9 are shown; Figure 6.2C) and an antibody against vinculin was used as a control for protein loading (Figure 6.2D). MEF cell lines A3-12 (Figure 6.2A+B), A4, A5 and A8 (Figure 6.2C), and A11 (not shown) were identified as both male and deficient in A-Raf (*A-raf* $^{-/Y}$). MEF cell lines A3-14, (Figure 6.2A+B), A3, A6 and A9 (Figure 6.2C), and A1 and A2 (not shown), were identified as both male and wild-type (*A-raf* $^{+/Y}$). Only primary MEFs originating from *A-raf* $^{-/Y}$ and *A-raf* $^{+/Y}$ embryos were used for subsequent experiments. Also, western blot analysis using an anti-A-Raf antibody was performed to confirm that the two *A-raf* $^{-/Y}$ ES

Fig. 6.2 Generation of *A-raf* $^{-/Y}$ primary MEFs and ES cells. (**A**) PCR analysis of DNA from MEFs arising from a timed mating between C57BL/6 male animals and *A-raf* $^{+/-}$ female animals. PCR using primers Ocp10 and Ocp90 amplified the wild-type PCR product of 500 bp from A3-4 and A3-14. PCR using primers Ocp66 and Ocp90 amplified the targeted PCR product of 250 bp from A3-4 and A3-12. (**B**) PCR using primers Ocp26 and Ocp27 amplified the *sry* specific PCR product of 250 bp from A3-14 and A3-12. (**C**) Western blot analysis to detect A-Raf. (**D**) Western blot analysis of the same blot in **C** to detect vinculin as a control for protein loading. M = 1 kb DNA marker.

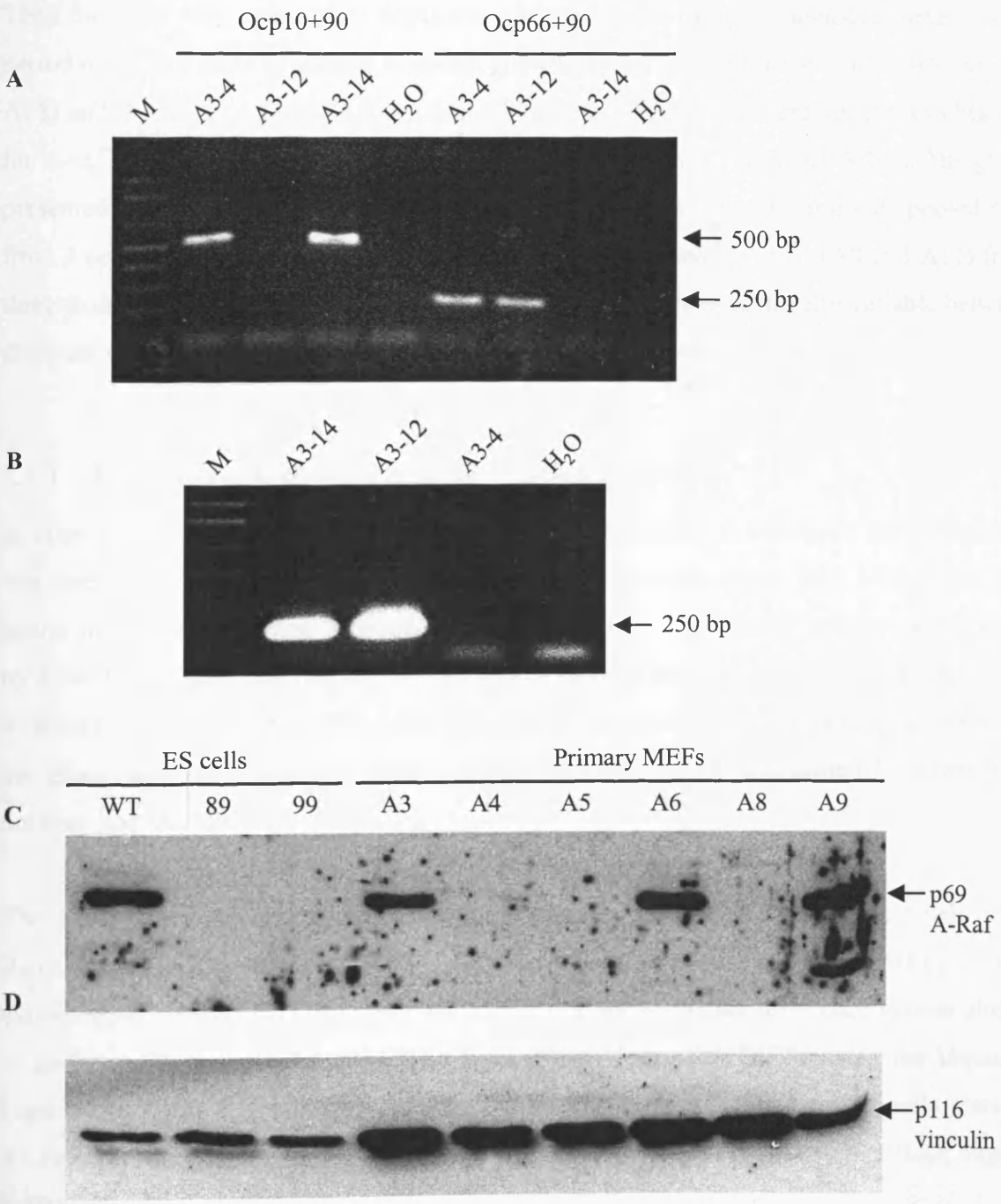

cell lines 89 and 99 that were used to generate mice did not express A-Raf protein (Figure 6.2C).

6.3.2 *Analysis of the growth characteristics of A-raf$^{-/Y}$ primary MEFs*

In order to analyse the growth of MEFs, total cell numbers were measured daily. Primary MEFs of all genotypes were plated onto 24 well plates at a density of $1x10^4$ cells per well. Then the cells were counted in triplicate every 24 hours using a haemocytometer over a period of up to 6 days in culture to obtain growth curves for both *A-raf*$^{-/Y}$ (A4, A5, A8 and A11) and *A-raf*$^{+/Y}$ (A3, A6, A9, A1 and A2) primary MEFs. The growth curves obtained for *A-raf*$^{-/Y}$ primary MEFs were similar to those of the *A-raf*$^{+/Y}$ primary MEFs. The graph presented in Figure 6.3A is representative of all data recorded and represents pooled data from 2 cell lines of each genotype; *A-raf*$^{-/Y}$ (A3 and A6) and *A-raf*$^{+/Y}$ (A8 and A11) from three data sets. In general, the growth curves obtained were occasionally variable between different experiments. However this was not reflective of the genotype.

6.3.3 *Analysis of proliferation of A-raf$^{-/Y}$ primary MEFs*

In order to analyse the ability of MEFs to progress through the cell cycle, DNA synthesis was measured. MEFs were made quiescent and then stimulated with 10% foetal calf serum in media containing bromodeoxyuridine (BrdU). Cell proliferation was measured by detection of cells that had incorporated BrdU by the addition of an anti-BrdU antibody, followed by addition of a FITC-conjugated secondary antibody. A minimum of 100 cells per experiment were analysed using a fluorescent microscope and scored for whether or not they had fluorescent nuclei.

The graph presented in Figure 6.3B represents pooled data from 6 different cell lines; *A-raf*$^{-/Y}$ (A4, A11 and A3-12) and *A-raf*$^{+/Y}$ (A1, A9 and A3-14) primary MEFs from 9 experiments. The *A-raf*$^{-/Y}$ primary MEFs showed no significant difference in their ability to undergo DNA synthesis compared with *A-raf*$^{+/Y}$ primary MEFs using the unpaired t test. The *A-raf*$^{+/Y}$ cells showed 49.87% proliferation and the *A-raf*$^{-/Y}$ cells showed 41.29% proliferation (n=9; 95% CI for difference –5.68% to 22.83%, p = 0.22; Figure 6.3B).

Fig. 6.3 Analysis of primary MEFs with respect to growth. (**A**) Growth profiles of *A-raf*$^{-/Y}$ primary MEFs (closed circles) compared to *A-raf*$^{+/Y}$ primary MEFs (open circles) over six days in culture. The data represent pooled data from 2 cell lines of each genotype (A3, A6, A8, A11) from three data sets. (**B**) DNA synthesis of *A-raf*$^{-/Y}$ primary MEFs (grey bar) compared to *A-raf*$^{+/Y}$ primary MEFs (white bar). The data represent pooled data from three experiments of cells of each genotype. Standard deviation bars are shown.

A

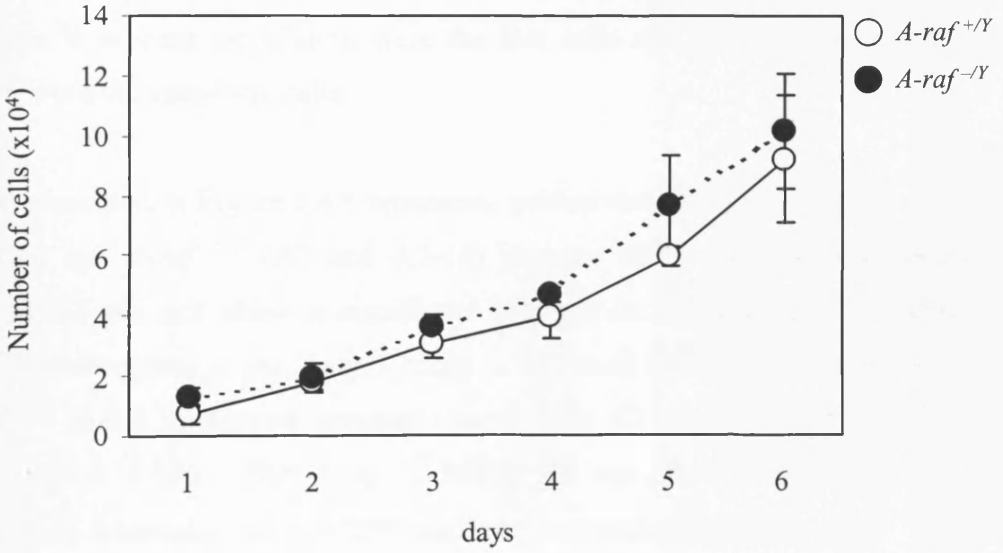

B

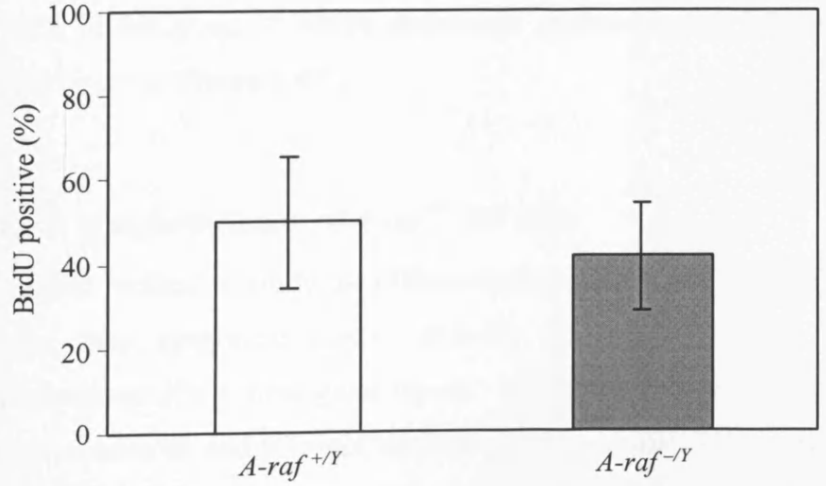

6.3.4 Analysis of apoptosis of A-raf$^{-/Y}$ primary MEFs

The primary *A-raf*$^{-/Y}$ MEFs derived from the C57/BL6 background did not show evidence of spontaneous apoptosis under normal growth conditions. Apoptosis was induced by treatment of *A-raf* $^{+/Y}$ and *A-raf* $^{-/Y}$ MEFs with 50 μM etoposide, 50 ng/ml α-CD95 antibody plus 0.5 μM cycloheximide or by serum withdrawal for 20 hours, and cell death was assessed by harvesting both attached and suspension MEFs followed by annexin V staining staining and flow cytometric analysis. The cell population was split into two; the low annexin V staining population were the live cells and the high annexin V staining population were the apoptotic cells.

The graph presented in Figure 6.4A represents pooled data from 4 cell lines; *A-raf*$^{-/Y}$ (A8 and A3-12.) and *A-raf* $^{+/Y}$ (A3 and A3-14) primary MEFs from 5 experiments. The *A-raf* $^{-/Y}$ MEFs did not show a significant increase in apoptosis upon treatment with etoposide in comparison to the *A-raf*$^{+/Y}$ cells as 27.7% of the *A-raf*$^{-/Y}$ MEFs and 29.3% of the *A-raf* $^{+/Y}$ MEFs underwent apoptosis (n=5; 95% CI for difference –5.8% to 2.5%, p =0.326; Figure 6.4A). The *A-raf* $^{-/Y}$ MEFs did not show a significant increase in apoptosis upon treatment with α-CD95 antibody in comparison to the *A-raf* $^{+/Y}$ MEFs, as 47.3% of the *A-raf* $^{-/Y}$ MEFs and 55% of the *A-raf* $^{+/Y}$ MEFs underwent apoptosis (n=5; 95% CI for difference –48.6% to 33.2%, p =0.63; Figure 6.4A). The *A-raf*$^{-/Y}$ MEFs did not show a significant increase in apoptosis upon serum withdrawal as 22% of the *A-raf*$^{-/Y}$ MEFs and 22% of the *A-raf* $^{+/Y}$ MEFs underwent apoptosis (n=5; 95% CI for difference –17.9% to 17.9%, p =1; Figure 6.4A).

6.3.5 Analysis of differentiation of A-raf$^{-/Y}$ ES cells

A well established method to study the differentiation potential of ES cells is to inject them subcutaneously into syngeneic hosts, whereby they form benign, solid teratomas containing derivatives of all three germ layers. Wild-type E14.1a ES cells (*A-raf* $^{+/Y}$) and *A-raf*$^{-/Y}$ ES cell clones 89 and 99 were injected subcutaneously into syngeneic hosts where they all formed teratomas of approximately equal weight. The tumours originating from E14.1a ES cells had a mean weight 0.58g (n=3) and the tumours originating from *A-raf*$^{-/Y}$ ES clones had a mean weight of 0.60g (n=5). The tumours were subjected to histological

Fig. 6.4 Analysis of primary MEFs with respect to apoptosis induced by either serum free media, 50 μM etoposide or 50 ng/ml α-CD95 antibody plus 0.5 μM cycloheximide. **(A)** Percentage of annexin positive staining cells as assessed by flow cytometric analysis of *A-raf*$^{-/Y}$ primary MEFs compared to *A-raf*$^{+/Y}$ primary MEFs. The data represent pooled data from five experiments of cells of each genotype. Standard deviation bars are shown.

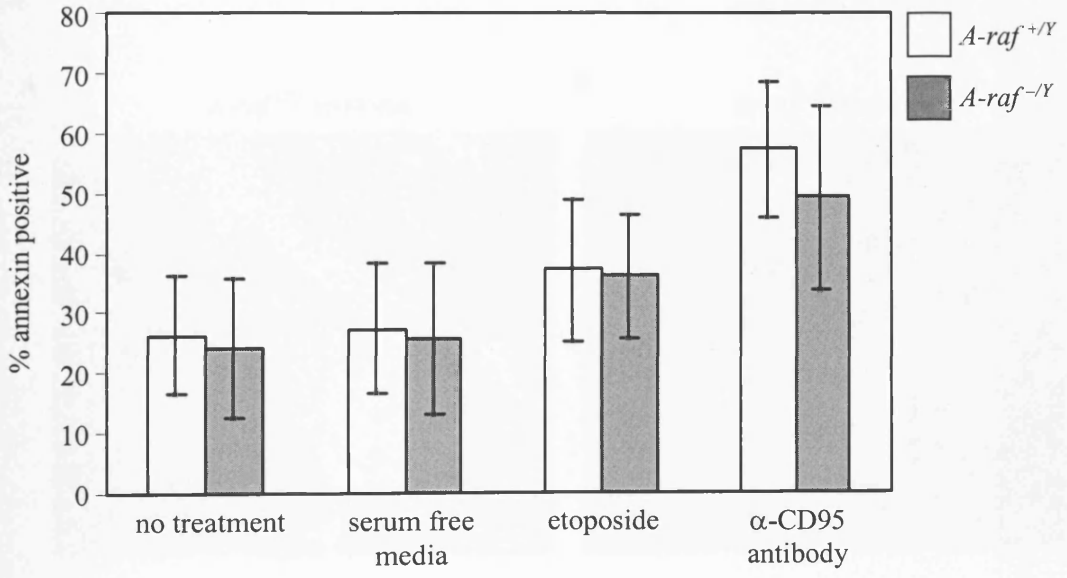

Fig. 6. 5. Histological analysis of teratomas derived from the subcutaneous injection of ES cells. **(A)** Teratoma that resulted from the injection of *A-raf*$^{+/Y}$ ES cells. **(B)** Teratoma that resulted from the injection of *A-raf*$^{-/Y}$. Scale bar represents 100μm. M = muscle, BV = blood vessel, E = epithelia, C = cartilage.

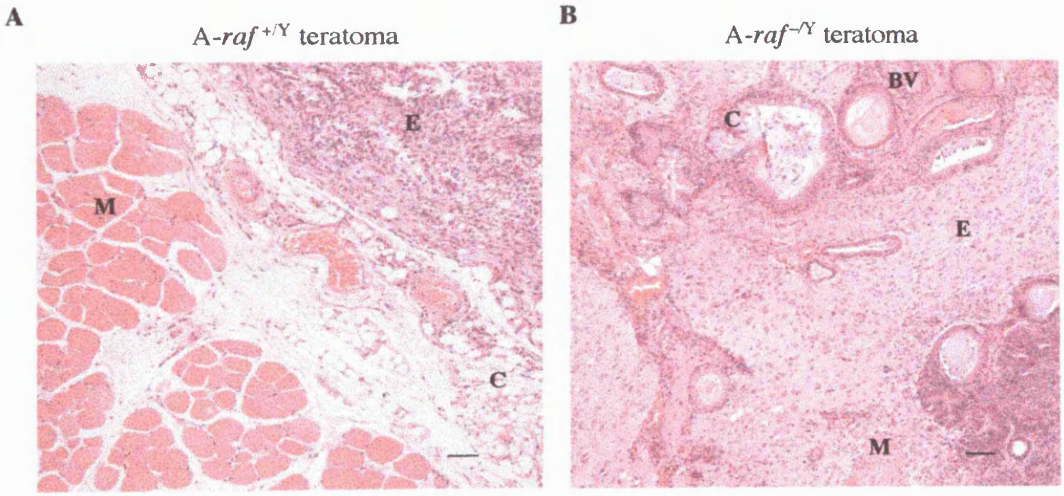

analysis and tumours from all of the ES cell lines looked similar and exhibited a chaotic arrangement of various tissues including cartilage, epithelium, muscle and blood vessels (Figure 6.5).

6.4 Conclusions

This chapter describes the derivation of primary MEFs that lack A-Raf (*A-raf*$^{-/Y}$) and the analysis of the role of A-Raf in growth, proliferation, differentiation and apoptosis using these MEFs.

Firstly, no difference was observed in the growth profiles of the *A-raf*$^{-/Y}$ MEFs as compared with the *A-raf*$^{+/Y}$ MEFs. Secondly, no significant difference was observed in the proliferation of the *A-raf*$^{-/Y}$ MEFs as compared with the *A-raf*$^{+/Y}$ MEFs. Thirdly, no difference was observed in the induced apoptosis of the *A-raf*$^{-/Y}$ MEFs as compared with the *A-raf*$^{+/Y}$ MEFs. Fourthly, no difference was observed in the differentiation ability of the *A-raf*$^{-/Y}$ ES cells as compared with the *A-raf*$^{+/Y}$ ES cells as assessed by the ability to form multiple cell types in teratomas. Therefore the role of A-Raf in intracellular signalling is unclear.

The lack of a requirement for A-Raf in these diverse cellular processes has been primarily demonstrated in primary MEFs. However this does not exclude the possibility that A-Raf is essential for these processes in other cell types. Another possibility is that the other Raf proteins or other protein kinases are compensating for its loss. *A-raf*$^{-/Y}$ mice are normal in size at birth which indicates that there is no problem with proliferation, differentiation or apoptosis during development and supports these findings in primary MEFs (Pritchard *et al.*, 1996).

In line with these observations, the levels of ERK activation in the *A-raf*$^{-/Y}$ MEFs as determined by phosphorylation status is identical to that in the *A-raf*$^{+/Y}$ MEFs (Mercer *et al.*, 2002). This indicates that A-Raf is not required for participation in the Ras/Raf/MEK/ERK cascade in this particular cell type or that its lack is compensated for by Raf-1, B-Raf or other MEK kinases. Further support for this lack of a requirement for A-Raf in the Ras/Raf/MEK/ERK cascade comes from the data showing that the kinase

domain of A-Raf has a very poor ability to phosphorylate and activate MEK in MEFs (Pritchard *et al.*, 1995; Marais *et al.*, 1997; Papin *et al.*, 1998; Huser *et al.*, 2001).

An interesting observation in the *A-raf* $^{-/Y}$ MEFs was that B-Raf activity is significantly elevated and Raf-1 activity is elevated but to a lesser extent (Mercer *et al.*, 2002). This either suggests a compensatory response for the loss of A-Raf, or that the function of A-Raf is to regulate the activities of these two Raf proteins possibly by regulating access to MEK.

A-Raf has been shown to co-localise to the mitochondria rather than the plasma membrane (Yuryev *et al.*, 2000). This implicates its potential involvement in mitochondrial-specific functions such as apoptosis. However, the primary MEF data shows that A-Raf is not involved in apoptosis in MEFs, although this does not eliminate the possibility that A-Raf may be required for the regulation of apoptosis in other cell types.

In addition to the data suggesting that A-Raf is not required for ERK activation in MEFs (Mercer *et al.*, 2002), ERK activation by Raf-1 may also have no physiological role as discussed in Chapter 5 (Huser *et al.*, 2001; Mikula *et al.*, 2001). Therefore it appears that B-Raf is the main Raf protein participating in the Ras/Raf/MEK/ERK cascade in MEFs. Further support for this hypothesis is provided by the finding that ERK activation is disrupted in *B-raf* $^{-/-}$ MEFs (Wojnowski *et al.*, 1997). Further studies on the Ras/Raf/MEK/ERK cascade therefore need to focus on B-Raf.

7 SUMMARY AND DISCUSSION

7.1 Generation of a floxed *raf-1* allele by homologous recombination in ES cells

When this project began, the only reported generation of a null mutation for the *raf-1* gene was by Wojnowski *et al.* (1998). This targeting event however generated a truncated Raf-1 protein with residual kinase activity. Therefore deletion of the whole of the *raf-1* gene was the safest option and was only feasible using Cre/*lox*P technology.

Two separate targeting vectors harbouring *lox*P sites were generated so that the *lox*P sites once integrated, would be approximately 26.8 kb apart with the intervening sequence containing exons 3 to 17. pTC7 was introduced first which, when homologously recombined, introduced a *lox*P site and a neo^R gene at the 5' end of *raf-1* in intron 2. A targeting frequency of 1: 3.9 of the selected clones was obtained. Eight of these positive clones were then chosen to go through the next round of gene targeting with pTC8. When pTC8 homologously recombined, this introduced a *lox*P sequence and a hyg^R gene at the 3' end of *raf-1* after the 3' untranslated region. A targeting frequency of 1: 33 of the selected clones was obtained. All eight clones identified as having undergone homologous recombination with pTC8 were analysed further to ensure disruption to the production of Raf-1 protein had not occurred and that the ES cells had a normal genotype. Each of these clones, except clone number 7, were then used to generate mice by the injection of these cells into 3.5 day blastocysts followed by implantation into a pseudopregnant female mouse to generate chimaeric mice. These mice were then used to breed with MF-1 mice to test for germline transmission of the targeted ES cells. ES cells derived from ES cell clone number 9 were shown to contribute to the germline of one of the male chimaeric mice as assessed by the transmission of coat colour to the offspring. However, analysis of tail DNA from these mice showed the presence of the 3' *lox*P targeting event but an absence of the 5' *lox*P targeting event. Further analysis of the germline transmitting chimaeric male showed the absence of the 5' *lox*P targeting event. It was concluded that the 5' *lox*P targeting event was unstable and therefore was lost from a proportion of the ES cells that were originally used to generate chimaeric mice. However, the 5' and 3' *lox*P sites were retained in chimeras originating from ES cell clones 29 and 55, but germline transmission has not yet been achieved from these clones.

Unfortunately, it was recently discovered that the 3' *lox*P targeting event had integrated between exons 6 and 7 of *MKRN2*, a gene encoding for makorin RING zinc-finger 2 that overlaps in an antisense orientation with the 3' UTR of the mouse *raf-1* gene (Gray *et al.*, 2001). Upon Cre-mediated recombination between the two *lox*P sites the deletion of exons 7 and 8 of *MKRN2* would occur in addition to the deletion of *raf-1*.

7.2 Cre-mediated deletion of a neomycin resistance gene flanked by *lox*P sites in MEFs and the *raf-1* gene flanked by *lox*P sites in ES cells

Conditions for the use of Cre-mediated deletion of floxed sequences were established to test the efficiency of this technique in tissue culture. A Cre expression vector was used to successfully delete a floxed neo^R gene in immortalised $raf\text{-}1^{FF/FF}$ MEFs with high efficiency. Therefore these results show that Cre can efficiently delete a floxed gene in tissue culture cells and that the deletion is stable.

A different Cre expression vector was used to identify that ES cell clone number 29 generated in Chapter 3 had acquired both *lox*P targeting events on the same chromosome. This was shown by the use of PCR analysis resulting in loss of a product upon deletion of *raf-1*. The clones originating from ES cell clone number 29 appeared to efficiently delete the *raf-1* gene. This ES cell clone is now being used to generate additional chimaeric mice.

7.3 Maintenance of a Cre expressing transgenic mouse colony

A colony of MLC2vCre mice obtained from Dr. K. Chien (Department of Medicine and Center for Molecular Genetics, University of California, San Diego) were established on both the MF-1 and the C57/BL6 background strains. These mice will eventually be mated with the *raf-1* floxed mice derived from ES cell clone 29 with an aim to delete Raf-1 specifically in the heart. The aim is to isolate cardiac myocytes and investigate the activation of the Ras/Raf/MEK/ERK cascade in response to hypertrophic stimuli.

7.4 Characterisation of *raf-1*$^{-/-}$ and *raf-1*$^{FF/FF}$ MEFs with regards to growth and proliferation and apoptosis

No differences were observed in the growth and proliferation of the *raf-1*$^{-/-}$ MEFs in comparison to *raf-1*$^{+/+}$ MEFs. This result is consistent with the normal Ki67 staining of embryos (Huser *et al.*, 2001). However they exhibited an increased susceptibility to undergo apoptosis upon treatment with etoposide or α-CD95 antibody plus cycloheximide, but not upon serum withdrawal. These results indicate that Raf-1 is required for the promotion of cell survival/inhibition of apoptosis in primary MEFs. In contrast, however, no difference in the susceptibility of the *raf-1*$^{FF/FF}$ MEFs in comparison to *raf-1*$^{+/+}$ MEFs was observed. It has been shown that Raf-1 kinase activity towards MEK is undetectable in the *raf-1*$^{FF/FF}$ MEFs indicating an essential role of tyrosine 340/341 phosphorylation for Raf-1 activity (Huser *et al.*, 2001). Moreover, ERK phosphorylation in response to various stimuli in *raf-1*$^{-/-}$ and *raf-1*$^{FF/FF}$ MEFs is similar to that in *raf-1*$^{+/+}$ MEFs. This indicates a unique role for Raf-1 in the regulation of apoptosis that is probably independent of its role in the Ras/Raf/MEK/ERK cascade. The results of this work were published in Hüser *et al.*, 2001.

ERK and p38MAPK phosphorylation were measured in response to α-CD95 antibody plus cycloheximide over a timecourse of stimulation to see if there were any differences in the phosphorylation states between *raf-1*$^{-/-}$ and *raf-1*$^{+/+}$ primary MEFs which would account for the increased apoptosis susceptibility of the *raf-1*$^{-/-}$ primary MEFs. No difference was detected in phosphorylation status between the *raf-1*$^{-/-}$ and *raf-1*$^{+/+}$ primary MEFs, further supporting the idea that the MEK kinase function of Raf-1 is not essential for its role in cell survival.

The final analysis of the *raf-1*$^{-/-}$ MEFs was to see if the increased apoptosis susceptibility could be rescued by the expression of wild-type Raf-1. The reason these experiments were performed was to ensure that the disruption in the *raf-1* gene had not affected other genes in close proximity. In particular, a gene has been identified that overlaps with and is antisense to *raf-1* at the 3' end of Raf-1 by 91 bp, called makorin RING zinc finger-2 (Gray *et al.*, 2001). Both stable clones out of a total of two that expressed wild-type Raf-1 rescued the apoptosis susceptibility apoptosis susceptibility due to the absence of Raf-1 in

response to α-CD95 antibody plus cycloheximide indicating that the makorin RING zinc finger-2 gene was not affected by the *raf-1* targeting event. To identify whether the kinase activity of Raf-1 is required for its role in apoptosis suppression, a construct expressing kinase inactive Raf-1 was transfected into the *raf-1*$^{-/-}$ MEFs. However just one stable clone out of a total of three that expressed kinase inactive Raf-1 rescued the apoptosis susceptibility due to the absence of Raf-1. More experiments on different stable clones need to be performed to assess the significance of these results.

7.5 Characterisation of A-Raf $^{-/Y}$ MEFs with regards to growth and proliferation, apoptosis and differentiation

No differences were observed in the growth, proliferation or differentiation of the A-Raf$^{-/Y}$ MEFs in comparison to A-Raf $^{+/Y}$ MEFs or in their ability to undergo apoptosis upon induction by treatment with serum free media, etoposide or α-CD95 antibody plus cycloheximide. These data imply that A-Raf is not essential for the regulation of these important cellular processes in MEFs. However, this does not exclude the possibility that A-Raf is essential for these processes in other cell types. The results of this work were published in Mercer *et al.*, 2002.

7.6 Conclusion

The use of knockout/transgenic technology has in this study revealed the major role for Raf-1; that of its role in cell survival rather than involvement in the Ras/Raf/MEK/ERK cascade as highlighted efficiently by the lack of phenotype in the RafFF mice or MEFs with regards to apoptosis. Many of the previous reports on the role of Raf-1 were performed by overexpression studies and as a result gave misleading clues as to the correct physiological role of Raf-1. Therefore transgenic technologies remains a valuable tool for studying the true function of endogenous proteins and in combination with the Cre/*lox*P system, provides a critical way to analyse intracellular signalling pathways.

REFERENCES

Abdel-Hafiz, H. A., Heasley, L. E., Kyriakis, J. M., Avruch, J., Kroll, D. J., Johnson, G. L., and Hoeffler, J. P. (1992). Activating transcription factor-2 DNA-binding activity is stimulated by phosphorylation catalyzed by p42 and p54 microtubule-associated protein kinases. *Mol Endocrinol* **6**: 2079-89.

Abraham, D., Podar, K., Pacher, M., Kubicek, M., Welzel, N., Hemmings, B. A., Dilworth, S. M., Mischak, H., Kolch, W., and Baccarini, M. (2000). Raf-1-associated protein phosphatase 2A as a positive regulator of kinase activation. *J Biol Chem* **275**: 22300-4.

Albanese, C., Johnson, J., Watanabe, G., Eklund, N., Vu, D., Arnold, A., and Pestell, R. G. (1995). Transforming p21ras mutants and c-Ets-2 activate the cyclin D1 promoter through distinguishable regions. *J Biol Chem* **270**: 23589-97.

Alessi, D. R., Saito, Y., Campbell, D. G., Cohen, P., Sithanandam, G., Rapp, U., Ashworth, A., Marshall, C. J., and Cowley, S. (1994). Identification of the sites in MAP kinase kinase-1 phosphorylated by p74raf-1. *EMBO J* **13**: 1610-9.

Allende, J. E., and Allende, C. C. (1995). Protein kinases. 4. Protein kinase CK2: an enzyme with multiple substrates and a puzzling regulation. *FASEB J* **9**: 313-23.

Altschuler, D., and Lapetina, E. G. (1993). Mutational analysis of the cAMP-dependent protein kinase-mediated phosphorylation site of Rap1b. *J Biol Chem* **268**: 7527-31.

Altschuler, D. L., Peterson, S. N., Ostrowski, M. C., and Lapetina, E. G. (1995). Cyclic AMP-dependent activation of Rap1b. *J Biol Chem* **270**: 10373–10376.

Alvarez, E., Northwood, I. C., Gonzalez, F. A., Latour, D. A., Seth, A., Abate, C., Curran, T., and Davis, R. J. (1991). Pro-Leu-Ser/Thr-Pro is a consensus primary sequence for substrate protein phosphorylation. Characterization of the phosphorylation of c-myc and c-jun proteins by an epidermal growth factor receptor threonine 669 protein kinase. *J Biol Chem* **266**: 15277-85.

Ambrosio, L., Mahowald, A. P., and Perrimon, N. (1989). Requirement of the Drosophila raf homologue for torso function. *Nature* **342**: 288-91.

Anderson, N. G., Li, P., Marsden, L. A., Williams, N., Roberts, T. M., and Sturgill, T. W. (1991). Raf-1 is a potential substrate for mitogen-activated protein kinase in vivo. *Biochem J* **277**: 573-6.

Angel, P., and Karin, M. (1991). The role of Jun, Fos and the AP-1 complex in cell-proliferation and transformation. *Biochim Biophys Acta* **1072**: 129-57.

Aronheim, A., Engelberg, D., Li, N., al-Alawi, N., Schlessinger, J., and Karin, M. (1994). Membrane targeting of the nucleotide exchange factor Sos is sufficient for activating the Ras signaling pathway. *Cell* **78**: 949-61.

Ashkenazi, A., and Dixit, V. M. (1998). Death receptors: Signaling and modulation. *Science* **281**: 1305-08.

Baeuerle, P. A., and Baltimore, D. (1988). I kappa B: a specific inhibitor of the NF-kappa B transcription factor. *Science* **242**: 540-6.

Bagrodia, S., and Cerione, R. A. (1999). PAK to the future. *Trends Cell Biol* **9**: 350-5.

Barak, Y., Juven, T., Haffner, R., and Oren, M. (1993). mdm2 expression is induced by wild type p53 activity. *EMBO J* **12**: 461-8.

Barnard, D., Diaz, B., Clawson, D., and Marshall, M. (1998). Oncogenes, growth factors and phorbol esters regulate Raf-1 through common mechanisms. *Oncogene* **17**: 1539-47.

Barnier, J. V., Papin, C., Eychene, A., Lecoq, O., and Calothy, G. (1995). The mouse B-raf gene encodes multiple protein isoforms with tissue-specific expression. *J Biol Chem* **270**: 23381-9.

Bar-Sagi, D. (1994). The Sos (Son of Sevenless) protein. *Trends Endocrinol Metab* **5**: 165-9.

Bar-Sagi, D., and Feramisco, J. R. (1985). Microinjection of the ras oncogene protein into PC12 cells induces morphological differentiation. *Cell* **42**: 841-8.

Bar-Sagi, D., and Hall, A. (2000). Ras and Rho GTPases: a family reunion. *Cell* **103**: 227-38.

Bates, S., Phillips, A. C., Clark, P. A., Stott, F., Peters, G., Ludwig, R. L., and Vousden, K. H. (1998). p14ARF links the tumour suppressors RB and p53. *Nature* **395**: 124-5.

Baumann, B., Weber, C. K., Troppmair, J., Whiteside, S., Israel, A., Rapp, U. R., and Wirth, T. (2000). Raf induces NF-kappaB by membrane shuttle kinase MEKK1, a

signaling pathway critical for transformation. *Proc Natl Acad Sci U S A* **97**: 4615-20.

Beck, T. W., Huleihel, M., Gunnell, M., Bonner, T. I., and Rapp, U. R. (1987). The complete coding sequence of the human A-raf-1 oncogene and transforming activity of a human A-raf carrying retrovirus. *Nucleic Acids Res* **15**: 595-609.

Beg, A. A., and Baltimore, D. (1996). An essential role for NF-kappaB in preventing TNF-alpha-induced cell death. *Science* **274**: 782-4.

Blain, S. W., Montalvo, E., and Massague, J. (1997). Differential interaction of the cyclin-dependent kinase (Cdk) inhibitor p27Kip1 with cyclin A-Cdk2 and cyclin D2-Cdk4. *J Biol Chem* **272**: 25863-72.

Bogoyevitch, M. A., Glennon, P. E., Andersson, M. B., Clerk, A., Lazou, A., Marshall, C. J., Parker, P. J., and Sugden, P. H. (1994). Endothelin-1 and fibroblast growth factors stimulate the mitogen-activated protein kinase signaling cascade in cardiac myocytes. The potential role of the cascade in the integration of two signaling pathways leading to myocyte hypertrophy. *J Biol Chem* **269**: 1110-9.

Bogoyevitch, M. A., Marshall, C. J., and Sugden, P. H. (1995). Hypertrophic agonists stimulate the activities of the protein kinases c-Raf and A-Raf in cultured ventricular myocytes. *J Biol Chem* **270**: 26303-10.

Boguski, M. S., and McCormick, F. (1993). Proteins regulating Ras and its relatives. *Nature* **366**: 643-54.

Boldyreff, B., and Issinger, O. G. (1997). A-Raf kinase is a new interacting partner of protein kinase CK2 beta subunit. *FEBS Lett* **403**: 197-9.

Bonner, T. I., Oppermann, H., Seeburg, P., Kerby, S. B., Gunnell, M. A., Young, A. C., and Rapp, U. R. (1986). The complete coding sequence of the human raf oncogene and the corresponding structure of the c-raf-1 gene. *Nucleic Acids Res* **14**: 1009-15.

Bonni, A., Brunet, A., West, A. E., Datta, S. R., Takasu, M. A., and Greenberg, M. E. (1999). Cell survival promoted by the Ras-MAPK signaling pathway by transcription-dependent and -independent mechanisms. *Science* **286**: 1358-62.

Bos, J. L. (1989). ras oncogenes in human cancer. *Cancer Res* **49**: 4682-9.

Bradley, A., Evans, M., Kaufman, M. H., and Robertson, E. (1984). Formation of germ-line chimaeras from embryo-derived teratocarcinoma cell lines. *Nature* **309**: 255-6.

Brand, A. H., and Perrimon, N. (1994). Raf acts downstream of the EGF receptor to determine dorsoventral polarity during Drosophila oogenesis. *Genes Dev* **8**: 629-39.

Brown, K., Gerstberger, S., Carlson, L., Franzoso, G., and Siebenlist, U. (1995). Control of I kappa B-alpha proteolysis by site-specific, signal-induced phosphorylation. *Science* **267**: 1485-8.

Brtva, T. R., Drugan, J. K., Ghosh, S., Terrell, R. S., Campbell-Burk, S., Bell, R. M., and Der, C. J. (1995). Two distinct Raf domains mediate interaction with Ras. *J Biol Chem* **270**: 9809-12.

Burgering, B. M. T., and Coffer, P. J. (1995). Protein kinase B (c-Akt) in phosphatidylinositol-3-OH kinase signal transduction. *Nature* **376**: 599-602.

Cairns, B. R., Ramer, S. W., and Kornberg, R. D. (1992). Order of action of components in the yeast pheromone response pathway revealed with a dominant allele of the STE11 kinase and the multiple phosphorylation of the STE7 kinase. *Genes Dev* **6**: 1305-18.

Carroll, M. P., and May, W. S. (1994). Protein kinase C-mediated serine phosphorylation directly activates Raf-1 in murine hematopoietic cells. *J Biol Chem* **269**: 1249-56.

Catling, A. D., Reuter, C. W., Cox, M. E., Parsons, S. J., and Weber, M. J. (1994). Partial purification of a mitogen-activated protein kinase kinase activator from bovine brain. Identification as B-Raf or a B-Raf-associated activity. *J Biol Chem* **269**: 30014-21.

Catling, A. D., Schaeffer, H. J., Reuter, C. W., Reddy, G. R., and Weber, M. J. (1995). A proline-rich sequence unique to MEK1 and MEK2 is required for raf binding and regulates MEK function. *Mol Cell Biol* **15**: 5214-25.

Chang, H. Y., Nishitoh, H., Yang, X., Ichijo, H., and Baltimore, D. (1998). Activation of apoptosis signal-regulating kinase 1 (ASK1) by the adapter protein Daxx. *Science* **281**: 1860-3.

Chao, T. H., Hayashi, M., Tapping, R. I., Kato, Y., and Lee, J. D. (1999). MEKK3 directly regulates MEK5 activity as part of the big mitogen-activated protein kinase 1 (BMK1) signaling pathway. *J Biol Chem* **274**: 36035-8.

Chen, C., Edelstein, L. C., and Gelinas, C. (2000). The Rel/NF-kappaB family directly activates expression of the apoptosis inhibitor Bcl-x(L). *Mol Cell. Biol.* **20**: 2687-95.

Chen, J., Fujii, K., Zhang, L., Roberts, T., and Fu, H. (2001). Raf-1 promotes cell survival by antagonizing apoptosis signal-regulating kinase 1 through a MEK-ERK independent mechanism. *Proc Natl Acad Sci U S A* **98**: 7783-8.

Chen, J., Kubalak, S. W., and Chien, K. R. (1998). Ventricular muscle-restricted targeting of the RXRα gene reveals a non-cell-autonomous requirement in cardiac chamber morphogenesis. *Development* **125**: 1943-1949.

Chen, R. H., Abate, C., and Blenis, J. (1993). Phosphorylation of the c-Fos transrepression domain by mitogen-activated protein kinase and 90-kDa ribosomal S6 kinase. *Proc Natl Acad Sci U S A* **90**: 10952-6.

Chen, R. H., Sarnecki, C., and Blenis, J. (1992). Nuclear localization and regulation of erk- and rsk-encoded protein kinases. *Mol Cell Biol* **12**: 915-27.

Chen, Z., Hagler, J., Palombella, V. J., Melandri, F., Scherer, D., Ballard, D., and Maniatis, T. (1995). Signal-induced site-specific phosphorylation targets I kappa B alpha to the ubiquitin-proteasome pathway. *Genes Dev* **9**: 1586-97.

Chiloeches, A., Mason, C. S., and Marais, R. (2001). S338 phosphorylation of Raf-1 is independent of phosphatidylinositol 3-kinase and Pak3. *Mol Cell Biol* **21**: 2423-34.

Chong, H., Lee, J., and Guan, K. L. (2001). Positive and negative regulation of Raf kinase activity and function by phosphorylation. *Embo J* **20**: 3716-27.

Chu, Z. L., McKinsey, T. A., Liu, L., Gentry, J. J., Malim, M. H., and Ballard, D. W. (1997). Suppression of tumor necrosis factor-induced cell death by inhibitor of apoptosis c-IAP2 is under NF-kappaB control. *Proc Natl Acad Sci U S A* **94**: 10057-62.

Chuang, E., Barnard, D., Hettich, L., Zhang, X. F., Avruch, J., and Marshall, M. S. (1994). Critical binding and regulatory interactions between Ras and Raf occur through a small, stable N-terminal domain of Raf and specific Ras effector residues. *Mol Cell Biol* **14**: 5318-25.

Clark, G. J., Drugan, J. K., Rossman, K. L., Carpenter, J. W., Rogers-Graham, K., Fu, H., Der, C. J., and Campbell, S. L. (1997). 14-3-3 zeta negatively regulates raf-1 activity by interactions with the Raf-1 cysteine-rich domain. *J Biol Chem* **272**: 20990-3.

Cleveland, J. L., Troppmair, J., Packham, G., Askew, D. S., Lloyd, P., Gonzalez-Garcia, M., Nunez, G., Ihle, J. N., and Rapp, U. R. (1994). v-raf suppresses apoptosis and promotes growth of interleukin-3-dependent myeloid cells. *Oncogene* **9**: 2217-26.

Cohen, G. M. (1997). Caspases: the executioners of apoptosis. *Biochem J* **326**: 1-16.

Collins, S., Caron, M. G., and Lefkowitz, R. J. (1992). From ligand binding to gene expression: new insights into the regulation of G-protein-coupled receptors. *Trends Biochem Sci* **17**: 37-9.

Cook, S. J., Rubinfeld, B., Albert, I., and McCormick, F. (1993). RapV12 antagonizes Ras-dependent activation of ERK1 and ERK2 by LPA and EGF

in Rat-1 fibroblasts. *EMBO J* **12**: 3475-85.

Countaway, J. L., Nairn, A. C., and Davis, R. J. (1992). Mechanism of desensitization of the epidermal growth factor receptor protein-tyrosine kinase. *J Biol Chem* **267**: 1129-40.

Cowley, S., Paterson, H., Kemp, P., and Marshall, C. J. (1994). Activation of MAP kinase kinase is necessary and sufficient for PC12 differentiation and for transformation of NIH 3T3 cells. *Cell* **77**: 841-52.

Crews, C. M., Alessandrini, A. A., and Erikson, R. L. (1991). Mouse Erk-1 gene product is a serine/threonine protein kinase that has the potential to phosphorylate tyrosine. *Proc Natl Acad Sci* **88**: 8845-9.

Crews, C. M., and Erikson, R. L. (1992). Purification of a murine protein-tyrosine/threonine kinase that phosphorylates and activates the Erk-1 gene product: relationship to the fission yeast byr1 gene product. *Proc Natl Acad Sci* **89**: 8205-9.

Currie, R. A., Walker, K. S., Gray, A., Deak, M., Casamayor, A., Downes, C. P., Cohen, P., Alessi, D. R., and Lucocq, J. (1999). Role of phosphatidylinositol 3,4,5-triphosphate in regulating the activity and localisation for 3-phosphoinositide-dependent protein kinase-1. *Biochem J* **337**: 575-83.

Cutler, R. E., Jr., Stephens, R. M., Saracino, M. R., and Morrison, D. K. (1998). Autoregulation of the Raf-1 serine/threonine kinase. *Proc Natl Acad Sci U S A* **95**: 9214-9.

Daniels, R. H., and Bokoch, G. M. (1999). p21 activated protein kinase: a crucial component of morphological signaling? *Trends Biochem Sci* **24**: 350-4.

Datta, S. R., Bellacosa, A., Chan, T. O., and Tsichlis, P. N. (1996). Akt is a direct target of the phosphatidylinositol 3-kinase. Activation by growth factors, v-src and v-Ha-ras, in Sf9 and mammalian cells. *J Biol Chem* **271**: 30835-9.

Datta, S. R., Dudek, H., Tao, X., Masters, S., Fu, H., Gotoh, Y., and Greenberg, M. E. (1997). Akt phosphorylation of BAD couples survival signals to the cell-intrinsic death machinery. *Cell* **91**: 231-41.

Daum, G., Eisenmann-Tappe, I., Fries, H. W., Troppmair, J., and Rapp, U. R. (1994). The ins and outs of Raf kinases. *Trends Biochem Sci* **19**: 474-80.

De Smaele, E., Zazzeroni, F., Papa, S., Nguyen, D. U., Jin, R., Jones, J., Cong, R., and Franzoso, G. (2001). Induction of gadd45beta by NF-kappaB downregulates pro-apoptotic signalling. *Nature* **414**: 308-13.

de Vries-Smits, A. M. M., Burgering, B. M. T., Leevers, S. J., Marshall, C. J., and Bos, J. L. (1992). Involvement of p21ras in activation of extracellular signal-regulated kinase 2. *Nature* **357**: 602-4.

Delhase, M., Hayakawa, M., Chen, Y., and Karin, M. (1999). Positive and negative regulation of IkB kinase activity through IKKb subunit phosphorylation. *Science* **284**: 309-13.

Dent, P., Haser, W., Haystead, T. A., Vincent, L. A., Roberts, T. M., and Sturgill, T. W. (1992). Activation of mitogen-activated protein kinase kinase by v-Raf in NIH 3T3 cells and in vitro. *Science* **257**: 1404-7.

Dent, P., and Sturgill, T. W. (1994). Activation of (His)6-Raf-1 in vitro by partially purified plasma membranes from v-Ras-transformed and serum-stimulated fibroblasts. *Proc Natl Acad Sci U S A* **91**: 9544-8.

Derijard, B., Hibi, M., Wu, I., Barrett, T., Su, B., Deng, T., Karin, M., and Davis, R. J. (1994). JNK1: a protein kinase stimulated by UV light and Ha-Ras that binds and phosphorylates the c-Jun activation domain. *Cell* **76**: 1025-37.

Derijard, B., Raingeaud, J., Barrett, T., Wu, I. H., Han, J., Ulevitch, R. J., and Davis, R. J. (1995). Independent human MAP-kinase signal transduction pathways defined by MEK and MKK isoforms. *Science* **267**: 682-5.

Dhillon, A. S., Meikle, S., Yazici, Z., Eulitz, M., and Kolch, W. (2002a). Regulation of Raf-1 activation and signalling by dephosphorylation. *EMBO J* **21**: 64-71.

Dhillon, A. S., Pollock, C., Steen, H., Shaw, P. E., Mischak, H., and Kolch, W. (2002b). Cyclic AMP-dependent kinase regulates Raf-1 kinase mainly by phosphorylation of serine 259. *Mol Cell Biol* **22**: 3237-46

Diaz, B., Barnard, D., Filson, A., MacDonald, S., King, A., and Marshall, M. (1997). Phosphorylation of Raf-1 serine 338-serine 339 is an essential regulatory event for Ras-dependent activation and biological signaling. *Mol Cell Biol* **17**: 4509-16.

Dickson, B., Sprenger, F., Morrison, D., and Hafen, E. (1992). Raf functions downstream of Ras1 in the Sevenless signal transduction pathway. *Nature* **360**: 600-3.

DiDonato, J. A., Hayakawa, M., Rothwarf, D. M., Zandi, E., and Karin, M. (1997). A cytokine-responsive IkB kinase that activates the transcription factor NFkB. *Nature* **388**: 548-54.

Dikic, I., Schlessinger, J., and Lax, I. (1994). PC12 cells overexpressing the insulin receptor undergo insulin-dependent neuronal differentiation. *Curr Biol* **4**: 702-8.

Downward, J. (1995). KSR: a novel player in the RAS pathway. *Cell* **83**: 831-4.

Drewes, G., Lichtenberg-Kraag, B., Doring, F., Mandelkow, E. M., Biernat, J., Goris, J., Doree, M., and Mandelkow, E. (1992). Mitogen activated protein (MAP) kinase transforms tau protein into an Alzheimer-like state. *EMBO J* **11**: 2131-8.

Drugan, J. K., Khosravi-Far, R., White, M. A., Der, C. J., Sung, Y. J., Hwang, Y. W., and Campbell, S. L. (1996). Ras interaction with two distinct binding domains in Raf-1 may be required for Ras transformation. *J Biol Chem* **271**: 233-7.

Erhardt, P., Schremser, E. J., and Cooper, G. M. (1999). B-Raf inhibits programmed cell death downstream of cytochrome c release from mitochondria by activating the MEK/Erk pathway. *Mol Cell Biol* **19**: 5308-15.

Esteban, L. M., Vicario-Abejon, C., Fernandez-Salguero, P., Fernandez-Medarde, A., Swaminathan, N., Yienger, K., Lopez, E., Malumbres, M., McKay, R., Ward, J. M., Pellicer, A., and Santos, E. (2001). Targeted genomic disruption of H-ras and N-ras, individually or in combination, reveals the dispensability of both loci for mouse growth and development. *Mol Cell Biol* **21**: 1444-52.

Evans, M. J., and Kaufman, M. H. (1981). Establishment in culture of pluripotential cells from mouse embryos. *Nature* **292**: 154-6.

Fabian, J. R., Daar, I. O., and Morrison, D. K. (1993). Critical tyrosine residues regulate the enzymatic and biological activity of Raf-1 kinase. *Mol Cell Biol* **13**: 7170-9.

Fantl, W. J., Muslin, A. J., Kikuchi, A., Martin, J. A., MacNicol, A. M., Gross, R. W., and Williams, L. T. (1994). Activation of Raf-1 by 14-3-3 proteins. *Nature* **371**: 612-4.

Farrar, M. A., Alberol, I., and Perlmutter, R. M. (1996). Activation of the Raf-1 kinase cascade by coumermycin-induced dimerization. *Nature* **383**: 178-81.

Feil, R., Brocard, J., Mascrez, B., LeMeur, M., Metzger, D., and Chambon, P. (1996). Ligand-activated site-specific recombination in mice. *Proc Natl Acad Sci U S A* **93**: 10887-10890.

Feramisco, J. R., Gross, M., Kamata, T., Rosenberg, M., and Sweet, R. W. (1984). Microinjection of the oncogene form of the human H-ras (T-24) protein results in rapid proliferation of quiescent cells. *Cell* **38**: 109-17.

Freed, E., Symons, M., Macdonald, S. G., McCormick, F., and Ruggieri, R. (1994). Binding of 14-3-3 proteins to the protein kinase Raf and effects on its activation. *Science* **265**: 1713-6.

Fu, H., Xia, K., Pallas, D. C., Cui, C., Conroy, K., Narsimhan, R. P., Mamon, H., Collier, R. J., and Roberts, T. M. (1994). Interaction of the protein kinase Raf-1 with 14-3-3 proteins. *Science* **266**: 126-9.

Galaktionov, K., Jessus, C., and Beach, D. (1995). Raf1 interaction with Cdc25 phosphatase ties mitogenic signal transduction to cell cycle activation. *Genes Dev* **9**: 1046-58.

Galcheva-Gargova, Z., Derijard, B., Wu, I., and Davis, R. J. (1994). An osmosensing signal transduction pathway in mammalian cells. *Science* **265**: 806-8.

Gartner, A., Nasmyth, K., and Ammerer, G. (1992). Signal transduction in Saccharomyces cerevisiae requires tyrosine and threonine phosphorylation of FUS3 and KSS1. *Genes Dev* **6**: 1280-92.

Gerwins, P., Blank, J. L., and Johnson, G. L. (1997). Cloning of a novel mitogen-activated protein kinase kinase kinase, MEKK4, that selectively regulates the c-Jun amino terminal kinase pathway. *J Biol Chem* **272**: 8288-95.

Ghosh, S., Xie, W. Q., Quest, A. F., Mabrouk, G. M., Strum, J. C., and Bell, R. M. (1994). The cysteine-rich region of raf-1 kinase contains zinc, translocates to liposomes, and is adjacent to a segment that binds GTP-ras. *J Biol Chem* **269**: 10000-7.

Gille, H., Sharrocks, A. D., and Shaw, P. E. (1992). Phosphorylation of transcription factor p62TCF by MAP kinase stimulates ternary complex formation at c-fos promoter. *Nature* **358**: 414-7.

Giroux, S., Tremblay, M., Bernard, D., Cadrin-Girard, J. F., Aubry, S., Larouche, L., Rousseau, S., Huot, J., Landry, J., Jeanotte, L., and Charron, J. (1999). Embryonic death of Mek1-deficient mice reveals a role for this kinase in angiogenesis in the labrinthe region of the placenta. *Curr Biol* **9**: 369-72.

Glading, A., Chang, P., Lauffenburger, D. A., and Wells, A. (2000). Epidermal growth factor receptor activation of calpain is required for fibroblast motility and occurs via an ERK/MAP kinase signaling pathway. *J Biol Chem* **275**: 2390-8.

Grammatikakis, N., Lin, J. H., Grammatikakis, A., Tsichlis, P. N., and Cochran, B. H. (1999). p50(cdc37) acting in concert with Hsp90 is required for Raf-1 function. *Mol Cell Biol* **19**: 1661-72.

Gray, T. A., Azama, K., Whitmore, K., Min, A., Abe, S., and Nicholls, R. D. (2001). Phylogenetic conservation of the makorin-2 gene, encoding a multiple zinc-finger protein, antisense to the RAF1 proto-oncogene. *Genomics* **77**: 119-26.

Green, D. R., and Reed, J. C. (1998). Mitochondria and apoptosis. *Science* **281**: 1309-12.

Greene, L. A., and Tischler, A. S. (1976). Establishment of a noradrenergic clonal line of rat adrenal pheochromocytoma cells which respond to nerve growth factor. *Proc Natl Acad Sci* **73**: 2424-8.

Gross, A., McDonnell, J. M., and Korsmeyer, S. J. (1999). BCL-2 family members and the mitochondria in apoptosis. *Genes Dev* **13**: 1899-911.

Gu, H., Marth, J. D., Orban, P. C., Mossmann, H., and Rajewsky, K. (1994). Deletion of a polymerase B gene segment in T cells using cell type-specific gene targeting. *Science* **265**: 103-106.

Gu, H., Zou, Y. R., and Rajewsky, K. (1993). Independent control of immunoglobulin switch recombination at individual switch regions evidenced through Cre-loxP-mediated gene targeting. *Cell* **73**: 1155-64.

Guan, K. L., Figueroa, C., Brtva, T. R., Zhu, T., Taylor, J., Barber, T. D., and Vojtek, A. B. (2000). Negative regulation of the serine/threonine kinase B-Raf by Akt. *J Biol Chem* **275**: 27354-9.

Gupta, S., Campbell, D., Derijard, B., and Davis, R. J. (1995). Transcription factor ATF2 regulation by the JNK signal transduction family. *Science* **267**: 389-93.

Gupta, S., Seth, A., and Davis, R. J. (1993). Transactivation of gene expression by Myc is inhibited by mutation at the phosphorylation sites Thr-58 and Ser-62. *Proc Natl Acad Sci* **90**: 3216-20.

Hafner, S., Adler, H. S., Mischak, H., Janosch, P., Heidecker, G., Wolfman, A., Pippig, S., Lohse, M., Ueffing, M., and Kolch, W. (1994). Mechanism of inhibition of Raf-1 by protein kinase A. *Mol Cell Biol* **14**: 6696-703.

Hagemann, C., Kalmes, A., Wixler, V., Wixler, L., Schuster, T., and Rapp, U. R. (1997). The regulatory subunit of protein kinase CK2 is a specific A-Raf activator. *FEBS Lett* **403**: 200-2.

Hallberg, B., Rayter, S. I., and Downward, J. (1994). Interaction of Ras and Raf in intact mammalian cells upon extracellular stimulation. *J Biol Chem* **269**: 3913-6.

Han, J., Jiang, Y., Li, Z., Kravchenko, V., and Ulevitch, R. J. (1997). Activation of the transcription factor MEF2C by the MAP kinase p38 in inflammation. *Nature* **386**: 296-9.

Han, J., Lee, J. D., Bibbs, L., and Ulevitch, R. J. (1994). A MAP kinase targeted by endotoxin and hyperosmolarity in mammalian cells. *Science* **265**: 808-11.

Han, J., Lee, J. D., Jiang, Y., Li, Z., Feng, L., and Ulevitch, R. J. (1996). Characterization of the structure and function of a novel MAP kinase kinase (MKK6). *J Biol Chem* **271**: 2886-91.

Han, M., Golden, A., Han, Y., and Sternberg, P. W. (1993). C. elegans lin-45 raf gene participates in let-60 ras-stimulated vulval differentiation. *Nature* **363**: 133-40.

Harbour, J. W., Luo, R. X., Dei Santi, A., Postigo, A. A., and Dean, D. C. (1999). Cdk phosphorylation triggers sequential intramolecular interactions that progressively block Rb functions as cells move through G1. *Cell* **98**: 859-69.

Hatai, T., Matsuzawa, A., Inoshita, S., Mochida, Y., Kuroda, T., Sakamaki, K., Kuida, K., Yonehara, S., Ichijo, H., and Takeda, K. (2000). Execution of apoptosis signal-regulating kinase 1 (ASK1)-induced apoptosis by the mitochondria-dependent caspase activation. *J Biol Chem* **275**: 26576-81.

Haupt, Y., Maya, R., Kazaz, A., and Oren, M. (1997). Mdm2 promotes the rapid degradation of p53. *Nature* **387**: 296-9.

Hawkins, P. T., Eguinoa, A., Qui, R.-G., Stokoe, D., Cooke, F. T., Walters, R., Wennstrom, S., Claesoon-Welsh, L., Evans, T., Symons, M., and Stephens, L. (1995). PDGF stimulates an increase in GTP-Rac via activation of phosphoinositide 3-kinase. *Curr Biol* **5**: 393-403.

Heidecker, G., Huleihel, M., Cleveland, J. L., Kolch, W., Beck, T. W., Lloyd, P., Pawson, T., and Rapp, U. R. (1990). Mutational activation of c-raf-1 and definition of the minimal transforming sequence. *Mol Cell Biol* **10**: 2503-12.

Heldin, C.-H. (1995). Dimerisation of cell surface receptors in signal transduction. *Cell* **80**: 213-23.

Hiles, I. D., Otsu, M., Volinia, S., Fry, M. J., Gout, I., Dhand, R., Panayotou, G., Ruiz-Larrea, F., Thompson, A., and Totty, N. F. (1992). Phosphatidylinositol 3-kinase: structure and expression of the 110 kd catalytic subunit. *Cell* **70**: 419-29.

Hoess, R. H., and Abremski, K. (1984). Interaction of the bacteriophage P1 recombinase Cre with the recombining site loxP. *Proc Natl Acad Sci U S A* **81**: 1026-9.

Hoess, R. H., and Sternberg, N. (1982). P1 site-specific recombination: nucleotide sequence of the recombining sites. *Proc Natl Acad Sci* **79**: 3398-402.

Hollstein, M., Sidransky, D., Vogelstein, B., and Harris, C. C. (1991). p53 mutations in human cancers. *Science* **253**: 49-53.

Hooper, M., Hardy, K., Handyside, A., Hunter, S., and Monk, M. (1987). HPRT-deficient (Lesch-Nyhan) mouse embryos derived from germline colonisation by cultured cells. *Nature* **326**: 292-5.

Howe, L. R., Leevers, S. J., Gomez, N., Nakielny, S., Cohen, P., and Marshall, C. J. (1992). Activation of the MAP kinase pathway by the protein kinase raf. *Cell* **71**: 335-42.

Hu, C. D., Kariya, K., Tamada, M., Akasaka, K., Shirouzu, M., Yokoyama, S., and Kataoka, T. (1995). Cysteine-rich region of Raf-1 interacts with activator domain of post-translationally modified Ha-Ras. *J Biol Chem* **270**: 30274-7.

Huff, K., End, D., and Guroff, G. (1981). Nerve growth factor-induced alteration in the response of PC12 pheochromocytoma cells to epidermal growth factor. *J Cell Biol* **88**: 189-98.

Hughes, P. E., Renshaw, M. W., Pfaff, M., Forsyth, J., Keivens, V. M., Schwartz, M. A., and Ginsberg, M. H. (1997). Suppression of integrin activation: a novel function of a Ras/Raf-initiated MAP kinase pathway. *Cell* **88**: 521-30.

Huleihel, M., Goldsborough, M., Cleveland, J., Gunnell, M., Bonner, T., and Rapp, U. R. (1986). Characterization of murine A-raf, a new oncogene related to the v-raf oncogene. *Mol Cell Biol* **6**: 2655-62.

Huser, M., Luckett, J., Chiloeches, A., Mercer, K., Iwobi, M., Giblett, S., Sun, X. M., Brown, J., Marais, R., and Pritchard, C. (2001). MEK kinase activity is not necessary for Raf-1 function. *Embo J* **20**: 1940-51.

Ichijo, H., Nishida, E., Irie, K., ten Dijke, P., Saitoh, M., Moriguchi, T., Takagi, M., Matsumoto, K., Miyazono, K., and Gotoh, Y. (1997). Induction of apoptosis by ASK1, a mammalian MAPKKK that activates SAPK/JNK and p38 signaling pathways. *Science* **275**: 90-4.

Ikawa, S., Fukui, M., Ueyama, Y., Tamaoki, N., Yamamoto, T., and Toyoshima, K. (1988). B-raf, a new member of the raf family, is activated by DNA rearrangement. *Mol Cell Biol* **8**: 2651-4.

Irie, K., Gotoh, Y., Yashar, B. M., Errede, B., Nishida, E., and Matsumoto, K. (1994). Stimulatory effects of yeast and mammalian 14-3-3 proteins on the Raf protein kinase. *Science* **265**: 1716-9.

Ise, K., Nakamura, K., Nakao, K., Shimizu, S., Harada, H., Ichise, T., Miyoshi, J., Gondo, Y., Ishikawa, T., Aiba, A., and Katsuki, M. (2000). Targeted deletion of the H-ras gene decreases tumor formation in mouse skin carcinogenesis. *Oncogene* **15**: 2951-6.

Jackson, E. L., Willis, N., Mercer, K., Bronson, R. T., Crowley, D., Montoya, R., Jacks, T., and Tuveson, D. A. (2001). Analysis of lung tumor initiation and progression using conditional expression of oncogenic K-ras. *Genes Dev* **15**: 3243-8.

Jaiswal, R. K., Moodie, S. A., Wolfman, A., and Landreth, G. E. (1994). The mitogen-activated protein kinase cascade is activated by B-Raf in response to nerve growth factor through interaction with p21ras. *Mol Cell Biol* **14**: 6944-53.

Jaiswal, R. K., Weissinger, E., Kolch, W., and Landreth, G. E. (1996). Nerve growth factor-mediated activation of the mitogen-activated protein (MAP) kinase cascade

involves a signaling complex containing B-Raf and HSP90. *J Biol Chem* **271**: 23626-9.

Jat, P. S., and Sharp, P. A. (1989). Cell lines established by a temperature-sensitive simian virus40 large-T-antigen gene are growth restricted at the non-permissive temperature. *Mol Cell Biol* **9**: 1672-81.

Jesenberger, V., Procyk, K. J., Ruth, J., Schreiber, M., Theussl, H. C., Wagner, E. F., and Baccarini, M. (2001). Protective role of Raf-1 in Salmonella-induced macrophage apoptosis. *J Exp Med* **193**: 353-64.

Jiang, G., and Hunter, T. (1999). Receptor signaling: when dimerization is not enough. *Curr Biol* **9**: R568-71.

Jiang, Y., Chen, C., Li, Z., Guo, W., Gegner, J. A., Lin, S., and Han, J. (1996). Characterization of the structure and function of a new mitogen-activated protein kinase (p38beta). *J Biol Chem* **271**: 17920-6.

Johnson, L., Greenbaum, D., Cichowski, K., Mercer, K., Murphy, E., Schmitt, E., Bronson, R. T., Umanoff, H., Edelmann, W., Kucherlapati, R., and Jacks, T. (1997). K-ras is an essential gene in the mouse with partial functional overlap with N-ras. *Genes Dev* **11**: 2468-81.

Jove, R., and Hanafusa, H. (1987). Cell transformation by the viral src oncogene. *Annu Rev Cell Biol* **3**: 31-56.

Joyner, A. L. (1999). "Gene Targeting - A Practical Approach." Oxford University Press, Oxford, UK.

Karin, M. (1995). The regulation of AP-1 activity by mitogen-activated protein kinases. *J Biol Chem* **270**: 16483-6.

Kasibhatla, S., Brunner, T., Genestier, L., Echeverri, F., Mahboubi, A., and Green, D. R. (1998). DNA damaging agents induce expression of Fas ligand and subsequent apoptosis in T lymphocytes via the activation of NF-kappa B and AP-1. *Mol Cell* **1**: 543-51.

Kato, J., Matsushime, H., Hiebert, S. W., Ewen, M. E., and Sherr, C. J. (1993). Direct binding of cyclin D to the retinoblastoma gene product (pRb) and pRb phosphorylation by the cyclin D-dependent kinase CDK4. *Genes Dev* **7**: 331-42.

Kato, Y., Kravchenko, V., Tapping, R. I., Han, J., Ulevitch, R. J., and Lee, J. D. (1997). BMK1/ERK5 regulates serum-induced early gene expression through transcription factor MEF2C. *EMBO J* **16**: 7054-66.

Kauffmann-Zeh, A., Rodriguez-Viciana, P., Ulrich, E., Gilbert, C., Coffer, P., Downward, J., and Evan, G. (1997). Suppression of c-Myc-induced apoptosis by Ras signalling through PI(3)K and PKB. *Nature* **385**: 544-8.

Kaufmann, S. H., and Earnshaw, W. C. (2000). Induction of apoptosis by cancer chemotherapy. *Exp Cell Res* **256**: 42-9.

Kavanaugh, W. M., Turck , C. W., and Williams, L. T. (1995). PTB domain binding to signaling proteins through a sequence motif containing phosphotyrosine. *Science* **268**: 1177-9.

Kimura, Y., Rutherford, S. L., Miyata, Y., Yahara, I., Freeman, B. C., Yue, L., Morimoto, R. I., and Lindquist, S. (1997). Cdc37 is a molecular chaperone with specific functions in signal transduction. *Genes Dev* **11**: 1775-85.

King, A. J., Sun, H., Diaz, B., Barnard, D., Miao, W., Bagrodia, S., and Marshall, M. S. (1998). The protein kinase Pak3 positively regulates Raf-1 activity through phosphorylation of serine 338. *Nature* **396**: 180-3.

Klemke, R. L., Cai, S., Giannini, A. L., Gallagher, P. J., de Lanerolle, P., and Cheresh, D. A. (1997). Regulation of cell motility by mitogen-activated protein kinase. *J Cell Biol* **137**: 481-92.

Kluck, R. M., Bossy-Wetzel, E., Green, D. R., and Newmeyer, D. D. (1997). The release of cytochrome c from mitochondria: a primary site for Bcl-2 regulation of apoptosis. *Science* **275**: 1132-36.

Koide, H., Satoh, T., Nakafuku, M., and Kaziro, Y. (1993). GTP-dependent association of Raf-1 with Ha-Ras: identification of Raf as a target downstream of Ras in mammalian cells. *Proc Natl Acad Sci U S A* **90**: 8683-6.

Kolch, W. (2000). Meaningful relationships: the regulation of the Ras/Raf/MEK/ERK pathway by protein interactions. *Biochem J* **351 Pt 2**: 289-305.

Kolch, W., Heidecker, G., Kochs, G., Hummel, R., Vahidi, H., Mischak, H., Finkenzeller, G., Marme, D., and Rapp, U. R. (1993). Protein kinase C alpha activates RAF-1 by direct phosphorylation. *Nature* **364**: 249-52.

Kolch, W., Heidecker, G., Lloyd, P., and Rapp, U. R. (1991). Raf-1 protein kinase is required for growth of induced NIH/3T3 cells. *Nature* **349**: 426-8.

Kornfeld, K., Hom, D. B., and Horvitz, H. R. (1995). The ksr-1 gene encodes a novel protein kinase involved in Ras-mediated signaling in C. elegans. *Cell* **83**: 903-13.

Kubbutat, M. H., Jones, S. N., and Vousden, K. H. (1997). Regulation of p53 stability by Mdm2. *Nature* **387**: 299-303.

Kuehn, M. R., Bradley, A., Robertson, E. J., and Evans, M. J. (1987). A potential animal model for Lesch-Nyhan syndrome though introduction of HPRT mutations into mice. *Nature* **326**: 295-8.

Kuhn, R., Schwenk, F., Aguet, M., and Rajewsky, K. (1995). Inducible gene targeting in mice. *Science* **269**: 1427-1429.

Kyriakis, J. M., App, H., Zhang, X. F., Banerjee, P., Brautigan, D. L., Rapp, U. R., and Avruch, J. (1992). Raf-1 activates MAP kinase-kinase. *Nature* **358**: 417-21.

Lakin, N. D., and Jackson, S. P. (1999). Regulation of p53 in response to DNA damage. *Oncogene* **18**: 7644-55.

Lange-Carter, C. A., Pleiman, C. M., Gardner, A. M., Blumer, K. J., and Johnson, G. L. (1993). A divergence in the MAP kinase regulatory network defined by MEK kinase and Raf. *Science* **260**: 315-9.

Larue, L., Ohsugi, M., Hirchenhain, J., and Kemler, R. (1994). E-cadherin null mutant embryos fail to form a trophectoderm epithelium. *Proc Natl Acad Sci U S A* **91**: 8263-7.

Le Gall, M., Chambard, J. C., Breittmayer, J. P., Grall, D., Pouyssegur, J., and Van Obberghen-Schilling, E. (2000). The p42/p44 MAP kinase pathway prevents apoptosis induced by anchorage and serum removal. *Mol Biol Cell* **11**: 1103-12.

Lee, F. S., Peters, R. T., Dang, L. C., and Maniatis, T. (1998). MEKK1 activates both IkappaB kinase alpha and IkappaB kinase beta. *Proc Natl Acad Sci U S A* **95**: 9319-24.

Lee, J. C., Laydon, J. T., McDonnell, P. C., Gallagher, T. F., Kumar, S., Green, D., McNulty, D., Blumenthal, M. J., Heys, J. R., Landvatter, S. W., and al., e. (1994). A protein kinase involved in the regulation of inflammatory cytokine biosynthesis. *Nature* **372**: 739-46.

Lee, R. M., Cobb, M. H., and Blackshear, P. J. (1992). Evidence that extracellular signal-regulated kinases are the insulin-activated Raf-1 kinase kinases. *J Biol Chem* **267**: 1088-92.

Leevers, S. J., and Marshall, C. J. (1992). Activation of extracellular signal-regulated kinase, ERK2, by p21ras oncoprotein. *Embo J* **11**: 569-74.

Leevers, S. J., Paterson, H. F., and Marshall, C. J. (1994). Requirement for Ras in Raf activation is overcome by targeting Raf to the plasma membrane. *Nature* **369**: 411-4.

Lemmon, M. A., and Schlessinger, J. (1994). Regulation of signal transduction and signal diversity by receptor oligomerization. *Trends Biochem Sci* **19**: 459-63.

Li, H., Zhu, H., Xu, C. J., and Yuan, J. (1998). Cleavage of BID by caspase 8 mediates the mitochondrial damage in the Fas pathway of apoptosis. *Cell* **94**: 491-501.

Li, P., Nijhawan, D., Budihardjo, I., Srinivasula, S. M., Ahmad, M., Alnemri, E. S., and Wang, X. (1997). Cytochrome c and dATP-dependent formation of Apaf-1/caspase-9 complex initiates an apoptotic protease cascade. *Cell* **91**: 479-89.

Li, S., and Sedivy, J. M. (1993). Raf-1 protein kinase activates the NF-kappa B transcription factor by dissociating the cytoplasmic NF-kappa B-I kappa B complex. *Proc Natl Acad Sci U S A* **90**: 9247-51.

Li, W., Han, M., and Guan, K. L. (2000). The leucine-rich repeat protein SUR-8 enhances MAP kinase activation and forms a complex with Ras and Raf. *Genes Dev* **14**: 895-900.

Li, W., Nishimura, R., Kashishian, A., Batzer, A. G., Kim, W. J., Cooper, J. A., and Schlessinger, J. (1994). A new function for a phosphotyrosine phosphatase: linking GRB2-Sos to a receptor tyrosine kinase. *Mol Cell Biol* **14**: 509-17.

Lin, A., Minden, A., Martinetto, H., Claret, F. X., Lange-Carter, C., Mercurio, F., Johnson, G. L., and Karin, M. (1995). Identification of a dual specificity kinase that activates the Jun kinases and p38-Mpk2. *Science* **268**: 286-90.

Lin, L. L., Wartmann, M., Lin, A. Y., Knopf, J. L., Seth, A., and Davis, R. J. (1993). cPLA2 is phosphorylated and activated by MAP kinase. *Cell* **72**: 269-78.

Ling, L., Cao, Z., and Goeddel, D. V. (1998). NF-kappaB-inducing kinase activates IKK-alpha by phosphorylation of Ser-176. *Proc Natl Acad Sci U S A* **95**: 3792-7.

Liscovitch, M. (1992). Crosstalk among multiple signal-activated phospholipases. *Trends Biochem Sci* **17**: 393-9.

Liu, H., Nishitoh, H., Ichijo, H., and Kyriakis, J. M. (2000). Activation of apoptosis signal-regulating kinase 1 (ASK1) by tumor necrosis factor receptor-associated factor 2 requires prior dissociation of the ASK1 inhibitor thioredoxin. *Mol Cell Biol* **20**: 2198-208.

Lowy, D. R., Zhang, K., DeClue, J. E., and Willumsen, B. M. (1991). Regulation of p21ras activity. *Trends Genet* **7**: 346-51.

Luckett, J. C., Huser, M. B., Giagtzoglou, N., Brown, J. E., and Pritchard, C. A. (2000). Expression of the A-raf proto-oncogene in the normal adult and embryonic mouse. *Cell Growth Differ* **11**: 163-71.

Luo, Z., Diaz, B., Marshall, M. S., and Avruch, J. (1997). An intact Raf zinc finger is required for optimal binding to processed Ras and for ras-dependent Raf activation in situ. *Mol Cell Biol* **17**: 46-53.

Luo, Z., Tzivion, G., Belshaw, P. J., Vavvas, D., Marshall, M., and Avruch, J. (1996). Oligomerization activates c-Raf-1 through a Ras-dependent mechanism. *Nature* **383**: 181-5.

MacNicol, A. M., Muslin, A. J., and Williams, L. T. (1993). Raf-1 kinase is essential for early Xenopus development and mediates the induction of mesoderm by FGF. *Cell* **73**: 571-83.

Majewski, M., Nieborowska-Skorska, M., Salomoni, P., Slupianek, A., Reiss, K., Trotta, R., Calabretta, B., and Skorski, T. (1999). Activation of mitochondrial Raf-1 is involved in the antiapoptotic effects of Akt. *Cancer Res* **59**: 2815-9.

Mansour, S. L., Thomas, K. R., and Capecchi, M. R. (1988). Disruption of the proto-oncogene int-2 in mouse embryo-derived stem cells: a general strategy for targeting mutations to non-selectable genes. *Nature* **336**: 348-52.

Marais, R., Light, Y., Mason, C., Paterson, H., Olson, M. F., and Marshall, C. J. (1998). Requirement of Ras-GTP-Raf complexes for activation of Raf-1 by protein kinase C. *Science* **280**: 109-12.

Marais, R., Light, Y., Paterson, H. F., and Marshall, C. J. (1995). Ras recruits Raf-1 to the plasma membrane for activation by tyrosine phosphorylation. *Embo J* **14**: 3136-45.

Marais, R., Light, Y., Paterson, H. F., Mason, C. S., and Marshall, C. J. (1997). Differential regulation of Raf-1, A-Raf, and B-Raf by oncogenic ras and tyrosine kinases. *J Biol Chem* **272**: 4378-83.

Marais, R., Wynne, J., and Treisman, R. (1993). The SRF accessory protein Elk-1 contains a growth factor-regulated transcriptional activation domain. *Cell* **73**: 381-93.

Marinissen, M. J., Chiariello, M., Pallante, M., and Gutkind, J. S. (1999). A network of mitogen-activated protein kinases links G protein-coupled receptors to the c-jun promoter: a role for c-Jun NH2-terminal kinase, p38s, and extracellular signal-regulated kinase 5. *Mol Cell Biol* **19**: 4289-301.

Martin, G. R. (1981). Isolation of a pluripotent cell line from early mouse embryos cultured in medium conditioned by teratocarcinoma stem cells. *Proc Natl Acad Sci U S A* **78**: 7634-8.

Marx, M., Eychene, A., Laugier, D., Bechade, C., Crisanti, P., Dezelee, P., Pessac, B., and Calothy, G. (1988). A novel oncogene related to c-mil is transduced in chicken neuroretina cells induced to proliferate by infection with an avian lymphomatosis virus. *EMBO J* **7**: 3369-73.

Mason, C. S., Springer, C. J., Cooper, R. G., Superti-Furga, G., Marshall, C. J., and Marais, R. (1999). Serine and tyrosine phosphorylations cooperate in Raf-1, but not B-Raf activation. *Embo J* **18**: 2137-48.

Matsuda, M., Hashimoto, Y., Muroya, K., Hasegawa, H., Kurata, T., Tanaka, S., Nakamura, S., and Hattori, S. (1994). CRK protein binds to two guanine nucleotide-releasing proteins for the Ras family and modulates nerve growth factor-induced activation of Ras in PC12 cells. *Mol Cell Biol* **14**: 5495-500.

Matsuda, S., Gotoh, Y., and Nishida, E. (1993). Phosphorylation of Xenopus mitogen-activated protein (MAP) kinase kinase by MAP kinase kinase kinase and MAP kinase. *J Biol Chem* **268**: 3277-81.

Matsuda, S., Kosako, H., Takenaka, K., Moriyama, K., Sakai, H., Akiyama, T., Gotoh, Y., and Nishida, E. (1992). Xenopus MAP kinase activator: identification and function as a key intermediate in the phosphorylation cascade. *EMBO J* **11**: 973-82.

McCarthy, S. A., Chen, D., Yang, B. S., Garcia Ramirez, J. J., Cherwinski, H., Chen, X. R., Klagsbrun, M., Hauser, C. A., Ostrowski, M. C., and McMahon, M. (1997). Rapid phosphorylation of Ets-2 accompanies mitogen-activated protein kinase

activation and the induction of heparin-binding epidermal growth factor gene expression by oncogenic Raf-1. *Mol Cell Biol* **17**: 2401-12.

McCarthy, S. A., Samuels, M. L., Pritchard, C. A., Abraham, J. A., and McMahon, M. (1995). Rapid induction of heparin-binding epidermal growth factor/diphtheria toxin receptor expression by Raf and Ras oncogenes. *Genes Dev* **9**: 1953-64.

Mercer, K., Chiloeches, A., Hueser, M., Kiernan, M., Marais, R., and Pritchard, C. (2002). ERK signalling and oncogene transformation are not impaired in cells lacking A-Raf. *Oncogene* **21**: 347-55.

Meuwissen, R., Linn, S. C., van der Valk, M., Mooi, W. J., and Berns, A. (2001). Mouse model for lung tumorigenesis through Cre/lox controlled sporadic activation of the K-Ras oncogene. *Oncogene* **20**: 6551-8.

Michaud, N. R., Fabian, J. R., Mathes, K. D., and Morrison, D. K. (1995). 14-3-3 is not essential for Raf-1 function: identification of Raf-1 proteins that are biologically activated in a 14-3-3- and Ras-independent manner. *Mol Cell Biol* **15**: 3390-7.

Michaud, N. R., Therrien, M., Cacace, A., Edsall, L. C., Spiegel, S., Rubin, G. M., and Morrison, D. K. (1997). KSR stimulates Raf-1 activity in a kinase-independent manner. *Proc Natl Acad Sci U S A* **94**: 12792-6.

Mikula, M., Schreiber, M., Husak, Z., Kucerova, L., Ruth, J., Wieser, R., Zatloukal, K., Beug, H., Wagner, E. F., and Baccarini, M. (2001). Embryonic lethality and fetal liver apoptosis in mice lacking the c-raf-1 gene. *Embo J* **20**: 1952-62.

Miltenberger, R. J., Cortner, J., and Farnham, P. J. (1993). An inhibitory Raf-1 mutant suppresses expression of a subset of v-raf-activated genes. *J Biol Chem* **268**: 15674-80.

Mineo, C., Anderson, R. G., and White, M. A. (1997). Physical association with ras enhances activation of membrane-bound raf (RafCAAX). *J Biol Chem* **272**: 10345-8.

Mischak, H., Seitz, T., Janosch, P., Eulitz, M., Steen, H., Schellerer, M., Philipp, A., and Kolch, W. (1996). Negative regulation of Raf-1 by phosphorylation of serine 621. *Mol Cell Biol* **16**: 5409-18.

Momand, J., Zambetti, G. P., Olson, D. C., George, D., and Levine, A. J. (1992). The mdm-2 oncogene product forms a complex with the p53 protein and inhibits p53-mediated transactivation. *Cell* **69**: 1237-45.

Monkley, S. J., Zhou, X. H., Kinston, S. J., Giblett, S. M., Hemmings, L., Priddle, H., Brown, J. E., Pritchard, C. A., Critchley, D. R., and Fassler, R. (2000). Disruption of the talin gene arrests mouse development at the gastrulation stage. *Dev Dyn* **219**: 560-74.

Moodie, S. A., Paris, M. J., Kolch, W., and Wolfman, A. (1994). Association of MEK1 with p21ras.GMPPNP is dependent on B-Raf. *Mol Cell Biol* **14**: 7153-62.

Moriguchi, T., Kuroyanagi, N., Yamaguchi, K., Gotoh, Y., Irie, K., Kano, T., Shirakabe, K., Muro, Y., Shibuya, H., Matsumoto, K., Nishida, E., and Hagiwara, M. (1996). A novel kinase cascade mediated by mitogen-activated protein kinase kinase 6 and MKK3. *J Biol Chem* **271**: 13675-9.

Morrison, D. K. (1995). Mechanisms regulating Raf-1 activity in signal transduction pathways. *Mol Reprod Dev* **42**: 507-14.

Morrison, D. K., and Cutler, R. E. (1997). The complexity of Raf-1 regulation. *Curr Opin Cell Biol* **9**: 174-9.

Morrison, D. K., Heidecker, G., Rapp, U. R., and Copeland, T. D. (1993). Identification of the major phosphorylation sites of the Raf-1 kinase. *J Biol Chem* **268**: 17309-16.

Morrison, D. K., Kaplan, D. R., Rapp, U., and Roberts, T. M. (1988). Signal transduction from membrane to cytoplasm: growth factors and membrane-bound oncogene products increase Raf-1 phosphorylation and associated protein kinase activity. *Proc Natl Acad Sci U S A* **85**: 8855-9.

Mott, H. R., Carpenter, J. W., Zhong, S., Ghosh, S., Bell, R. M., and Campbell, S. L. (1996). The solution structure of the Raf-1 cysteine-rich domain: a novel ras and phospholipid binding site. *Proc Natl Acad Sci U S A* **93**: 8312-7.

Murai, H., Ikeda, M., Kishida, S., Ishida, O., Okazaki-Kishida, M., Matsuura, Y., and Kikuchi, A. (1997). Characterization of Ral GDP dissociation stimulator-like (RGL) activities to regulate c-fos promoter and the GDP/GTP exchange of Ral. *J Biol Chem* **272**: 10483-90.

Nakajima, T., Kinoshita, S., Sasagawa, T., Sasaki, K., Naruto, M., Kishimoto, T., and Akira, S. (1993). Phosphorylation at threonine-235 by a ras-dependent mitogen-activated protein kinase cascade is essential for transcription factor NF-IL6. *Proc Natl Acad Sci* **90**: 2207-11.

Nakano, H., Shindo, M., Sakon, S., Nishinaka, S., Mihara, M., Yagita, H., and Okumura, K. (1998). Differential regulation of IkappaB kinase alpha and beta by two upstream kinases, NF-kappaB-inducing kinase and mitogen-activated protein kinase/ERK kinase kinase-1. *Proc Natl Acad Sci U S A* **95**: 3537-42.

Nakielny, S., Cohen, P., Wu, J., and Sturgill, T. (1992). MAP kinase activator from insulin-stimulated skeletal muscle is a protein threonine/tyrosine kinase. *EMBO J* **11**: 2123-9.

Nantel, A., Huber, M., and Thomas, D. Y. (1999). Localization of endogenous Grb10 to the mitochondria and its interaction with the mitochondrial-associated Raf-1 pool. *J Biol Chem* **274**: 35719-24.

Nebreda, A. R., and Gavin, A.-C. (1999). Cell survival demands some rsk. *Science* **286**: 1309-10.

Nebreda, A. R., and Porras, A. (2000). p38 MAP kinases: beyond the stress response. *TIBS* **25**: 257-60.

Nemenoff, R. A., Winitz, S., Qian, N. X., Van Putten, V., Johnson, G. L., and Heasley, L. E. (1993). Phosphorylation and activation of a high molecular weight form of phospholipase A2 by p42 microtubule-associated protein 2 kinase and protein kinase C. *J Biol Chem* **268**: 1960-4.

Nevins, J. R. (1992). E2F: a link between the Rb tumor suppressor protein and viral oncoproteins. *Science* **258**: 424-9.

Nguyen, T. T., Scimeca, J. C., Filloux, C., Peraldi, P., Carpentier, J. L., and Van Obberghen, E. (1993). Co-regulation of the mitogen-activated protein kinase, extracellular signal-regulated kinase 1, and the 90-kDa ribosomal S6 kinase in PC12 cells. Distinct effects of the neurotrophic factor, nerve growth factor, and the mitogenic factor, epidermal growth factor. *J Biol Chem* **268**: 9803-10.

Nishitoh, H., Saitoh, M., Mochida, Y., Takeda, K., Nakano, H., Rothe, M., Miyazono, K., and Ichijo, H. (1998). ASK1 is essential for JNK/SAPK activation by TRAF2. *Mol Cell* **2**: 389-95.

Noda, M., Ko, M., Ogura, A., Liu, D. G., Amano, T., Takano, T., and Ikawa, Y. (1985). Sarcoma viruses carrying ras oncogenes induce differentiation-associated properties in a neuronal cell line. *Nature* **318**: 73-5.

Northwood, I. C., Gonzalez, F. A., Wartmann, M., Raden, D. L., and Davis, R. J. (1991). Isolation and characterization of two growth factor-stimulated protein kinases that phosphorylate the epidermal growth factor receptor at threonine 669. *J Biol Chem* **266**: 15266-76.

Ohtsubo, M., and Roberts, J. M. (1993). Cyclin-dependent regulation of G1 in mammalian fibroblasts. *Science* **259**: 1908-12.

Ohtsuka, T., Shimizu, K., Yamamori, B., Kuroda, S., and Takai, Y. (1996). Activation of brain B-Raf protein kinase by Rap1B small GTP-binding protein. *J Biol Chem* **271**: 1258-61.

Okada, T., Hu, C. D., Jin, T. G., Kariya, K., Yamawaki-Kataoka, Y., and Kataoka, T. (1999). The strength of interaction at the Raf cysteine-rich domain is a critical determinant of response of Raf to Ras family small GTPases. *Mol Cell Biol* **19**: 6057-64.

Olivier, R., Otter, I., Monney, L., Wartmann, M., and Borner, C. (1997). Bcl-2 does not require Raf kinase activity for its death-protective function. *Biochem J* **324**: 75-83.

Otsu, M., Hiles, I., Gout, I., Fry, M. J., Ruiz-Larrea, F., Panayotou, G., Thompson, A., Dhand, R., Hsuan, J., and Totty, N. (1991). Characterization of two 85 kd proteins that associate with receptor tyrosine kinases, middle-T/pp60c-src complexes, and PI3-kinase. *Cell* **65**: 91-104.

Pages, G., Guerin, S., Grall, D., Bonino, F., Smith, A., Anjuere, F., Auberger, P., and Pouyssegur, J. (1999). Defective thymocyte maturation in p44 MAP kinase (Erk 1) knockout mice. *Science* **286**: 1374-7.

Palmero, I., Pantoja, C., and Serrano, M. (1998). p19ARF links the tumour suppressor p53 to Ras. *Nature* **395**: 125-6.

Papin, C., Denouel, A., Calothy, G., and Eychene, A. (1996). Identification of signalling proteins interacting with B-Raf in the yeast two-hybrid system. *Oncogene* **12,** 2213-21.

Papin, C., Denouel-Galy, A., Laugier, D., Calothy, G., and Eychene, A. (1998). Modulation of kinase activity and oncogenic properties by alternative splicing reveals a novel regulatory mechanism for B-Raf. *J Biol Chem* **273**: 24939-47.

Pawson, T. (1995). Protein modules and signaling networks. *Nature* **373**: 573-80.

Payne, D. M., Rossomando, A. J., Martino, P., Erickson, A. K., Her, J. H., Shabanowitz, J., Hunt, D. F., Weber, M. J., and Sturgill, T. W. (1991). Identification of the regulatory phosphorylation sites in pp42/mitogen-activated protein kinase (MAP kinase). *EMBO J* **10**: 885-92.

Pear, W. S., Nolan, G. P., Scott, M. L., and Baltimore, D. (1993). Production of high-titer helper-free retroviruses by transient transfection. *Proc Natl Acad Sci U S A* **90**: 8392-6.

Peruzzi, F., Prisco, M., Morrione, A., Valentinis, B., and Baserga, R. (2001). Anti-apoptotic signaling of the insulin-like growth factor-I receptor through mitochondrial translocation of c-Raf and Nedd4. *J Biol Chem* **276**: 25990-6.

Pham, C. D., Arlinghaus, R. B., Zheng, C. F., Guan, K. L., and Singh, B. (1995). Characterization of MEK1 phosphorylation by the v-Mos protein. *Oncogene* **10**: 1683-8.

Picard, D. (1993). Steroid-binding domains for regulating the functions of heterologous proteins in cis. *Trends cell biol* **3**: 278-280.

Pizon, V., Chardin, P., Lerosey, I., Olofsson, B., and Tavitian, A. (1988). Human cDNAs rap1 and rap2 homologous to the Drosophila gene Dras3 encode proteins closely related to ras in the 'effector' region. *Oncogene* **3**: 201-4.

Pomerantz, J., Schreiber-Agus, N., Liegeois, N. J., Silverman, A., Alland, L., Chin, L., Potes, J., Chen, K., Orlow, I., Lee, H. W., Cordon-Cardo, C., and DePinho, R. A. (1998). The Ink4a tumor suppressor gene product, p19Arf, interacts with MDM2 and neutralizes MDM2's inhibition of p53. *Cell* **92**: 713-23.

Pritchard, C. A., Bolin, L., Slattery, R., Murray, R., and McMahon, M. (1996). Post-natal lethality and neurological and gastrointestinal defects in mice with targeted disruption of the A-Raf protein kinase gene. *Curr Biol* **6**: 614-7.

Pritchard, C. A., Samuels, M. L., Bosch, E., and McMahon, M. (1995). Conditionally oncogenic forms of the A-Raf and B-Raf protein kinases display different biological and biochemical properties in NIH 3T3 cells. *Mol Cell Biol* **15**: 6430-42.

Pulverer, B. J., Kyriakis, J. M., Avruch, J., Nikolakaki, E., and Woodgett, J. R. (1991). Phosphorylation of c-jun mediated by MAP kinases. *Nature* **353**: 670-4.

Qiu, W., Zhuang, S., von Lintig, F. C., Boss, G. R., and Pilz, R. B. (2000). Cell type-specific regulation of B-Raf kinase by cAMP and 14-3-3 proteins. *J Biol Chem* **275**: 31921-9.

Quelle, D. E., Ashmun, R. A., Shurtleff, S. A., Kato, J. Y., Bar-Sagi, D., Roussel, M. F., and Sherr, C. J. (1993). Overexpression of mouse D-type cyclins accelerates G1phase in rodent fibroblasts. *Genes Dev* **7**: 1559-71.

Qui, M. S., and Green, S. H. (1992). PC12 cell neuronal differentiation is associated with prolonged p21ras activity and consequent prolonged ERK activity. *Neuron* **9**: 705-17.

Qureshi, S. A., Joseph, C. K., Hendrickson, M., Song, J., Gupta, R., Bruder, J., Rapp, U., and Foster, D. A. (1993). A dominant negative Raf-1 mutant prevents v-Src-induced transformation. *Biochem Biophys Res Commun* **192**: 969-75.

Raingeaud, J., Whitmarsh, A. J., Barrett, T., Derijard, B., and Davis, R. J. (1996). MKK3- and MKK6-regulated gene expression is mediated by the p38 mitogen-activated protein kinase signal transduction pathway. *Mol Cell Biol* **16**: 1247-55.

Rana, A., Gallo, K., Godowski, P., Hirai, S., Ohno, S., Zon, L., Kyriakis, J. M., and Avruch, J. (1996). The mixed lineage kinase SPRK phosphorylates and activates the stress-activated protein kinase activator, SEK-1. *J Biol Chem* **271**: 19025-8.

Rapp, U. R. (1991). Role of Raf-1 serine/threonine protein kinase in growth factor signal transduction. *Oncogene* **6**: 495-500.

Rapp, U. R., Goldsborough, M. D., Mark, G. E., Bonner, T. I., Groffen, J., Reynolds, F. H., Jr., and Stephenson, J. R. (1983). Structure and biological activity of v-raf, a unique oncogene transduced by a retrovirus. *Proc Natl Acad Sci U S A* **80**: 4218-22.

Resnitzky, D., Gossen, M., Bujard, H., and Reed, S. I. (1994). Acceleration of the G1/S phase transition by expression of cyclins D1 and E with an inducible system. *Mol Cell Biol* **14**: 1669-79.

Reuter, C. W., Catling, A. D., Jelinek, T., and Weber, M. J. (1995). Biochemical analysis of MEK activation in NIH3T3 fibroblasts. Identification of B-Raf and other activators. *J Biol Chem* **270**: 7644-55.

Ries, S., Biederer, C., Woods, D., Shifman, O., Shirasawa, S., Sasazuki, T., McMahon, M., Oren, M., and McCormick, F. (2000). Opposing effects of Ras on p53: transcriptional activation of mdm2 and induction of p19ARF. *Cell* **103**: 321-30.

Rivera, V. M., Miranti, C. K., Misra, R. P., Ginty, D. D., Chen, R. H., Blenis, J., and Greenberg, M. E. (1993). A growth factor-induced kinase phosphorylates the serum response factor at a site that regulates its DNA-binding activity. *Mol. Cell. Biol.* **13**: 6260-73.

Robertson, E., Bradley, A., Kuehn, M., and Evans, M. (1986). Germ-line transmission of genes introduced into cultured pluripotential cells by retroviral vector. *Nature* **323**: 445-8.

Rodriguez-Viciana, P., Warne, P. H., Dhand, R., Vanhaesebroeck, B., Gout, I., Fry, M. J., Waterfield, M. D., and Downward, J. (1994). Phosphatidylinositol-3-OH kinase as a direct target of Ras. *Nature* **370**: 527-32.

Rommel, C., Radziwill, G., Lovric, J., Noeldeke, J., Heinicke, T., Jones, D., Aitken, A., and Moelling, K. (1996). Activated Ras displaces 14-3-3 protein from the amino terminus of c-Raf-1. *Oncogene* **12**: 609-19.

Rommel, C., Radziwill, G., Moelling, K., and Hafen, E. (1997). Negative regulation of Raf activity by binding of 14-3-3 to the amino terminus of Raf in vivo. *Mech Dev* **64**: 95-104.

Rordorf-Nikolic, T., Van Horn, D. J., Chen, D., White, M. F., and Backer, J. M. (1995). Regulation of phosphatidylinositol 3'-kinase by tyrosyl phosphoproteins. Full activation requires occupancy of both SH2 domains in the 85-kDa regulatory subunit. *J Biol Chem* **270**: 3662-6.

Rosario, M., Paterson, H. F., and Marshall, C. J. (1999). Activation of the Raf/MAP kinase cascade by the Ras-related protein TC21 is required for the TC21-mediated transformation of NIH 3T3 cells. *Embo J* **18**: 1270-9.

Roy, S., Lane, A., Yan, J., McPherson, R., and Hancock, J. F. (1997). Activity of plasma membrane-recruited Raf-1 is regulated by Ras via the Raf zinc finger. *J Biol Chem* **272**: 20139-45.

Rozakis-Adcock, M., Fernley, R., Wade, J., Pawson, T., and Bowtell, D. (1993). The SH2 and SH3 domains of mammalian Grb2 couple the EGF receptor to the Ras activator mSos1. *Nature* : 83-5.

Sadoshima, J., and Izumo, S. (1993). Mechanical stretch rapidly activates multiple signal transduction pathways in cardiac myocytes: potential involvement of an autocrine/paracrine mechanism. *EMBO J* **12**: 1681-92.

Saitoh, M., Nishitoh, H., Fujii, M., Takeda, K., Tobiume, K., Sawada, Y., Kawabata, M., Miyazono, K., and Ichijo, H. (1998). Mammalian thioredoxin is a direct inhibitor of apoptosis signal-regulating kinase (ASK) 1. *EMBO J* **17**: 2596-606.

Salmeron, A., Ahmad, T. B., Carlile, G. W., Pappin, D., Narsimhan, R. P., and Ley, S. C. (1996). Activation of MEK-1 and SEK-1 by Tpl-2 proto-oncoprotein, a novel MAP kinase kinase kinase. *EMBO J* **15**: 817-26.

Salomoni, P., Wasik, M. A., Riedel, R. F., Reiss, K., Choi, J. K., Skorski, T., and Calabretta, B. (1998). Expression of constitutively active Raf-1 in the mitochondria restores antiapoptotic and leukemogenic potential of a transformation-deficient BCR/ABL mutant. *J Exp Med* **187**: 1995-2007.

Samuels, M. L., Weber, M. J., Bishop, J. M., and McMahon, M. (1993). Conditional transformation of cells and rapid activation of the mitogen-activated protein kinase cascade by an estradiol-dependent human raf-1 protein kinase. *Mol Cell Biol* **13**: 6241-52.

Sanchez, I., Hughes, R. T., Mayer, B. J., Yee, K., Woodgett, J. R., Avruch, J., Kyriakis, J. M., and Zon, L. I. (1994). Role of SAPK/ERK kinase-1 in the stress-activated pathway regulating transcription factor c-Jun. *Nature* **372**: 794-8.

Sanghera, J. S., Peter, M., Nigg, E. A., and Pelech, S. L. (1992). Immunological characterization of avian MAP kinases: evidence for nuclear localization. *Mol Biol Cell* **3**: 775-87.

Sauer, B., and Henderson, N. (1989). Cre-stimulated recombination at loxP-containing DNA sequences placed into the mammalian genome. *Nucleic Acids Res* **17**: 147-61.

Scaffidi, C., Fulda, S., Srinivasan, A., Friesen, C., Li, F., Tomaselli, K. J., Debatin, K. M., Krammer, P. H., and Peter, M. E. (1998). Two CD95 (APO-1/Fas) signaling pathways. *EMBO J* **17**: 1675-87

Schaap, D., van der Wal, J., Howe, L. R., Marshall, C. J., and van Blitterswijk, W. J. (1993). A dominant-negative mutant of raf blocks mitogen-activated protein kinase activation by growth factors and oncogenic p21ras. *J Biol Chem* **268**: 20232-6.

Scheffler, J. E., Waugh, D. S., Bekesi, E., Kiefer, S. E., LoSardo, J. E., Neri, A., Prinzo, K. M., Tsao, K. L., Wegrzynski, B., Emerson, S. D., and Fry, D. C. (1994). Characterization of a 78-residue fragment of c-Raf-1 that comprises a minimal binding domain for the interaction with Ras-GTP. *J Biol Chem* **269**: 22340-6.

Schlessinger, J. (1988). Signal transduction by allosteric receptor oligomerization. *Trends Biochem Sci* **13**: 443-7.

Schlessinger, J. (1993). How receptor tyrosine kinases activate Ras. *Trends Biochem Sci* **18**: 273-5.

Schonwasser, D. C., Marais, R. M., Marshall, C. J., and Parker, P. J. (1998). Activation of the mitogen-activated protein kinase/extracellular signal-regulated kinase pathway by conventional, novel, and atypical protein kinase C isotypes. *Mol Cell Biol* **18**: 790-8.

Schulte, T. W., An, W. G., and Neckers, L. M. (1997). Geldanamycin-induced destabilization of Raf-1 involves the proteasome. *Biochem Biophys Res Commun* **239**: 655-9.

Schulte, T. W., Blagosklonny, M. V., Ingui, C., and Neckers, L. (1995). Disruption of the Raf-1-Hsp90 molecular complex results in destabilization of Raf-1 and loss of Raf-1-Ras association. *J Biol Chem* **270**: 24585-8.

Seger, R., Ahn, N. G., Boulton, T. G., Yancopoulos, G. D., Panayotatos, N., Radziejewska, E., Ericsson, L., Bratlien, R. L., Cobb, M. H., and Krebs, E. G. (1992a). Microtubule-associated protein 2 kinases, ERK1 and ERK2, undergo autophosphorylation on both tyrosine and threonine residues: implications for their mechanism of activation. *Proc Natl Acad Sci* **88**: 6142-6.

Seger, R., Ahn, N. G., Posada, J., Munar, E. S., Jensen, A. M., Cooper, J. A., Cobb, M. H., and Krebs, E. G. (1992b). Purification and characterization of mitogen-activated protein kinase activator(s) from epidermal growth factor-stimulated A431 cells. *J Biol Chem* **267**: 14373-81.

Seger, R., Seger, D., Lozeman, F. J., Ahn, N. G., Graves, L. M., Campbell, J. S., Ericsson, L., Harrylock, M., Jensen, A. M., and Krebs, E. G. (1992c). Human T-cell mitogen-activated protein kinase kinases are related to yeast signal transduction kinases. *J Biol Chem* **267**: 25628-31.

Seth, A., Gonzalez, F. A., Gupta, S., Raden, D. L., and Davis, R. J. (1992). Signal transduction within the nucleus by mitogen-activated protein kinase. *J Biol Chem* **267**: 24796-804.

Sewing, A., Wiseman, B., Lloyd, A. C., and Land, H. (1997). High-intensity Raf signal causes cell cycle arrest mediated by p21Cip1. *Mol Cell Biol* **17**: 5588-97.

Sherr, C. J., and Roberts, J. M. (1999). CDK inhibitors: positive and negative regulators of G1-phase progression. *Genes Dev* **13**: 1501-12.

Sidovar, M. F., Kozlowski, P., Lee, J. W., Collins, M. A., He, Y., and Graves, L. M. (2000). Phosphorylation of serine 43 is not required for inhibition of c-Raf kinase by the cAMP-dependent protein kinase. *J Biol Chem* **275**: 28688-94.

Sieburth, D. S., Sun, Q., and Han, M. (1998). SUR-8, a conserved Ras-binding protein with leucine-rich repeats, positively regulates Ras-mediated signaling in C. elegans. *Cell* **94**: 119-30.

Silverstein, A. M., Grammatikakis, N., Cochran, B. H., Chinkers, M., and Pratt, W. B. (1998). p50(cdc37) binds directly to the catalytic domain of Raf as well as to a site on hsp90 that is topologically adjacent to the tetratricopeptide repeat binding site. *J Biol Chem* **273**: 20090-5.

Sithanandam, G., Kolch, W., Duh, F. M., and Rapp, U. R. (1990). Complete coding sequence of a human B-raf cDNA and detection of B-raf protein kinase with isozyme specific antibodies. *Oncogene* **5**: 1775-80.

Sluss, H. K., Barrett, T., Derijard, B., and Davis, R. J. (1994). Signal transduction by tumour necrosis factor mediated by JNK protein kinases. *Mol Cell Biol* **14**: 8376-84.

Smeal, T., Binetruy, B., Mercola, D. A., Birrer, M., and Karin, M. (1991). Oncogenic and transcriptional cooperation with Ha-Ras requires phosphorylation of c-Jun on serines 63 and 73. *Nature* **354**: 494-6.

Smith, A. G., Heath, J. K., Donaldson, D. D., Wong, G. G., Moreau, J., Stahl, M., and Rogers, D. (1988). Inhibition of pluripotential embryonic stem cell differentiation by purified polypeptides. *Nature* **336**: 688-90.

Smith, A. J., De Sousa, M. A., Kwabi-Addo, B., Heppell-Parton, A., Impey, H., and Rabbitts, P. (1995). A site-directed chromosomal translocation induced in embryonic stem cells by Cre-loxP recombination. *Nat Genet* **9**: 376-85.

Smith, M. R., Heidecker, G., Rapp, U. R., and Kung, H. F. (1990). Induction of transformation and DNA synthesis after microinjection of raf proteins. *Mol Cell Biol* **10**: 3828-33.

Songyang, Z., Shoelson, S. E., Chaudhuri, M., Gish, G., Pawson, T., Haser, W. G., King, F., Roberts, T., Ratnofsky, S., and Lechleider, R. J. (1993). SH2 domains recognize specific phosphopeptide sequences. *Cell* **72**: 767-78.

Srinivasula, S. M., Ahmad, M., Fernandes-Alnemri, T., Litwack, G., and Alnemri, E. S. (1996). Molecular ordering of the Fas-apoptotic pathway: the Fas/APO-1 protease Mch5 is a CrmA-inhibitable protease that activates multiple Ced-3/ICE-like cysteine proteases. *Proc Natl Acad Sci U S A* **93**: 14486-91.

Stacey, D. W., and Kung, H.-F. (1984). Transformation of NIH3T3 cells by microinjection of Ha-ras p21 protein. *Nature* **310**: 508-11.

Stanton, V. P., Jr., and Cooper, G. M. (1987). Activation of human raf transforming genes by deletion of normal amino-terminal coding sequences. *Mol Cell Biol* **7**: 1171-9.

Stanton, V. P., Jr., Nichols, D. W., Laudano, A. P., and Cooper, G. M. (1989). Definition of the human raf amino-terminal regulatory region by deletion mutagenesis. *Mol Cell Biol* **9**: 639-47.

Stephens, R. M., Sithanandam, G., Copeland, T. D., Kaplan, D. R., Rapp, U. R., and Morrison, D. K. (1992). 95-kilodalton B-Raf serine/threonine kinase: identification of the protein and its major autophosphorylation site. *Mol Cell Biol* **12**: 3733-42.

Stevenson, B. J., Rhodes, N., Errede, B., and Sprague, G. F. (1992). Constitutive mutants of the protein kinase STE11 activate the yeast pheromone response pathway in the absence of the G protein. *Genes Dev* **6**: 1293-304.

Stewart, S., Sundaram, M., Zhang, Y., Lee, J., Han, M., and Guan, K.-L. (1999). Kinase suppressor of Ras forms a multiprotein signaling complex and modulates MEK localisation. *Mol. Cell. Biol.* **19**: 5523-5534.

Stokoe, D., Macdonald, S. G., Cadwallader, K., Symons, M., and Hancock, J. F. (1994). Activation of Raf as a result of recruitment to the plasma membrane. *Science* **264**: 1463-7.

Stokoe, D., and McCormick, F. (1997). Activation of c-Raf-1 by Ras and Src through different mechanisms: activation in vivo and in vitro. *Embo J* **16**: 2384-96.

Storm, S. M., Cleveland, J. L., and Rapp, U. R. (1990). Expression of raf family proto-oncogenes in normal mouse tissues. *Oncogene* **5**: 345-51.

Strasser, A., Harris, A. W., Huang, D. C., Krammer, P. H., and Cory, S. (1995). Bcl-2 and Fas/APO-1 regulate distinct pathways to lymphocyte apoptosis. *EMBO J* **14**: 6136-47.

Sturgill, T. W., Ray, L. B., Erikson, E., and Maller, J. L. (1988). Insulin-stimulated MAP-2 kinase phosphorylates and activates ribosomal protein S6 kinase II. *Nature* **334**: 715-8.

Suen, K. L., Bustelo, X. R., and Barbacid, M. (1995). Lack of evidence for the activation of the Ras/Raf mitogenic pathway by 14-3-3 proteins in mammalian cells. *Oncogene* **11**: 825-31.

Sun, H., King, A. J., Diaz, H. B., and Marshall, M. S. (2000). Regulation of the protein kinase Raf-1 by oncogenic Ras through phosphatidylinositol 3-kinase, Cdc42/Rac and Pak. *Curr Biol* **10**: 281-4.

Sundaram, M., and Han, M. (1995). The C. elegans ksr-1 gene encodes a novel Raf-related kinase involved in Ras-mediated signal transduction. *Cell* **83**: 889-901.

Sutrave, P., Bonner, T. I., Rapp, U. R., Jansen, H. W., Patschinsky, T., and Bister, K. (1984). Nucleotide sequence of avian retroviral oncogene v-mil: homologue of murine retroviral oncogene v-raf. *Nature* **309**: 85-8.

Takayama, S., Sato, T., Krajewski, S., Kochel, K., Irie, S., Millan, J. A., and Reed, J. C. (1995). Cloning and functional analysis of BAG-1: a novel Bcl-2-binding protein with anti-cell death activity. *Cell* **80**: 279-84.

Takishima, K., Griswold-Prenner, I., Ingebritsen, T., and Rosner, M. R. (1991). Epidermal growth factor (EGF) receptor T669 peptide kinase from 3T3-L1 cells is an EGF-stimulated "MAP" kinase. *Proc Natl Acad Sci* **88**: 2520-4.

Tao, W., and Levine, A. J. (1999). P19(ARF) stabilizes p53 by blocking nucleo-cytoplasmic shuttling of Mdm2. *Proc Natl Acad Sci U S A* **96**: 6937-41.

Taussig, R., and Gilman, A. G. (1995). Mammalian membrane-bound adenylyl cyclases. *J Biol Chem* **270**: 1-4.

Therrien, M., Chang, H. C., Solomon, N. M., Karim, F. D., Wassarman, D. A., and Rubin, G. M. (1995). KSR, a novel protein kinase required for RAS signal transduction. *Cell* **83**: 879-88.

Thomas, K. R., and Capecchi, M. R. (1987). Site-directed mutagenesis by gene targeting in mouse embryo-derived stem cells. *Cell* **51**: 503-12.

Thomas, S. M., DeMarco, M., D'Arcangelo, G., Halegoua, S., and Brugge, J. S. (1992). Ras is essential for nerve growth factor- and phorbol ester-induced tyrosine phosphorylation of MAP kinases. *Cell* **68**: 1031-40.

Thorburn, A., Thorburn, J., Chen, S. Y., Powers, S., Shubeita, H. E., Feramisco, J. R., and Chien, K. R. (1993). HRas-dependent pathways can activate morphological and genetic markers of cardiac muscle cell hypertrophy. *J Biol Chem* **268**: 2244-9.

Thorburn, J., Frost, J. A., and Thorburn, A. (1994a). Mitogen-activated protein kinases mediate changes in gene expression, but not cytoskeletal organization associated with cardiac muscle cell hypertrophy. *J Cell Biol* **126**: 1565-72.

Thorburn, J., McMahon, M., and Thorburn, A. (1994b). Raf-1 kinase activity is necessary and sufficient for gene expression changes but not sufficient for cellular morphology changes associated with cardiac myocyte hypertrophy. *J Biol Chem* **269**: 30580-6.

Thorson, J. A., Yu, L. W., Hsu, A. L., Shih, N. Y., Graves, P. R., Tanner, J. W., Allen, P. M., Piwnica-Worms, H., and Shaw, A. S. (1998). 14-3-3 proteins are required for maintenance of Raf-1 phosphorylation and kinase activity. *Mol Cell Biol* **18**: 5229-38.

Torres, R. M., and Kühn, R. (1997). "Laboratory Protocols for Conditional GeneTargeting." Oxford University Press, Oxford, UK.

Tournier, C., Hess, P., Yang, D. D., Xu, J., Turner, T. K., Nimnual, A., Bar-Sagi, D., Jones, S. N., Flavell, R. A., and Davis, R. J. (2000). Requirement of JNK for stress-induced activation of the cytochrome c-mediated death pathway. *Science* **288**: 870-4.

Traenckner, E. B., Pahl, H. L., Henkel, T., Schmidt, K. N., Wilk, S., and Baeuerle, P. A. (1995). Phosphorylation of human I kappa B-alpha on serines 32 and 36 controls I kappa B-alpha proteolysis and NF-kappa B activation in response to diverse stimuli. *EMBO J* **14**: 2876-83.

Traverse, S., and Cohen, P. (1994). Identification of a latent MAP kinase kinase kinase in PC12 cells as B-raf. *FEBS Lett* **350**: 13-8.

Traverse, S., Cohen, P., Paterson, H., Marshall, C., Rapp, U., and Grand, R. J. (1993). Specific association of activated MAP kinase kinase kinase (Raf) with the plasma membranes of ras-transformed retinal cells. *Oncogene* **8**: 3175-81.

Traverse, S., Gomez, N., Paterson, H., Marshall, C., and Cohen, P. (1992). Sustained activation of the mitogen-activated protein (MAP) kinase cascade may be required for differentiation of PC12 cells. Comparison of the effects of nerve growth factor and epidermal growth factor. *Biochem J* **288**: 351-5.

Traverse, S., Seedorf, K., Paterson, H., Marshall, C. J., Cohen, P., and Ullrich, A. (1994). EGF triggers neuronal differentiation of PC12 cells that overexpress the EGF receptor. *Curr Biol* **4**: 694-701.

Treisman, R. (1996). Regulation of transcription by MAP kinase cascades. *Curr Opin Cell Biol* **8**: 205-15.

Tzivion, G., Luo, Z., and Avruch, J. (1998). A dimeric 14-3-3 protein is an essential cofactor for Raf kinase activity. *Nature* **394**: 88-92.

Tzivion, G., Shen, Y. H., and Zhu, J. (2001). 14-3-3 proteins; bringing new definitions to scaffolding. *Oncogene* **20**: 6331-8.

Umanoff, H., Edelmann, W., Pellicer, A., and Kucherlapati, R. (1995). The murine N-ras gene is not essential for growth and development. *Proc Natl Acad Sci* **92**: 1709-13.

Urano, T., Emkey, R., and Feig, L. A. (1996). Ral-GTPases mediate a distinct downstream signaling pathway from ras that facilitates transformation. *EMBO J* **15**: 810-6.

Van Aelst, L., Barr, M., Marcus, S., Polverino, A., and Wigler, M. (1993). Complex formation between RAS and RAF and other protein kinases. *Proc Natl Acad Sci U S A* **90**: 6213-7.

Van Antwerp, D. J., Martin, S. J., Kafri, T., Green, D. R., and Verma, I. M. (1996). Suppression of TNF-alpha-induced apoptosis by NF-kappaB. *Science* **274**: 787-9.

Van Deursen, J., Fornerod, M., Van Rees, B., and Grosveld, G. (1995). Cre-mediated site-specific translocation between nonhomologous mouse chromosomes. *Proc Natl Acad Sci U S A* **92**: 7376-80.

Vojtek, A. B., Hollenberg, S. M., and Cooper, J. A. (1993). Mammalian Ras interacts directly with the serine/threonine kinase Raf. *Cell* **74**: 205-14.

Vossler, M. R., Yao, H., York, R. D., Pan, M. G., Rim, C. S., and Stork, P. J. (1997). cAMP activates MAP kinase and Elk-1 through a B-Raf- and Rap1-dependent pathway. *Cell* **89**: 73-82.

Wang, C., Deng, L., Hong, M., Akkaraju, G. R., Inoue, J., and Chen, Z. J. (2001). TAK1 is a ubiquitin-dependent kinase of MKK and IKK. *Nature* **412**: 346-51.

Wang, C. Y., Mayo, M. W., Korneluk, R. G., Goeddel, D. V., and Baldwin, A. S. J. (1998). NF-kappaB antiapoptosis: induction of TRAF1 and TRAF2 and c-IAP1 and c-IAP2 to suppress caspase-8 activation. *Science* **281**: 1680-3.

Wang, H. G., Miyashita, T., Takayama, S., Sato, T., Torigoe, T., Krajewski, S., Tanaka, S., Hovey, L., 3rd, Troppmair, J., Rapp, U. R., and et al. (1994). Apoptosis regulation by interaction of Bcl-2 protein and Raf-1 kinase. *Oncogene* **9**: 2751-6.

Wang, H. G., Rapp, U. R., and Reed, J. C. (1996a). Bcl-2 targets the protein kinase Raf-1 to mitochondria. *Cell* **87**: 629-38.

Wang, H. G., Takayama, S., Rapp, U. R., and Reed, J. C. (1996b). Bcl-2 interacting protein, BAG-1, binds to and activates the kinase Raf-1. *Proc Natl Acad Sci U S A* **93**: 7063-8.

Warne, P. H., Viciana, P. R., and Downward, J. (1993). Direct interaction of Ras and the amino-terminal region of Raf-1 in vitro. *Nature* **364**: 352-5.

Wartmann, M., and Davis, R. J. (1994). The native structure of the activated Raf protein kinase is a membrane-bound multi-subunit complex. *J Biol Chem* **269**: 6695-701.

Widmann, C., Gibson, S., and Johnson, G. L. (1998). Caspase-dependent cleavage of signaling proteins during apoptosis. A turn-off mechanism for anti-apoptotic signals. *J Biol Chem* **273**: 7141-7.

Williams, N. G., Roberts, T. M., and Li, P. (1992). Both p21ras and pp60v-src are required, but neither alone is sufficient, to activate the Raf-1 kinase. *Proc Natl Acad Sci U S A* **89**: 2922-6.

Wojnowski, L., Stancato, L. F., Zimmer, A. M., Hahn, H., Beck, T. W., Larner, A. C., Rapp, U. R., and Zimmer, A. (1998). Craf-1 protein kinase is essential for mouse development. *Mech Dev* **76**: 141-9.

Wojnowski, L., Zimmer, A. M., Beck, T. W., Hahn, H., Bernal, R., Rapp, U. R., and Zimmer, A. (1997). Endothelial apoptosis in Braf-deficient mice. *Nat Genet* **16**: 293-7.

Wolthuis, R. M., de Ruiter, N. D., Cool, R. H., and Bos, J. L. (1997). Stimulation of gene induction and cell growth by the Ras effector Rlf. *Embo J* **16**: 6748-61.

Wolthuis, R. M., Zwartkruis, F., Moen, T. C., and Bos, J. L. (1998). Ras-dependent activation of the small GTPase Ral. *Curr Biol* **8**: 471-4.

Wood, K. W., Qi, H., D'Arcangelo, G., Armstrong, R. C., Roberts, T. M., and Halegoua, S. (1993). The cytoplasmic raf oncogene induces a neuronal phenotype in PC12 cells: a potential role for cellular raf kinases in neuronal growth factor signal transduction. *Proc Natl Acad Sci U S A* **90**: 5016-20.

Wood, K. W., Sarnecki, C., Roberts, T. M., and Blenis, J. (1992). ras mediates nerve growth factor receptor modulation of three signal-transducing protein kinases: MAP kinase, Raf-1, and RSK. *Cell* **68**: 1041-50.

Woods, D., Parry, D., Cherwinski, H., Bosch, E., Lees, E., and McMahon, M. (1997). Raf-induced proliferation or cell cycle arrest is determined by the level of Raf activity with arrest mediated by p21Cip1. *Mol Cell Biol* **17**: 5598-611.

Wu, J., Dent, P., Jelinek, T., Wolfman, A., Weber, M. J., and Sturgill, T. W. (1993a). Inhibition of the EGF-activated MAP kinase signaling pathway by adenosine 3',5'-monophosphate. *Science* **262**: 1065-9.

Wu, J., Harrison, J. K., Dent, P., Lynch, K. R., Weber, M. J., and Sturgill, T. W. (1993b). Identification and characterization of a new mammalian mitogen-activated protein kinase kinase, MKK2. *Mol Cell Biol* **13**: 4539-48.

Wu, X., Bayle, J. H., Olson, D., and Levine, A. J. (1993c). The p53-mdm-2 autoregulatory feedback loop. *Genes Dev* **7**: 1126-32.

Wu, X., Noh, S. J., Zhou, G., Dixon, J. E., and Guan, K. L. (1996). Selective activation of MEK1 but not MEK2 by A-Raf from epidermal growth factor-stimulated Hela cells. *J Biol Chem* **271**: 3265-71.

Xia, Z., Dickens, M., Raingeaud, J., Davis, R. J., and Greenberg, M. E. (1995). Opposing effects of ERK and JNK-p38 MAP kinases on apoptosis. *Science* **270**: 1326-31.

Xing, H. R., and Kolesnick, R. (2001). Kinase suppressor of Ras signals through Thr269 of c-Raf-1. *J Biol Chem* **276**: 9733-41.

Yamamori, B., Kuroda, S., Shimizu, K., Fukui, K., Ohtsuka, T., and Takai, Y. (1995). Purification of a Ras-dependent mitogen-activated protein kinase kinase kinase from bovine brain cytosol and its identification as a complex of B-Raf and 14-3-3 proteins. *J Biol Chem* **270**: 11723-6.

Yamazaki, T., Komuro, I., and Yazaki, Y. (1998). Signalling pathways for cardiac hypertrophy. *Cell Signal* **10**: 693-8.

Yamazaki, T., Tobe, K., Hoh, E., Maemura, K., Kaida, T., Komuro, I., Tamemoto, H., Kadowaki, T., Nagai, R., and Yazaki, Y. (1993). Mechanical loading activates mitogen-activated protein kinase and S6 peptide kinase in cultured rat cardiac myocytes. *J Biol Chem* **268**: 12069-76.

Yan, M., Dai, T., Deak, J. C., Kyriakis, J. M., Zou, L. I., Woodgett, J. R., and J., T. D. (1994). Activation of stress-activated protein kinase by MEKK1 phosphorylation of its activator SEK1. *Nature* **372**: 798-800.

Yan, M., and Templeton, D. J. (1994). Identification of 2 serine residues of MEK-1 that are differentially phosphorylated during activation by raf and MEK kinase. *J Biol Chem* **269**: 19067-73.

Yang, J., Liu, X., Bhalla, K., Kim, C. N., Ibrado, A. M., Cai, J., Peng, T. I., Jones, D. P., and Wang, X. (1997). Prevention of apoptosis by Bcl-2: release of cytochrome c from mitochondria blocked. *Science* **275**: 1129-32.

Yao, B., Zhang, Y., Delikat, S., Mathias, S., Basu, S., and Kolesnick, R. (1995). Phosphorylation of Raf by ceramide-activated protein kinase. *Nature* **378**: 307-10.

Yeung, K., Janosch, P., McFerran, B., Rose, D. W., Mischak, H., Sedivy, J. M., and Kolch, W. (2000). Mechanism of suppression of the Raf/MEK/extracellular signal-regulated kinase pathway by the raf kinase inhibitor protein. *Mol Cell Biol* **20**: 3079-85.

Yeung, K., Seitz, T., Li, S., Janosch, P., McFerran, B., Kaiser, C., Fee, F., Katsanakis, K. D., Rose, D. W., Mischak, H., Sedivy, J. M., and Kolch, W. (1999). Suppression of Raf-1 kinase activity and MAP kinase signalling by RKIP. *Nature* **401**: 173-7.

Yin, X. M., Wang, K., Gross, A., Zhao, Y., Zinkel, S., Klocke, B., Roth, K. A., and Korsmeyer, S. J. (1999). Bid-deficient mice are resistant to Fas-induced hepatocellular apoptosis. *Nature* **400**: 886-91.

York, R. D., Yao, H., Dillon, T., Ellig, C. L., Eckert, S. P., McCleskey, E. W., and Stork, P. J. S. (1998). Rap1 mediates sustained MAP kinase activation induced by nerve growth factor. *Nature* **392**: 622-6.

Yu, W., Fantl, W. J., Harrowe, G., and Williams, L. T. (1998). Regulation of the MAP kinase pathway by mammalian Ksr through direct interaction with MEK and ERK. *Curr Biol* **8**: 56-64.

Yuryev, A., Ono, M., Goff, S. A., Macaluso, F., and Wennogle, L. P. (2000). Isoform-specific localization of A-RAF in mitochondria. *Mol Cell Biol* **20**: 4870-8.

Zandi, E., Chen, Y., and Karin, M. (1998). Direct phosphorylation of IkB by IKKa and IKKb: discrimination between free and NF-kB-bound substrate. *Science* **281**: 1360-3.

Zha, J., Harada, H., Yang, E., Jockel, J., and Korsmeyer, S. J. (1996). Serine phosphorylation of death agonist BAD in response to survival factor results in binding to 14-3-3 not BCL-X(L). *Cell* **87**: 619-28.

Zhang, B. H., and Guan, K. L. (2000). Activation of B-Raf kinase requires phosphorylation of the conserved residues Thr598 and Ser601. *Embo J* **19**: 5429-39.

Zhang, B. H., Tang, E. D., Zhu, T., Greenberg, M. E., Vojtek, A. B., and Guan, K. L. (2001). Serum- and glucocorticoid-inducible kinase SGK phosphorylates and negatively regulates B-Raf. *J Biol Chem* **276**: 31620-6.

Zhang, X. F., Settleman, J., Kyriakis, J. M., Takeuchi-Suzuki, E., Elledge, S. J., Marshall, M. S., Bruder, J. T., Rapp, U. R., and Avruch, J. (1993). Normal and oncogenic p21ras proteins bind to the amino-terminal regulatory domain of c-Raf-1. *Nature* **364**: 308-13.

Zhang, Y., Yao, B., Delikat, S., Bayoumy, S., Lin, X.-H., Basu, S., McGinley, M., Chan-Hui, P.-Y., Lichenstein, H., and Kolesnick, R. (1997). Kinase suppressor of Ras is ceramide-activated protein kinase. *Cell* **89**: 63-72.

Zheng, C. F., and Guan, K. L. (1993). Cloning and characterization of two distinct human extracellular signal-regulated kinase activator kinases, MEK1 and MEK2. *J Biol Chem* **268**: 11435-9.

Zheng, C. F., and Guan, K. L. (1994). Activation of MEK family kinases requires phosphorylation of two conserved Ser/Thr residues. *EMBO J* **13**: 1123-31.

Zimmermann, S., and Moelling, K. (1999). Phosphorylation and regulation of Raf by Akt (protein kinase B). *Science* **286**: 1741-4.

Zou, H., Henzel, W. J., Liu, X., Lutschg, A., and Wang, X. (1997). Apaf-1, a human protein homologous to C. elegans CED-4, participates in cytochrome c-dependent activation of caspase-3. *Cell* **90**: 405-13.

Zou, H., Li, Y., Liu, X., and Wang, X. (1999). An APAF-1 cytochrome c multimeric complex is a functional apoptosome that activates procaspase-9. *J Biol Chem* **274**: 11549-56.

Appendix

Publications

M. Hüser, J. Luckett, A. Chiloeches, **K. Mercer**, M. Iwobi, S. Giblett, X. M. Sun, J. Brown, R. Marais, C. Pritchard. 2001. MEK kinase activity is not necessary for Raf-1 function. EMBO J. **20**, 1940-1951.

K. Mercer, A. Chiloeches, M. Hüser, M. Kiernan, R. Marais, C. Pritchard. 2002. ERK signalling and oncogene transformation are not impaired in cells lacking A-Raf. Oncogene **21**, 347-355.

The EMBO Journal Vol. 20 No. 8 pp. 1940–1951, 2001

MEK kinase activity is not necessary for Raf-1 function

Martin Hüser, Jeni Luckett, Antonio Chiloeches[1], Kathryn Mercer, Mabel Iwobi, Susan Giblett, Xiao-Ming Sun[2], Jane Brown[3], Richard Marais[1] and Catrin Pritchard[4]

Department of Biochemistry, [2]MRC Toxicology Unit and [3]Division of Biomedical Services, University of Leicester, University Road, Leicester LE1 7RH and [1]Institute of Cancer Research, 237 Fulham Road, London SW3 6JB, UK

[4]Corresponding author
e-mail: cap8@le.ac.uk

M.Hüser, J.Luckett and A.Chiloeches contributed equally to this work

Raf-1 protein kinase has been identified as an integral component of the Ras/Raf/MEK/ERK signalling pathway in mammals. Activation of Raf-1 is achieved by Ras.GTP binding and other events at the plasma membrane including tyrosine phosphorylation at residues 340/341. We have used gene targeting to generate a 'knockout' of the *raf-1* gene in mice as well as a *rafFF* mutant version of endogenous Raf-1 with Y340FY341F mutations. *Raf-1*$^{-/-}$ mice die in embryogenesis and show vascular defects in the yolk sac and placenta as well as increased apoptosis of embryonic tissues. Cell proliferation is not affected. Raf-1 from cells derived from *raf-1*$^{FF/FF}$ mice has no detectable activity towards MEK *in vitro*, and yet *raf-1*$^{FF/FF}$ mice survive to adulthood, are fertile and have an apparently normal phenotype. In cells derived from both the *raf-1*$^{-/-}$ and *raf-1*$^{FF/FF}$ mice, ERK activation is normal. These results strongly argue that MEK kinase activity of Raf-1 is not essential for normal mouse development and that Raf-1 plays a key role in preventing apoptosis.

Keywords: apoptosis/knockout/MEK kinase/Raf-1/tyrosine phosphorylation

Introduction

The mammalian *raf-1* gene was first identified as the cellular homologue of v-*raf*, the oncogene responsible for the induction of sarcomas in mice by the MSV3611 virus. Two other genes highly homologous to *raf-1* have been cloned: A-*raf* and B-*raf*. All three *raf* genes code for serine/threonine protein kinases and they share a high degree of sequence similarity. The N-terminal region encodes the regulatory domain and binds essential cofactors including Ras while the C-terminal region contains the catalytic kinase domain. Deletion of the N-terminal regulatory regions of all three kinases gives rise to proteins that are constitutively active and are oncogenic in a wide variety of cell types. The kinase domain of B-*raf* appears to be the most potent of the three in these assays (Pritchard *et al.*, 1995). In the mouse, transcripts for all three *raf* genes are detectable in all cells (Storm *et al.*, 1990; Barnier *et al.*, 1995).

Of the three Raf isotypes, most biochemical studies have focused on Raf-1. Inactive Raf-1 is normally cytosolic, but Raf-1 binds to Ras.GTP *in vitro* and *in vivo* and so translocates to the plasma membrane in the presence of active Ras (Marais and Marshall, 1996 and references therein). However, binding to Ras is not sufficient for full Raf-1 activation (Traverse *et al.*, 1993; Marais *et al.*, 1995, 1997; Mason *et al.*, 1999) and additional signals at the plasma membrane including phosphorylation are required (Marais and Marshall, 1996). Our previous studies in COS cells have shown that activation of Raf-1 requires phosphorylation of Y340 and/or Y341. Substitution of these residues to phenylalanine, creating RafFF, blocks activation of Raf-1 by oncogenic Ras and Src, and by ligand stimulation (Marais *et al.*, 1995, 1997; Diaz *et al.*, 1997; Stokoe and McCormick, 1997; Barnard *et al.*, 1998). Recent data have also suggested that phosphorylation of Raf-1 at serine 338 is required for activation, demonstrating that complex phosphorylation events take place within this region of Raf-1 (Diaz *et al.*, 1997; Barnard *et al.*, 1998; Mason *et al.*, 1999). However, the physiological importance of these phosphorylation events is unclear.

The principal functions of the Raf protein kinases appear to be participation in the highly conserved Ras/Raf/MEK/ERK intracellular signalling pathway (Marshall 1994). This pathway is activated by different classes of cell surface receptors including receptor tyrosine kinases (RTKs) and G protein coupled seven transmembrane receptors, all of which confer their biological effects through Ras (Dickson and Hafen, 1994; Marshall, 1994). ERK activation has been associated with many of the downstream consequences of Ras activation and the Raf proteins provide a vital link between activated Ras proteins and the ERKs. A variety of biochemical and genetic data point to the importance of Raf-1 as a MEK activator. Activation of an inducible version of oncogenic Raf-1 induces the rapid activation of MEK and ERK as well as immediate early gene expression in NIH 3T3 cells (Samuels *et al.*, 1993; Kerkhoff and Rapp, 1997). Immunoprecipitated endogenous Raf-1 can phosphorylate MEK1 and -2 *in vitro* (Howe *et al.*, 1992; Kyriakis *et al.*, 1992; Marais *et al.*, 1998) and the Raf/MEK/ERK cascade can be reconstituted *in vitro* using proteins expressed in Sf9 cells (Macdonald *et al.*, 1993). Kinase inactive Raf-1 cannot activate MEK in this system. Finally, dominant-negative Raf-1 mutants block growth factor and oncogenic ras-stimulated activation of ERKs in fibroblasts (Schaap *et al.*, 1993; Chao *et al.*, 1994; Troppmair *et al.*, 1994).

Intriguingly, a number of observations do not entirely fit with the view that the endogenous Raf-1 protein is a physiologically important MEK activator (Marais and Marshall, 1996). First, only a small proportion (<10%) of the entire cellular Raf-1 is activated upon treatment of cells with growth factors (Dent *et al.*, 1995; Reuter *et al.*, 1995; Jelinek *et al.*, 1996). Secondly, B-Raf has been identified as the major MEK activator in neuronal cell types and NIH 3T3 cells, despite Raf-1 also being expressed in these cells (Moodie *et al.*, 1993, 1994; Catling *et al.*, 1994; Jaiswal *et al.*, 1994; Traverse and Cohen, 1994; Reuter *et al.*, 1995). The kinase domain of B-Raf is a considerably stronger activator of MEK and has a higher affinity for MEK than the kinase domain of Raf-1 (Pritchard *et al.*, 1995; Marais *et al.*, 1997; Papin *et al.*, 1998). Finally, Raf-1 and ERK activation are not coincident in some circumstances (Wood *et al.*, 1992, 1993; Kuo *et al.*, 1996). A pool of Raf-1 is also thought to be located in mitochondria (Wang *et al.*, 1996) and an ERK-independent role for mitochondrial Raf-1 in apoptosis has been postulated (Neshat *et al.*, 2000).

Many of the previous studies designed to address the involvement of Raf-1 in mediating signals between Ras and ERKs have used antisense or dominant-negative constructs overexpressed in tissue culture cell lines to inhibit its expression or activity (Kolch *et al.*, 1991; Chao *et al.*, 1994; Troppmair *et al.*, 1994). These approaches have the disadvantage that they may sequester the function/expression of other Raf isotypes (A-Raf and B-Raf) or other Ras effectors. To achieve the required specificity, gene targeting has been used to ablate individual *raf* genes (Pritchard *et al.*, 1996; Wojnowski *et al.*, 1997, 1998). In this study, we describe the generation of Raf-1 deficient mice (*raf-1*$^{-/-}$) as well as mice with a 'knockin' mutation of the endogenous 340/341 tyrosines to phenylalanine (*raf-1*$^{FF/FF}$). Although there is no detectable Raf-1 activity in cells derived from either strain of mouse, ERK activation was not compromised in either. However, the *raf-1*$^{-/-}$ animals die in embryogenesis due to vascularization defects and increased apoptosis, while the *raf-1*$^{FF/FF}$ animals survive to adulthood and have an apparently normal phenotype. Our results show that the full-length Raf-1 protein is essential for normal mouse development and for protection against apoptosis, but they argue that Raf-1 kinase activity towards MEK is not necessary for these processes.

Results

Generation and phenotype analysis of raf-1$^{-/-}$ *and raf-1*$^{FF/FF}$ *mutant mice*

The generation of the mutant mice is described in the Supplementary data (available at *The EMBO Journal* Online.) Both mutations were established on the mixed 129Ola/C57BL6 and 129Ola/MF-1 backgrounds. For the *raf-1* knockout, *raf-1*$^{+/-}$ animals were intercrossed and PCR genotype analysis was performed on tail DNAs from surviving offspring. No surviving animals with the *raf-1*$^{-/-}$ genotype were obtained (n = 14 matings) but *raf-1*$^{+/-}$ animals were born at the expected Mendelian frequency and were indistinguishable from *raf-1*$^{+/+}$ littermates. Therefore, *raf-1*$^{+/-}$ intercrosses were set up and embryos were genotyped. On the 129Ola/C57BL6 background, at E9.5, a number of abnormal embryos were observed and these all PCR genotyped as *raf-1*$^{-/-}$ (Table I). On the 129Ola/MF-1 background, in early backcross generations, a phenotype similar to that on the 129Ola/C57BL6 background was observed (Table II). However, a number of normal embryos at E9.5–E10.5 also typed as *raf-1*$^{-/-}$ (Table II). When the *raf-1* mutation was further backcrossed to the MF-1 strain, *raf-1*$^{-/-}$ embryos were observed at E12.5 up to birth but these were small and morphologically abnormal.

On the 129Ola/C57BL6 background, at E9.5, *raf-1*$^{-/-}$ embryos were morphologically smaller and were reduced in size by approximately one-third (Figure 1A and B). They were developmentally arrested, had fewer somites and were anaemic, but were still alive as judged by the presence of a regular heartbeat. Strikingly, all of the mutants lacked small and large blood vessels in the yolk sac (Figure 1C and D), as visualized by staining with an antibody to platelet endothelial cell adhesion molecule-1 (PECAM-1; Figure 1E). PECAM-1 staining of the *raf-1*$^{-/-}$ embryos also revealed abnormal vascular network formation (Figure 1F–I). In the head region, there was a reduction in the number of large and small blood vessels, the vessels were disorganized and there were no capillary sprouts into the neuroectoderm (Figure 1H and I). Haemorrhaging was observed in approximately one-quarter of the mutant embryos (data not shown). There was a significant reduction in the number and density of cells throughout the mutant embryos but cell size appeared larger (Figure 1J and K). Staining of the embryonic brain with the Ki67 antibody, a marker for cells in S phase, showed that there was no significant reduction in the numbers of proliferating cells in the *raf-1*$^{-/-}$ embryos (Figure 1L and M). However, the terminal deoxynucleotidyl transferase-mediated dUTP nick end labelling (TUNEL) assay indicated that there was an increase in the numbers of apoptotic cells throughout the mutant embryos (Figure 1N and O).

On the 129Ola/MF-1 background, the *raf-1*$^{-/-}$ embryos died within a few hours of birth. They were 50–60% lighter in weight than the *raf-1*$^{+/+}$ embryos and they were anaemic (Figure 2A). The placenta was considerably smaller than the *raf-1*$^{+/+}$ placenta and was disorganized (Figure 2B and C). The spongiotrophoblast layer was considerably reduced in size, a number of the mesenchymal cells of the labyrinthine layer were undifferentiated and there were fewer blood vessels (Figure 2D and E). As with the 129Ola/C57BL6 *raf-1*$^{-/-}$ embryos, there were fewer cells in the mutant liver than the wild-type liver, but the mutant cells appeared to be greater in size (Figure 2F–K). In addition, there were notably fewer areas of haemopoiesis (Figure 2F and G). There did not appear to be any difference in the number of proliferating cells in the *raf-1*$^{-/-}$ liver compared with the *raf-1*$^{+/+}$ liver (Figure 2H and I). There was also no significant difference in the number of TUNEL positive cells in the *raf-1*$^{-/-}$ liver sections compared with the *raf-1*$^{+/+}$ liver sections (Figure 2J and K), indicating no significant difference in levels of spontaneous apoptosis. The fact that the *raf-1*$^{-/-}$ livers are hypocellular is likely to have been caused by increased susceptibility to apoptosis at earlier developmental stages (see below).

Table I. Genotyping data from *raf-1*$^{+/-}$ intercrosses: C57BL6 background

Age	*raf-1*$^{+/+}$	*raf-1*$^{+/-}$	*raf-1*$^{-/-}$ normal	*raf-1*$^{-/-}$ abnormal	Resorbed[a]	Untyped[b]
E3.5	2	5	3	0	–	3
E8.5	2	4	3	0	0	0
E9.5	17	26	0	12	1	0
E10.5	7	16	0	10	9	0
E11.5	14	20	0	6	14	0
E12.5	4	2	0	0	0	0
E15.5	0	2	0	0	2	0
Total	46	75	6	28	26	3

[a]Resorbed tissue had degenerated too much to dissect cleanly.
[b]DNA samples did not PCR amplify.

Table II. Genotyping data from *raf-1*$^{+/-}$ intercrosses: MF-1 background

Age	*raf-1*$^{+/+}$	*raf-1*$^{+/-}$	*raf-1*$^{-/-}$ normal	*raf-1*$^{-/-}$ abnormal	Resorbed[a]	Untyped[b]
E8.5	2	6	1	0	0	0
E9.5	3	14	1	1	0	0
E10.5	3	1	3	2	0	1
E12.5	3	4	0	1	3	3
E13.5	7	9	0	1	1	1
E14.5	6	6	0	3	2	7
E18.5	16	20	0	3	0	2
Birth (P1)	3	10	0	5[c]	–	2
Total	43	70	5	16	6	16

[a]Resorbed tissue had degenerated too much to dissect cleanly.
[b]DNA samples did not PCR amplify.
[c]Animals died a few hours after birth.

To assess the *raf-1*$^{FF/FF}$ phenotype, *raf-1*$^{+/FF}$ animals on the 129Ola/C57BL6 and 129Ola/MF-1 backgrounds were intercrossed and PCR genotype analysis was performed on tail DNAs from surviving offspring. Of 148 animals assessed, 45 typed as *raf-1*$^{+/+}$, 67 as *raf-1*$^{+/FF}$ and 36 as *raf-1*$^{FF/FF}$ (n = 19 matings). Therefore, there was no significant difference in the ratio of *raf-1*$^{+/+}$ to *raf-1*$^{FF/FF}$ animals surviving to adulthood (P = 0.15). The *raf-1*$^{FF/FF}$ animals on both genetic backgrounds survived for >1 year, were normal in weight and had no behavioural abnormalities. T-cell development was normal in these animals as judged by CD4 and CD8 staining of T cells (data not shown).

Analysis of proliferation and apoptosis in raf-1$^{-/-}$ and raf-1$^{FF/FF}$ MEFs

Mouse embryonic fibroblasts (MEFs) were derived from the *raf-1*$^{-/-}$ and *raf-1*$^{FF/FF}$ embryos and characterized for their ability to proliferate and undergo apoptosis *in vitro*. We consistently failed to culture *raf-1*$^{-/-}$ MEFs from E10.5 on the 129Ola/C57BL6 background as most of the cells were dead following embryo homogenization. This may be because of the apparent spontaneous apoptosis of the *raf-1*$^{-/-}$ embryos observed on this genetic background (Figure 1N and O). However, we successfully obtained *raf-1*$^{-/-}$ MEFs from E14.5 embryos on the 129Ola/MF-1 background. *Raf-1*$^{FF/FF}$ MEFs were isolated from E14.5 embryos resulting from *raf-1*$^{+/FF}$ intercrosses on both genetic backgrounds. Sibling *raf-1*$^{+/+}$ MEFs were also isolated in each case.

There was no detectable difference between the growth rates of the *raf-1*$^{-/-}$ cells compared with *raf-1*$^{+/+}$ cells over 8 days in culture (Figure 3A), or the *raf-1*$^{FF/FF}$ cells compared with the *raf-1*$^{+/+}$ cells (data not shown). Cell proliferation was measured by assessing bromodeoxyuridine (BrdU) incorporation in MEFs that had been made quiescent and then stimulated with 10% fetal calf serum (FCS). Again, the *raf-1*$^{-/-}$ and *raf-1*$^{FF/FF}$ MEFs showed no difference in their ability to undergo DNA synthesis as measured by this assay compared with *raf-1*$^{+/+}$ MEFs (Figure 3B).

Except for the C57BL6 *raf-1*$^{-/-}$ MEFs, the primary MF-1 *raf-1*$^{-/-}$ and *raf-1*$^{FF/FF}$ MEFs did not show evidence of spontaneous apoptosis under normal growth conditions (Figure 3C–E). Apoptosis was induced by treatment of *raf-1*$^{+/+}$, *raf-1*$^{-/-}$ and *raf-1*$^{FF/FF}$ MEFs with etoposide, anti-Fas antibody or by serum withdrawal, and cell death was assessed by annexin V or Hoechst 33258 staining. The *raf-1*$^{FF/FF}$ cells showed no increase or decrease in programmed cell death (PCD) upon treatment with these apoptotic agents compared with *raf-1*$^{+/+}$ cells (Figure 3C). In contrast, *raf-1*$^{-/-}$ cells showed a significant increase in PCD (Figure 3D–F). Upon treatment with etoposide, the *raf-1*$^{+/+}$ cells showed 21.1% PCD whereas the *raf-1*$^{-/-}$ cells showed 30.0% PCD (n = 7; 95% CI for difference 0.5–17.2%, P = 0.04; Figure 3D and E). Upon treatment with anti-Fas antibody, the *raf-1*$^{+/+}$ cells showed 29.9% PCD whereas the *raf-1*$^{-/-}$ cells showed 48.3% PCD (n = 7; 95% CI for difference 9.5–27.4%, P = 0.0007; Figure 3D and E). The *raf-1*$^{-/-}$ cells did not show a significant increase in PCD upon serum withdrawal as this treatment induced 26.0% PCD for the *raf-1*$^{-/-}$ cells and 18.7% for the *raf-1*$^{+/+}$ cells (n = 7; 95% CI for difference –6.8 to 21.4%, P = 0.284; Figure 3D and E). Hoechst 33258 staining

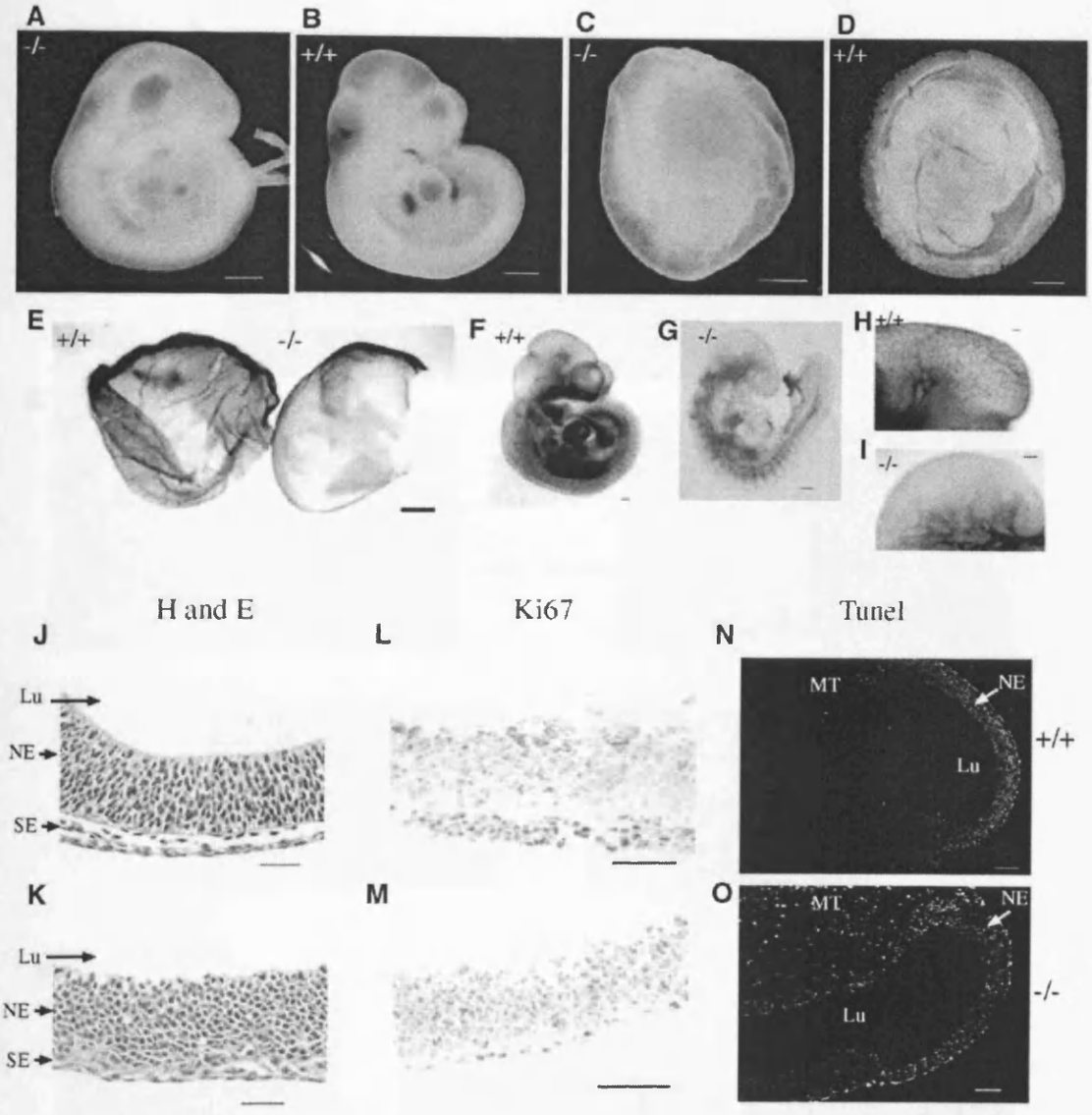

Fig. 1. Phenotype of the 129Ola/C57BL6 *raf-1*$^{-/-}$ embryos. (**A**) *raf-1*$^{-/-}$ embryo at E9.5; (**B**) *raf-1*$^{+/+}$ littermate embryo at E9.5; (**C**) *raf-1*$^{-/-}$ embryo at E9.5 in yolk sac; (**D**) *raf-1*$^{+/+}$ littermate embryo at E9.5 in yolk sac; (**E**) PECAM-1 immunostaining of yolk sacs from wild-type embryo at E9.5 (left) and from mutant embryo (right). (**F–I**) PECAM-1 staining of *raf-1*$^{+/+}$ embryo (F and H) and *raf-1*$^{-/-}$ embryo (G and I) at E9.5. (H) and (I) are magnifications of the embryonic brain regions. (**J–O**) Longitudinal sections through forebrain of *raf-1*$^{+/+}$ (J, L and N) and *raf-1*$^{-/-}$ (K, M and O) embryos at E9.5. (J) and (K) were stained with haematoxylin and eosin, (L) and (M) were immunostained with a Ki67 antibody, and (N) and (O) were processed for TUNEL staining. Scale bars: A–E, 250 μm; F and G, 100 μm; H and I, 25 μm, J–M, 50 μm; N and O, 100 μm. NE, neural ectoderm; SE, surface ectoderm; Lu, lumen of prospective forebrain; MT, cephalic mesenchyme tissue.

confirmed that the *raf-1*$^{-/-}$ cells were more susceptible to PCD induced by the anti-Fas antibody than the *raf-1*$^{+/+}$ cells, as assessed by nuclear morphology (Figure 3F).

Raf kinase activities in the mutant cells

For measuring Raf kinase activities, primary MEFs were immortalized with the SV40 large T antigen and permanent cell lines were derived. Only cells expressing similar levels of the T antigen and with similar growth rates were analysed and compared (data not shown). We first compared the activities of the endogenous Raf proteins in *raf-1*$^{+/+}$ MEFs using the immunoprecipitation kinase cascade assay (Marais *et al.*, 1997). For these initial studies, the conditions were optimized for B-Raf activity, since B-Raf is the most active isotype under our assay conditions (Mason *et al.*, 1999). In agreement with our previous studies, B-Raf had elevated basal activity in unstimulated cells, whereas both Raf-1 and A-Raf were inactive (Figure 4A). When stimulated with epidermal growth factor (EGF), B-Raf activity in *raf-1*$^{+/+}$ cells was

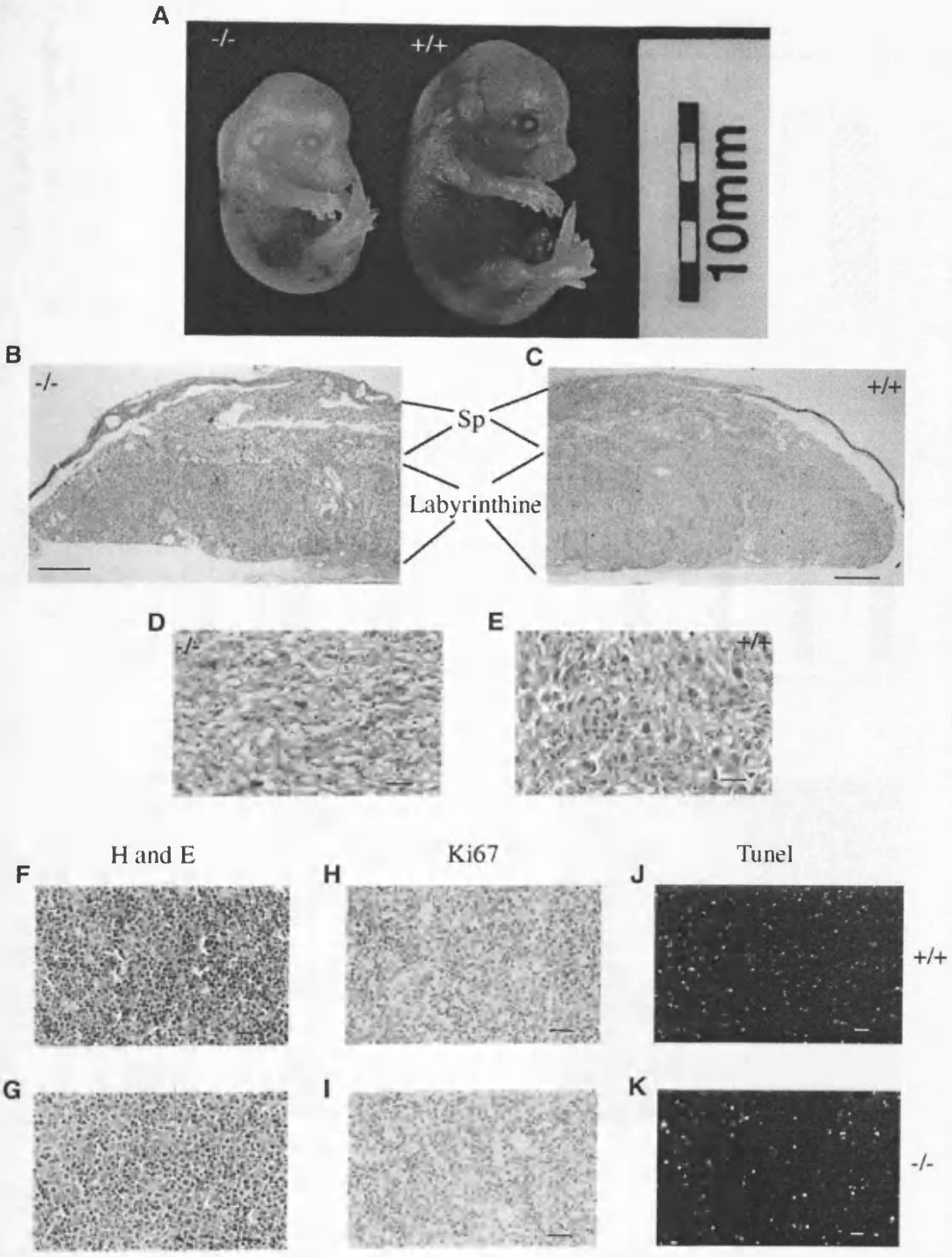

Fig. 2. Phenotype of the 129Ola/MF-1 *raf-1*$^{-/-}$ embryos. (**A**) Photograph of *raf-1*$^{-/-}$ embryo (left) and *raf-1*$^{+/+}$ littermate embryo (right) at E15.5. (**B** and **C**) Cross-sections of placentas from *raf-1*$^{-/-}$ (B) and *raf-1*$^{+/+}$ (C) embryos showing the labyrinthine and spongiotrophoblast (Sp) layers. (**D** and **E**) Cross-sections of labyrinthine layer of placentas from *raf-1*$^{-/-}$ (D) and *raf-1*$^{+/+}$ (E) embryos. (**F–K**) Cross-sections of liver from littermate *raf-1*$^{-/-}$ (G, I and K) and *raf-1*$^{+/+}$ embryos at E15.5. These sections were either stained with haematoxylin and eosin (F and G), immunostained with the Ki67 antibody (H and I) or processed for TUNEL staining (J and K). Scale bars: B and C, 400 μm; D–K, 50 μm.

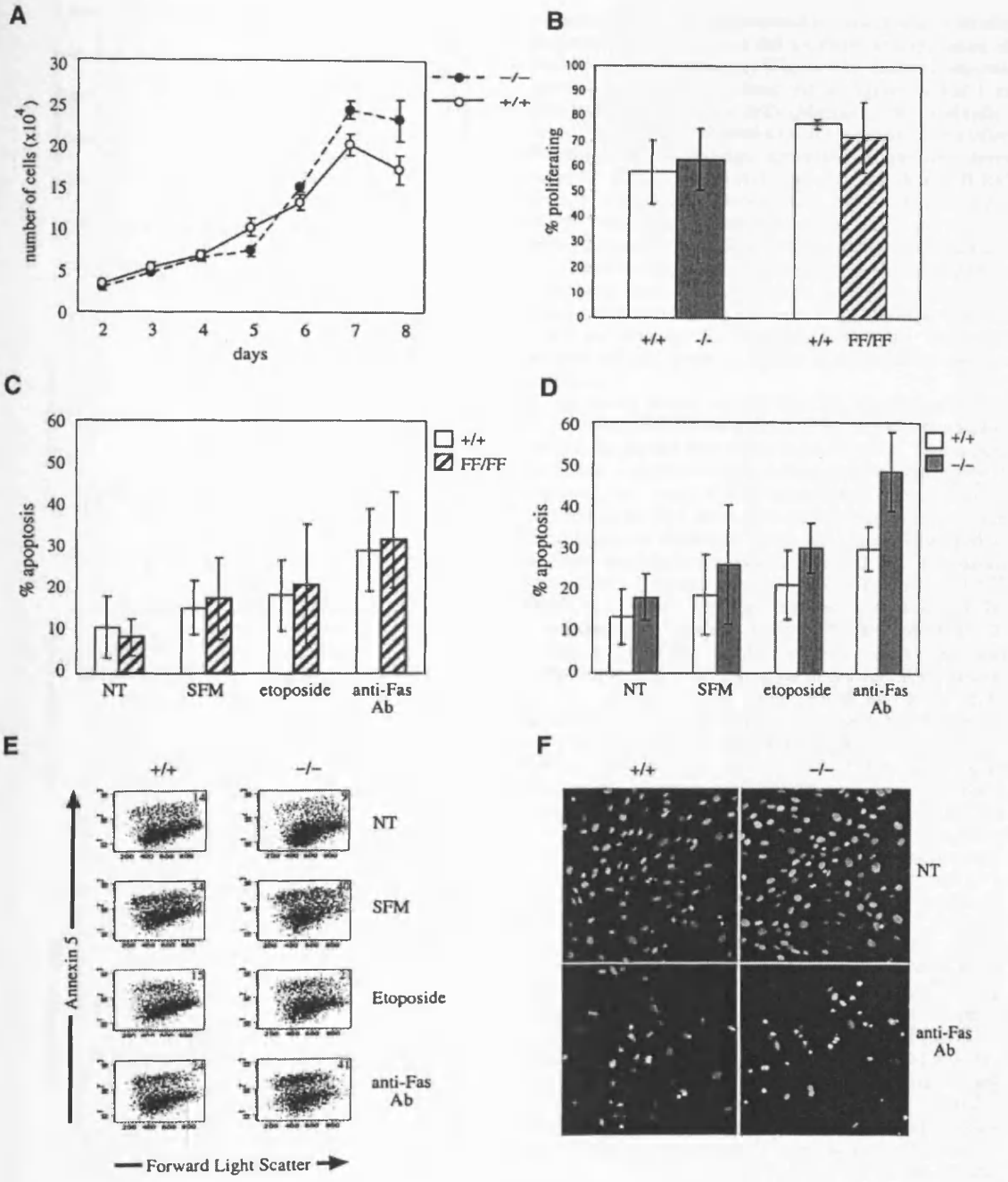

Fig. 3. Proliferation and apoptosis analysis of MEFs. (**A**) Growth curves of *raf-1*$^{+/+}$ MEFs (open circles) compared with *raf-1*$^{-/-}$ MEFs (closed circles) over 8 days in culture are shown. (**B**) DNA synthesis of *raf-1*$^{-/-}$ and *raf-1*$^{FF/FF}$ primary MEFs compared with *raf-1*$^{+/+}$ cells induced by 10% serum. The data represent pooled data from four experiments of cells with each genotype. (**C** and **D**) Levels of apoptosis in *raf-1*$^{FF/FF}$ cells compared with *raf-1*$^{+/+}$ cells (C) and in *raf-1*$^{-/-}$ cells compared with *raf-1*$^{+/+}$ cells (D). Cells were either not treated (NT) or treated with serum-free media (SFM), etoposide or anti-Fas antibody for 20 h. The percentage of cells undergoing apoptosis was quantified by flow cytometric analysis of annexin V staining. Each experiment was performed seven times and the data show mean values ± standard deviation. (**E**) An example of flow cytometric analysis of annexin V staining of cells for data presented in (C) and (D). The percentage of annexin V positive cells is indicated. (**F**) Hoechst 33258 staining of apoptotic cells. *raf-1*$^{+/+}$ cells (left panels) and *raf-1*$^{-/-}$ cells (right panels) were either untreated (top panels) or treated with anti-Fas antibody (bottom panels).

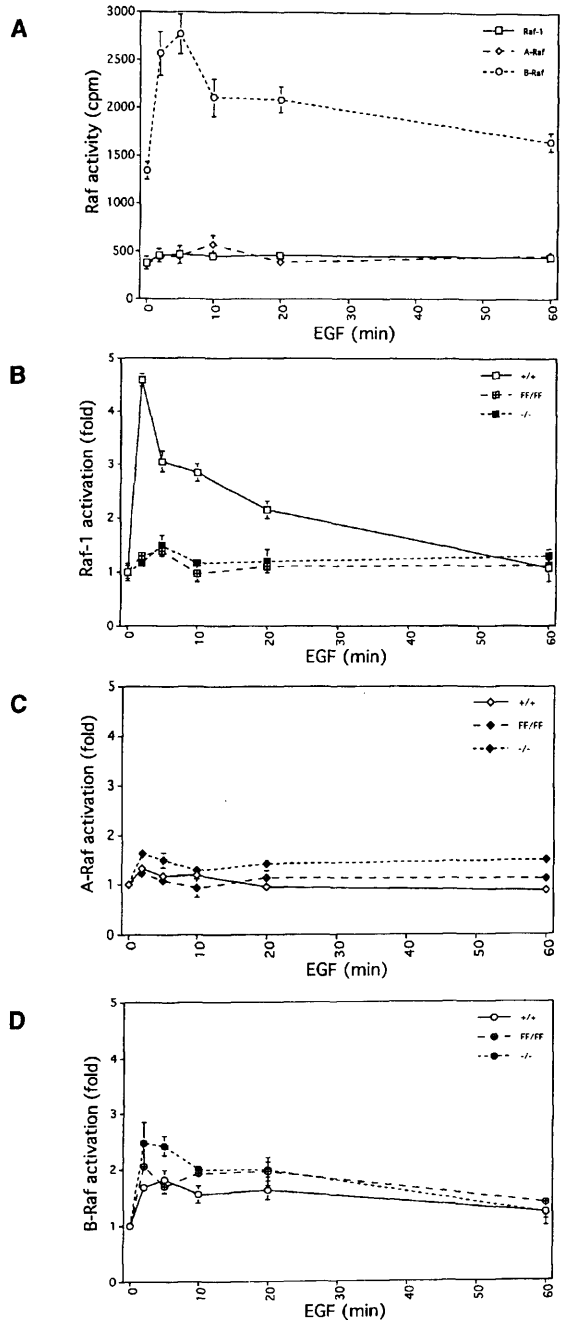

Fig. 4. Raf kinase activities. (**A**) Time course of activation of immunoprecipitated A-Raf, B-Raf and Raf-1 in the kinase cascade assay in *raf-1*$^{+/+}$ cells following stimulation with EGF. The conditions for the assay were the same as those used for routinely measuring B-Raf activity. (**B**) Time course showing the fold Raf-1 activation in *raf-1*$^{+/+}$, *raf-1*$^{-/-}$ and *raf-1*$^{FF/FF}$ MEFs following EGF stimulation. Standard conditions for measuring Raf-1 activity were utilized. (**C**) Time course showing the fold A-Raf activation in MEFs following EGF stimulation. The conditions were the same as for the Raf-1 assay. (**D**) Time course showing the fold B-Raf activation in MEFs following EGF stimulation. The B-Raf assay conditions were utilized. Each experiment was performed in triplicate and error bars show standard deviations.

increased by ~2-fold and returned to basal levels by 60 min (Figure 4A). However, we did not detect any activation of Raf-1 or A-Raf in this assay (Figure 4A), despite numerous reports previously describing the activation of Raf-1 in growth factor stimulated cells (Marshall, 1994 and references therein). We obtained similar results using two other B-Raf-specific antibodies, generated to peptides from different regions of B-Raf, but did not detect B-Raf activity with these antibodies in MEFs derived from B-*raf*$^{-/-}$ embryos (Wojnowski *et al.*, 1997; our unpublished data). However, despite this extremely strong kinase activity of B-Raf, the protein could not be detected in these cells with these antibodies even by ^{35}S-labelling or by immunoprecipitation combined with western analysis (data not shown). By contrast, A-Raf and Raf-1 are present at high levels in MEFs as detected by western analysis.

The above results suggest that the specific activity of B-Raf towards MEK as measured by this kinase cascade assay is far greater than either Raf-1 or A-Raf. To examine Raf-1 and A-Raf activation, we increased the sensitivity of the assay by using 10-fold more lysate (1 mg) and by increasing the first incubation period from 15 to 30 min (Materials and methods). These have been developed as standard conditions for measuring Raf-1 activity (Marais *et al.*, 1997). Immortalized *raf-1*$^{+/+}$, *raf-1*$^{-/-}$ and *raf-1*$^{FF/FF}$ MEFs were made quiescent and stimulated with EGF, platelet-derived growth factor (PDGF), phorbol 12-myristate 13-acetate (PMA) or lysophosphatidic acid (LPA) over a time course of up to 60 min. Raf-1 kinase activity was stimulated 4- to 6-fold in *raf-1*$^{+/+}$ cells following 2–5 min treatment with EGF and returned to basal levels within 60 min (Figure 4B). As expected, no Raf-1 kinase activity was detected in the *raf-1*$^{-/-}$ cells (Figure 4B). In the *raf-1*$^{FF/FF}$ MEFs, no activation of Raf-1 was detected in response to EGF; the level of activity observed was comparable to that in the *raf-1*$^{-/-}$ cells and to background levels in assays performed without substrate. The same Raf-1 activation results were obtained upon stimulation with PDGF, PMA and LPA (data not shown). In *raf-1*$^{+/+}$ cells, A-Raf kinase activity was much lower than Raf-1 activity and was stimulated only by 1.3-fold upon 2 min treatment with EGF. Similar levels of A-Raf activity were detected in the *raf-1*$^{-/-}$ and *raf-1*$^{FF/FF}$ cells compared with *raf-1*$^{+/+}$ cells (Figure 4C). We compared B-Raf activation in the *raf-1*$^{+/+}$, *raf-1*$^{-/-}$ and *raf-1*$^{FF/FF}$ cells using the assay conditions described above for B-Raf. The levels of basal B-Raf kinase activity in the *raf-1*$^{-/-}$ and *raf-1*$^{FF/FF}$ cells were similar to that observed in *raf-1*$^{+/+}$ cells (Figure 4D). The time course of activation by EGF was similar in the three cell lines, although the level of induction of B-Raf in *raf-1*$^{-/-}$ and *raf-1*$^{FF/FF}$ was elevated slightly compared with *raf-1*$^{+/+}$ cells.

ERK activation in the mutant cells

To measure ERK activation, cells were made quiescent and stimulated with EGF and levels of phospho-ERK were assessed. In the *raf-1*$^{+/+}$ cells, phospho-ERK increased following 2 min of EGF treatment and continued to increase up to 5 min of treatment but reached basal levels after 60 min (Figure 5A). For the *raf-1*$^{-/-}$ and *raf-1*$^{FF/FF}$ cells, the level of phospho-ERK was similar to that in the *raf-1*$^{+/+}$ cells (Figure 5A). ERK phosphorylation was

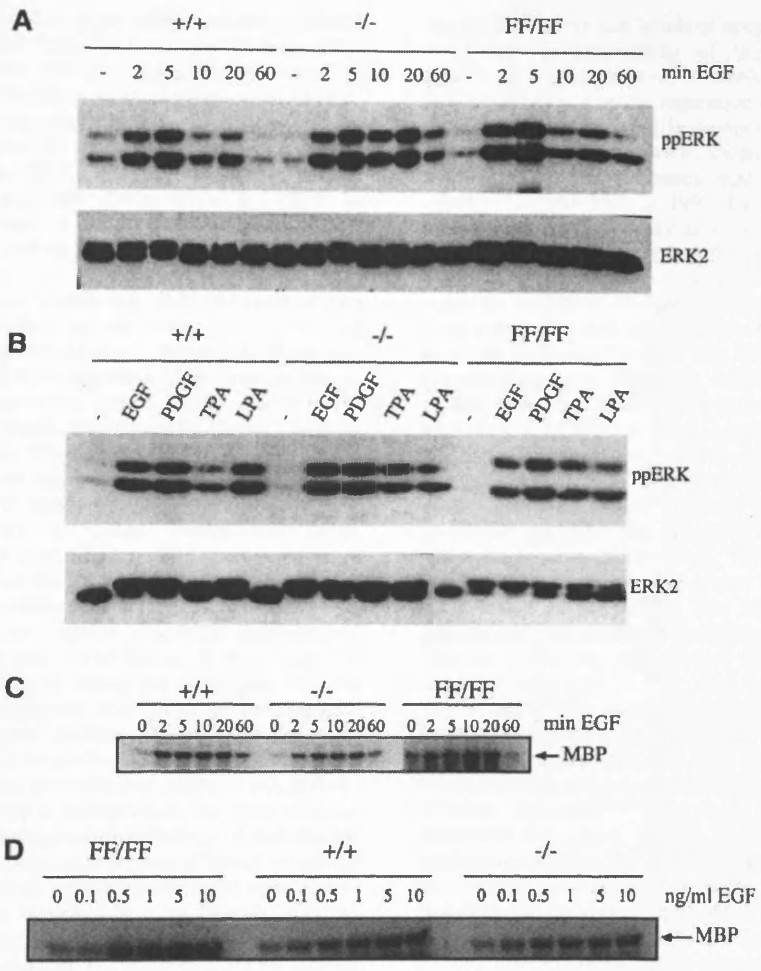

Fig. 5. ERK activation. (**A**) Stimulation of ERK phosphorylation in *raf-1*$^{+/+}$, *raf-1*$^{-/-}$ and *raf-1*$^{FF/FF}$ MEFs over a time course of EGF treatment. (**B**) Stimulation of ERK phosphorylation in *raf-1*$^{+/+}$, *raf-1*$^{-/-}$ and *raf-1*$^{FF/FF}$ MEFs following treatment with different stimuli for 10 min. The blots in (A) and (B) were incubated with an anti-phosphoERK antibody (top panels) and an anti-ERK2 antibody (bottom panels) to control for protein loading. (**C**) ERK activation in *raf-1*$^{+/+}$, *raf-1*$^{-/-}$ and *raf-1*$^{FF/FF}$ MEFs over a time course of EGF treatment as measured by the immunocomplex MBP kinase assay. (**D**) ERK activation in *raf-1*$^{+/+}$, *raf-1*$^{-/-}$ and *raf-1*$^{FF/FF}$ MEFs following stimulation with different concentrations of EGF for 10 min as measured by the MBP kinase assay.

assessed in cells that were made quiescent and then stimulated with EGF, PDGF, serum, LPA and PMA for 10 min (Figure 5B). In the *raf-1*$^{+/+}$ cells, ERK phosphorylation was induced following treatment with all stimuli. A similar level of ERK phosphorylation was observed in the *raf-1*$^{-/-}$ and *raf-1*$^{FF/FF}$ cells with all stimuli (Figure 5B). ERK activation was also measured by using myelin basic protein (MBP) as a substrate for immunoprecipitated p42ERK. As with the ERK phosphorylation data, ERK activation increased in all cells following 2 min EGF treatment and reached maximum at 10 min (Figure 5C). There was no difference observed in either the time course or level of ERK activity between the *raf-1*$^{+/+}$, *raf-1*$^{-/-}$ or *raf-1*$^{FF/FF}$ cells following EGF treatment (Figure 5C). ERK activation was also assessed upon stimulation of quiescent cells with sub-saturating amounts of EGF. MEFs of each genotype were made quiescent and then stimulated with varying concentrations of EGF from 0 to 10 ng/ml for 10 min. With increasing doses of EGF, a greater level of ERK activation was observed in all cell lines (Figure 5D). However, no difference was observed in the level of MBP phosphorylation upon treatment with any given dose of EGF between the *raf-1*$^{+/+}$, *raf-1*$^{-/-}$ and *raf-1*$^{FF/FF}$ cells (Figure 5D).

Discussion

The Ras/Raf/MEK/ERK cascade links the activation of cell surface receptors at the membrane with downstream events in the nucleus (Marshall, 1994). A wealth of biochemical data have indicated a role for the Raf-1 protein kinase in this pathway (Dent *et al.*, 1992; Howe *et al.*, 1992; Kyriakis *et al.*, 1992; Samuels *et al.*, 1993). Genetic data in *Drosophila* and *Caenorhabditis elegans* have provided evidence that the Raf homologues in these species stimulate MEK and ERK activation and mediate

many of the proliferative and differentiation signals induced by RTKs and Ras (Dickson and Hafen, 1994; Eisenmann and Kim, 1994). Inhibition of Raf-1 in fibroblasts using antisense or dominant-negative expressing constructs disrupts proliferation induced by serum, transformation induced by oncogenic Ras and growth factor activation of the ERKs (Kolch *et al.*, 1991; Schaap *et al.*, 1993; Chao *et al.*, 1994; Troppmair *et al.*, 1994). In this study we show that, although Raf-1 is not the only physiological MEK activator, it is essential for mouse development.

The *raf-1*$^{-/-}$ embryo phenotype reported here shows defects in vascularization and placenta development as well as increased apoptosis of many tissues. On the mixed inbred 129Ola/C57BL6 background there was an earlier lethal phenotype than on the mixed 129Ola/MF-1 background. This strain-specific phenotype is almost identical to that described by Wojnowski *et al.* (1998), who generated homozygous mice with a hypomorphic allele for *raf-1* that had 10% residual kinase activity on inbred (C57BL6) and outbred (CD-1) genetic backgrounds. In the manuscript by Mikula *et al.* (2001), *raf-1*$^{-/-}$ embryos were established primarily on the inbred 129Sv background and these also showed increased apoptosis of fetal liver cells and MEFs as well as similar placental deficiencies. However, those embryos survived to a later stage of development (E12.5–16.5) than the embryos on the 129Ola/C57BL6 background and they did not possess yolk sac vascularization defects. These differences in phenotype are likely to be attributable to different genetic modifiers in each strain, the nature of which is not known.

On the 129Ola/C57BL6 background, the most striking defect in the *raf-1*$^{-/-}$ embryos is the absence of endothelial cells in the yolk sac and disorganization of blood vessels in the embryo (Figure 1E–I). The establishment and modelling of blood vessels is controlled by ligands such as vascular endothelial growth factors (VEGFs), angiopoietins and ephrins that modulate the activity of RTKs (Risau, 1997). Vasculogenesis appears to be mediated by VEGF through the VEGF–R2 RTK while angiogenesis is mediated by VEGF through the VEGF–R1 RTK as well as angiopoietins at later stages of development (Fong *et al.*, 1995; Sato *et al.*, 1995; Shalaby *et al.*, 1995; Hanahan *et al.*, 1997). The lack of vascularization in the yolk sac of the *raf-1*-deficient mice suggests a link between Raf-1 and VEGF–R2 signalling and/or VEGF/VEGFR expression *in vivo* that cannot be compensated by other Raf proteins. VEGF–R2 has also been implicated in the determination of the haematoangioblast progenitor (Shalaby *et al.*, 1995; Risau, 1997) and the data presented by Mikula *et al.* (2001) confirm that 129Sv/*raf-1*$^{-/-}$ embryos have defects in early stages of haemopoiesis. In cultured endothelial cell lines, VEGF induces Raf-1/ERK activities and stimulates mitogenesis (Takahashi *et al.*, 1999). However, the fact that the *raf-1*$^{FF/FF}$ mutant mice do not show defects in vasculogenesis and the fact that ERK activation is not disrupted in the *raf-1*$^{-/-}$ MEFs argue that the role of Raf-1 in this process is largely ERK independent.

The placental and yolk sac deficiencies could clearly contribute to the generalized growth retardation and developmental delay observed in the *raf-1*$^{-/-}$ embryos on both genetic backgrounds (Figures 1 and 2). However, in addition to this, the *raf-1*$^{-/-}$ embryos and MEFs clearly demonstrate increased levels of apoptosis, whereas there is no defect in the ability of these cells to undergo proliferation (Figures 1–3). Therefore, either endogenous Raf-1 has no role in the regulation of the cell cycle or its function in proliferation is compensated by other MEK activators. A role for Raf-1 in apoptosis has been indicated from a number of biochemical studies (Wang *et al.*, 1996; Pritchard and McMahon, 1997; Lau *et al.*, 1998) and Ras has been reported to induce apoptosis through activation of Raf-1/ERKs (Dudek *et al.*, 1997; Kauffmann-Zeh *et al.*, 1997; Downward, 1998). Activated Ras is also thought to suppress apoptosis through PKB/Akt and recently it has been shown that Akt can suppress Raf-1 activity by direct phosphorylation of serine 259 (Rommel *et al.*, 1999; Zimmermann and Moelling, 1999). The anti-apoptotic protein Bcl-2 has been shown to interact with Raf-1 and this interaction appears to be independent of Raf-1 kinase activity (Wang *et al.*, 1994). One function of this interaction may be to target Raf-1 to the outer mitochondrial membrane where it could promote resistance to apoptosis through phosphorylation of BAD, a pro-apoptotic protein (Wang *et al.*, 1996). This inhibition of BAD appears to require PI3-kinase but is ERK-independent (Neshat *et al.*, 2000). The fact that the *raf-1*$^{FF/FF}$ animals have no increased apoptosis also suggests that the role of Raf-1 in suppression of apoptosis is ERK independent *in vivo*.

The *raf-1*$^{FF/FF}$ animals have no detectable mutant phenotype although we cannot yet exclude the possibility that they are not more or less susceptible to stressful situations such as bacterial infections or tumorigenesis. In addition, the *raf-1*$^{FF/FF}$ phenotype has so far only been examined on mixed genetic backgrounds and further backcrossing to the MF-1 and C57BL6 strains may reveal phenotypic heterogeneity between strains, as has been revealed for the *raf-1*$^{-/-}$ animals. The *raf-1*$^{FF/FF}$ animals express a mutant version of Raf-1 that shows no detectable activity towards MEK in the immunoprecipitation kinase cascade assay (Figure 4B), a result that supports our previous data in COS cells, demonstrating that overexpressed RafFF has virtually no MEK kinase activity (Marais *et al.*, 1995). It is possible that RafFF possesses extremely low levels of MEK kinase activity that are beyond experimental detection but are sufficient to allow survival of the RafFF animals. This would then suggest that in some cell types, Raf-1 is the limiting MEK activator, and would explain the difference in survival between the *raf-1*$^{-/-}$ and *raf-1*$^{FF/FF}$ animals. However, in the studies of Wojnowski *et al.* (1998), 10% residual Raf-1 activity was found to be insufficient for mouse survival and we were unable to detect this level of Raf-1 activity in the *raf-1*$^{FF/FF}$ MEFs. We also observed no difference in the level or profile of ERK activation in the *raf-1*$^{-/-}$ and *raf-1*$^{FF/FF}$ MEFs compared with the *raf-1*$^{+/+}$ cells (as also shown by Mikula *et al.*, 2001) and, furthermore, MEK activity was detected in both the *raf-1*$^{-/-}$ and *raf-1*$^{FF/FF}$ cells (data not shown; see also Mikula *et al.*, 2001). Thus, Raf-1 activity is not required for MEK and ERK activation, at least in some cell types, presumably because other Raf isoforms or MEK activators (such as the MEKK proteins) compensate for the loss of Raf-1. We did find a slight increase in B-Raf activity in the *raf-1*$^{-/-}$ MEFs, which may in part compensate for the loss of Raf-1. Taken

together these data show that Raf-1 is not required for ERK activation at least in some cell types and yet animals expressing RafFF, a version of Raf-1 that is unable to activate MEK, survive.

Even in the *raf-1*$^{+/+}$ MEFs, the kinase activity of endogenous Raf-1 towards MEK in the immunocomplex kinase cascade assay is difficult to measure unless sensitive assay conditions are utilized (Figure 4A and B). In contrast, immunoprecipitated B-Raf from MEFs has extremely strong kinase activity towards MEK under much less sensitive assay conditions (Figure 4A), even though the B-Raf protein is difficult to detect (data not shown). In *B-raf*$^{-/-}$ MEFs, ERK activation was reduced compared with wild-type MEFs (M.Hüser, unpublished; Wojnowski *et al.*, 2000). Taken together, these data provide strong evidence that B-Raf, rather than Raf-1, is the primary Raf isotype that activates MEK/ERKs in MEFs, if not more cell types. B-Raf regulation differs from that of Raf-1. Unlike Raf-1 and A-Raf, B-Raf does not require tyrosine phosphorylation for activation, and B-Raf is reported to be activated by Rap1a, notably in PC12 cells (York *et al.*, 1998) and by TC21 (Rosario *et al.*, 1999). B-Raf also has strong basal kinase activity towards MEK that is independent of Ras, although oncogenic Ras does stimulate B-Raf activity further through a mechanism involving translocation of B-Raf to the membrane (Marais *et al.*, 1997; Mason *et al.*, 1999). Thus, although the induction of B-Raf activity by growth factors in MEFs appears to be weak (2- to 3-fold), it is possible that it is the relocation of active B-Raf to the plasma membrane in the presence of active Ras that gives the large induction of MEK/ERK activity.

What then is the role of Raf-1? Our data imply that the MEK kinase activity of Raf-1 is not essential for normal mouse development, but that the protein is required. A number of other substrates for Raf-1 have been reported including the dual specificity phosphatase Cdc25A (Galaktionov *et al.*, 1995) and the ankyrin repeat protein Tvl-1 (Lin *et al.*, 1999). Possibly, the *raf-1*$^{-/-}$ phenotype may be manifested through disruption of the activities of these other substrates, whereas RafFF may be able to phosphorylate and activate these substrates. Alternatively, the main function of Raf-1 may not be as a kinase. Raf-1 forms part of a multiprotein complex in the cell including HSP90, p50 and 14-3-3 proteins, and binding of these scaffold proteins is thought to be important for maintaining the stability of Raf-1 (Stancato *et al.*, 1993; Wartmann and Davis, 1994; Reuter *et al.*, 1995). Many of the proteins that interact with Raf-1 also interact with KSR (kinase suppressor of Ras), a putative Ras-effector protein kinase that was identified by genetic studies in *Drosophila* and *C.elegans* (Kornfeld *et al.*, 1995; Sundaram and Han, 1995; Therrien *et al.*, 1995). Studies in *C.elegans* have shown that the kinase activity of KSR is not important for its function (Stewart *et al.*, 1999). Thus, at least in some circumstances, Raf-1, like KSR, may not require its kinase activity for function, and like KSR, one of its main functions may be as a scaffold protein (Denouel-Galy *et al.*, 1998; Yu *et al.*, 1998).

During evolution, three highly conserved *raf* genes have arisen from a single prototypic gene as a result of genome duplication followed by functional adaptation. Biochemical data indicate that the three mammalian Raf enzymes are differentially utilized and the results presented here suggest that the Raf-1 protein has evolved such that its kinase activity towards MEK is not essential for mouse development, or that sufficient redundancy exists to overcome the need for Raf-1 kinase activity, but not for Raf-1 protein. A-Raf has extremely weak, if any, activity towards MEK (Figure 4 and Marais *et al.*, 1997) and is primarily located in mitochondria (Yuryev *et al.*, 2000), suggesting that it too has evolved alternative functions. Interestingly, *Drosophila raf* is more homologous to *B-raf* in many domains than *A-raf* or *raf-1*. It is now important to identify the non-MEK kinase functions of Raf-1 and A-Raf.

Materials and methods

Histology

Tissues and embryos were prepared, sectioned and then either stained with haematoxylin and eosin or processed for Ki67 immunostaining or TUNEL assay (Monkley *et al.*, 2000). The Ki67 antibody was a rabbit polyclonal antibody supplied by Dianova (Germany). Embryos and yolk sacs for whole mount staining with PECAM-1 were processed by the method described by Schlaeger *et al.* (1995).

Derivation of MEFs and immortalization

Individual embryos were dissected and cut, washed several times with cold phosphate-buffered saline (PBS) and then incubated at 4°C for 2 (*raf-1*/C57BL6) or 6 h (*raf-1*/MF-1 and *rafFF*) in 0.25% (w/v) trypsin. An aliquot of Dulbecco's modified Eagle's medium (DMEM) containing 10% FCS and 100 U/ml penicillin/streptomycin was added and the suspension was transferred to tissue culture plates and cultured. Primary cells were immortalized with the ZIPTEX virus expressing the SV40 large T antigen (Sladek and Jacobberger, 1992). Virus and cells were co-incubated in 8 μg/ml polybrene for 4–24 h and immortalized cells were grown out by continuous culture.

Proliferation and apoptosis assays

For growth curves, 2×10^4 primary cells were plated and counted at 24 h intervals in triplicate using a haemocytometer. For DNA synthesis assays the method described by Treinies *et al.* (1999) was followed. To induce apoptosis, primary cells at 80% confluency on 6 cm dishes were treated with 50 μm etoposide, 50 ng/ml anti-Fas antibody with 0.5 μm cycloheximide or serum-free medium for 20 h in a 37°C humidifying incubator. Suspension and attached cells were collected, incubated for 20 min at 37°C in fresh media and stained with annexin V (Bender MedSystems). Stained cells were assessed by FACS analysis (Becton Dickinson). Alternatively, treated cells were stained with 5 μg/ml Hoechst 33258 in PBS for 1 h at 37°C. Data were analysed by using the two-tailed unpaired *t*-test.

Kinase assays and immunoblotting

MEFs were made quiescent by culturing in DMEM containing 0.5% (v/v) FCS for at least 24 h. They were stimulated by addition of 10 ng/ml EGF, 50 ng/ml PDGF, 40 μM PMA, 200 ng/ml LPA or 20% (v/v) FCS and incubated over a time course of 0–60 min. Protein lysates were prepared as described in Luckett *et al.* (2000) for the ERK analysis or Marais *et al.* (1997) for the Raf kinase assays. Western blots were prepared and processed as described previously (Luckett *et al.*, 2000). Primary antibodies were a mouse monoclonal antibody against Thr202/Tyr204 phospho-p44/42 ERK (New England Biolabs) and a rabbit polyclonal antibody for ERK2 (Leevers and Marshall, 1992). Raf proteins were immunoprecipitated for 2 h at 4°C from 0.1–1 mg cell extract with 2 μg of anti-Raf-1 antibody (Transduction Laboratories), 4 μg of anti-B-Raf rabbit polyclonal antibody (Mason *et al.*, 1999), 2 μg of anti-B-Raf goat polyclonal antibody (Santa Cruz Biotechnology, Santa Cruz, CA) and 2 μg of anti-A-Raf mouse monoclonal antibody (Transduction Laboratories). p42 ERK was immunoprecipitated by using 5 μl rabbit anti-p42ERK polyclonal antibody (no. 122; Treinies *et al.*, 1999). The activity of each Raf protein was assessed by using the Raf kinase cascade assay using glutathione *S*-transferase (GST)–MEK, GST–ERK and MBP together with [γ-^{32}P]ATP as sequential substrates (Marais *et al.*, 1997). For B-Raf, 0.1 mg of lysate was used and the first kinase incubation period with GST–MEK and GST–ERK was for 15 min whereas for Raf-1

and A-Raf, 1 mg of lysate was used and the first incubation period was extended to 30 min. ERK activity was measured using the MBP kinase assay (Samuels *et al.*, 1993).

Supplementary data

Supplementary data for this paper are available at *The EMBO Journal* Online.

Acknowledgements

We thank Jim Norman, David Critchley, Gerry Cohen and Chris Marshall for critical reading of the manuscript, members of the Marais and Pritchard laboratories for their support, Lee Topping for help with statistics and the Division of Biomedical Services for their help. We also thank Phil Soriano for providing the ZIPTEX virus, Hugh Paterson for providing the DNA synthesis protocol and reagents, Martin McMahon for providing the C-terminal Raf-1 antibody and Rich Murray for providing targeting vectors. This work was supported by a Royal Society fellowship to C.P., BBSRC studentships to J.L. and K.M., and project grants from the Cancer Research Campaign and The Wellcome Trust. We thank these organizations for their invaluable support.

References

Barnard,D., Diaz,B., Clawson,D. and Marshall,M. (1998) Oncogenes, growth factors and phorbol esters regulate Raf-1 through common mechanisms. *Oncogene*, **17**, 1539–1547.

Barnier,J.V., Papin,C., Eychene,A., Lecoq,O. and Calothy,G. (1995) The mouse B-*raf* gene encodes multiple protein isoforms with tissue-specific expression. *J. Biol. Chem.*, **270**, 23381–23389.

Catling,A.D., Reuter,C.W., Cox,M.E., Parsons,S.J. and Weber,M.J. (1994) Partial purification of a mitogen-activated protein kinase kinase activator from bovine brain. Identification as B-Raf or a B-Raf-associated activity. *J. Biol. Chem.*, **269**, 30014–30021.

Chao,T.O., Foster,D.A., Rapp,U.R. and Rosner,M.R. (1994) Differential Raf requirement for activation of mitogen-activated protein kinase by growth factors, phorbol esters, and calcium. *J. Biol. Chem.*, **269**, 7337–7341.

Denouel-Galy,A., Douville,E.M., Warne,P.H., Papin,C., Laugier,D., Calothy,G., Downward,J. and Eychene,A. (1998) Murine Ksr interacts with MEK and inhibits Ras-induced transformation. *Curr. Biol.*, **8**, 46–55.

Dent,P., Haser,W., Haystead,T.A.J., Vincent,L.A., Roberts,T.M. and Sturgill,T.W. (1992) Activation of the mitogen-activated protein kinase kinase by v-raf in NIH3T3 cells and *in vitro*. *Science*, **257**, 1404–1407.

Dent,P., Jelinek,T., Morrison,D.K., Weber,M.J. and Sturgill,T.W. (1995) Reversal of Raf-1 activation by purified and membrane-associated protein phophatases. *Science*, **268**, 1902–1906.

Diaz,B., Barnard,D., Filson,A., Macdonald,S., King,A. and Marshall,M. (1997) Phosphorylation of Raf-1 serine 338–serine 339 is an essential regulatory event for Ras-dependent activation and biological signalling. *Mol. Cell. Biol.*, **17**, 4509–4516.

Dickson,B. and Hafen,E. (1994) Genetics of signal transduction in invertebrates. *Curr. Opin. Genet. Dev.*, **4**, 64–70.

Downward,J. (1998) Ras signalling and apoptosis. *Curr. Opin. Genet. Dev.*, **8**, 49–54.

Dudek,H., Datta,S.R., Franke,T.F., Birnbaum,M.J., Yao,R., Cooper,G.M., Segal,R.A., Kaplan,D.R. and Greenberg,M.E. (1997) Regulation of neuronal survival by the serine-threonine protein kinase Akt. *Science*, **275**, 661–665.

Eisenmann,D.M. and Kim,S.K. (1994) Signal transduction and cell fate specification during *Caenorhabditis elegans* vulval development. *Curr. Opin. Genet. Dev.*, **4**, 508–516.

Fong,G.-H., Rossant,J., Gertsenstein,M. and Breitman,M.L. (1995) Role of the flt-1 receptor tyrosine kinase in regulating the assembly of vasacular endothelium. *Nature*, **376**, 66–70.

Galaktionov,K., Jessus,C. and Beach,D. (1995) Raf1 interaction with Cdc25 phosphatase ties mitogenic signal transduction to cell cycle activation. *Genes Dev.*, **9**, 1046–1058.

Hanahan,D. (1997) Signaling vascular morphogenesis and maintenance. *Science*, **277**, 48–50.

Howe,L.R., Leevers,S.J., Gomez,N., Nakielny,S., Cohen,P. and Marshall,C.J. (1992) Activation of the MAP kinase pathway by the protein kinase raf. *Cell*, **71**, 335–342.

Jaiswal,R.K., Moodie,S.A., Wolfman,A. and Landreth,G. (1994) The mitogen-activated protein kinase cascade is activated by B-Raf in response to nerve growth factor through interaction with p21^{ras}. *Mol. Cell. Biol.*, **14**, 6944–6953.

Jelinek,T., Dent,P., Sturgill,T.W. and Weber,M.J. (1996) Ras-induced activation of Raf-1 is dependent on tyrosine phosphorylation. *Mol. Cell. Biol.*, **16**, 1027–1034.

Kauffmann-Zeh,A., Rodriguez-Viciana,P., Ulrich,E., Gilbert,C., Coffer,P., Downward,J. and Evan,G. (1997) Suppression of c-Myc-induced apoptosis by Ras signalling through PI(3)K and PKB. *Nature*, **385**, 544–548.

Kerkhoff,E. and Rapp,U.R. (1997). Induction of cell proliferation in quiescent NIH3T3 cells by oncogenic c-Raf-1. *Mol. Cell. Biol.*, **17**, 2576–2586.

Kolch,W., Heidecker,G., Lloyd,P. and Rapp,U.R. (1991) Raf-1 protein kinase is required for growth of induced NIH/3T3 cells. *Nature*, **349**, 426–428.

Kornfeld,K., Hom,D.B. and Horvitz,H.R. (1995) The *ksr*-1 gene encodes a novel protein kinase involved in ras-mediated signaling in *C.elegans*. *Cell*, **83**, 903–913.

Kuo,W.-L., Abe,M., Rhee,J., Eves,E.M., McCarthy,S.A., Yan,M., Templeton,D.J., McMahon,M. and Rich Rosner,M. (1996) Raf, but not MEK or ERK is sufficient for differentiation of hippocampal neuronal cells. *Mol. Cell. Biol.*, **16**, 1458–1470.

Kyriakis,J.M., App,H., Zhang,X.-F., Banerjee,P., Brautigan,D.L., Rapp,U.R. and Avruch,J. (1992) Raf-1 activates MAP kinase-kinase. *Nature*, **358**, 417–421.

Lau,Q.C., Brusselbach,S. and Muller,R. (1998) Abrogation of c-Raf expression induces apoptosis in tumor cells. *Oncogene*, **16**, 1899–1902.

Leevers,S.J. and Marshall,C.J. (1992) Activation of extracellular signal-regulated kinase ERK2 by p21^{ras} oncoprotein. *EMBO J.*, **11**, 569–574.

Lin,J.H., Makris,A., McMahon,C., Bear,S.E., Patriotis,C., Prasad,V.R., Brent,R., Golemis,E.A. and Tsichlis,P.N. (1999) The ankyrin repeat-containing adaptor protein Tvl-1 is a novel substrate and regulator of Raf-1. *J. Biol. Chem.*, **274**, 14706–14715.

Luckett,J.C.A., Hüser,M.B., Giagtzoglou,N., Brown,J.E. and Pritchard, C.A. (2000) Expression of the A-*raf* proto-oncogene in the normal adult and embryonic mouse. *Cell Growth Differ.*, **11**, 163–171.

Macdonald,S.G., Crews,C.M., Wu,L., Driller,J., Clark,R., Erikson,R.L. and McCormick,F. (1993) Reconstitution of the Raf-1–MEK–ERK signal transduction pathway *in vitro*. *Mol. Cell. Biol.*, **13**, 6615–6620.

Marais,R. and Marshall,C.J. (1996) Control of the ERK MAP kinase cascade by Ras and Raf. *Cancer Surv.*, **27**, 101–125.

Marais,R., Light,Y., Paterson,H.F. and Marshall,C.J. (1995) Ras recruits Raf-1 to the plasma membrane for activation by tyrosine phosphorylation. *EMBO J.*, **14**, 3136–3145.

Marais,R., Light,Y., Paterson,H.F., Mason,C.S. and Marshall,C.J. (1997) Differential regulation of Raf-1, A-Raf and B-Raf by oncogenic ras and tyrosine kinases. *J. Biol. Chem.*, **272**, 4378–4383.

Marais,R., Light,Y., Mason,C., Paterson,H., Olson,M.F. and Marshall,C.J. (1998) Requirement of Ras–GTP–Raf complexes for activation of Raf-1 by protein kinase C. *Science*, **280**, 109–112.

Marshall,C.J. (1994) MAP kinase kinase kinase, MAP kinase kinase and MAP kinase. *Curr. Opin. Genet. Dev.*, **4**, 82–89.

Mason,C.S., Springer,C.J., Cooper,R.G., Superti-Furga,G., Marshall,C.J. and Marais,R. (1999) Serine and tyrosine phophorylations cooperate in Raf-1, but not B-Raf activation. *EMBO J.*, **18**, 2137–2148.

Mikula,M. *et al.* (2001) Embryonic lethality and fetal liver apoptosis in mice lacking the *c-raf-1* gene. *EMBO J.*, **20**, 1952–1962.

Monkley,S.J. *et al.* (2000) Disruption of the *talin* gene arrests mouse development at the gastrulation stage. *Dev. Dyn.*, **219**, 560–574.

Moodie,S.A., Willumsen,B.M., Weber,M.J. and Wolfman,A. (1993) Complexes of Ras.GTP with Raf-1 and mitogen-activated protein kinase kinase. *Science*, **260**, 1658–1661.

Moodie,S.A., Paris,M., Kolch,W. and Wolfman,A. (1994) Association of MEK1 with p21^{ras}.GMPPNP is dependent on B-Raf. *Mol. Cell. Biol.*, **14**, 7153–7162.

Neshat,M.S., Raitano,A.B., Wang,H.-G., Reed,J.C. and Sawyers,C.L. (2000) The survival of the Bcr-Abl oncogene is mediated by Bad-dependent and independent pathways: roles for phosphatidylinositol 3-kinase and Raf. *Mol. Cell. Biol.*, **20**, 1179–1186.

Papin,C., Denouel-Galy,A., Laugier,D., Calothy,G. and Eychene,A. (1998) Modulation of kinase activity and oncogenic properties by alternative splicing reveals a novel regulatory mechanism for B-Raf. *J. Biol. Chem.*, **273**, 24939–24947.

Pritchard,C. and McMahon,M. (1997) Raf revealed in life-or-death decisions. *Nature Genet.*, **16**, 214–215.

Pritchard,C.A., Samuels,M.L., Bosch,E. and McMahon,M. (1995) Conditionally oncogenic forms of the A-Raf and B-Raf protein kinases display different biological and biochemical properties in NIH 3T3 cells. *Mol. Cell. Biol.*, **15**, 6430–6442.

Pritchard,C.A., Bolin,L., Slattery,R., Murray,R. and McMahon,M. (1996) Post-natal lethality and neurological and gastrointestinal defects in mice with targeted disruption of the A-Raf protein kinase gene. *Curr. Biol.*, **6**, 614–617.

Reuter,C.W.M., Catling,A.D., Jelinek,T. and Weber,M.J. (1995) Biochemical analysis of MEK activation in NIH3T3 fibroblasts. *J. Biol. Chem.*, **270**, 7644–7655.

Risau,W. (1997) Mechanisms of angiogenesis. *Nature*, **386**, 671–674.

Rommel,C., Clarke,B.A., Zimmermann,S., Nunez,L., Rossman,R., Reid,K., Moelling,K., Yancopoulos,G.D. and Glass,D.J. (1999) Differentiation stage-specific inhibition of the Raf–MEK–ERK pathway by Akt. *Science*, **286**, 1738–1741.

Rosario,M., Paterson,H.F. and Marshall,C.J. (1999) Activation of the Raf/MAP kinase cascade by the Ras-related protein TC21 is required for the TC21-mediated transformation of NIH 3T3 cells. *EMBO J.*, **18**, 1270–1279.

Samuels,M.L., Weber,M.J., Bishop,J.M. and McMahon,M. (1993) Conditional transformation of cells and rapid activation of the mitogen-activated protein kinase cascade by an estradiol-dependent human Raf-1 protein kinase. *Mol. Cell. Biol.*, **13**, 6241–6252.

Sato,T.N. *et al.* (1995) Distinct roles of the receptor tyrosine kinases Tie-1 and Tie-2 in blood vessel formation. *Nature*, **376**, 70–74.

Schaap,D., van der Wal,J., Howe,L.R., Marshall,C.J. and van Blitterswijk,W.J. (1993) A dominant-negative mutant of raf blocks mitogen-activated protein kinase activation by growth factors and oncogenic $p21^{ras}$. *J. Biol. Chem.*, **268**, 20232–20236.

Schlaeger,T.M., Qin,Y., Fujiwara,Y., Magram,J. and Sato,T.N. (1995) Vascular endothelial cell lineage-specific promoter in transgenic mice. *Development*, **121**, 1089–1098.

Shalaby,F., Rossant,J., Yamaguchi,T.P., Gertsenstein,M., Wu,X.-F., Breitman,M.L. and Schuh,A.C. (1995) Failure of blood-island formation and vasculogenesis in Flk-1-deficient mice. *Nature*, **376**, 62–66.

Sladek,T.L. and Jacobberger,J.W. (1992) Dependence of SV40 large T-antigen cell cycle regulation on T-antigen expression levels. *Oncogene*, **7**, 1305–1313.

Stancato,L.F., Chow,Y.F., Hutchison,K.A., Perdew,G.H., Jove,R. and Pratt,W.B. (1993) Raf exists in a native heterocomplex with hsp90 and p50 that can be reconstituted in a cell-free system. *J. Biol. Chem.*, **268**, 21711–21716.

Stewart,S., Sundaram,M., Zhang,Y., Lee,J., Han,M. and Guan,K.-L. (1999) Kinase suppressor of Ras forms a multiprotein signaling complex and modulates MEK localization. *Mol. Cell. Biol.*, **19**, 5523–5534.

Stokoe,D. and McCormick,F. (1997) Activation of c-raf-1 by Ras and Src through different mechanisms: activation *in vivo* and *in vitro*. *EMBO J.*, **16**, 2384–2396.

Storm,S.M., Cleveland,J.L. and Rapp,U.R. (1990) Expression of *raf* family of proto-oncogenes in normal mouse tissues. *Oncogene*, **5**, 345–351.

Sundaram,M. and Han,M. (1995) The *C.elegans ksr-1* gene encodes a novel Raf-related kinase involved in ras-mediated signal transduction. *Cell*, **83**, 889–901.

Takahashi,T., Ueno,H. and Shibuya,M. (1999) VEGF activates protein kinase C-dependent, but Ras-independent Raf–MEK–MAP kinase pathway for DNA synthesis in primary endothelial cells. *Oncogene*, **18**, 2221–2230.

Therrien,M., Chang,H.C., Solomon,N.M., Karim,F.D., Wassarman,D.A. and Rubin,G.M. (1995) KSR, a novel protein kinase required for RAS signal transduction. *Cell*, **83**, 879–888.

Traverse,S. and Cohen,P. (1994) Identification of a latent MAP kinase kinase kinase in PC-12 cells as B-Raf. *FEBS Lett.*, **350**, 13–18.

Traverse,S., Cohen,P., Paterson,H., Marshall,C., Rapp,U. and Grand,R.J. (1993) Specific association of activated MAP kinase kinase kinase (Raf) with the plasma membranes of ras-transformed retinal cells. *Oncogene*, **8**, 3175–3181.

Treinies,I., Paterson,H.F., Hooper,S., Wilson,R. and Marshall,C.J. (1999) Activated MEK stimulates expression of AP-1 components independently of phosphatidylinositol 3-kinase (PI3-kinase) but requires a PI3-kinase signal to stimulate DNA synthesis. *Mol. Cell. Biol.*, **19**, 321–329.

Troppmair,J., Bruder,J.T., Munoz,H., Lloyd,P.A., Kyriakis,J., Banerjee,P., Avruch,J. and Rapp,U.R. (1994) Mitogen-activated protein kinase/extracellular signal-regulated protein kinase activation by oncogenes, serum, and 12-*O*-tetradecanoylphorbol-13-acetate requires Raf and is necessary for transformation. *J. Biol. Chem.*, **269**, 7030–7035.

Wang,H.-G. *et al.* (1994) Apoptosis regulation by interaction of bcl-2 protein and Raf-1 kinase. *Oncogene*, **9**, 2751–2756.

Wang,H.-G., Rapp,U.R. and Reed,J.C. (1996) Bcl-2 targets the protein kinase Raf-1 to mitochondria. *Cell*, **87**, 629–638.

Wartmann,M. and Davis,R.J. (1994) The native structure of the activated Raf protein kinase is a membrane-bound multi-subunit complex. *J. Biol. Chem.*, **269**, 6695–6701.

Wojnowski,L., Zimmer,A.M., Beck,T.W., Hahn,H., Bernal,R., Rapp,U.R. and Zimmer,A. (1997) Endothelial apoptosis in Braf-deficient mice. *Nature Genet.*, **16**, 293–297.

Wojnowski,L., Stancato,L.F., Zimmer,A.M., Hahn,H., Beck,T.W., Larner,A.C., Rapp,U.R. and Zimmer,A. (1998) Craf-1 protein kinase is essential for mouse development. *Mech. Dev.*, **76**, 141–149.

Wojnowski,L., Stancato,L.F., Larner,A., Rapp,U.R. and Zimmer,A. (2000) Overlapping and specific functions of Braf and Craf-1 proto-oncogenes during mouse embryogenesis. *Mech. Dev.*, **91**, 97–104.

Wood,K.W., Sarnecki,C., Roberts,T.M. and Blenis,J. (1992) Ras mediates nerve growth factor receptor modulation of three signal-transducing protein kinases: MAP kinase, Raf-1 and RSK. *Cell*, **68**, 1041–1050.

Wood,K.W., Qi,H., D'Arcangelo,G., Armstrong,R.C., Roberts,T.M. and Halegoua,S. (1993) The cytoplasmic *raf* oncogene induces a neuronal phenotype in PC12 cells: A potential role for cellular *raf* kinases in neuronal factor signal transduction. *Proc. Natl Acad. Sci. USA*, **90**, 5016–5020.

York,R.D., Yao,H., Dillon,T., Ellig,C.L., Eckert,S.P., McCleskey,E.W. and Stork,P.J.S. (1998) Rap1 mediates sustained MAP kinase activation induced by nerve growth factor. *Nature*, **392**, 622–626.

Yu,W., Fantl,W.J., Harrowe,G. and Williams,L.T. (1998) Regulation of the MAP kinase pathway by mammalian Ksr through direct interaction with MEK and ERK. *Curr. Biol.*, **8**, 56–64.

Yuryev,A., Ono,M., Goff,S.A., Macaluso,F. and Wennogle,L.P. (2000) Isoform-specific localization of A-RAF in mitochondria. *Mol. Cell. Biol.*, **20**, 4870–4878.

Zimmermann,S. and Moelling,K. (1999) Phosphorylation and regulation of Raf by Akt (protein kinase B). *Science*, **286**, 1741–1744.

Received January 2, 2001; revised February 20, 2001; accepted February 23, 2001

SPECIAL NOTE

THIS ITEM IS BOUND IN SUCH A MANNER AND WHILE EVERY EFFORT HAS BEEN MADE TO REPRODUCE THE CENTRES, FORCE WOULD RESULT IN DAMAGE

Oncogene (2002) 21, 347–355

www.nature.com/onc

ERK signalling and oncogene transformation are not impaired in cells lacking A-Raf

Kathryn Mercer[1], Antonio Chiloeches[2], Martin Hüser[1], Michelle Kiernan[3], Richard Marais[2] and Catrin Pritchard*,[1]

[1]*Department of Biochemistry, University of Leicester, University Road, Leicester LE1 7RH, UK;* [2]*Institute of Cancer Research, 237 Fulham Road, London SW3 6JB, UK;* [3]*Department of Biological Sciences, University of Plymouth, Plymouth PL4 8AA, UK*

Previous studies have indicated an important role for the Raf family of protein kinases in controlling cellular responses to extracellular stimuli and activated oncogenes, through their ability to activate the MEK/ERKs. To investigate the specific role of A-Raf in this process we generated A-Raf deficient mouse embryonic fibroblasts (MEFs) and embryonic stem (ES) cells by gene targeting and characterized their ability to undergo proliferation, differentiation, apoptosis, ERK activation, and transformation by oncogenic Ras and Src. The A-Raf deficient cells are not disrupted for any of these processes, despite the fact that this protein is normally expressed at high levels in both cell types. This implies either that A-Raf plays no role in MEK/ERK activation, that its function is fully compensated by other Raf proteins or MEK kinases or that its role in MEK/ERK activation is highly tissue-specific. Interestingly, B-Raf and Raf-1 activity towards MEK as measured by the immunoprecipitation kinase cascade assay are both significantly increased in the A-Raf deficient MEFs.
Oncogene (2002) **21**, 347–355. DOI: 10.1038/sj/onc/1205101

Keywords: A-Raf; knockout; ERK activation; oncogene transformation

Introduction

The Raf proteins are highly conserved serine–threonine protein kinases that are integral members of intracellular signalling cascades. In mammals, the Raf family comprises three members, A-Raf, B-Raf and Raf-1, that share a high degree of sequence similarity (Daum *et al.*, 1994). The N-terminal part of the proteins comprises the regulatory domain that binds essential cofactors while the C-terminal domain comprises the catalytic kinase domain. All three kinases are known to bind Ras.GTPases and all three are translocated to the plasma membrane by oncogenic Ras (Marais *et al.*, 1997). All three proteins bind to MEK and can phosphorylate MEK in immunecomplex kinase assays (Pritchard *et al.*, 1996; Marais *et al.*, 1997; Hüser *et al.*, 2001). All three genes are ubiquitously expressed although their expression levels vary enormously between different tissues (Storm *et al.*, 1990; Barnier *et al.*, 1995; Luckett *et al.*, 2000). The best characterized signalling cascade involving the Raf proteins is the Ras/Raf/MEK/ERK cascade which is activated by a wide variety of activated cell surface receptors. The function of activated Raf proteins in this cascade appears to be to provide a signalling link between Ras and ERKs by activating MEK, the upstream activator of the ERKs. ERKs have multiple targets in the cell and allow the cell to respond appropriately to proliferative, apoptotic and differentiation signals. This cascade is also involved in mediating some of the transforming effects of activated oncogenes and inhibition studies using dominant negative and antisense constructs have shown that Raf proteins are required for transformation by v-Ha-ras and v-*src* (Kolch *et al.*, 1991; Qureshi *et al.*, 1993).

Immunoprecipitated Raf proteins differ widely in their ability to activate MEK/ERK as measured by the kinase cascade assay (Pritchard *et al.*, 1995; Marais *et al.*, 1997). B-Raf immunoprecipitated from growth factor-stimulated mouse embryonic fibroblasts (MEFs) is the strongest activator of MEK/ERK even though it is expressed at extremely low levels in this cell type (Hüser *et al.*, 2001). By contrast, A-Raf immunoprecipitated from the same cells does not measurably activate MEK/ERK (Hüser *et al.*, 2001) and A-Raf activity towards MEK have so far only been detected in primary rat ventricular myocytes stimulated with powerful hypertrophic agonists (Bogoyevitch *et al.*, 1995). Raf-1 immunoprecipitated from growth factor-stimulated MEFs also has extremely low activity towards MEK/ERK compared to B-Raf (Hüser *et al.*, 2001). On the basis of these differential activities it has been suggested that the Raf proteins may determine whether a cell undergoes cell cycle progression or arrest in response to an extracellular stimulus, by controlling the level of ERK activation (Woods *et al.*, 1997).

Despite the well established role of the Raf proteins in MEK/ERK activation, other functions for the Raf proteins have been proposed (Hagemann and Rapp,

*Correspondence: C Pritchard; E-mail: cap8@le.ac.uk
Received 16 August 2001; revised 19 October 2001; accepted 27 October 2001

1999). Besides MEK and Ras, A-Raf has also been shown to bind to the β subunit of CK2 (Hagemann *et al.*, 1997) and to pyruvate kinase M2 (M2-PK). A recent study showed that A-Raf interacts with hTOM and hTIM, two proteins involved in the mitochondrial transport system, leading to the discovery that A-Raf is located exclusively in mitochondria (Yuryev *et al.*, 2000). Recently, we (Hüser *et al.*, 2001) and others (Mikula *et al.*, 2001) provided evidence that the major function of Raf-1 is in preventing apoptosis and that this function may be independent of any effect on ERK. MEFs derived from *raf-1*$^{-/-}$ mice demonstrated increased programmed cell death (PCD) in response to several apoptotic stimuli, but ERK activation was not affected. Furthermore, we generated mice containing a Y340FY341F knockin mutation of Raf-1 and showed that, while this mutated version of Raf-1 is not able to phosphorylate and activate MEK/ERK, the apoptosis phenotype of the *raf-1*$^{-/-}$ mice is not detected (Hüser *et al.*, 2001).

To further investigate the *in vivo* role of A-Raf we have derived A-Raf deficient mice and cell lines (Pritchard *et al.*, 1996). The *A-raf* gene is X chromosome linked and, therefore, through one targeting event in male embryonic stem (ES) cells, we were able to generate *A-raf*$^{-/Y}$ ES cells. We have previously shown that male mice generated from these cells survive to birth but suffer from progressive wasting, have a variety of postnatal neurological abnormalities, and eventually die 10–21 days after birth (Pritchard *et al.*, 1996). In this report we have derived *A-raf*$^{-/Y}$ MEFs and characterized these cells for their ability to proliferate, to undergo apoptosis, to activate the ERKs and to be transformed by Ras and Src oncogenes. The potential of A-*raf*$^{-/Y}$ ES cells to form differentiated tissues in teratomas was also tested. Our data show that A-Raf is not involved in mediating any of these cellular responses suggesting that this Raf isoform is not an important component of the Ras/Raf/MEK/ERK cascade, at least in the cell types studied.

Results

Generation of A-Raf$^{-/Y}$ *ES cells and MEFs*

Two independent A-Raf deficient (*A-raf*$^{-/Y}$) ES cell lines, clones 89 and 99, were generated by gene targeting of E14.1a ES cells with the pTCA–Raf targeting vector as previously reported (Pritchard *et al.*, 1996). To obtain *A-raf*$^{-/Y}$ MEFs and sibling control *A-raf*$^{+/Y}$ MEFs, female *A-raf*$^{+/-}$ mice on the C57BL6 genetic background were mated to C57BL6 wild-type males. Embryos were collected at E14.5 and fibroblasts were grown out from the embryos by standard procedures (Pritchard *et al.*, 1996; Hüser *et al.*, 2001). Genotypes of each cell line were confirmed by PCR analysis of DNA obtained from each individual culture (Figure 1a). Western blot analysis with an anti-A-Raf antibody was used to confirm that the ES cells and

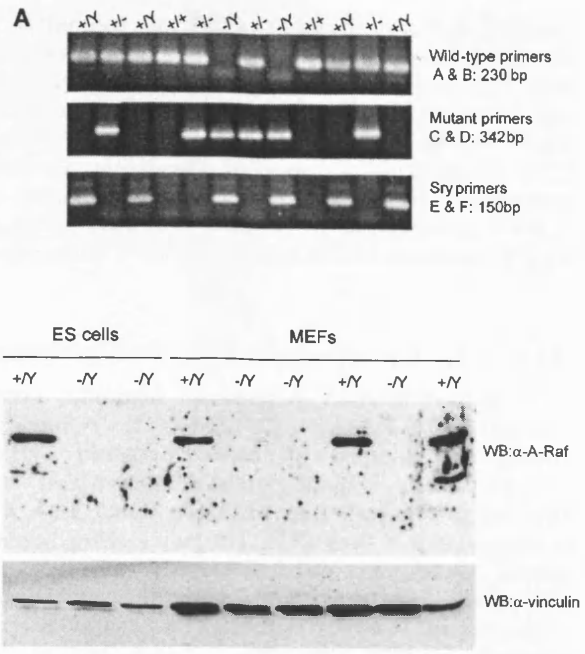

Figure 1 (**a**) PCR genotyping of MEFs from a typical litter arising from an *A-raf*$^{+/-}$ × C57BL6 intercross. PCR genotyping results for wild-type primers A/B (230 bp product), mutant primers C/D (342 bp product) and Sry primers E/F (approx. 150 bp product) are indicated. The genotype of each MEF is indicated at the top of each lane. (**b**) Western blot analysis of ES cells and MEFs. Western blot analysis with an anti-A-Raf antibody (top panel) was used to confirm the presence/absence of the A-Raf protein in each cell line. The blot was analysed with an antibody against vinculin to confirm protein loading (bottom panel)

MEFs were indeed deficient for the A-Raf protein and that no truncated protein products were expressed from the targeted gene (Figure 1b; top panel). The *A-raf*$^{-/Y}$ MEFs and ES cells were normal in morphology compared to *A-raf*$^{+/Y}$ cells and showed no difference in contact inhibited growth, cell adhesion, cell shape or motility (data not shown).

A-raf$^{-/Y}$ *cells do not show significant defects in cell proliferation or apoptosis*

The growth rates of the A-*raf*$^{-/Y}$ primary MEFs were compared to the growth rates of the A-*raf*$^{+/Y}$ MEFs over 6 days in the culture. While some variation was observed between the growth rates of individual MEF cell lines, this did not reflect on the genotype of the MEF cell line (Figure 2a). The *A-raf*$^{-/Y}$ ES cells also did not show any difference in growth over 7 days in culture compared to *A-raf*$^{+/Y}$ cells (data not shown). DNA synthesis was measured by assessing bromodeoxyuridine incorporation in three different A-*raf*$^{+/Y}$ MEFs and three different A-*raf*$^{-/Y}$ MEFs that had been made quiescent and then stimulated with 10% foetal calf serum. Each MEF line was analysed at least twice and the data were pooled. While the A-*raf*$^{-/Y}$ MEFs appeared to show a slight reduction in DNA

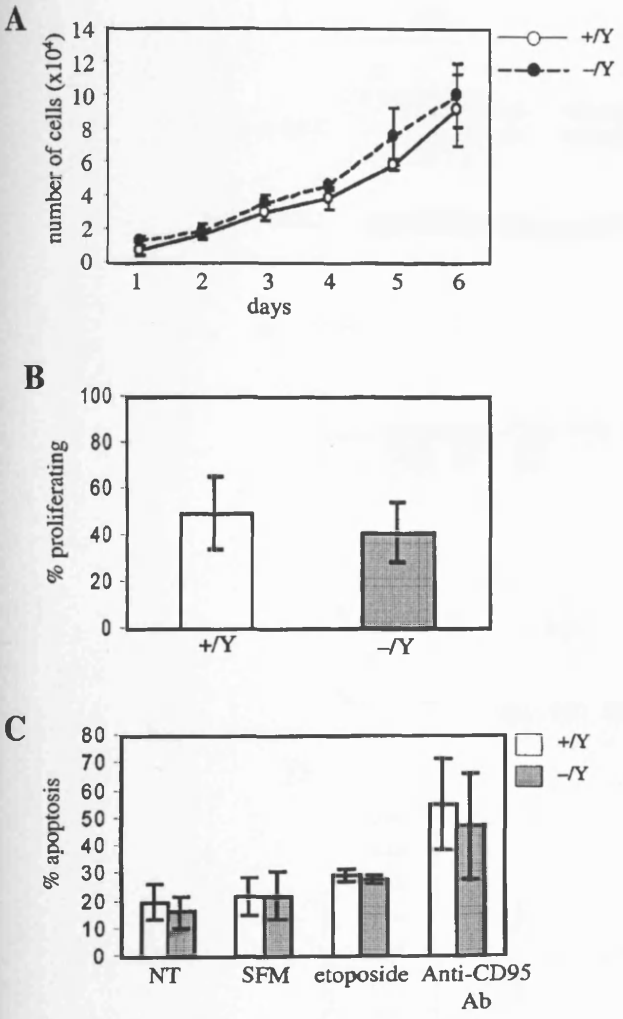

Figure 2 Apoptosis and proliferation analysis of MEFs. (**a**) Growth curves of A-*raf*$^{+/Y}$ MEFs (open circles) compared to A-*raf*$^{-/Y}$ MEFs (closed circles) over 6 days in culture are shown. (**b**) DNA synthesis of A-*raf*$^{+/Y}$ primary MEFs compared to A-*raf*$^{-/Y}$ cells induced by 10% serum. The data represent pooled data from nine experiments of cells with each genotype. (**c**) Levels of apoptosis in A-*raf*$^{+/Y}$ cells compared to A-*raf*$^{-/Y}$ cells. Cells were either not treated (NT) or treated with serum-free media (SFM), etoposide or anti-CD95 antibody for 20 h. The percentage of cells undergoing apoptosis was quantified by flow cytometric analysis of annexin V staining. Each experiment was performed three times and the data shows mean values ± standard deviation

synthesis (Figure 2b), this difference was not significant, as measured by the unpaired *t*-test ($n=9$; 95% CI for difference -5.68% to 22.83%, $P=0.22$). Apoptosis was induced by treatment of primary MEFs with etoposide, anti-CD95 antibody or by serum withdrawal (SFM), and cell death was assessed by annexin V staining using conditions identical to those previously used to assess the *raf-1*$^{-/-}$ apoptotic phenotype (Hüser *et al*., 2001). For the A-*raf*$^{+/Y}$ cells, significant levels of apoptosis were observed with each of the apoptosis inducers, although more PCD was observed with the anti-CD95 antibody than either etoposide or SFM. This difference in PCD induced by the different treatments appears to be a general characteristic of primary MEFs as the same results were obtained with *raf-1*$^{+/+}$ cells (Hüser *et al*., 2001). However, in contrast to *raf-1*$^{-/-}$ cells (Hüser *et al*., 2001) the A-*raf*$^{-/Y}$ cells showed no significant increase or decrease in PCD upon treatment with these apoptotic agents compared to A-*raf*$^{+/Y}$ cells ($P=1$ for serum withdrawal, $P=0.33$ for etoposide; $P=0.63$ for anti-CD95 antibody; Figure 2c).

Assessment of ERK and Raf activation in A-raf$^{-/Y}$ *MEFs*

We next examined the level of ERK activation in A-*raf*$^{+/Y}$ and A-*raf*$^{-/Y}$ MEFs by assessment of the level of ERK phosphorylation in response to growth factor treatment. Primary *A-raf*$^{+/Y}$ and *A-raf*$^{-/Y}$ MEFs were made quiescent and then stimulated with epidermal growth factor (EGF) over a time course of up to 10 min (Materials and methods). Protein lysates were prepared and Western blots were incubated with an antibody specific for phospho-ERK. In the *A-raf*$^{+/Y}$ cells, the level of phospho-ERK increased following treatment with EGF and the level of phospho-ERK was similar in the *A-raf*$^{-/Y}$ cells (Figure 3a). ERK phosphorylation was also assessed in three other *A-raf*$^{-/Y}$ MEF clones and in three other *A-raf*$^{+/Y}$ clones following EGF treatment for 10 min and a similar level of ERK phosphorylation was observed for clones of all genotypes (data not shown). ERK activation was also measured by performing an immunecomplex kinase assay using myelin basic protein (MBP) as a substrate for immunoprecipitated p42ERK. As with the ERK phosphorylation data, no difference in ERK activity was observed between the A-*raf*$^{+/Y}$ and A-*raf*$^{-/Y}$ cells following EGF treatment (Figure 3b). In addition, no difference in ERK activation was observed upon stimulation of the cells with platelet-derived growth factor or serum (data not shown).

No difference in the level of expression of Raf-1 was observed in the A-*raf*$^{-/Y}$ cells compared to the A-*raf*$^{+/Y}$ cells (Figure 3c). It was not possible to assess the level of B-Raf expression in these cells since this protein is expressed at extremely low levels in primary MEFs (Hüser *et al*., 2001). Therefore, we analysed whether there were changes in Raf-1 and B-Raf activities in the A-*raf*$^{-/Y}$ cells by using the immunoprecipitation MEK/ERK kinase cascade assay (Marais *et al*., 1997; Hüser *et al*., 2001). Since B-Raf is the most active Raf isotype in these assays in MEFs, we used the conditions optimized for the Raf-1 assay and decreased the sensitivity of the assay for B-Raf by using 10 times less protein lysate than for the Raf-1 assay (Materials and methods). Immortalized *A-raf*$^{+/Y}$ and *A-raf*$^{-/Y}$ MEFs were made quiescent and stimulated with EGF over a time course of up to 10 min. Consistent with our previous observations, when stimulated with EGF, B-Raf activity in A-*raf*$^{+/Y}$ cells was increased by ~1.5-fold and Raf-1 activity was increased by ~2.4-fold (Figure 3d). Both activities reached maximum stimulation at the 5 min time point

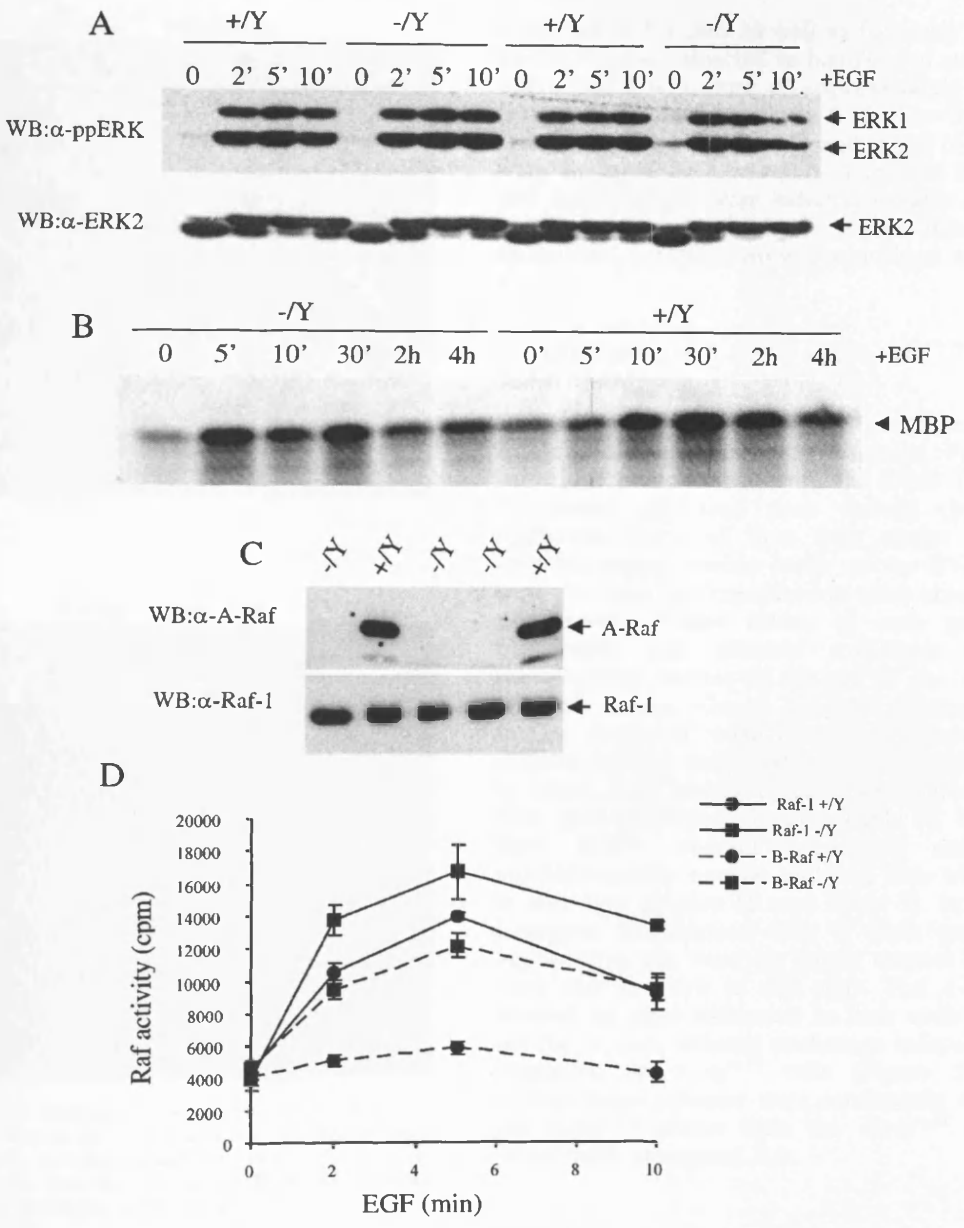

Figure 3 (**a**) Induction of ERK phosphorylation by EGF in MEFs. Primary A-*raf*$^{+/Y}$ and A-*raf*$^{-/Y}$ MEFs were treated with EGF over a time course of 0, 2, 5 and 10 min, and protein cell lysates were harvested. Western blots were prepared and analysed with an antibody against phosphoERK (top) or against total ERK2 (bottom). No difference in the level or time course of ERK phosphorylation was observed between the cell lines of each genotype. (**b**) Induction of ERK activation by EGF in MEFs. Primary A-*raf*$^{+/Y}$ and A-*raf*$^{-/Y}$ MEFs were made quiescent and then treated with EGF over a time course of 0, 5, 10, 30 min, and 2 and 4 h. Protein cell lysates were harvested and p42ERK was immunoprecipitated. ERK activity was measured by using the MBP kinase assay. No difference in the level or time course of ERK activation was observed between the cell lines of each genotype. (**c**) Assessment of Raf-1 expression levels in MEFs. Western blots were prepared and analysed with an antibody against A-Raf (top panel) or Raf-1 (bottom panel). Similar levels of Raf-1 are expressed in the A-*raf*$^{+/Y}$ and A-*raf*$^{-/Y}$ samples. (**d**) Measurement of B-Raf and Raf-1 kinase activities. Immortalized MEFs were made quiescent and treated with EGF over a time course of 0, 2, 5 and 10 min. Protein cell lysates were harvested and B-Raf or Raf-1 was immunoprecipitated. Raf activity was measured using the cascade assay (Materials and methods). Both B-Raf and Raf-1 activities are elevated in the A-*raf*$^{-/Y}$ cells compared to the A-*raf*$^{+/Y}$ cells. Each experiment was performed three times in triplicate and error bars show standard deviations

(Figure 3d). In A-*raf*$^{-/Y}$ cells stimulated with EGF, B-Raf activity increased by ~2.4-fold and Raf-1 activity increased by ~3.1-fold. Therefore, both B-Raf and Raf-1 kinase activities were significantly increased in the A-*raf*$^{-/Y}$ cells compared to the A-*raf*$^{+/Y}$ cells. At the 5 min time point the mean difference between the Raf-1 activities in the A-*raf*$^{+/Y}$ and A-*raf*$^{-/Y}$ cells was 4704 c.p.m. ($n=6$; 95% CI for difference 2381–

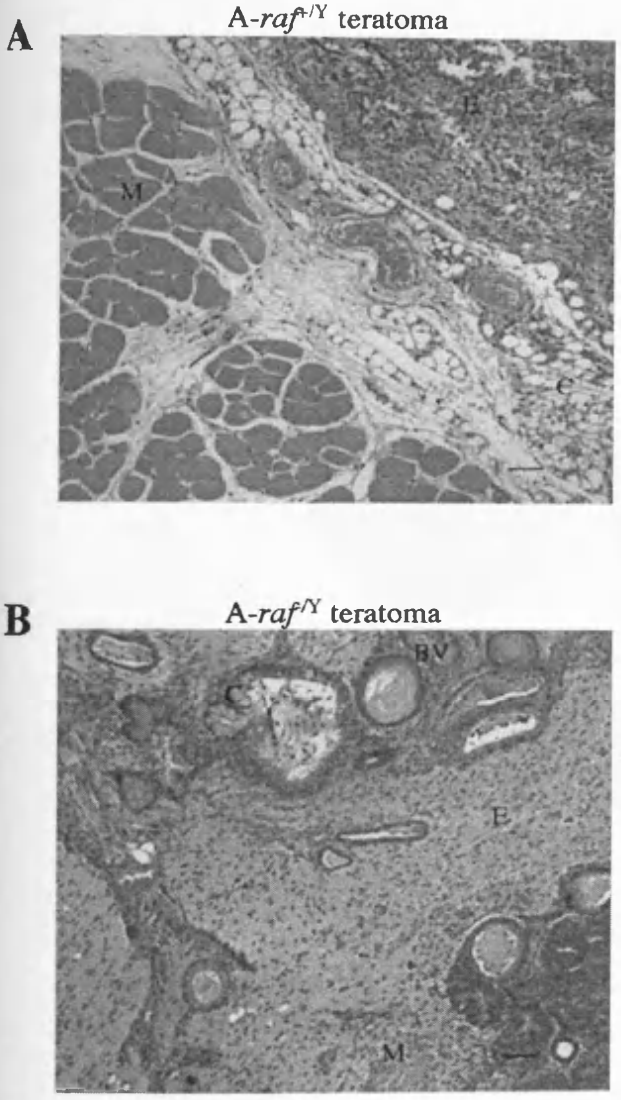

Figure 4 Histological analysis of teratomas derived from A-*raf*$^{+/Y}$ ES cells (**a**) and A-*raf*$^{-/Y}$ ES cells (**b**). Teratomas were fixed, embedded in paraffin, sectioned and stained with haematoxylin and eosin. Scale bar represents 100 μm. M = muscle, BV = blood vessel, E = epithelia, C = cartilage

7028 c.p.m. $P = 0.0006$) whereas the mean difference between the B-Raf activities was 7272 c.p.m. ($n = 6$; 95% CI for difference 4470 – 10073 c.p.m. $P < 0.0001$). Therefore the increase in B-Raf activity in the A-*raf*$^{-/Y}$ cells is slightly higher than the increase in Raf-1 activity. Similar results were obtained in three independent assays for two different MEFs of each genotype.

A-raf$^{-/Y}$ *ES cells are capable of differentiating to various cell lineages*

A well established method to study the differentiation potential of ES cells is to inject them subcutaneously into syngeneic hosts, whereby they form benign, solid teratomas containing derivatives of all three germ layers. Therefore, teratomas were produced for wild-type E14.1a ES cells as well as for *A-raf*$^{-/Y}$ ES clones 89 and 99 and subjected to histological analysis. All ES cells formed teratomas of approximately equal weight (For *A-raf*$^{+/Y}$ mean weight = 0.58 *g*, $n = 3$; for *A-raf*$^{-/Y}$ mean weight = 0.6 *g*, $n = 5$) and none of the tumours were invasive or metastatic. Tumours from *A-raf*$^{+/Y}$ and A-*raf*$^{-/Y}$ cells were indistinguishable and exhibited a chaotic arrangement of various tissues including epithelium, cartilage, muscle and blood vessels (Figure 4).

Transformation of A-raf$^{-/Y}$ *and* A-raf-1$^{+/Y}$ *MEFs by* ras *and* src *oncogenes*

The ability of the *A-raf*$^{-/Y}$ MEFs to be transformed by Ras and Src oncogenes was assessed. Primary MEFs were first immortalized with the SV40 T antigen and permanent cell lines were derived (Materials and methods). Only cell lines with similar growth rates and expressing similar levels of the SV40 T antigen were analysed and compared in these experiments (data not shown). Three clones of each genotype were transfected with plasmid constructs expressing a transforming variant of Ha-ras or the chicken v-Src tyrosine kinase. Clones of each genotype expressing similar levels of v-Ha-Ras or v-Src were analysed (Figure 5a) and subjected to soft agar assays in order to assess their ability to undergo anchorage independent growth (Figure 5b and Table 1). The immortalized MEFs without a second oncogene were morphologically normal and had little ability to grow in soft agar (Figure 5b and Table 1). In contrast, the oncogene transformed cells of both genotypes were highly refractile, were no longer contact inhibited and were able to grow in soft agar. The *A-raf*$^{-/Y}$ MEFs showed no clear difference in their ability to undergo Ha-*ras* or v-*src* induced anchorage independent growth compared to *A-raf*$^{+/Y}$ cells (Figure 5b), although slightly more colonies were consistently obtained with the A-*raf*$^{-/Y}$ clones than the A-*raf*$^{+/Y}$ clones transfected with oncogenic Ras.

Discussion

The A-*raf* gene was originally identified by screening a mouse spleen cDNA library with a v-*raf* probe at low stringency (Huleihel *et al*., 1986). The gene was subsequently mapped to the X chromosome and shown to have 70 – 80% nucleotide sequence identity to *raf-1*. Compared to Raf-1 and B-Raf, relatively few biochemical studies have focussed on A-Raf function, despite the fact that this protein is expressed at high levels in many cell types (Luckett *et al*., 2000). We have taken the approach of using gene knockout technology to further understand the function of A-Raf in intracellular signalling *in vivo*.

As with all Raf proteins, A-Raf has been shown to bind to Ras and MEK *in vitro* (Hagemann and Rapp, 1999). However, in comparison to the other Raf proteins, the kinase domain of A-Raf has a much

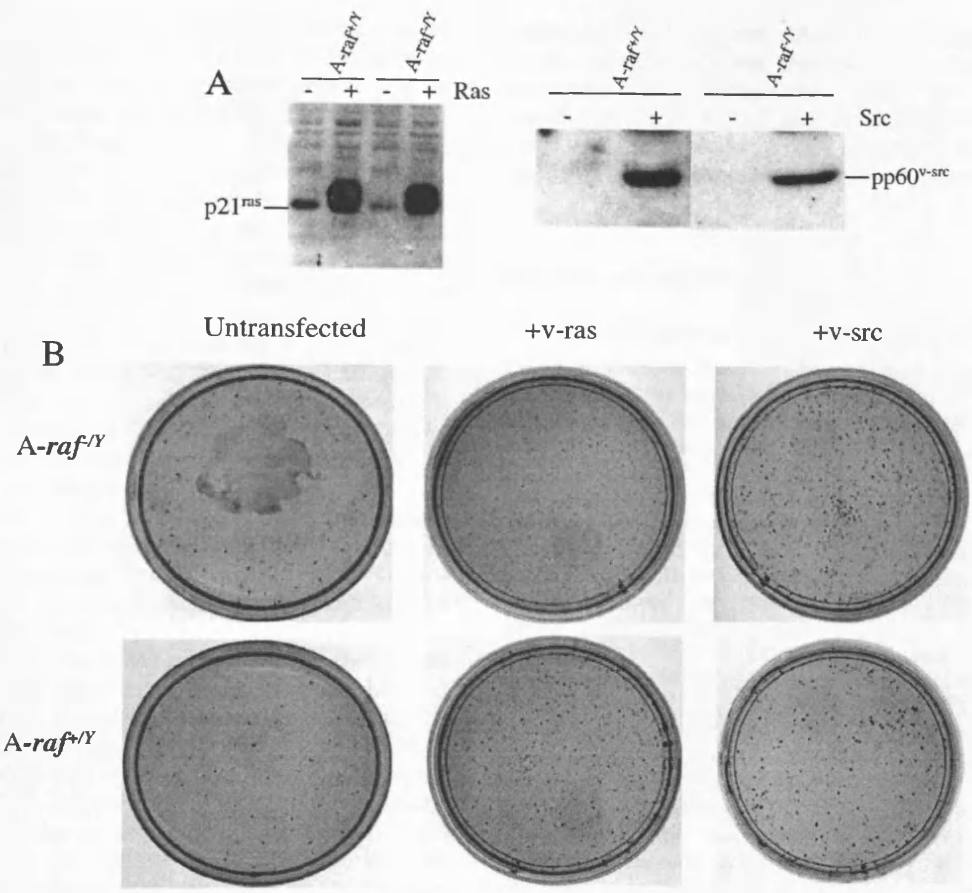

Figure 5 Transformation of MEFs with Ras and Src oncogenes. (**a**) Expression of $p21^{ras}$ (left panel) and $pp60^{v-src}$ (right panel) in A-*raf*$^{-/Y}$ and A-*raf*$^{+/Y}$ MEFs transfected with pZAS4ras and pZAS4src plasmids. Expression levels of the oncogenes are similar in the MEFs of each genotype. Although endogenous p21ras expression is also detected in the untransfected cells, expression of oncogenic Ha-Ras is evident from the higher levels of expression in the transfected cells. (**b**) Anchorage independent growth of MEFs transfected with Ras and Src oncogenes. Soft agar assays were performed as described in Materials and methods. Many colonies were detected in the Ras and Src transfected cells of both genotypes, but not in the untransfected cells

Table 1 Quantification of numbers of colonies obtained in soft agar assays of A-*raf*$^{+/Y}$ and A-*raf*$^{-/Y}$ MEFs transformed with Ras or Src oncogenes

MEF genotype	*Oncogene*	*Soft agar colonies*
+/Y Clone 3	–	14
	Ras	29
	Src	47
+/Y Clone 6	–	0
	Ras	68
	Src	78
+/Y Clone 9	–	0
	Ras	39
	Src	22
−/Y Clone 4	–	0
	Ras	76
	Src	49
−/Y Clone 5	–	15
	Ras	76
	Src	44
−/Y Clone 11	–	0
	Ras	92
	Src	30

Data represent number of colonies obtained with 10^4 cells in assay. All assays were performed in triplicate and the mean value is given for each assay

weaker ability to phosphorylate and activate MEK/ERK when over-expressed in tissue culture cells (Pritchard *et al*., 1995; Marais *et al*., 1997). When expressed in Sf9 cells the kinase domain of B-Raf is over 500 times more efficient at phosphorylating MEK1 and MEK2 than the kinase domain of A-Raf (Pritchard *et al*., 1995). In addition, A-Raf immunoprecipitated from growth factor-stimulated MEFs cannot detectably activate MEK as measured by the kinase cascade assay (Hüser *et al*., 2001). The results presented in this report further support the view that A-Raf does not play a role in the Ras/Raf/MEK/ERK cascade *in vivo* as there is no defect in ERK activation in A-*raf*$^{-/Y}$ MEFs in response to growth stimulation (Figure 3a,b). Since recent data also indicate that ERK activation by Raf-1 may have no physiological role (Mikula *et al*., 2001; Hüser *et al*., 2001), B-Raf seems to be the main, if not the only, Raf isotype participating in the Ras/Raf/MEK/ERK cascade in MEFs. The observation that ERK activation is significantly disrupted in B-*raf*$^{-/-}$ MEFs is consistent with this conclusion (Wojnowski *et al*., 2000).

Previous investigations using over-expression in 3T3 cells have shown that Raf proteins can either induce cell cycle progression or cell cycle arrest depending on their level of activity towards the MEK/ERK pathway (Pritchard *et al.*, 1995; Woods *et al.*, 1997). Low levels of Raf activity elicits cell cycle progression by inducing expression of cyclin D1 and cyclin E whereas high levels of Raf activity can induce the expression of $p21^{Cip1}$ which inhibits cell cycle progression (Pritchard *et al.*, 1995; Woods *et al.*, 1997). Therefore, it was interesting to assess whether there were any defects in the cell cycle in MEFs and mice lacking A-Raf. The A-*raf*$^{-/Y}$ mice survive to birth and are normal in size at birth, suggesting that proliferation in embryogenesis is not significantly disrupted. Consistent with this observation, we found no clear difference in the ability of A-*raf*$^{-/Y}$ MEFs to progress through the cell cycle compared to A-*raf*$^{+/Y}$ MEFs (Figure 2a,b). Although the A-*raf*$^{-/Y}$ mice demonstrate progressive wasting in the infant phase onwards, recent studies have shown that this is due to a feeding ataxia (C Pritchard and M Iwobi; unpublished data).

We also examined the ability of A-*raf*$^{-/Y}$ MEFs to undergo programmed cell death (PCD) in response to a variety of apoptosis inducers compared to A-*raf*$^{+/Y}$ cells and observed no significant difference in PCD (Figure 2c), unlike *raf-1*$^{-/-}$ cells which are more susceptible to PCD induced by etoposide and anti-CD95 antibody (Hüser *et al.*, 2001). The A-*raf*$^{-/Y}$ ES cells also showed no defect in their ability to differentiate into multiple cell lineages in teratomas (Figure 4), a result consistent with the observation that all tissues of the A-*raf*$^{-/Y}$ mice develop normally (Pritchard *et al.*, 1996).

The A-*raf*$^{-/Y}$ MEFs can be transformed efficiently with the Src and Ha-Ras oncogenes (Figure 5 and Table 1) and the ability of A-*raf*$^{-/Y}$ ES cells to form teratomas is not disrupted. These results indicate that A-Raf is not important for the manifestation of the tumour phenotype. Previous studies using antisense or dominant inhibitory constructs in NIH3T3 cells showed the importance of Raf proteins for mediating the oncogenic effects of Ras and Src (Kolch *et al.*, 1991; Qureshi *et al.*, 1993). Our data argue that A-Raf does not play a role in this process, indicating that Raf-1 or B-Raf are more important for oncogene transformation.

What then is the role of A-Raf? Our results have shown that A-Raf does not play a unique role in the Ras/Raf/MEK/ERK cascade or in mediating the downstream responses of this cascade, at least in MEFs. B-Raf activity is substantially elevated in the A-Raf deficient cells and Raf-1 activity to a lesser degree (Figure 3d), suggesting that A-Raf may be involved in regulating the activities of these Raf isotypes. However, it is conceivable that the role of A-Raf as an ERK activator is highly tissue-specific and that the phenotype of the A-*raf*$^{-/Y}$ mice can be explained by tissue-specific disruption of this pathway. The localization of A-Raf to mitochondria in rat liver (Yuryev *et al.*, 2000) raises the distinct possibility that A-Raf has mitochondrial-specific functions that may include apoptosis. While we have shown that A-Raf is not involved in apoptosis in MEFs, this does not exclude the possibility that A-Raf has a tissue-specific apoptotic role. So far, we have not detected an increase in apoptosis in the liver or thymus of A-*raf*$^{-/Y}$ animals.

Materials and methods

Derivation and genotyping of MEFs and ES cells

Two independent A-*raf*$^{-/Y}$ ES cell lines (clones 89 and 99) were derived by undertaking one round of gene targeting with the pTCA-Raf knockout targeting vector in E14.1a ES cells as previously described (Pritchard *et al.*, 1996). Untargeted E14.1a ES cells represented A-*raf*$^{+/Y}$ controls. The A-*raf* primary MEFs were derived from E14.5 embryos arising from intercrosses between A-*raf*$^{+/-}$ females maintained on the C57BL6 background and wild-type C57BL6 males. MEFs from individual embryos were derived by standard procedures (Pritchard *et al.*, 1996; Hüser *et al.*, 2001). PCR genotyping was performed with primers A (GGCGATGTAGCTGTGAAAGTG) and B (5′-GCTCA-GAGGAGAAAGGGTCA-3′) for the wild-type allele, with primers C (CTTCCTGAGCACCTGCATCTC) and D (5′-CGTGCAATCCATCTTGTTCA) for the mutant allele and primers E (5′-GACTAGACATGTCTTAACATCTGTCC) and F (5′-CCTATTGCATGGACTGCAGCTTATG-3′) for the *Sry* gene (Gubbay *et al.*, 1992). All PCR reactions were performed using Ready-To-Go PCR beads (Amersham Pharmacia Biotech Inc.) and primers at 1 pM/μl. PCR reactions were performed at 94°C for 5 min followed by 35 cycles at 94°C for 30 s, 60°C for 30 s and 72°C for 30 s. PCR products were electrophoresed on 1.2% (w/v) agarose gels. Primary cells were immortalized with the ZIPTEX virus expressing the SV40 large T-antigen (Sladek and Jacobberger, 1992). Virus and cells were co-incubated in 8 μg/ml polybrene for 4–24 h and immortalized cells were grown out by continuous culture.

Cell culture and plasmid transfections

ES cells were cultured in high glucose (4.5 g/l) Dulbecco's modified Eagle's medium (DMEM; Life Technologies) containing 15% foetal calf serum (Life Technologies), 100 U/ml penicillin/streptomycin, 20 mM L-glutamine, 10 mM sodium pyruvate, non-essential amino acids, 115 μm β-mercaptoethanol and ESGRO Leukaemia Inhibitory Factor (LIF; Chemicon) on gelatin-treated plates. Primary and immortalized MEFs were cultured in low glucose DMEM (1 g/l) containing 10% foetal calf serum and 100 U/ml penicillin/streptomycin at 10% CO_2 in a humidified incubator. Primary cultures were not passaged more than eight times. For growth factor stimulation, MEFs were made quiescent by culturing in DMEM containing 0.5% (v/v) FCS for at least 24 h. They were stimulated by addition of EGF (10 ng/ml) over a time course of up to 24 h. Oncogene plasmids, pZAS4ras and pZAS4src (supplied by M McMahon, University of California, San Francisco, USA), expressing the v-Ha-Ras and chicken v-Src oncogenes respectively and containing the *Eco*gpt selectable marker were transfected into A-*raf*$^{-/Y}$ or A-*raf*$^{+/Y}$ MEFs by using lipofectamine according to the manufacturer's instructions (Life Technologies). Transfected cells were selected with medium containing hypoxanthine (15 μg/ml), aminopterin

(2 μg/ml), thymidine (10 μg/ml), xanthine (250 μg/ml) and mycophenolic acid (25 μg/ml) and the resulting colonies were pooled.

Kinase assays and immunoblotting

Triton X-100 soluble protein lysates and Western blots were prepared as described previously (Marais *et al.*, 1997; Luckett *et al.*, 2000). Primary antibodies used were: a 1 : 1000 dilution of an anti-p69^{A-raf} polyclonal antiserum (Santa Cruz Biotechnology), a 1 : 1000 dilution of the F9 vinculin monoclonal antibody (a gift from Dr V Koteliansky, CNRS, Paris), 1 : 2000 dilution of a mouse monoclonal antibody against Thr202/Tyr204 phospho-p44/42 ERK (New England Biolabs), a 1 : 1000 dilution of a rabbit polyclonal antibody against ERK2 (Zymed Laboratories Inc.), a 1 : 1000 dilution of an anti-avian Src mouse monoclonal antiserum against chicken v-Src (Clone EC10; Upstate Biotechnology, Inc.) and a 1 : 500 dilution of an anti-Ras mouse monoclonal antibody (Transduction Laboratories). Detection of the antigen–antibody complexes was performed as described previously with the appropriate secondary antibody (Luckett *et al.*, 2000). Raf proteins were immunoprecipitated for 2 h at 4°C from 0.1–1 mg of cell extracts with 2 μg of the anti-Raf-1 antibody (Transduction Laboratories) or 4 μg of an anti-B-Raf rabbit polyclonal antibody (Mason *et al.*, 1999). The activity of each Raf protein was assessed as described by Marais *et al.*, 1997. For B-Raf, 0.1 mg of lysate was used whereas for Raf-1, 1 mg of lysate was used. p42 ERK was immunoprecipitated by using 5 μl of a rabbit anti-p42ERK polyclonal antibody and ERK activity was measured using the MBP kinase assay (Samuels *et al.*, 1993).

Proliferation and apoptosis analysis

For growth curves, 2×10^4 primary cells were plated per well of a 24- or 12-well plate. Cells were counted at 24 h intervals in triplicate using a haemocytometer. For DNA synthesis assays the method described by Treinies *et al.* (1999) and Hüser *et al.* (2001) was followed. To induce apoptosis, primary cells at 80% confluency on 6 cm dishes were treated with etoposide (50 μm), anti-CD95 antibody (50 ng/ml) with 0.5 μm cycloheximide or serum-free medium for 20 h in a 37°C humidifying incubator. Annexin V staining and FACS analysis were performed as described in Hüser *et al.* (2001). Data were analysed by using the unpaired 2-tailed independent *t*-test to assess the significance of the results.

Transformation assays

For soft agar assays, cells were trypsinized and counted using a haemocytometer. 10^3, 10^4 and 10^5 cells were then placed in medium containing 0.35% (w/v) low-melting-temperature agarose. For the Ras and Src transformed cells HAT selection was also included in the medium. After 21 days, cells were stained with MTT (3-[4,5-dimethylthiazol-2-yl]-2,5-diphenyltetrazolium bromide). The stained plates were photographed and the colonies were counted using a Gel Doc 2000 system (BioRad) and Quantity One software with the sensitivity level set at 3.0.

Teratoma formation

ES cells were cultured, trypsinized, washed with PBS and 5×10^6 cells in PBS were injected subcutaneously into the flank of 8-week-old syngeneic 129Ola male mice. After 3 weeks, tumours were collected, weighed, fixed in 4% (w/v) paraformaldehyde, embedded in paraffin and 5 μm sections were prepared and stained with haematoxylin and eosin. Sections were analysed under a Leica DMLB light microscope.

Acknowledgments

We thank Susan Giblett for embedding and sectioning the teratomas, Mabel Iwobi for the PCR data, Martin McMahon for providing the pZAS4ras and pZAS4src vectors and Lee Topping for help with statistics. We are also grateful to the Division of Biomedical Services at Leicester for their technical assistance. This work was supported by a BBSRC studentship to K Mercer, a Royal Society fellowship to C Pritchard, and project grants from the Medical Research Council and the Cancer Research Campaign. We thank these organisations for their invaluable support.

References

Barnier JV, Papin C, Eychene A, Lecoq O and Calothy G. (1995). *J. Biol. Chem.*, **270,** 23381–23389.

Bogoyevitch MA, Marshall CJ and Sugden PH. (1995). *J. Biol. Chem.*, **270,** 26303–26310.

Daum G, Eisenmann-Tappe I, Fries HW, Troppmair J and Rapp UR. (1994). *Trends Biochem. Sci.*, **19,** 474–480.

Gubbay J, Vivian N, Economou A, Jackson D, Goodfellow P and Lovell-Badge R. (1992). *Proc. Natl. Acad. Sci. USA*, **89,** 7953–7957.

Hagemann C, Kalmes A, Wixler L, Schuster T and Rapp UR. (1997). *FEBS Let.*, **403,** 200–202.

Hagemann C and Rapp UR. (1999). *Exp. Cell Res.*, **253,** 34–46.

Huleihel M, Goldsborough M, Cleveland J, Gunnell M, Bonner T and Rapp UR. (1986). *Mol. Cell. Biol.*, **6,** 2655–2662.

Hüser H, Luckett J, Chiloeches A, Mercer K, Iwobi M, Giblett S, Sun X-M, Brown J, Marais R and Pritchard C. (2001). *EMBO J.*, **20,** 1940–1951.

Kolch W, Heidecker G, Lloyd P and Rapp UR. (1991). *Nature*, **349,** 426–428.

Luckett JCA, Huser MB, Giagtzoglou N, Brown JE and Pritchard CA. (2000). *Cell Growth Differ.*, **11,** 163–171.

Marais R, Light Y, Paterson HF, Mason CS and Marshall CJ. (1997). *J. Biol. Chem.*, **272,** 4378–4383.

Mason CS, Springer CJ, Cooper RG, Superti-Furga G, Marshall CJ and Marais R. (1999). *EMBO J.*, **18,** 2137–2148.

Mikula M, Schreiber M, Husak Z, Kucerova L, Ruth J, Wieser R, Zatloukal K, Beug H, Wagner EF and Baccarini M. (2001). *EMBO J.*, **20,** 1952–1962.

Pritchard CA, Samuels ML, Bosch E and McMahon M. (1995). *Mol. Cell. Biol.*, **15,** 6430–6442.

Pritchard CA, Bolin L, Slattery R, Murray R and McMahon M. (1996). *Curr. Biol.*, **6,** 614–617.

Qureshi SA, Joseph CK, Hendrickson M, Song J, Gupta R, Bruder J, Rapp U and Foster DA. (1993). *Biochem. Biophys. Res. Comm.*, **30,** 969–975.

Samuels ML, Weber MJ, Bishop JM and McMahon M. (1993). *Mol. Cell. Biol.*, **13**, 6241–6252.
Sladek TL and Jacobberger JW. (1992). *Oncogene.*, **7**, 1305–1313.
Storm SM, Cleveland JL and Rapp UR. (1990). *Oncogene*, **5**, 345–351.
Treinies I, Paterson HF, Hooper S, Wilson R and Marshall CJ. (1999). *Mol. Cell. Biol.*, **19**, 321–329.
Wojnowski L, Stancato LF, Larner A, Rapp UR and Zimmer A. (2000). *Mech. Devel.*, **91**, 97–104.
Woods D, Parry D, Cherwinsky H, Bosch E, Lees E and McMahon M. (1997). *Mol. Cell. Biol.*, **17**, 5598–5611.
Yuryev A, Ono M, Goff SA, Macaluso F and Wennogle LP. (2000). *Mol. Cell. Biol.*, **20**, 4870–4878.